

**University of Nottingham**  
**School of Chemical, Environmental and Mining Engineering**

**Geometric Effects on Phase Split at a  
Large Diameter T-junction**

by

**Elisabeth Wren M.Eng.**

**Thesis submitted to the University of Nottingham for the degree of  
Doctor of Philosophy**

**September 2001**

## **Abstract**

The separation of gas-liquid flows is a necessary part of many industrial processes. Thus, it has received much attention over the years with the ultimate aim of reducing equipment costs whilst maintaining or improving efficiency. Traditionally, the Petroleum Industry has relied heavily on conventional vessel separators which are bulky, expensive and have a high inventory. Research has indicated that a cheap alternative may be a simple pipe junction. It has been shown that gas-liquid flows can be divided at pipe junctions in such a manner that there is a partial separation of the phases. The result is two streams – one richer in gas than the initial feed and the other richer in liquid. If the phases can be separated, albeit partially, at a simple pipe junction then the need for a large separator is diminished.

Within this thesis the use of a simple T-junction is considered as a continuous, compact, economical partial phase separator with a minimal inventory for use within the oil industry. The main objective was to gain a better understanding of how a gas-liquid flow is divided at a large diameter T-junction and how the flow split is affected by T-junction geometry. Firstly, the orientation of the side arm from the horizontal was considered with both a regular (inlet arm diameter = branch arm diameter = 0.127m) T-junction and a reduced (branch arm to inlet diameter ratio = 0.6) T-junction. The side arm was placed horizontally ( $0^\circ$ ), vertically upwards ( $+90^\circ$ ) and vertically downwards ( $-90^\circ$ ) and the phase split of air-water annular and stratified flows were investigated. To improve the phase separation characteristics of the regular T-junction, inserts protruding from the side arm into the main pipe were considered and for the junction with a vertically downwards side arm a U-bend was used to reduce the fraction of gas pulled through. The experimental investigation was expanded to incorporate the effect of placing two regular T-junctions in series. With the branch arm of the first placed vertically upwards ( $+90^\circ$ ), and the second vertically downwards ( $-90^\circ$ ) a pure gas stream and a liquid rich stream were created from the multi-phase inlet. Reducing the sidearm diameter of the second junction lowered the fraction of gas drawn off in the liquid rich stream. The physical separation distance the T-junctions was found to have little effect on phase split. The interaction of the two junctions are interdependent and the phase split results from the two junction

---



system was found to be more complex than simply considering the results of two individual T-junctions.

Being able to predict the phase split at a junction is vital if they are to be considered seriously within industrial settings. The case of a regular T-junction with a vertically downwards ( $-90^\circ$ ) side arm has received little specific attention. From the linear nature of the phase split results it was determined that if two key points could be accurately predicted then the phase split results can be determined. The “onset of gas take off”, the fraction of liquid diverted down the branch arm when the first fraction of gas is pulled through, was successfully related to the bubble rise velocity of the gas entrained in the liquid column trapped in the branch arm. The “critical gas take off”, the fraction of gas diverted when all the liquid is drawn down the branch arm, was determined by relating the fluid flow to the motion of a falling particle.

## **Acknowledgements**

I would like to express my gratitude to my supervisor Prof. B. J. Azzopardi. Guidance and support has been given willingly throughout my research and has been invaluable both in the pursuit of new ideas and in the preparation of this thesis.

Many thanks to the technical staff of the Workshop. Their expertise and patience have ensured that my ideas have been taken successfully from concept to reality with few complications.

I would like thank Brian Oswald of BPX, Sunbury for his time and comments, placing an industrial relevance on the present research. The financial support of both BPX and the EPSRC is gratefully acknowledged.

Special thanks to my colleagues Glen, Wayne and Richard. Their support and assistance during all stages of my research has been deeply appreciated. Many thanks to the rest my colleagues, past and present, in the post-graduate office who have tried to educate me in the world of computers and have all helped make the duration of my PhD a valuable experience.

I would also like to thank Prof. H. Soliman who visited Nottingham in the summer of 2001 from the University of Manitoba, Canada. His enthusiasm and knowledge on the subject led to many interesting discussions and opened up new avenues of thought.

To my family and close friends I am grateful for their continuing encouragement and unwavering belief that I would get there one day – and one day I did.



# Contents

<b>ABSTRACT</b>	<b>i</b>
<b>ACKNOWLEDGEMENTS</b>	<b>iii</b>
<b>CONTENTS</b>	<b>iv</b>
<b>LIST OF FIGURES</b>	<b>vii</b>
<b>LIST OF TABLES</b>	<b>xii</b>
<b>CHAPTER 1 MULTIPHASE FLOWS</b>	<b>1</b>
1.1 WHAT IS MULTIPHASE FLOW?	1
1.2 TWO-PHASE FLOW PATTERNS	2
1.2.1 Vertical Upflow in Pipes	3
1.2.2 Horizontal Flow in Pipes	4
1.3 PREDICTING HORIZONTAL TWO-PHASE FLOW PATTERNS	6
1.4 SEPARATING TWO-PHASE FLOWS	8
1.4.1 Introducing junctions and two-phase flow	10
<b>CHAPTER 2 T-JUNCTIONS AND TWO-PHASE FLOW</b>	<b>14</b>
2.1 THE “SIMPLE” T-JUNCTION	15
2.1.1 Dominant forces around a T-junction	15
2.1.2 Associated variables with a T-junction	16
2.1.3 Ways of representing phase split data	17
2.2 GEOMETRICAL EFFECTS ON FLOW SPLIT AT A T-JUNCTION	19
2.2.1 Effect of main pipe orientation	21
2.2.2 Effects of altering the side arm diameter	24
2.2.3 Effect of branch arm orientation	30
2.2.4 Effect of altering the physical dimensions of the T-junction	35
2.2.5 T-junctions in alternative combinations	38

<b>CHAPTER 3</b>	<b>EXPERIMENTAL ARRANGEMENT.....</b>	<b>40</b>
3.1	THE FLOW FACILITY .....	40
3.1.1	<i>Altering side arm orientation .....</i>	<i>44</i>
3.1.2	<i>Downwards side arm with U-bend .....</i>	<i>47</i>
3.1.3	<i>Two T-junctions in series .....</i>	<i>48</i>
3.1.4	<i>The T-junctions and inserts .....</i>	<i>49</i>
3.2	EXPERIMENTAL PROCEDURE FOR A SINGLE T-JUNCTION.....	50
3.2.1	<i>Operation with the side arm lying horizontally (0°) and vertically upwards (+90°).....</i>	<i>51</i>
3.2.2	<i>Operation with the inserts .....</i>	<i>53</i>
3.2.3	<i>Operation with the side arm vertically downwards (-90°) with and without a U-bend..</i>	<i>54</i>
3.3	EXPERIMENTAL PROCEDURE WITH TWO T-JUNCTIONS IN SERIES .....	55
3.4	THE FLOW PATTERNS INVESTIGATED.....	56
3.5	VISUAL OBSERVATIONS AND HIGH SPEED CAMERA FOOTAGE .....	60
<b>CHAPTER 4</b>	<b>EFFECT OF GEOMETRY ON PHASE SPIT AT A SINGLE T-JUNCTION....</b>	<b>61</b>
4.1	COMPARISONS WITH PUBLISHED DATA.....	62
4.2	EFFECT OF SIDE ARM DIAMETER .....	63
4.2.1	<i>Horizontal side arm (0°).....</i>	<i>63</i>
4.2.2	<i>Vertically upwards side arm (+90°).....</i>	<i>73</i>
4.2.3	<i>Vertically downwards side arm (-90°) .....</i>	<i>79</i>
4.2.4	<i>Downwards side arm with U-bend .....</i>	<i>90</i>
4.3	VISUAL OBSERVATIONS AT THE T-JUNCTION WITH A DOWNWARDS SIDE ARM .....	93
4.4	CONCLUSIONS .....	97
<b>CHAPTER 5</b>	<b>PLACING AN INSERT AT A SINGLE T-JUNCTION.....</b>	<b>99</b>
5.1	PREVIOUS WORK ON T-JUNCTIONS AND INSERTS .....	100
5.2	ADDING AN INSERT AT THE LARGE DIAMETER T-JUNCTIONS.....	102
5.2.1	<i>Altering the angle of cut of the insert.....</i>	<i>102</i>
5.2.2	<i>Altering the protrusion depth of the insert .....</i>	<i>106</i>
5.2.3	<i>Insert and the reduced T-junction.....</i>	<i>109</i>
5.3	CONCLUSIONS .....	111



<b>CHAPTER 6 TWO T-JUNCTIONS IN SERIES.....</b>	<b>113</b>
6.1 GRAPHICAL REPRESENTATION OF THE PHASE SEPARATION .....	114
6.1.1 <i>Conventional Phase Separation Graphs</i> .....	116
6.1.2 <i>Triangular phase separation plots</i> .....	120
6.1.3 <i>Combining two outlets</i> .....	124
6.2 USING A REDUCED T-JUNCTION .....	126
6.3 ALTERING THE SEPARATION DISTANCE .....	128
6.4 TWO T-JUNCTIONS IN SERIES AND SINGLE T-JUNCTIONS .....	131
6.4.1 <i>Comparing the phase separation</i> .....	131
6.4.2 <i>Predicting the phase separation of two T-junctions</i> .....	138
6.5 VISUAL OBSERVATIONS IN THE TWO T-JUNCTION SYSTEM .....	143
6.6 CONCLUSIONS .....	146
 <b>CHAPTER 7 PREDICTING THE PHASE SPLIT AT A T-JUNCTION.....</b>	 <b>148</b>
7.1 PHASE REDISTRIBUTION MODELS .....	149
7.1.1 <i>The general methods for modelling two phase flow</i> .....	149
7.1.2 <i>The distribution of the two phases</i> .....	153
7.1.3 <i>Predicting the phase split with a downwards side arm</i> .....	154
7.2 THE ONSET OF GAS TAKE OFF .....	158
7.2.1 <i>Predictions using small break theory</i> .....	159
7.2.2 <i>Predictions considering the gas-liquid flow in the branch arm</i> .....	163
7.3 THE CRITICAL GAS FRACTION AND GAS PULL THROUGH .....	170
7.3.1 <i>Empirical relationships</i> .....	170
7.3.2 <i>Considering the pressure drop across the T-junction</i> .....	171
7.3.3 <i>Considering the drag forces</i> .....	176
7.4 LIMITATIONS OF THESE PREDICTIONS .....	180
 <b>CHAPTER 8 CONCLUSIONS AND FURTHER WORK .....</b>	 <b>183</b>
8.1 FINAL CONSIDERATIONS AND CONCLUSIONS .....	183
8.2 FUTURE WORK .....	186
 <b>BIBLIOGRAPHY .....</b>	 <b>188</b>

---

<b>NOMENCLATURE .....</b>	<b>197</b>
<b>APPENDIX A    ERROR ANALYSIS AND DATA OBTAINED FROM EXPERIMENTAL RESULTS</b>	
<b>APPENDIX B    PHASE SPLIT DATA</b>	
<b>APPENDIX C    CONSIDERING SINGLE PHASE PRESSURE DROP</b>	
<b>APPENDIX D    CONSIDERING DRAG FORCES</b>	

## List of Figures

Figure 1-1: The major flow patterns observed during two-phase vertical upflow .....	3
Figure 1-2: The major flow regimes observed during horizontal two-phase flow .....	5
Figure 1-3: Horizontal flow pattern map for the experimental facility based on the methodology of Taitel and Dukler (1976) .....	8
Figure 1-4: Industrial separation of two-phase flow into storage tanks .....	11
Figure 2-1: A typical T-junction and the parameters associated with it .....	16
Figure 2-2: Phase split representation for annular flow at a horizontal regular T-Junction .....	18
Figure 2-3: The geometric arrangement proposed, utilising a T-junction as a partial phase separator, Azzopardi <i>et al.</i> (2001) .....	20
Figure 2-4: Comparing the phase split of a vertical and a horizontal T-junction, UKAEA (Harwell) ..	23
Figure 2-5: Effect of diameter ratio on phase split, Azzopardi (1984) .....	25
Figure 2-6: Dividing T- and 45° Y-junctions .....	25
Figure 2-7: The pressure drop at a regular T-junction, Buell <i>et al.</i> (1994) .....	26
Figure 2-8: Pressure drop across a regular and reduced T-junction, Walters <i>et al.</i> (1988) .....	27
Figure 2-9: Baffle positions of Fouda and Rhodes (1974) .....	36
Figure 2-10: Schematic diagram showing the insert positions used by Butterworth (1980) .....	36
Figure 2-11: T- and Y- configurations investigated by Beveilacqua <i>et al.</i> (2000) .....	38
Figure 3-1: Schematic flow diagram of the T-junction rig .....	41
Figure 3-2: Horizontal side arm .....	44
Figure 3-3: Vertically upwards side arm .....	45

---



Figure 3-4: Vertically downwards side arm without U-bend .....	46
Figure 3-5: Vertically downwards side arm with U-bend .....	47
Figure 3-6: Two T-junctions in series.....	48
Figure 3-7: Inserts placed in the side arm of both T-junctions .....	49
Figure 3-8: Inserts facing forwards at protrusion depth $\frac{1}{2}D$ and backwards at protrusion depth $\frac{3}{4}D$ ...	50
Figure 3-9: Typical flow split results for annular flow with the side arm positioned horizontally and vertically upwards.....	52
Figure 3-10: Typical phase split for stratified flow with the $45^\circ$ insert facing forwards and backwards at a protrusion depth of $\frac{1}{2}D$ .....	53
Figure 3-11: Typical phase split results for stratified flow with a the side arm positioned vertically downwards .....	54
Figure 3-12: Phase split results annular flow with two regular T-junctions in series .....	56
Figure 3-13: Flow pattern map from predictions of Taitel and Dukler for a 0.127m diameter horizontal pipe compared with the experimental inlet flow conditions .....	57
Figure 4-1: The effects of inlet flow pattern on a horizontal reduced T-junction, $U_{gs} = 12\text{m/s}$ .....	64
Figure 4-2: Phase split for stratified flow at a horizontal regular and reduced T-junctions, $U_{gs} = 4\text{m/s}$ .....	66
Figure 4-3: Slug flow data of Buell <i>et al.</i> (1994) with similar void fractions to the current data, $U_{ls} = 0.18\text{m/s}$ .....	66
Figure 4-4: Phase split for stratified flow at a horizontal regular and reduced T-junction, $U_{gs} = 12\text{m/s}$ .....	69
Figure 4-5: Phase split for stratified flow at a horizontal regular and reduced T-junction, $U_{gs} = 24\text{m/s}$ .....	69
Figure 4-6: Comparison of current stratified flow data ( $U_{gs} = 12\text{m/s}$ ) with that of Azzopardi <i>et al.</i> (1988) based on CISE void fraction of 0.934 .....	71
Figure 4-7: Comparison of current stratified flow data ( $U_{gs} = 24\text{m/s}$ ) with that of Reimann <i>et al.</i> (1988) based on CISE void fraction of 0.96 .....	71
Figure 4-8: Phase split for annular flow at a horizontal regular and reduced T-junction, $U_{gs} = 12\text{m/s}$ .....	72
Figure 4-9: Phase split for stratified flow at a regular and reduced T-junction with a vertically upwards branch arm, $U_{gs} = 4\text{m/s}$ .....	75
Figure 4-10: Phase split for stratified flow at a regular and reduced T-junction with a vertically upwards branch arm, $U_{gs} = 12\text{m/s}$ .....	77
Figure 4-11: Phase split for stratified flow at a regular and reduced T-junction with a vertically upwards branch arm, $U_{gs} = 24\text{m/s}$ .....	77
Figure 4-12: Phase split comparison of different side arm orientations, $U_{gs} = 8\text{m/s}$ , $U_{ls} = 0.31\text{m/s}$ .....	82
Figure 4-13: Effect of $U_{gs}$ on phase split at a regular T-junction with a downwards side arm, $U_{ls} = 0.31\text{m/s}$ .....	83



Figure 4-14: Effect of $U_{ls}$ on phase split at a regular T-junction with a downwards side arm, $U_{gs} = 8\text{m/s}$ .....	83
Figure 4-15: Phase split for stratified flow at a regular and reduced T-junction with a vertically downwards side arm, $U_{gs} = 6\text{m/s}$ .....	85
Figure 4-16: Comparison of current stratified flow data ( $U_{ls} = 0.186\text{m/s}$ ) with published data, CISE void fraction of 0.837.....	86
Figure 4-17: Phase split for stratified flow at a regular and reduced T-junction with a downwards side arm, $U_{ls} = 0.186\text{m/s}$ .....	86
Figure 4-18: Phase split for annular flow at a regular and reduced T-junction with vertically downwards side arm, $U_{gs} = 12\text{m/s}$ .....	88
Figure 4-19: Phase split for annular flow at a regular horizontal T-junction, $U_{gs} = 12\text{m/s}$ .....	89
Figure 4-20: Phase split for stratified and annular flow at a reduced T-junction with and without a U-bend, $U_{gs} = 12\text{m/s}$ .....	91
Figure 4-21: Phase split for stratified flow at reduced T-junction with and without a U-bend, $U_{gs} = 4\text{m/s}$ .....	91
Figure 4-22: Stratified flow (low gas-liquid interface) at the regular T-junction .....	94
Figure 4-23: High liquid, high gas flowrates approaching the regular T-junction.....	94
Figure 4-24: High liquid, low gas flowrates approaching the T-junction .....	94
Figure 4-25: Gas pull through at a small break in a large diameter pipe, Reimann & Khan (1982).....	96
Figure 5-1: The insert positions used by Butterworth (1980).....	100
Figure 5-2: The T-junction with baffle as used by Fouda and Rhodes (1974) .....	101
Figure 5-3: Annular flow, $\frac{1}{2}D$ protrusion, $45^\circ$ insert.....	103
Figure 5-4: Annular flow, $\frac{1}{2}D$ protrusion , $30^\circ$ insert.....	103
Figure 5-5: Annular flow, $\frac{3}{4}D$ protrusion, $45^\circ$ insert.....	104
Figure 5-6: Annular flow, $\frac{3}{4}D$ protrusion, $30^\circ$ insert.....	104
Figure 5-7: Profile of the insert seen by the on-coming flow in the main run arm .....	105
Figure 5-8: Stratified-wavy flow, $\frac{1}{2}D$ protrusion, $45^\circ$ insert.....	108
Figure 5-9: Stratified-wavy flow, $\frac{3}{4}D$ protrusion, $45^\circ$ insert.....	108
Figure 5-10: Reduced T-junction, annular flow, $\frac{1}{2}D$ protrusion, $45^\circ$ insert.....	110
Figure 5-11: Reduced T-junction, annular flow, $\frac{3}{4}D$ protrusion, $45^\circ$ insert .....	110
Figure 6-1: Schematic diagram of the two T-junction system.....	115
Figure 6-2: Phase split results for the up arm, $U_{gs} = 12\text{m/s}$ and $U_{ls} = 0.31\text{m/s}$ .....	117
Figure 6-3: Phase split results for the down arm based on inlet, $U_{gs} = 12\text{m/s}$ and $U_{ls} = 0.31\text{m/s}$ .....	117
Figure 6-4: Phase split results for down arm based on stream 3, $U_{gs} = 12\text{m/s}$ and $U_{ls} = 0.31\text{m/s}$ .....	119
Figure 6-5: Overall phase split results for $U_{gs} = 12\text{m/s}$ and $U_{ls} = 0.31\text{m/s}$ .....	119
Figure 6-6: Triangular plot of gas phase split, $U_{gs} = 12\text{m/s}$ and $U_{ls} = 0.31\text{m/s}$ .....	122
Figure 6-7: Triangular plot of the phase separation for the system, $U_{gs} = 12\text{m/s}$ and $U_{ls} = 0.31\text{m/s}$ ...	122
Figure 6-8: The effects of combining the different outlets. $U_{gs} = 12\text{m/s}$ and $U_{ls} = 0.31\text{m/s}$ .....	124



Figure 6-9: Effects of using a reduced diameter T-junction, $U_{gs} = 12\text{m/s}$ , $U_{ls} = 0.31\text{m/s}$ .....	127
Figure 6-10: Effect on T-junction separation distance with two regular T-junctions, $U_{gs} = 12\text{m/s}$ and $U_{ls} = 0.31\text{m/s}$ . Hollow symbols represent separation distance 0.5m and full symbols 1.2m.....	129
Figure 6-11: Effect of T-junction separation distance with reduced T -junction, $U_{gs} = 12\text{m/s}$ , $U_{ls} = 0.31\text{m/s}$ . Hollow symbols represent separation distance 0.5m, the full symbols 1.2m .....	129
Figure 6-12: Effect of T-junction separation distance with two regular T -junctions, $U_{gs} = 4\text{m/s}$ . $U_{ls} = 0.043\text{m/s}$ . Hollow symbols represent separation distance 0.5m, the full symbols 1.2m ....	130
Figure 6-13: Schematic representation of the different outlets being compared .....	132
Figure 6-14: Comparison of phase split with one and two T-junctions. Annular flow, $U_{gs} = 12\text{m/s}$ and $U_{ls} = 0.31\text{m/s}$ . .....	133
Figure 6-15: Comparison of phase split with one and two T-junctions. Stratified flow, $U_{gs} = 4\text{m/s}$ and $U_{ls} = 0.434\text{m/s}$ .....	133
Figure 6-16: Comparison of phase split with one and two T-junctions. Stratified flow, $U_{gs} = 8\text{m/s}$ and $U_{ls} = 0.186\text{m/s}$ .....	134
Figure 6-17: Comparison of phase separation with a reduced diameter T-junction for the one and two T-junction systems. $U_{gs} = 12\text{m/s}$ and $U_{ls} = 0.31\text{m/s}$ .....	136
Figure 6-18: Comparison of phase separation with a reduced diameter T-junction for the one and two T-junction systems. $U_{gs} = 4\text{m/s}$ and $U_{ls} = 0.434\text{m/s}$ .....	136
Figure 6-19: Comparison of phase separation with a reduced diameter T-junction for the one and two T-junction systems. $U_{gs} = 8\text{m/s}$ and $U_{ls} = 0.186\text{m/s}$ .....	137
Figure 6-20: Can the two T-junction system be represented by two individual T-junctions? .....	138
Figure 6-21: Phase separation of a single T-junction with a vertically upwards side arm compared with the up arm of the first T of the two in series. $U_{gs} = 12\text{m/s}$ , $U_{ls} = 0.31\text{m/s}$ .....	139
Figure 6-22: Various phase separation curves of a single T with downwards side arm compared with the down arm of the second T of the two in series. Annular Flow, $U_{gs} = 12\text{m/s}$ , $U_{ls} = 0.31\text{m/s}$	141
Figure 6-23: Various phase separation curves of a single T with downwards side arm compared with the down arm of the second T of the two in series. Stratified Flow, $U_{gs} = 12\text{m/s}$ , $U_{ls} = 0.186\text{m/s}$ .....	141
Figure 6-24: Schematic diagram of the two T-junction system indicating the four viewing points....	143
Figure 6-25: Video stills of the gas-liquid flows at a two T-junction system.....	144
 Figure 7-1: The different zones of influence used within phenomenological models.....	151
Figure 7-2: The model of Seeger <i>et al.</i> (1986) compared with the data of Peng <i>et al.</i> (1993).....	155
Figure 7-3: The model of Ballyk and Shoukri (1990) compared with the data of Peng <i>et al.</i> (1993). 155	
Figure 7-4: Typical phase split results with the side arm vertically downwards $U_{gs} = 8\text{m/s}$ and $U_{ls} = 0.556\text{m/s}$ .....	157
Figure 7-5: Onset of gas pull through, Maciaszek and Micaelli (1988).....	160
Figure 7-6: The effect on the predicted value of $L_{onset}$ for different inlet conditions.....	162

---

Figure 7-7: Variation of experimental values of $L'_{onset}$ with inlet gas and liquid superficial velocities .....	163
Figure 7-8: Liquid build up at the butterfly valve in the downwards side arm .....	164
Figure 7-9: Calculated versus measured values of $L'_{onset}$ .....	167
Figure 7-10: The industrial partial phase T-junction separator at BP/Amoco, Hull .....	169
Figure 7-11: Empirical phase split predictions for a large diameter regular T-junction, $U_{gs} = 10\text{m/s}$ .	170
Figure 7-12: Downwards regular T-junction where all the liquid is drawn down the side arm.....	172
Figure 7-13: The comparison of measured film thickness to those calculated using the methodology of Taitel and Dukler (1976) highlighted by Rea (1998) .....	175
Figure 7-14: The dependence of horizontal distance travelled on particle diameter $U_{gs} = 10\text{m/s}$ and $U_{ls} = 0.434\text{m/s}$ .....	177
Figure 7-15: Predicted phase split knowing $L'_{onset}$ and $G'_{crit}$ for $U_{gs} = 10\text{m/s}$ , $U_{ls} = 0.434\text{m/s}$ .....	178
Figure 7-16: Phase split predictions for different particle diameters, $U_{gs} = 6\text{m/s}$ and $U_{ls} = 0.556\text{m/s}$ .....	179
Figure 7-17: Low liquid flow $U_{gs} = 6\text{m/s}$ .....	181



List of Tables

Table 2-1: Inlet conditions referring to the UKAEA (Harwell) data in Figure 2-4 ..... 23

Table 2-2: Previous work where the effect of diameter ratio has been studied ..... 30

Table 2-3: Previous work where the effect of orientation has been studied ..... 34

Table 2-4: Previous work where the effect of altering the physical dimensions of the T-junction has been studied..... 37

Table 3-1: Summary of all experiments performed with corresponding T-junction geometry..... 59

Table 4-1: Comparison of all gas take off limits in a vertically upwards T-junction ( $D_3/D_1 = 0.6$ )..... 78

Table 7-1: Comparison of the predicted and experimental values for the fraction of liquid drawn into the branch arm at the onset of gas take off,  $L'_{onset}$  for different inlet flow conditions for the large diameter regular T-junction using the small break theory ..... 161

Table 7-2: Comparison of the predicted and experimental values for the fraction of liquid drawn into the branch arm at the onset of gas take off,  $L'_{onset}$  for different inlet flow conditions for the data of Reimann *et al.* (1988)..... 168

---

To Dr Wren *Snr.*

*Parturient montez, nascetur ridiculus mus*

Horace, *Ars Poetica*

*The wren goes to't*

Shakespeare, *King Lear*, Act IV, Scene VI

---



# CHAPTER 1

## Multiphase Flows

Central to this thesis is an understanding of multiphase flow and how it behaves. The term “multiphase flow” can cover many different phase combinations travelling together within a pipeline, or piece of equipment, hence a general introduction is presented which concentrates on two-phase gas-liquid flow. The various different flow patterns that can occur in both vertical and horizontal pipelines with co-current gas-liquid flow have been discussed in detail. Particular attention has been applied to horizontal flow patterns and how these may be predicted since the inlet pipeline of the flow facility used during the experimental investigations is horizontal.

The separation of gas-liquid flows is a necessary part of many industrial processes. Thus, it has received much attention over the years with the ultimate aim of reducing equipment costs whilst maintaining or improving efficiency. Alternatives to the conventional methods have been found and one such potential is the basis of the two-phase gas-liquid research presented within this thesis.

### ***1.1 What is Multiphase Flow?***

On examination of many pieces of equipment within the chemical, power generation and hydrocarbon production industries, such as separators, reactors, heat exchangers and pipelines, it can be observed that they contain flows that are of more than one phase. The simultaneous flow through equipment of two or more phases is termed “multiphase flow”. In many cases the two phases are vapour and liquid, for example in reboilers and condensers; fluidised beds and pneumatic conveying are concerned with solid-gas streams; the oil industry regularly has to handle immiscible liquids, specifically oil and water. In many cases they actually deal with gas, oil and water all



flowing together and hydraulic conveying deals with solid-liquid flows. Multiphase flows may also occur in single phase pipelines which are subjected to a large pressure drop or temperature rise.

The science of multiphase flows is complex but the industrial need to understand how to handle and process such streams has spurred research. Over the years many equations and correlations have been derived to describe as correctly as possible the motion and reaction of multiphase flows under various conditions. Due to their complex nature and the many variations of multiphase flows, two-phase gas-liquid flows have gained the most attention and this thesis has concentrated on such flows.

## ***1.2 Two-Phase Flow Patterns***

When a gas-liquid mixture flows in a pipe, the combined flow can assume different characteristics caused by the interface between the two phases. Some of the formations are clearly identifiable and others are more chaotic and difficult to classify. Since gas-liquid two-phase flows are commonplace throughout industry, various different configurations have been defined, grouping together two-phase flows that have the same characteristics. These relate to the distribution of the phase and the mechanisms dominating pressure drop and heat and mass transfer. Understanding and determining which of these flow regimes is present in a given section of pipeline is crucial as the hydrodynamics and the two-phase properties of the stream can vary significantly.

The exact character of the two-phase stream depends on the relative ratios of the gas and liquid present and the velocities of each phase relative to one another. Pipeline orientation also significantly effects the flow pattern as gravity exerts a greater influence on the liquid phase. Obviously, the multiplicity of factors affecting the two-phase flow pattern can lead to many variations but they can be divided into two distinct groups depending on pipe orientation – horizontal and vertical. Under these two headings, the different ways the gas and liquid flow together can then be

---



described. Sections 1.2.1 and 1.2.2 describe the main flow patterns associated with vertical and horizontal gas-liquid flow respectively.

### 1.2.1 Vertical Upflow in Pipes

The flow patterns for co-current vertical upflow flow patterns are shown in Figure 1-1. With vertical upflow gravity acts axially and the four major flow patterns have been described below.

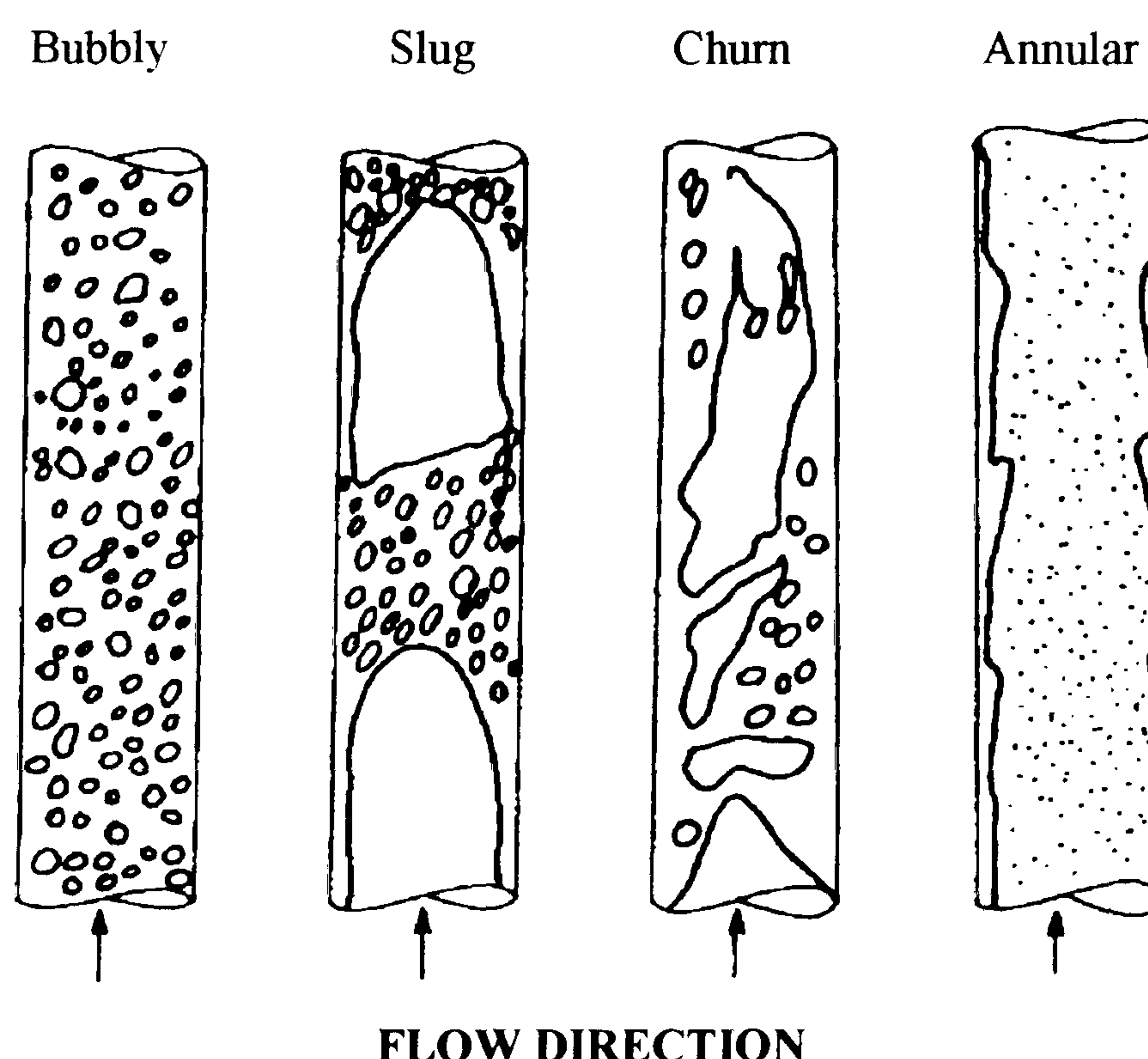


Figure 1-1: The major flow patterns observed during two-phase vertical upflow

*Bubbly Flow:* the gas phase is uniformly distributed as non-uniform sized bubbles in a continuous liquid phase. The bubbles travel with a complex motion and may be seen to coalesce.

*Slug Flow:* most of the gas travels upwards in large bullet-shaped bubbles that have a similar diameter as that of the pipe. These bubbles are often referred to as “Taylor bubbles” and between them and the pipe wall a thin liquid film is seen to flow

downwards, as the Taylor bubble rises. In the wake of the Taylor bubble the liquid often contains a dispersion of much smaller bubbles. This flow regime is sometimes referred to as plug flow.

*Churn Flow:* at higher gas velocities the Taylor bubbles in slug flow break down and the motion of the liquid becomes less predictable and more oscillatory. In general the flow pattern is more chaotic, frothy and disordered than either slug or bubbly flow. This flow pattern covers a wide range of flow rates.

*Annular Flow:* this flow is characterised by part of the liquid travelling as a thin film on the channel walls with the gas forming a continuous core along the centre of the pipe. The remainder of the liquid is entrained as fast moving liquid droplets within the gas core. These droplets may be deposited later back into the liquid film on the pipe walls.

### **1.2.2 Horizontal Flow in Pipes**

Unlike vertical upflow, in co-current two-phase horizontal flow, gravity acts perpendicular to the direction of motion. This causes the two phases to be dispersed in a different manner, generally with the denser liquid phase flowing along the bottom of the pipe. The major flow patterns can be seen in Figure 1-2 and are described below.

*Bubbly flow:* this flow pattern is similar to the equivalent pattern in vertical upflow and consists of gas bubbles dispersed within a liquid continuum. However, gravity tends to force the bubbles to accumulate at the top of the pipe except at very high liquid velocities when turbulence is enough to disperse the bubbles about the entire pipe cross section.



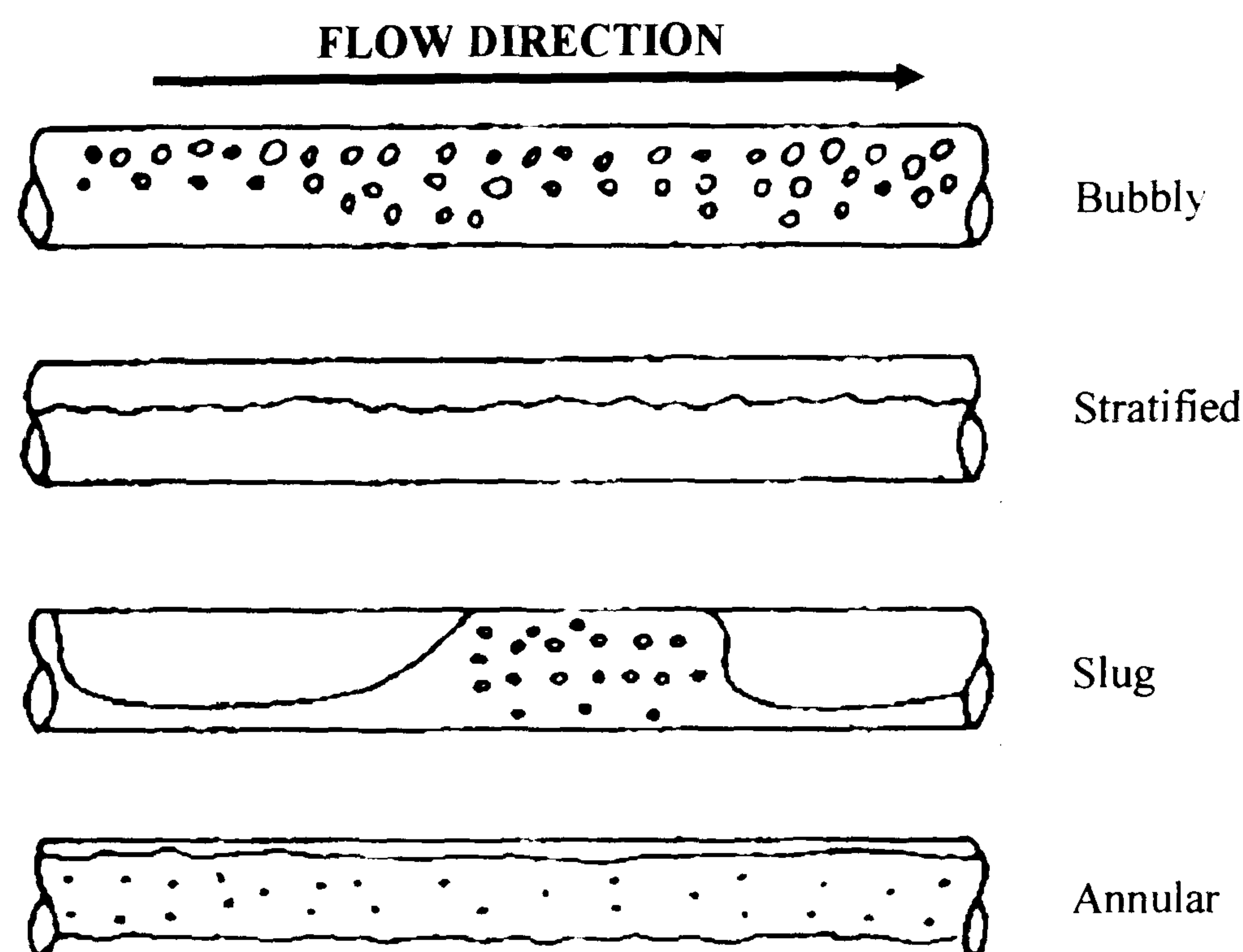


**Figure 1-2: The major flow regimes observed during horizontal two-phase flow**

*Stratified flow:* here the liquid flows as a continuous layer in the lower section of the pipe and the gas flows above it in a separated layer. The interface may be smooth. At higher gas velocities waves are caused at the liquid interface and this may be described as *stratified wavy flow*.

*Slug Flow:* as for vertical upflow, this is an intermittent flow pattern. The gas travels as large gas pockets in the upper section of the pipe separated by liquid slugs. The slugs may contain smaller gas bubbles.

*Annular Flow:* as with the equivalent pattern in vertical flow, the liquid flows as a thin film on the pipe walls and the gas as a continuous core which may contain liquid droplets. Gravity causes the liquid film to be thicker at the bottom of the pipe but, as the gas velocity is increased, the film becomes circumferentially more uniform.

### ***1.3 Predicting Horizontal Two-Phase Flow Patterns***

When designing a section of pipeline or piece of equipment it is necessary to know how the two phases are flowing together, as the different flow patterns can have serious design implications. For example, slug flow can cause vibration damage if a piece of equipment is continually hit by a slug of liquid and then a gas pocket and is therefore best avoided. On the other hand, the large number of dispersed gas bubbles within bubbly flow gives the stream a large mass transfer area and is therefore beneficial to induce in certain situations.

Detecting which flow pattern is present by visual observation is very subjective. If clear observation is not possible then high-speed photography can be used, however, this technique can only be employed in limited situations. Barnea and Taitel (1985) describe various instrumental techniques (conductance probes, hot wire probes,  $\gamma$ -ray densitometer) for measuring void fractions or pressure fluctuations of the two-phase flow. By comparison with an idealised response the flow pattern may be detected.

The drawback of both visual and instrumental techniques for determining which flow pattern is present is that they cannot be used in the design stage of a process plant and this may lead to the formation of undesirable flow patterns. Through experimental investigations, it was discovered that flow patterns and their boundaries could be mapped onto a two-dimensional plot. These plots became known as flow pattern maps and can be used to predict the flow regime under specific conditions.

Flow pattern maps are useful tools but the results are not foolproof due to the subjectivity of the determination of the flow pattern, especially around the transition boundaries, and the limited range of data used for making the maps. The pipe diameter and inclination, system pressures and the properties of the two fluids flowing together all have a great effect, further indication that one map may predict different results compared to the observed flow pattern and suggests that two-dimensional plots are not adequate enough for exact predictions of flow regimes. They have however

---



been accepted by the industry and still remain the only method of predicting two-phase flow regimes.

One of the oldest and perhaps the most widely used, especially within the petroleum industry, is the flow pattern map created by Baker (1954). Based on industrially relevant data, the map was created by visually determining the different flow regimes. A later map by Eaton *et al.* (1967) used two-phase dimensionless correlations but for ease of use Mandhane *et al.* (1974) mapped relatively accurately a large bank of data from various sources using superficial gas and liquid velocities as co-ordinates. Taitel and Dukler (1976) used a more rigorous theoretical approach based around the stratified flow regime. Starting from a one dimensional momentum balance on each phase for stratified flow, they analysed the conditions for transition between five basic flow regimes – stratified, stratified-wavy, slug, annular and bubbly. They approached the problem by visualizing a stratified liquid and then determining the mechanism by which a change from stratified flow can be expected to occur, as well as the flow pattern that can be expected to result from the change. The fact that stratified flow may not actually exist is not important, since it is well established that the existence of a specific flow pattern at specified gas and liquid flowrates is independent of how they arrived at that state. This methodology could also be applied to slightly inclined flows. From the mechanistic modelling of Taitel and Dukler a flow pattern map was devised that can help predict two-phase flow patterns for a wide variety of system conditions. Hence, using their methodology a flow pattern map was created for the horizontal 0.127m diameter pipe used within the current investigations. Figure 1-3 shows the flow pattern map for the experimental facility operated at atmospheric pressure at various inlet air and water superficial velocities.

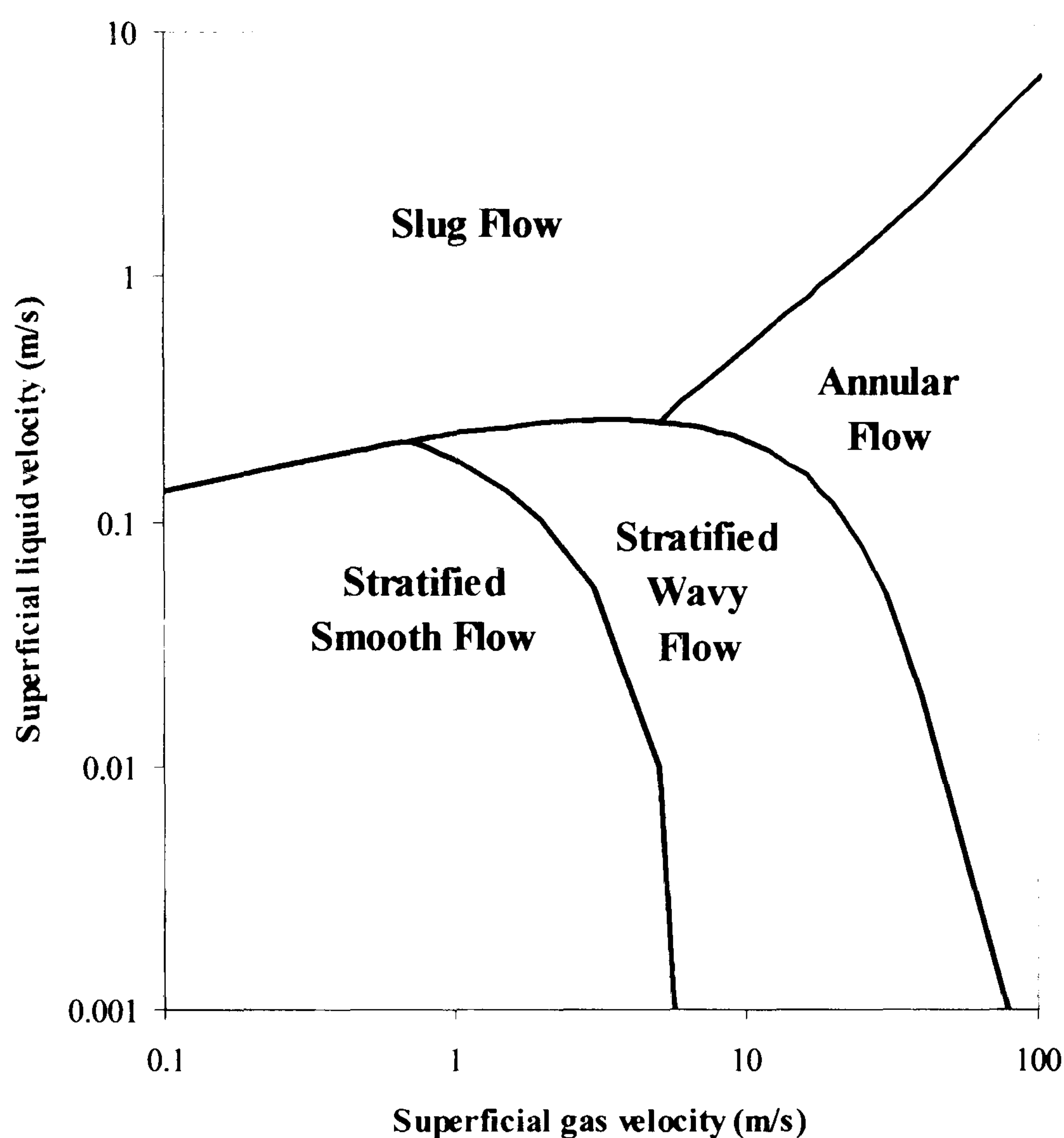


**Figure 1-3: Horizontal flow pattern map for the experimental facility based on the methodology of Taitel and Dukler (1976)**

## ***1.4 Separating Two-Phase Flows***

The brief introduction to two-phase gas-liquid flows in the previous sections has shown that they can be complex, difficult to predict and therefore difficult to process. Within industrial settings, gas-liquid separators are very common since the separation of the phases helps prevent equipment corrosion, yield loss, damage or malfunction, and the transportation of single phase streams is safer, more efficient and economical. A vast amount of technical information is available for various designs from the separation of liquid droplets from a gas stream to the removal of gas and water from crude oil during production.



Traditionally, the Petroleum Industry has relied heavily on conventional vessel-type separation technology, which has changed little over the years, to separate out the crude oil from the multiphase mixture that is produced from the well-head. Traditional separators must be sized to allow adequate time for the immiscible gas, oil and water phases to separate by gravity and to provide sufficient volume in the gas space to accommodate the rise and fall in liquid level that result from production surges. This makes gravity separators bulky, heavy and expensive in both capital and operating costs. These limitations are felt most severely during off-shore developments, where platform costs are continually escalating as remaining oil fields become more inaccessible. Moreover, bulky gravity separators contain a large inventory of highly flammable material which the Cullen report on the Piper Alpha disaster recommended should be minimised.

The growing costs of off-shore drilling, the need to exploit smaller, marginal oil fields and tightening safety regulations have motivated the Petroleum Industry to explore the development and application of alternative separator technologies. The Gas Liquid Cylindrical Cyclone (GLCC) represents one such example of a simple, compact, low-cost, small inventory separator. Davies and Watson (1979) showed that the easy operation and significant reduction in size, and therefore cost, of such separators was promising. The hesitation from industry came from the lack of available knowledge about optimum design and performance of GLCCs plus the limitation of existing mathematical models to single phase flows with a low concentration of the second dispersed phase. Industry may be conservative but research has continued to provide cheaper, safer alternatives to the bulky gravity separator.

Research has indicated that a cheap alternative may be a simple pipe junction. It has been shown that gas-liquid flows can be divided at pipe junctions in such a manner that there is a partial separation of the phases. The result is two streams – one richer in gas than the initial feed and the other richer in liquid. If the phases can be separated, albeit partially, at a simple pipe junction then the need for a large separator is diminished. Within this thesis the use of a simple junction is considered as a

---



continuous, compact, economical partial phase separator with a minimal inventory for use within the oil industry.

#### **1.4.1 Introducing junctions and two-phase flow**

The need to separate gas-liquid flows is paramount and junctions are a necessary configuration in a pipe network. Together and in the right combination a simple solution may be found to one of industries' largest capital costs – separating gas-liquid flows. The following sections explore this possibility and the ideas are expanded on and developed in the rest of this thesis.

There are many variations of junction that exist but the simplest is where two pipes meet at right angles to one another and this is termed a “T-junction”. For single-phase flows sufficient knowledge is available allowing engineers to perform adequate design calculations to predict the flow split and thus design efficient downstream equipment. In the case of two-phase flow the number of variables is much larger and is complicated by the constant mixing and separating of the phases. The presence of dividing junctions creates further problems as either phase could pass preferentially into the branch.

The division of the two-phase flow at a T-junction can be considered from two points of view. The first is as a simple flow divider where equal amounts of the approaching flow are divided between the two outlets. The second considers the junction to act as a partial phase separator. This is where a gas rich and a liquid rich stream are produced from a multiphase inlet flow. Being able to predict the behaviour of gas-liquid flows at junctions is a necessary part of efficient plant operation. Since the split of multiphase flows at T-junctions is a complex issue, relying on many more variables than single phase flow splitting, an in-depth study has been performed here to further increase our knowledge and understanding in an attempt to predict phase split accurately.



Without understanding such phenomena, equipment downstream of the junction can be over/under designed and its efficiency reduced. For example, Figure 1-4 shows the isometric pipe layout for an industrial plant in Kuwait\*. The contents of a low pressure separator are fed into two storage tanks. It was soon noted both tanks had to cope with severe slugging conditions and that Tank 1 was continually full whilst Tank 2 was under utilised.

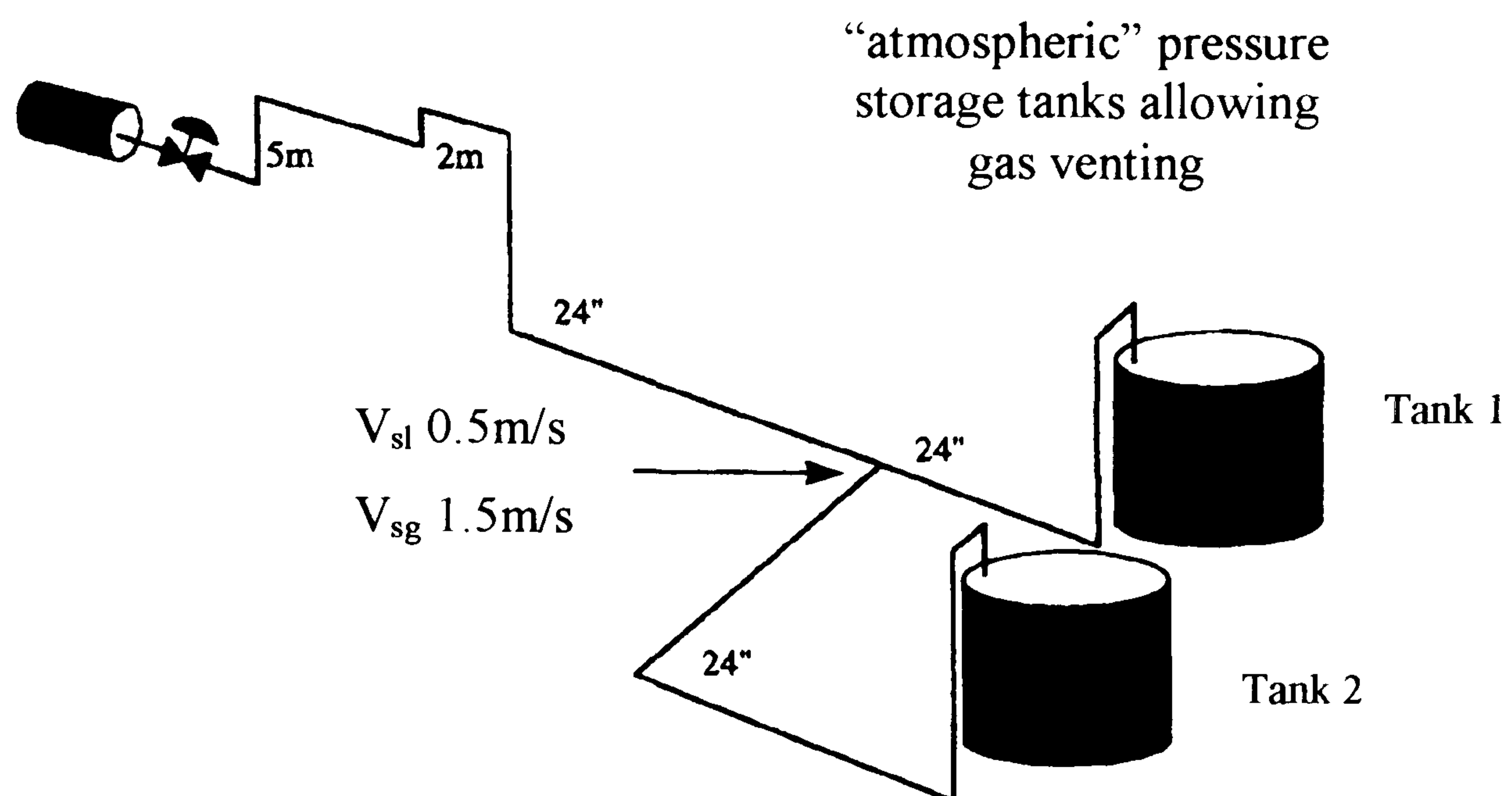


**Figure 1-4: Industrial separation of two-phase flow into storage tanks**

Both of these problems were due to the layout of the pipework. The asymmetric split of the flow at the T-junction was due to the difference in downstream resistances, the flow path to Tank 1 is far straighter and therefore provides an easier route to the storage tank. The slugging was induced within the system by having both pipelines ending in a riser to the storage tanks.

This example highlights that by not understanding how the two-phase flow present is affected by a simple T-junction or risers, can lead to poor equipment efficiency. Changing the geometry of the pipework after the T-junction so that it was identical leading to both tanks solved the problem. This ensured that an even split was obtained and both tanks were efficiently used. The rerouting of the pipework also

---

\* Case study highlighted at the BP Amoco "Multiphase Flow Course", Aberdeen, September 1999

avoided the need for a riser and thus the vibration problems associated with slugging were diminished.

In the above example, the T-junction was used to divide the flow between the two storage tanks; conversely, two well-known examples of where phase separation at a junction has been encouraged are given by Fryar (1980) and Oranje (1983). Fryar was one of the first to publish a paper on the use of T-junctions as partial phase separators. A horizontal main pipe with a vertically downwards branch arm was used to separate out the liquid from a two-phase stream. The liquid exiting down the branch was collected in a separator type arrangement to allow any steam drawn down to be removed and returned to the main pipe. Oranje noted some gas stations were receiving large amount of condensate whilst others received none at all. By reproducing the results within the laboratory he managed to create some “rules of thumb” for predicting the phase split at T-junctions. These were, however, limited by strict boundary conditions but the beginnings of predicting phase split at T-junctions prompted further research in the area. Both authors highlight that the continuous separation of two-phase mixtures is dependent on how the two phases are travelling together in the pipe and the downstream geometry of the system.

Having highlighted the main areas of concern when a two-phase flow approaches a junction, namely T-junction orientation and approaching flow pattern, the research presented in this thesis aims to increase knowledge in these areas in the following ways:

1. by placing a T-junction in large diameter pipework to act as a partial phase separator
2. using different T-junction geometries to draw off a gas or liquid rich stream from the approaching air-water two-phase flow
3. considering minor modifications of the junction to enhance the phase split



Additionally, the main objectives of this research are to:

1. examine the viability of a simple T-junction as a partial phase separator
2. improve phase separation by minor modifications of the T-junction
3. improve existing knowledge on the phase split at a T-junction with a downwards sidearm and to predict the phase split at such junctions

Having introduced the topic of two-phase flows and how they react at T-junctions, the complexity of the problem is described in more detail in Chapter 2. The flow facility used and how it was modified to accommodate the different T-junction orientations is described within Chapter 3. Chapter 4 considers the phase split results for the various side arm orientations with stratified and annular flow approaching the junction. Chapter 5 looks at the benefits of adding inserts at the junction and Chapter 6 considers whether two T-junctions in series improves the phase split over a single junction. Chapter 7 considers how the phase split at junctions may be predicted and presents a method for calculating the phase separation at a junction with a horizontal main pipe and vertically downwards side arm. All these ideas are summarised in Chapter 8, which provides final overview with conclusions and areas of investigation for future work.

## CHAPTER 2

### **T-Junctions and Two-Phase Flow**

As mentioned in Chapter 1, the division of two-phase flow at a T-junction can be considered from two differing viewpoints. The first considers the effects and problems caused to downstream equipment because of the uneven flow split that can occur at a T-junction. The second looks at the T-junction as a partial phase separator, which is the main motivation behind the research in this thesis.

Trying to utilise the natural, uneven distribution of the phases at a T-junction, so that the device acts as a partial separator, is not a new idea but one that has been expanded on during recent years. The size of the T-junction is its main advantage over conventional separators. Having a much smaller footprint, compared with a gravity separator or a GLCC, it lends itself to be installed where space is at a premium, for example on an off-shore platform. Performing a crude separation at a T-junction, placed either on the sea bed or on the platform itself, before the flow enters the main separator could mean that the majority of the gas could already be drawn off thus reducing the separator's load. Reducing its loading would have the knock-on effect of minimising the area it requires on the platform and hence allowing it to be significantly cheaper to build and instal. A second use, where the size could play an important role, is in the handling of flammable fluids. T-junctions have a naturally low inventory making them ideal to use when handling and separating highly flammable fluids although caution would have to be exercised as the reduced inventory may be off-set by the system being more difficult to control.



## **2.1 The “Simple” T-junction**

The T-junction may be the simplest coupling together of two sections of pipe but there are many physical factors and dominant forces that affect how the two-phase flow approaching the junction may be divided between the outlets.

### **2.1.1 Dominant forces around a T-junction**

At a T-junction it can be considered that there are three dominate forces controlling the phase split:

1. *Gravity.* The effect of gravitational acceleration acts predominantly on the liquid phase and can either promote liquid displacement down the branch arm, when it is orientated in a downwards direction, or help reduce liquid drawn off, when the branch arm is vertically upwards.

2. *Inertia.* The higher axial momentum flux of the liquid phase tends to force the liquid to continue flowing along the pipe, bypassing the entrance to the branch arm. This effect can be more pronounced when the diameter of the branch arm is smaller than the main run pipe. The liquid will pass the smaller opening quicker and thus have less time to be affected by any draw off effects.

3. *Pressure.* Pressure drop at the T-junction when the branch arm has a smaller diameter is larger compared to a T-junction where all branches are the same diameter. For the same gas fraction intake into the smaller branch arm, the gas velocity increases significantly and hence, by Bernoulli, creates a larger pressure drop. This in turn draws liquid into the branch arm.

### 2.1.2 Associated variables with a T-junction

The geometrical properties of the T-junction can affect the flow split as well as the properties of the fluid flowing in the pipe. Such parameters include the diameters of the inlet, run and branch arms; the inclination angles of the main pipe and side arm; the angle of the junction and the radius of curvature where the branch arm meets the main pipe.

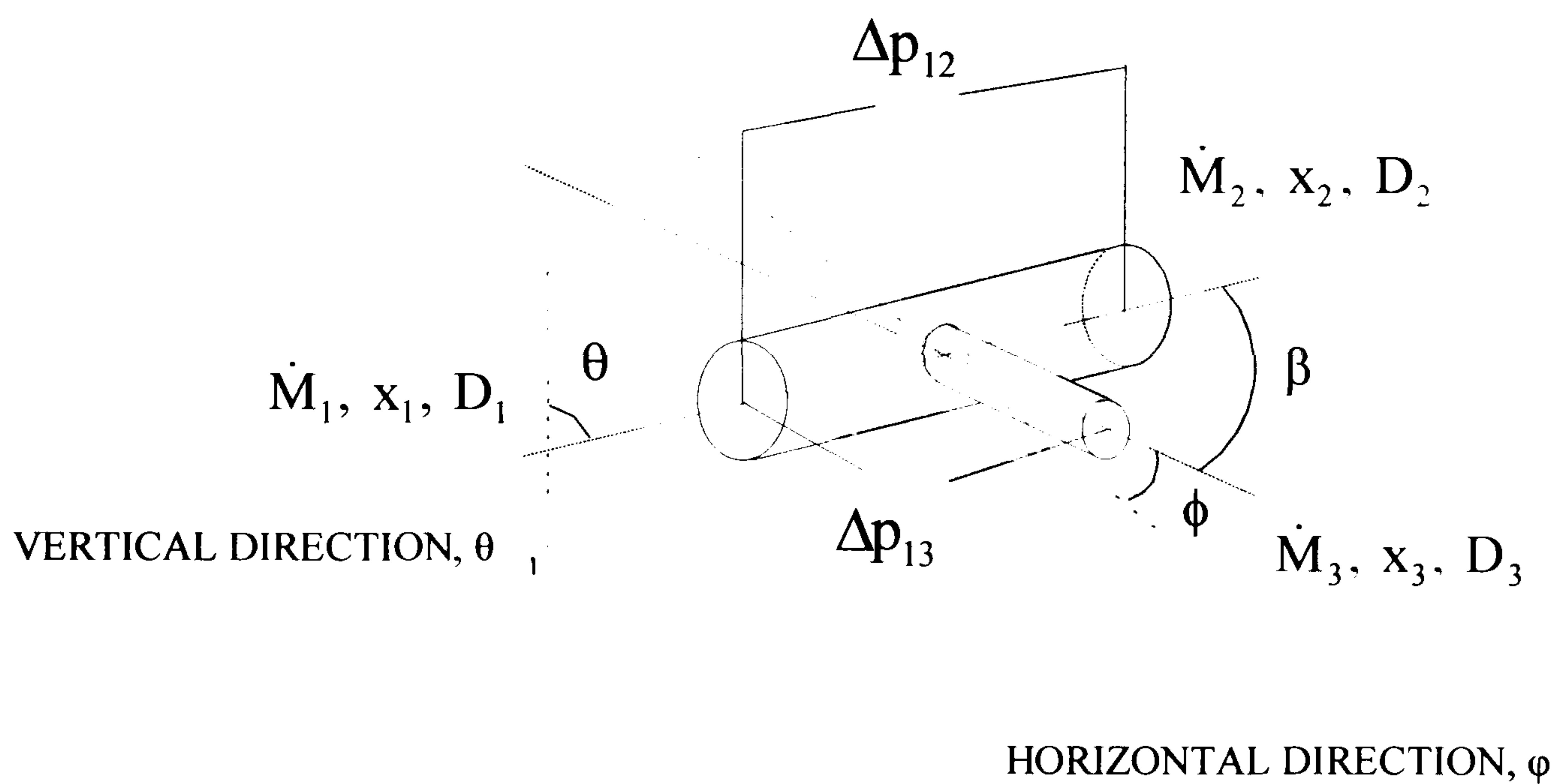


**Figure 2-1: A typical T-junction and the parameters associated with it**

Figure 2-1 shows there are many variables beyond the physical geometry of the T-junction that must be considered when trying to predict what is likely to happen for a given flow pattern approaching the junction. The geometry includes the angles associated with the junction – the angle of the main pipe from the horizontal ( $\theta$ ); the angle of the branch arm from the main pipe (if  $\beta$  is  $90^\circ$  the junction is classed as a T-junction) and the orientation of the branch arm, whether it lies in the horizontal plane ( $\phi = 0^\circ$ ), vertically upwards ( $\phi = +90^\circ$ ), vertically downwards ( $\phi = -90^\circ$ ) or at an angle in-between. There are eight other variables that also define the flow split - the mass flowrates of the gas and liquid,  $\dot{M}_1$ ,  $\dot{M}_2$  and  $\dot{M}_3$  plus the quality,  $x_1, x_2, x_3$  of



each arm of the junction and the two associated pressure drops,  $\Delta P_{12}$  and  $\Delta P_{13}$ . For all variables subscripts 1, 2 and 3 denote the inlet, run and branch arms respectively.

For a given pipeline, normally three of the above variables will be known thus leaving five unknown parameters, and five equations to be solved. Of the five unknown parameters, mass balances over the system and on either the gas or the liquid phase would provide two of the required equations. Energy or momentum balances for the branch and the run arms would provide two more and the remaining relationship is provided by the locus of the phase split at the junction, normally obtained by experimental observations. Trying to predict this equation has stimulated extensive research into the phase split at T-junctions.

### **2.1.3 Ways of representing phase split data**

Section 2.1.2 mentioned that in order to close the T-junction problem the locus of the phase split at the junction must be obtained and this traditionally has been arrived at by experimental methods. Chapter 7 describes various methods that try to predict the phase split at T-junctions through mathematical models but experimental data are still required for verification.

Conventionally, experimental observations used to obtain the locus of phase split have been plotted in one of two ways:

1. fraction of inlet liquid diverted down the branch arm,  $L'$  versus  $G'$ , fraction of inlet gas diverted down the branch arm
2. branch to inlet quality,  $x_3/x_1$  versus  $\dot{M}_3/\dot{M}_1$ , total mass flow fraction removed through the branch

Both methods have their merits but within this thesis all data has been plotted using the first method. Using this method Figure 2-2 shows the typical phase split for annular flow approaching a horizontal regular T-junction. The  $x = y$  line, between

---



points (0,0) and (1,1), represents the line of equal flow split between the two branch arms of the junction. If the junction acts as a flow divider and the locus falls along this line and the quality of both branch arms will be the same and identical to that of the inlet flow. Points lying to the left side of the  $x = y$  line indicate liquid dominated flow down the branch arm compared to inlet flow. Points lying to the right of the diagonal represent gas dominated flow within the branch arm. Complete vapour and liquid extraction are represented by the straight lines  $G' = 1$  and  $L' = 1$  respectively.

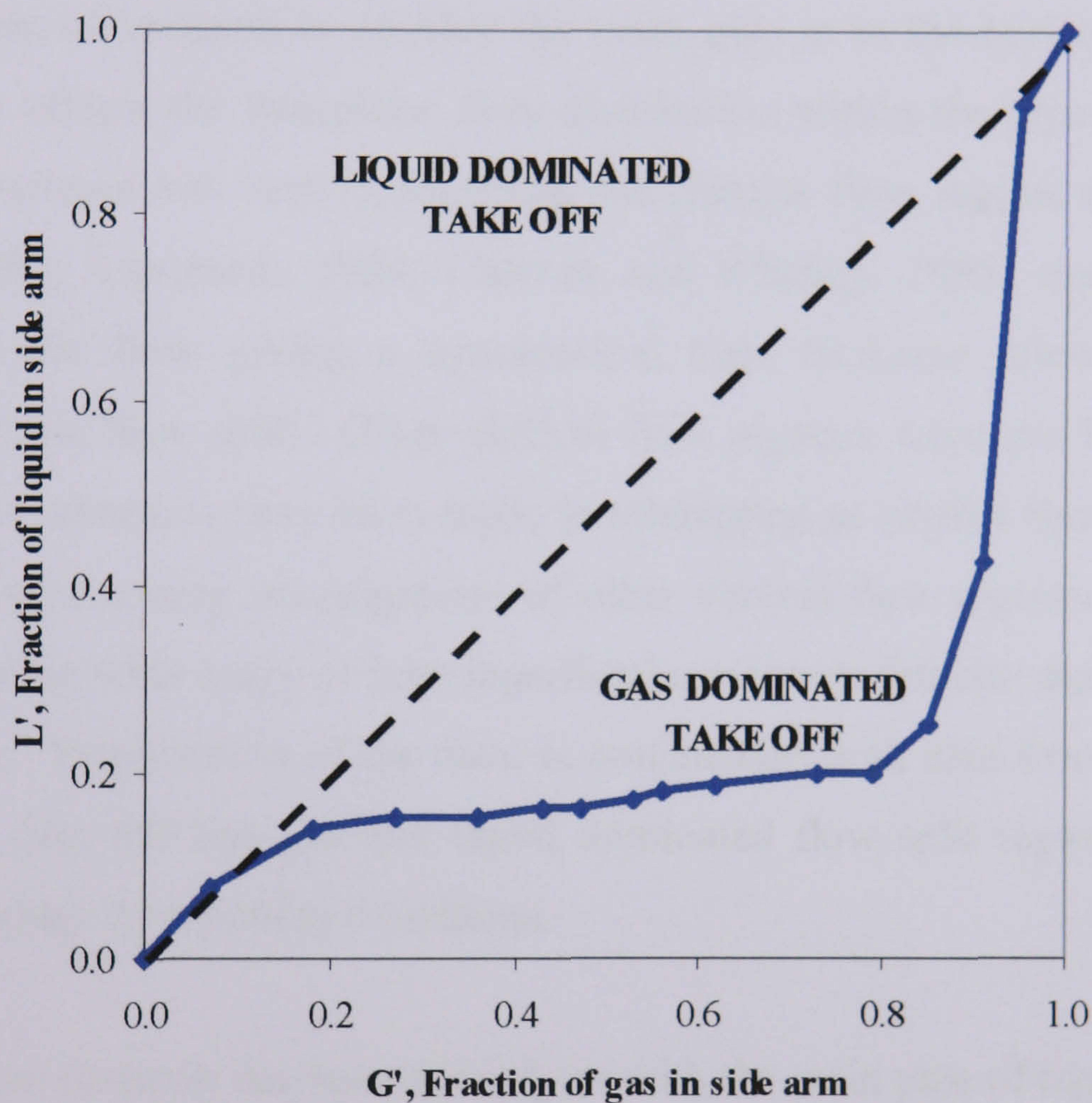


**Figure 2-2: Phase split representation for annular flow at a horizontal regular T-Junction**

Overall, this method is particularly useful for showing at a glance the flow behaviour of the junction. Over the years, much effort has been put into trying to understand how this locus is affected by inlet flow regime, up and down stream pipe geometry, junction geometry and inlet quality.



## **2.2 Geometrical effects on Flow Split at a T-Junction**

Chapter 1 indicated the various flow patterns associated with two-phase flow and Figure 2-1 highlighted the many variables associated with a T-junction thus highlighting the difficulty of being able to predict the phase separation as such flows pass a T-junction. The problem has therefore been tackled from many different perspectives over the years and many findings published. The chief distinction that separates areas of research is whether the main pipe is in the horizontal or vertical plane as this affects the two-phase flow distribution within the pipe. Most data in vertical T-junctions has been collected in the annular flow regime (Azzopardi and Whalley, 1982; Azzopardi, 1984; Charron and Whalley, 1995) since gravity acts evenly over the flow giving a symmetrical film thickness allowing successful modelling of the flow split. Other vertical flow regimes have not been studied as rigorously but advances have been made in attempting to predict flow split. One of the more comprehensive investigations of other vertical flow regimes was by Conte (2000) where the wide range of inlet superficial conditions fell into the slug and churn flow patterns. Examination of the data, in conjunction with data from other authors, showed that data fell into gas and liquid dominated flow split regions that did not coincide with any flow pattern transitions.

More extensive research has been carried out with the main pipe of the junction in the horizontal plane. Much of the research concentrates in the annular and stratified regimes although slug flow has been investigated due to its detrimental effects on equipment. Kolnes and Asheim (1990) proposed placing a T-junction with a vertically upwards branch arm in the main pipeline on the seabed. Their idea was to produce a separator that could cope with terrain induced slugs hence diminishing the need for expensive on-shore slug catchers. This idea was extended by Katsaounis *et al.* (1997) whose dynamic separator systems would also avoid the presence of slugging within multiphase pipelines. However, to date none of these proposed T-junction separators have been installed within the field. This could be because the separation performance of T-junctions is known to be so dependent on inlet flow

regime that as the oil field grows older the three phase oil/water/gas flow that passes through the system will change in ratio and thus alter the separation characteristics of the T-junction.

Given the technical difficulties involved, oil companies tend to stick to tried and tested equipment. However, a break through for T-junction technology has recently occurred. A T-junction is now being used as a partial phase separator at BP/Amoco Chemicals, Hull. They were finding that only part of the liquid product from a reactor was flashed to vapour on passing through a valve before reaching a distillation column. Within the column the liquid was being carried upwards with the vapour, reducing the column efficiency. The standard solution would be to install a conventional separator, allowing the remaining liquid and vapour to be fed into different points of the column, not only is this expensive but time consuming and awkward with the plant already operational. With the present knowledge of phase split across T-junctions it was thought that this would provide the perfect solution for this type of problem. Azzopardi *et al.* (2001) examined the possibility and proposed the geometric arrangement shown in Figure 2-3.

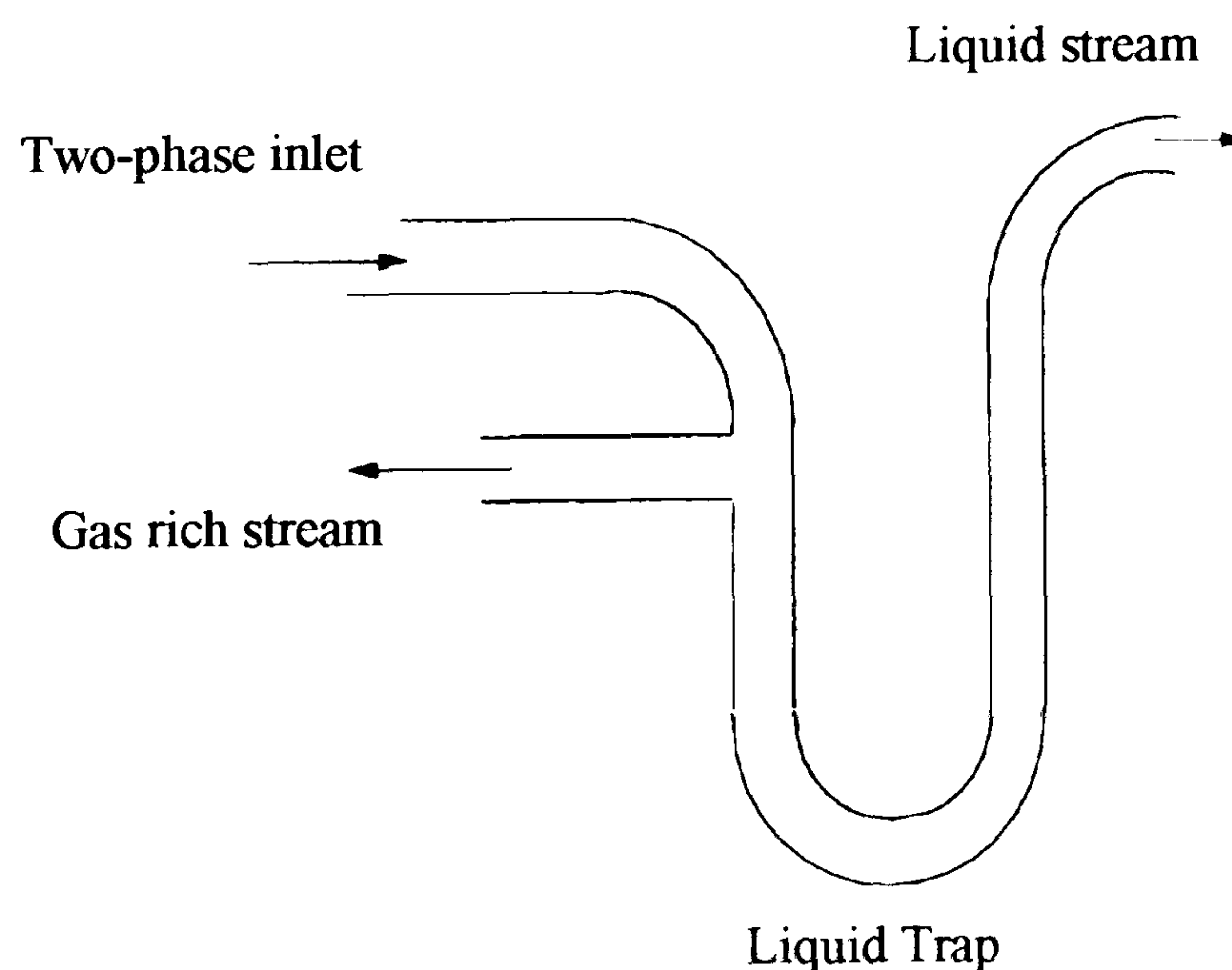


**Figure 2-3: The geometric arrangement proposed, utilising a T-junction as a partial phase separator, Azzopardi *et al.* (2001)**



The two-phase flow enters the arrangement and as it passes round the first bend the liquid droplets, entrained within the gas, hit the far wall. The liquid falls as a film downwards, collecting within the U-bend, forcing the “cleaner” gas to leave down the branch arm of the T-junction. Thus the simple pipe arrangement, centred around a T-junction, acts as a partial phase separator drawing off a gas rich stream and leaving a liquid rich stream. This proposed geometrical arrangement has since been installed and found to be a fully operational with sufficient separation of the liquid from the vapour stream allowing the gas rich and liquid rich streams to enter more appropriate points in the column. Efficiency has been restored at very little cost or inconvenience so maybe T-junctions will be considered as a serious alternative to the conventional separator in the future.

The effectiveness of the partial phase separation occurring at the T-junction arrangement described above may motivate other companies to apply T-junction technology to their problems hence there is a very real need for the continued research on the phase split at T-junctions. This thesis goes some way to further knowledge by investigating the effects on phase separation at T-junctions with different physical geometries including side arm diameter, side arm orientation and modification of the junction itself. As there has been much research investigating the many aspects that can affect phase split at a junction only relevant literature will be cited here. A number of comprehensive reviews covering all aspects of T-junctions and phase separation have been published, notably by Lahey (1987), Muller and Reinman (1991), Azzopardi and Hervieu (1994) and Azzopardi (1999).

### **2.2.1 Effect of main pipe orientation**

As described briefly at the beginning of this chapter, research can be divided into two main groups depending on the orientation of the main pipeline – horizontal T-junctions and vertical T-junctions. Due to the difference in influence of gravity on the two phases with orientation, phase separation at the junction is altered and thus they

are treated independently. All experimental investigations performed for this thesis considered the main pipeline lying horizontally.

Several authors have, however, noted that the orientation of the main pipe seems not to exert a strong influence on the phase redistribution at the junction. Seeger *et al.* (1986) as well as Hwang *et al.* (1988) mentioned that the phase split data taken for a horizontal T-junction by Saba and Lahey (1984) closely follows that of Honan and Lahey (1981) taken using a vertical T-junction. Several examples can also be found within the data amassed by the UKAEA (Harwell) laboratories. Figure 2-4 compares the data for four similar runs, two with the main pipe vertically and two with the main pipe lying horizontally. As can be seen the data in all cases shows a near identical split. The vertical T-junction data was published by Hewitt *et al.* (1990) following the horizontal T-junction data by Azzopardi *et al.* (1988). Conditions for each of the four cases are given in Table 2-1.

More dramatic effects on phase split can be achieved, however, by reducing the diameter of the side arm compared to that of the main pipe or by altering the orientation of the side arm by a few degrees up or down from the horizontal. These are taken in turn and their effects on phase split are described in sections 2.2.2 and 2.2.3 respectively.



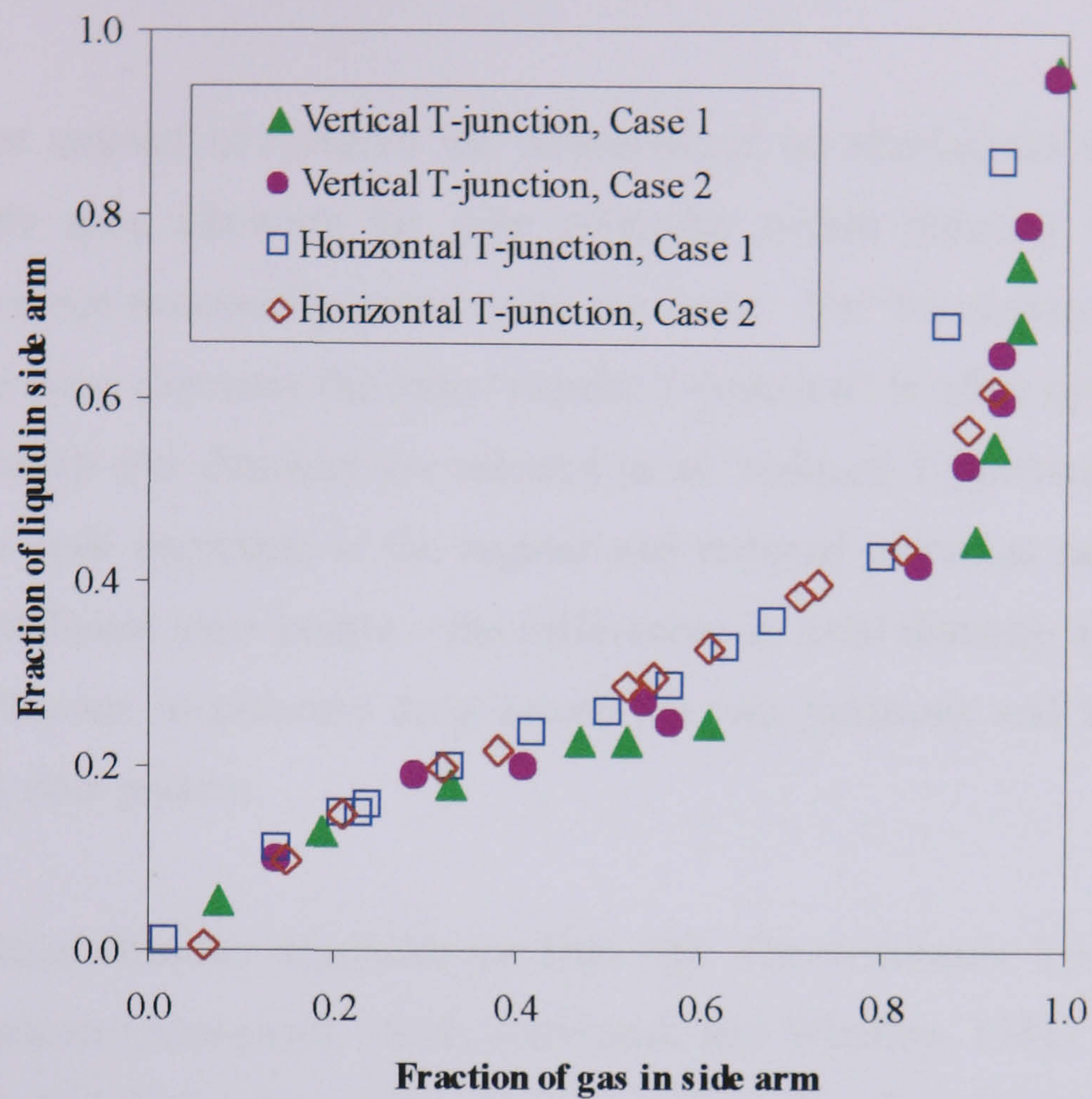


Figure 2-4: Comparing the phase split of a vertical and a horizontal T-junction, UKAEA (Harwell)

Table 2-1: Inlet conditions referring to the UKAEA (Harwell) data in Figure 2-4

Data	$U_{gs}$ (kg/s)	$U_{ls}$ (kg/s)	System Pressure Bar
Vertical T-junction - Case 1	0.0117	1.23	3.7
Vertical T-junction – Case 2	0.0117	1.23	4.4
Horizontal T-junction – Case 1	0.044	0.062	3
Horizontal T-junction – Case 2	0.050	0.076	3



### **2.2.2 Effects of altering the side arm diameter**

A significant amount of research has concentrated on altering the diameter ratio of main to side arm, allowing for pipe networks within industry where pipework diameters are not necessarily going to be the same. For T-junctions where all three arms are the same diameter the term “regular T-junction” is often applied; those with a smaller branch arm diameter are referred to as “reduced T-junctions”. Differences in the phase split occurring at the regular and reduced junctions can be considered from three different view points – the differences in axial distance available for take off; the difference in pressure drop across the two junctions and the effect of the approaching flow pattern.

1. *Axial Distance Available for Take Off.* The systematic look at the effect of sidearm diameter (Azzopardi, 1984; Azzopardi and Whalley, 1982) for a vertical T-junction concluded that there was an obvious but not always a clean cut trend of diameter ratio. A systematic variation with diameter ratio was observed with the larger the diameter ratio the greater the take off, see Figure 2-5.

This is not unexpected, since the larger the side arm diameter the longer the axial distance available for gas take off. For smaller side arm diameters much of the liquid film that is dragged towards the side arm by the gas being removed may only arrive at the side wall after passing the opening of the side arm. Hence, the reduced fraction of liquid take off observed.



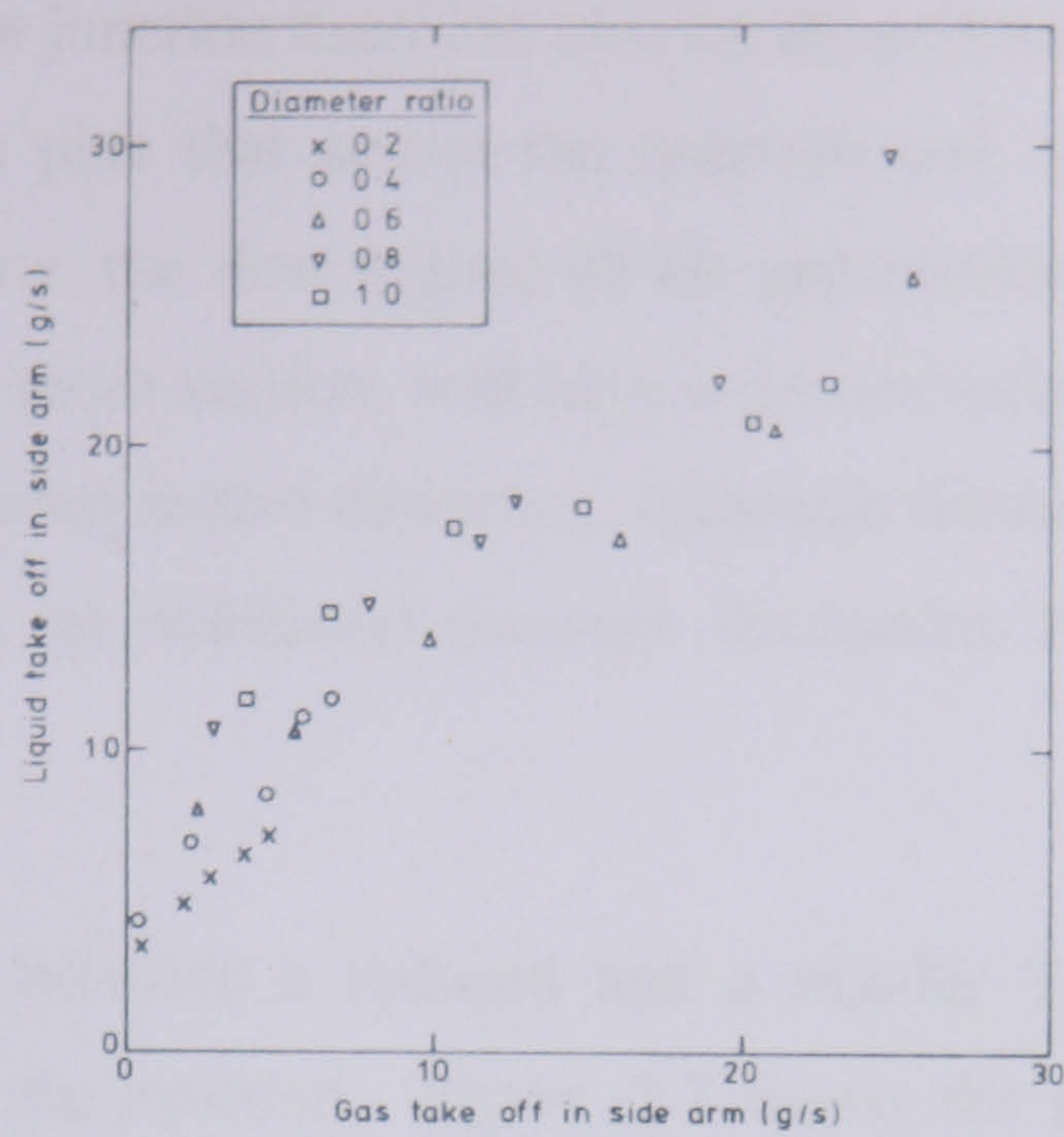


Figure 2-5: Effect of diameter ratio on phase split, Azzopardi (1984)

Such qualitative results can be confirmed by looking at the results of Lahey (1987). Consider the geometry of a regular T-junction and a dividing 45° Y-junction, see Figure 2-6. For the same main pipe to side arm diameter ratio the axial distance covered by the entrance to the Y-junction is 1.4 times longer than that for the regular T-junction. Hence, the liquid phase, which normally has a higher axial inertia than the vapour phase, has more time to be influenced to change direction and so be drawn off down the side arm.

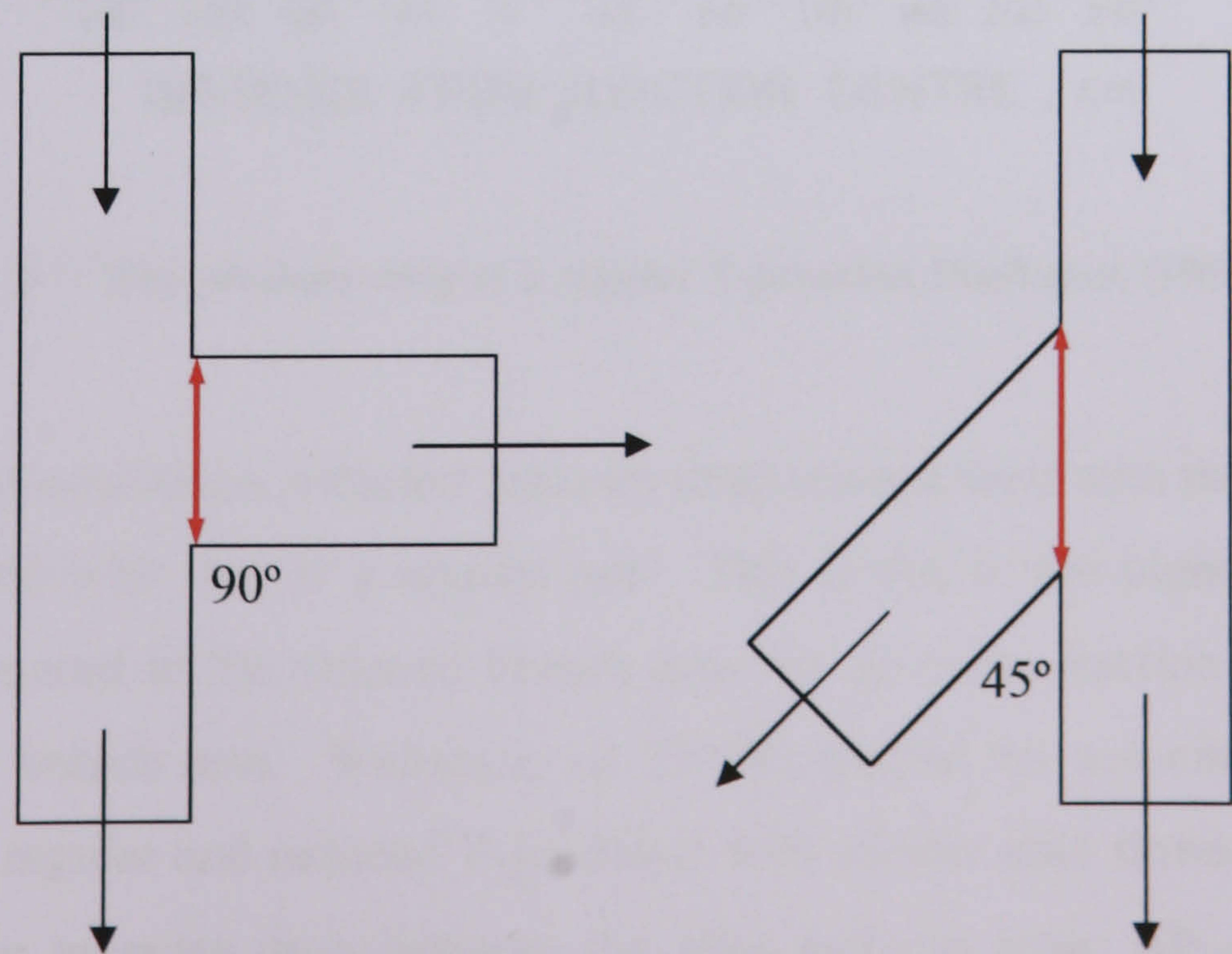


Figure 2-6: Dividing T- and 45° Y-junctions



2. *Pressure Drop.* The division of the phases at T-junctions depends not only on the geometry of the junction itself but also on the pressures of the pipework in the two downstream legs plus that across the junction and, as already mentioned but explained further below, the flow regime of the approaching fluids. The outlet with the lower pressure, or more suction, will have a greater influence on the passing fluid thus more will be diverted in that direction. Although friction, fixtures and fittings all cause pressure drops, an additional pressure fluctuation is experienced across the junction itself.

The main difference between a reduced and a regular T-junction is the pressure redistribution around the junction. Figure 2-7 shows the pressure drops associated with a regular 37.6mm (i.d) T-junction measured by Buell *et al.* (1994).

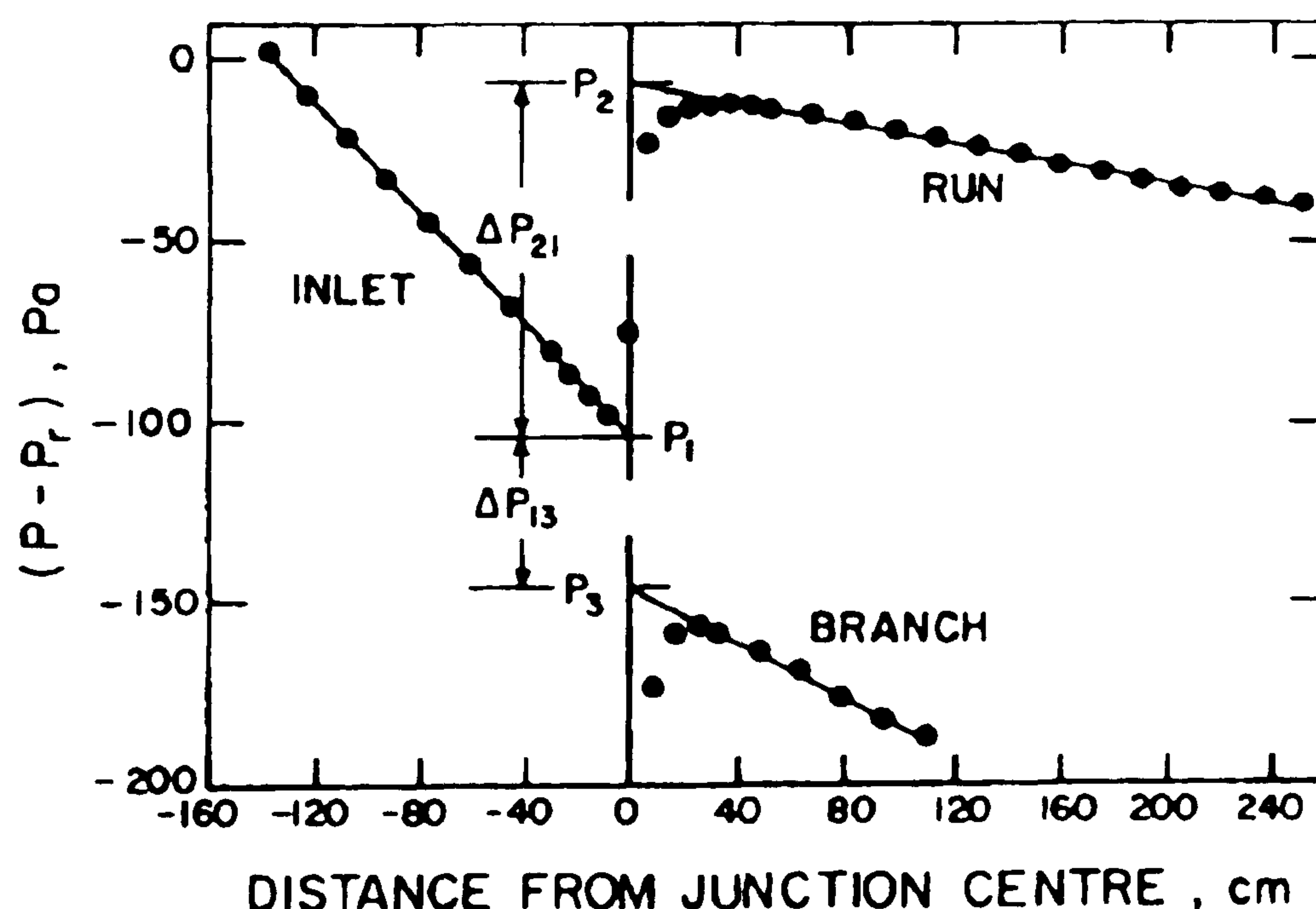


Figure 2-7: The pressure drop at a regular T-junction, Buell *et al.* (1994)

For the same inlet conditions, a higher pressure drop is associated with the reduced T-junction compared with that of a regular one. This is due to the higher gas phase velocities encountered in the reduced branch arm for the same fraction of inlet gas drawn down the branch arm. Walters *et al.* (1998) studied the associated pressure drops for both a regular and reduced T-junctions with similar inlet flows. As shown in Figure 2-8 the pressure drop between the inlet and run arms,  $\Delta P_{12}$  is minimal whether across a regular or reduced T-junction. Conversely, and as expected, the



pressure drop between the inlet and the branch arm,  $\Delta P_{13}$  increases significantly with decreasing side arm ratio.

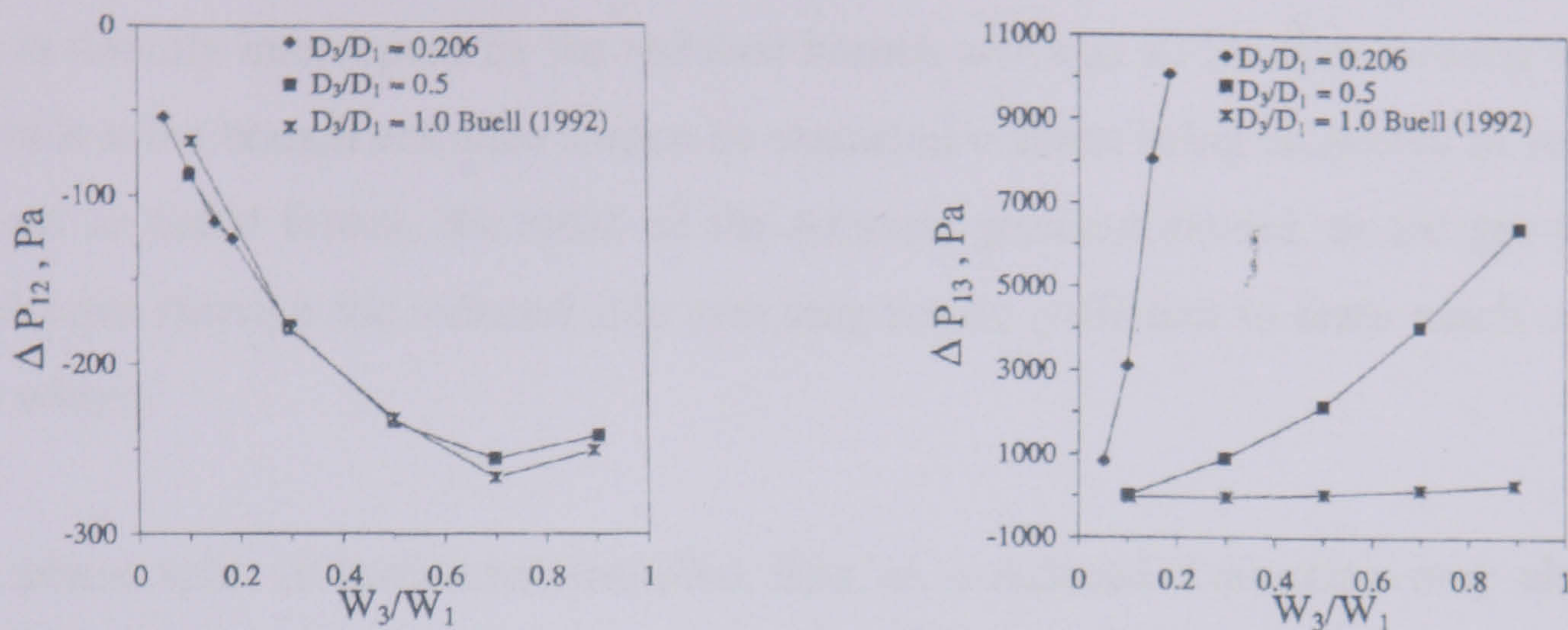


Figure 2-8: Pressure drop across a regular and reduced T-junction, Walters *et al.* (1988)

This pressure drop can be related to the effects of Bernoulli's equation. For example, if the branch-to-inlet diameter ratio is 2:1, the gas velocity in the reduced branch arm increases fourfold for the same fraction of gas to be diverted. This acceleration of the gas goes some way in overcoming the axial momentum of the liquid phase and thus it draws more liquid into the branch arm for the same fraction of gas drawn off which is often the case of the reduced T-junction.

3. *Approaching Flow Pattern.* Effects of inlet superficial velocities of both phases have been methodically investigated in tests (Domanski *et al.*, 1987; Azzopardi *et al.*, 1988; Reimann *et al.*, 1988; Shoham *et al.*, 1989; Peng *et al.*, 1998 and Walters *et al.*, 1998) covering a wide range of inlet flow regimes. Shoham *et al.* (1989) extended their earlier work using a regular T-junction and low liquid holdup flow patterns, namely stratified smooth, stratified wavy and annular flow, by comparison with a reduced T-junction. For the reduced T-junction, the fraction of gas removed increased for the same fraction of liquid drawn off. This can be related to the reduced axial distance of the smaller side arm available for gas and liquid take off



into the branch and hence the larger pull required by the gas to overcome the inertia forces of the liquid, especially for stratified flow. For annular flow conditions, the effect of the reduced side arm is diminished since centripetal forces dominate liquid take off as the liquid phase flows as an asymmetrical film around the pipe wall. Less film is directly intercepted by the reduced branch arm and so the film flowing above and below the branch entrance cannot be extracted without being subjected to vertical as well as radial forces, the result of the pressure gradient caused, as the gas phase accelerates through the reduced side arm may not be sufficient to draw much of this film with it.

The phase split of horizontal stratified flow in a reduced T-junction may also be affected by the elevation difference between the bottom of the main pipe wall and the branch arm opening. This may also explain the reduced fraction of liquid entering the side arm since the liquid phase will have to “climb” up into it before being drawn off. However, as noted by Shoham *et al.* (1989), even at low inlet liquid flowrates, corresponding to lower liquid levels in the pipe, a larger proportion of the inlet liquid is drawn off than at higher inlet liquid flowrates. The lower inertia forces occurring at lower liquid flowrates must therefore override the significance of the “jump” into the raised branch arm and hence allow the liquid phase to be drawn off with ease. Shoham *et al.* (1989) extended their previous model for a regular T-junction to incorporate reduced side arm junctions with reasonable agreement with their data. The steam-water data by Peng *et al.* (1998) exhibited similar results. An enhanced phase split was observed with the reduced T-junction branch to inlet diameter ratio of 0.33 in this case, and characterised by higher branch qualities for all flow split ratios. The effects of increasing inlet vapour flow rates were similar for a regular T-junction and are described in detail by Peng *et al.* (1998).

Both Ballyk *et al.* (1991) and Azzopardi *et al.* (1988) show that for some inlet conditions, the effect of reducing the branch arm diameter becomes less pronounced. However, Walters *et al.* (1998) found that with a very small side arm diameter ratio of 0.2 the fractional liquid take off was greater than for a diameter ratio of 0.5. This was confined to higher values of gas take off ( $>0.5$ ). Ballyk *et al.* (1991) compared diameter ratios of 1, 0.82 and 0.5 using steam-water annular flow. They discovered

---



that the data obtained for the two reduced T-junction experiments were closer to each other than 0.82 ratio was to the regular T-junction. This was attributed to the loss of liquid film removal from the bottom of the pipe by direct extraction being greater for the initial reduction in branch to inlet ratios and this becoming less pronounced as this ratio was reduced. In addition, for the gas take off, as the side arm diameter is reduced the branching acceleration, and hence the velocity of the gas phase, must increase for the same fraction of gas to be removed, enhancing carry over mechanisms (reduced pressure drop and entrainment) off-setting the reduction in liquid film removal by direct extraction. Azzopardi *et al.* (1988) state that under certain circumstances gas take off may be unaffected by diameter ratio. They attributed this observation to a phenomenon they described as “break point” which is similar to “film stop” described by Azzopardi (1988) for annular flow. It was noted that the slope of the phase split curve sharply increased at higher gas take off, causing more liquid to be taken off from this point than expected. The break point was seen to decrease as inlet gas flowrate decreases since, for annular flow at lower gas flowrates the liquid film is seen to increase in depth and the thicker, slower moving film is more susceptible to take off. A similar finding was found with stratified flow (Azzopardi *et al.* 1990) where, beyond a critical gas take off, a sharp increase in gradient of the phase split curve can be seen, but this critical gas take off limit seems not to depend strongly on diameter ratio. A comparison was made with their data, which covered both annular and stratified flow regimes, with previously published models and this clearly highlighted, once more, the importance of considering inlet flow regime as the comparisons with models were restricted to those for a specific flow regime. The data of Shoham *et al.* (1987) also exhibits similar trends.

Published data, which deals with the effect of varying the side arm diameter are listed in Table 2-2. From this experimental data base, it can be seen that research thus far has been confined to small main pipe diameters and predominantly air/water, steam/water low pressure systems. As our understanding of the physical actions of either phase at the junction slowly increases perhaps confidence will enable research to expand into broader, more industrially relevant conditions.



Table 2-2: Previous work where the effect of diameter ratio has been studied

Source	Main pipe diameter (m)	Main pipe orientation	Diameter Ratio	Flow patterns studied
Azzopardi & Whalley (1982) Azzopardi (1984)	0.032	Vertical	0.2 0.4 0.6 0.8 1.0	Annular
Shoham <i>et al.</i> (1987,1989)	0.051	Horizontal	0.5 1.0	Annular Stratified
Reimann <i>et al.</i> (1988)	0.05	Horizontal	0.084 0.2 0.52 1.0	Annular Stratified Slug
Azzopardi <i>et al.</i> (1988, 1990)	0.026	Horizontal	0.333 0.667 1.0	Annular
Ballyk <i>et al.</i> (1991)	0.038	Horizontal	0.5 0.82 1.0	Annular Stratified
Buell <i>et al.</i> (1994) Waters <i>et al.</i> (1998)	0.038	Horizontal	0.2 0.5 1.0	Annular Stratified
Penmatcha <i>et al.</i> (1996) Marti & Shoham (1997)	0.05	Horizontal	0.5 1.0	Stratified
Peng <i>et al.</i> (1998)	0.076	Horizontal	0.333 1.0	Stratified

### 2.2.3 Effect of branch arm orientation

Gravity forces have a strong effect on the flow split especially as the orientation of the branch arm is altered. More liquid is drawn into the side arm when it is inclined downwards. Conversely, for upward inclinations a significant amount of the inlet gas has to be diverted up the side arm before any of the liquid is drawn off. Once the liquid has started to flow up the branch arm, only a little extra gas has to be diverted to draw up all of the liquid. At inclinations over  $30^\circ$  upwards, nearly all of the gas has to be drawn up the side arm before any liquid flows up the branch arm.

Most researchers who have investigated phase split at reduced diameter T-junctions have also investigated the effect of side arm orientation. This has helped to increase the database of knowledge currently available for systematic changes on the same



experimental equipment. For ease of reference an inclination angle of  $0^\circ$  represents all branches in the horizontal plane. Positive inclination angles indicate the branch arm being raised upwards to a maximum of  $+90^\circ$ , vertically upwards. Negative inclination angles represent downward movement of the branch arm to  $-90^\circ$ , vertically downwards.

One of the first researchers to investigate the observations of Oranje (1983), who initially noted the uneven split of gas condensate at T-junctions as mentioned in Chapter 1, was Hong (1978). For the relatively small T-junction used in the investigation, as predicted, the orientation of the side arm significantly affected the fraction of liquid entering the branch arm. With the side arm straight up,  $+90^\circ$ , the liquid stream tended to split almost evenly with the gas. Moving the side arm towards  $-90^\circ$  increased the fraction of liquid take off, increasing to total take off when more than 40% of the gas entered the side arm. Similar results were obtained by Penmatcha *et al.* (1996) who stated for their stratified-wavy system branch arm inclinations lower than  $-60^\circ$  resulted in total removal of the liquid phase through the branch arm. Results from a reduced T-junction, used in the same experimental facility under similar conditions, by Marti and Shoham (1997) clearly indicate that a reduced T-junction significantly alters gas and liquid take off rates with less gas being drawn down the side arm for the same fraction of liquid take off as the side arm was rotated downwards. This is due to the accelerated gas velocities in the reduced T-junction forcing a greater proportion of the liquid phase to be drawn off its axial course and down the side arm. Liquid removal would become easier with increasing downward orientation of the branch arm, gravity forces also forcing more liquid into the branch arm. However, at very low gas fraction intakes, less liquid is diverted for reduced T-junctions than for regular T-junctions as the pressure drop at the T-junction, due to increased gas velocity in the reduced diameter side arm, is not yet significant enough to compensate for the dominating axial inertia forces within the liquid phase. A mechanistic model was developed and expanded with relatively good agreement between the theoretical and experimental results.

Seeger *et al.* (1986) noted the influence inlet flow pattern had on the amount of liquid drawn into the vertically downwards side arm of a regular T-junction. For low gas

---



take off the range over which only liquid enters the branch arm increases the more stratified the inlet flow pattern is. If the inlet superficial liquid velocity is kept constant and the inlet gas superficial velocity is raised, as explained in Chapter 1, the flow pattern changes to a more homogenous type of flow where gravity has little influence, i.e. dispersed bubble and annular flow at high velocities. The increased momentum fluxes of both phases have more of a pronounced effect on phase split than if gas superficial velocity is kept constant and liquid superficial velocity is increased.

Unlike Seeger *et al.* (1986), Peng *et al.* (1998) confined their study to increasing gas and liquid superficial velocities within the stratified-wavy regime. For their steam-water system comparisons were drawn between a regular and reduced T-junction with a vertically downwards ( $-90^\circ$ ) side arm. The onset of vapour extraction was found to occur at liquid flow split ratios above 40%, compared with Marti and Shoham (1997) who considered their reduced T-junction to act as a phase separator at an inclination of  $-60^\circ$ . Peng *et al.* (1998) defended their findings by considering that before the vapour can be extracted it must first be pulled through the layer of liquid flowing along the bottom of the pipe. The faster the inlet superficial vapour velocity, the thinner the liquid layer and the lower the flow split ratio at the onset of vapour pull through.

The effect of branch orientation with annular flow was found to have a significant effect on phase split, as was changing the inlet quality due to its effects on film thickness (Peng *et al.*, 1996; Ballyk *et al.*, 1991).

For upward side arm inclinations, phase separation is quite distinct due to the fact that both gravity and inertia forces in the inlet and branch are acting in the same direction. This means any entrained liquid drops deposited on the pipe wall will fall as a film back towards the junction, creating vertical churn flow with corresponding pressure variations at the T-junction, making this orientation particularly hard to predict and hence model. Even very small inclination angles,  $<1^\circ$ , (Ottens *et al.*, 1999) have been found to reduce the initial fraction of liquid drawn up through the side arm.



A systematic investigation (Penmatcha *et al.*, 1996; Marti and Shoham, 1997) has shown that a significant amount of gas has to be diverted into the branch before any liquid is diverted. The closer the branch arm is orientated to the vertically upwards position the greater the fraction of gas that has to be diverted. However, once the liquid is flowing into the branch arm relatively little extra gas is required before all the liquid is diverted down the side arm. Reducing the side arm diameter diminishes the fraction of gas required to divert any liquid by about 20%. It can also be noted that phase split become independent of inlet liquid velocities indicating that the most important factors in determining the fraction of liquid taken off are the gas splitting ratios and the inclination angle of the side arm up from the horizontal. This phenomenon was also noted by Seeger *et al.* (1986) who found that good separation was achieved for all inlet flow patterns with the exception of dispersed bubble flow.

The effect of viscosity and inclination angle was investigated by Ottens *et al.* (1999) after the initial findings of Hong (1978). In both cases, it was shown that increasing liquid viscosity initially decreased the fraction of liquid taken off down the side arm for a constant fraction of gas diverted until around 70% of the liquid has been extracted. After this point, only a small increase in the fraction of gas drawn off causes a greater fraction of the liquid to be removed than for less viscous cases. Thus, care has to be taken when combining the two effects of liquid viscosity and branch arm inclination.

Whilst the majority of experimentalists have worked with small diameter pipework, two sets of experiments have been performed on more industrial sized equipment: Maciaszek and Micaelli (1988) and Mudde *et al.* (1993). Despite their large diameter pipework they noted a significant effect of downstream flow regime on phase split at the T-junction. Downstream geometry was considered to have a strong effect as the findings of Azzopardi and Smith (1992) confirm. Both sets of data for the large diameter pipes were compared with previously published models for smaller diameter pipes. General trends were observed but accurate predictions were only obtained with the model based on mass, energy and momentum balances presented by Maciaszek and Micaelli (1988).



Table 2-3 summarises previous work where T-junctions with inclined branch arms have been studied. As can be seen, a significant amount of research has combined the effects of reduced side arm diameter and side arm orientation.

**Table 2-3: Previous work where the effect of orientation has been studied**

Source	Main pipe diameter (m)	Diameter ratio	Branch orientation	Flow patterns studied
Fouda & Rhodes (1974)	0.051	0.5	+90	Annular
Hong (1978)	0.0095	1.0	0, $\pm(45, 90)$	Annular Stratified
Whalley & Azzopardi (1980)	0.032	0.4	0, $\pm(30, 60, 90)$	Annular
Seeger <i>et al.</i> (1986)	0.05	1.0	0, $\pm 90$	Annular Bubbly Slug
Maciaszek & Momponteil (1986)	0.135	0.15	0, $\pm 90$	Stratified
Katsaounis & Schultheiss (1985)	0.203	0.40	+90	Plug Slug Stratified
Reimann <i>et al.</i> (1988) Domanski <i>et al.</i> (1987)	0.05	1.0 0.52 0.2 0.084	0, $\pm 90$	Annular Stratified Slug
Ballyk <i>et al.</i> (1991) Peng <i>et al.</i> (1993)	0.0256	1.0	0, $-(45, 90)$	Annular
Hart <i>et al.</i> (1991) Ottens <i>et al.</i> (1999)	0.051	0.75 1.0	0, $+(0.25, 0.5)$	Stratified
Mudde <i>et al.</i> (1993)	0.23	0.43	+90	Stratified Bubbly
Penmatcha <i>et al.</i> (1996) Marti & Shoham (1997)	0.05	1.0 0.5	0, $+(1, 5, 10, 20, 35)$ $-(5, 10, 25, 40, 60)$	Stratified Stratified-wavy
Peng <i>et al.</i> (1998)	0.076	0.33	0, -90	Annular



#### **2.2.4 Effect of altering the physical dimensions of the T-junction**

Relatively little work has been published where the dimensions of the T-junction have been altered, either physically or by the addition of inserts or baffles. In both cases one of two objectives is aimed for: either to improve phase separation or to create a predictable flow divider.

The simplest modification was experimented with by Katsaounis and Schultheiss (1985). They used a large diameter main pipe (203mm) with a vertically upwards branch arm with initial diameter of 52mm widening to 82mm (over a length of 125mm). The effects on pressure drop of this “nose cone” were predominately investigated although for all flow patterns almost total separation of the gas into the branch arm was noted despite conventional flow split measurements not being taken. This modified T-junction formed the basis of the dynamic slug catcher proposed by Katsaounis *et al.* (1997).

Baffles being placed at a T-junction have been considered (Fouda and Rhodes, 1974; Azzopardi and Smith, 1992) and were thought to homogenise the flow sufficiently to produce an adequate flow divider, rather than phase separator. Fouda and Rhodes (1974) performed a complete set of experiments with two-phase annular flow through a horizontal T-junction with a vertical side arm to study the effects of baffles and homogenisers on downstream qualities. The baffles used were a quarter ( $\frac{1}{4}D$ ), half ( $\frac{1}{2}D$ ) and three-quarters ( $\frac{3}{4}D$ ) of the tube diameter in height and were placed off centre, at the base of the T-junction as indicated in Figure 2-9. They demonstrated that without a baffle present the two-phase flow split unevenly between the two outlets. However, it was only the presence of the largest baffle that significantly reduced this effect.



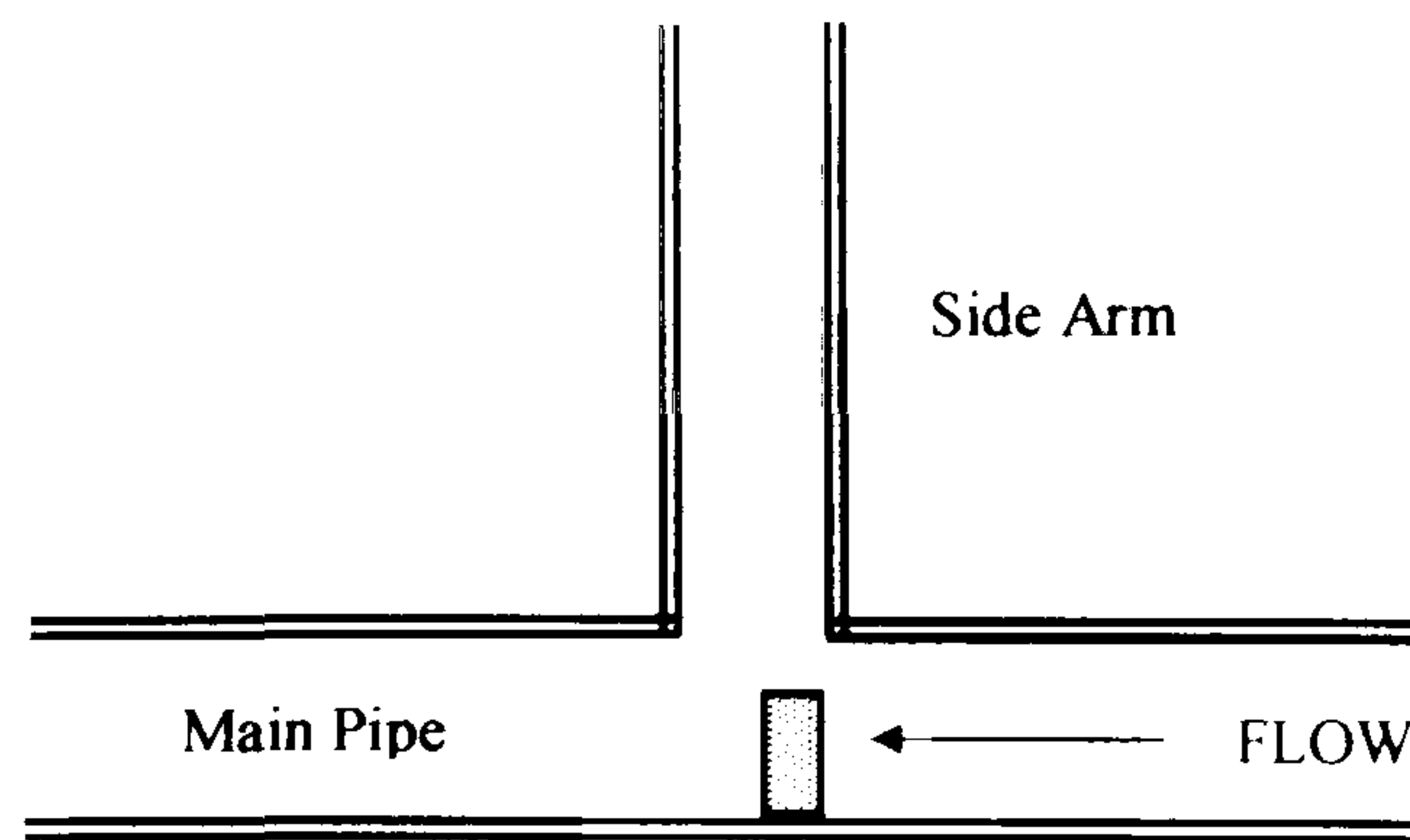


**Figure 2-9: Baffle positions of Fouda and Rhodes (1974)**

Comparable in effectiveness to the largest baffle was an homogenising orifice placed downstream of the T-junction. This idea was extended by Azzopardi and Smith (1992) who positioned a  $\frac{1}{2}D$  high baffle  $4.7D$  downstream of the T-junction. Unlike the orifice the baffle did not affect phase split when either annular or stratified flow approached the junction. A  $90^\circ$  bend, from the horizontal to vertically downwards, was also placed beyond the T-junction however; its presence only marginally increased the effectiveness of the phase split with stratified flow approaching the junction. For annular flow no difference was observed with the side arm in either the horizontal or vertically upwards position.

Butterworth (1980) reported limited tests on air-water two-phase flow through a modified horizontal T-junction. The T-junction was  $0.038 / 0.025\text{m}$  and the side arm had a piece of  $0.025\text{m}$  o.d. /  $0.022\text{m}$  i.d. tubing inserted into it with the end of it cut at an angle of  $45^\circ$ . The insert was made such that it could be turned thus allowing the orientation of the plane of the cut to be changed with respect to flow direction, see Figure 2-10.

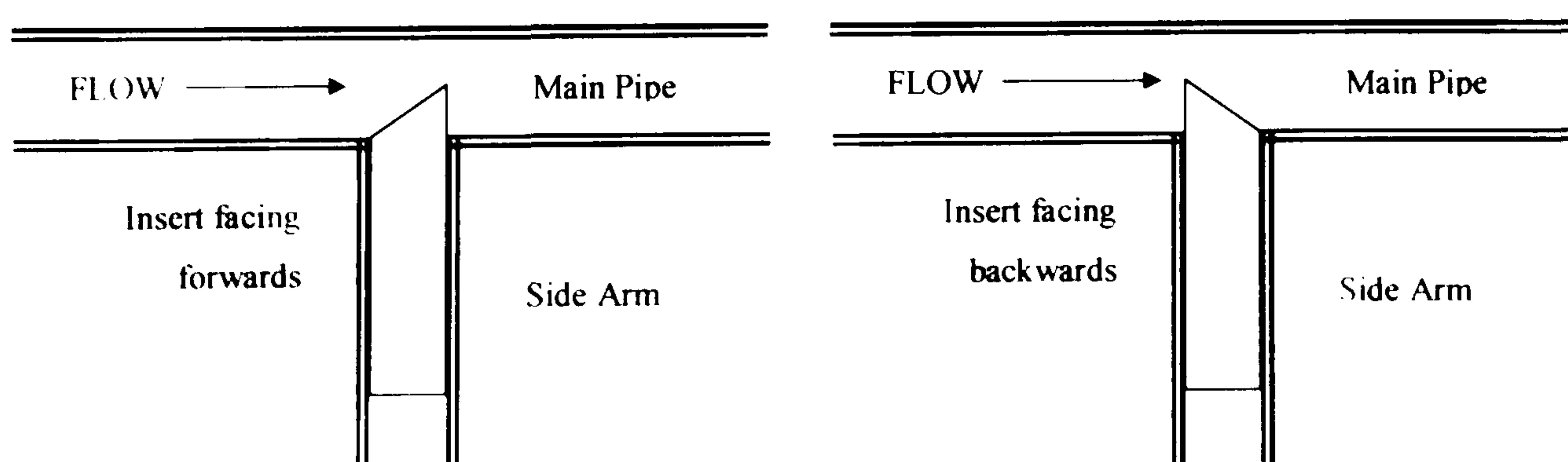


**Figure 2-10: Schematic diagram showing the insert positions used by Butterworth (1980)**



Results were compared with the insert facing forwards (scooped section facing direction of flow), with insert facing backwards (scooped section not facing direction of flow) and for a non-protruding case. Only three experiments were performed in the annular, wavy and stratified flow regimes.

For annular flow it was found that the forward facing insert decreased the maldistribution of the phases but increased flow division, compared to the split without any insert present, whilst the backwards facing insert increased the phase separation. In contrast, in wavy flow the forwards facing insert reduced the maldistribution at low gas take off but had very little effect at higher gas take off. The backwards facing insert had little effect. As these were the only experiments performed they raised more questions than they answered but as a first step at introducing inserts to modify phase split some interesting observations were noted. Some of the questions posed have been investigated further for a large diameter T-junction and the results can be seen in Chapter 5.

A summary of previous work where the physical dimensions of the T-junction have been altered can be seen in Table 2-4.

**Table 2-4: Previous work where the effect of altering the physical dimensions of the T-junction has been studied**

Source	Main pipe diameter (m)	T-junction modifications	Flow patterns studied
Fouda & Rhodes (1974)	0.051	$\frac{1}{4}D$ , $\frac{1}{2}D$ , $\frac{3}{4}D$ baffles placed at junction	Annular
Butterworth (1980)	0.038	45° rotational inserts protruding from side arm into main pipe	Annular Stratified
Katsaounis & Schultheiss (1985)	0.203	Widening of branch arm from 52mm to 82mm (in 125mm)	Plug Slug Stratified
Azzopardi & Smith (1992)	0.038	$\frac{1}{2}D$ baffle plus a 90° bend downstream of T-junction	Annular Stratified



### 2.2.5 T-junctions in alternative combinations

Manifolds, or junctions close together on a main pipe, have formed the bases of a limited number of earlier studies (Collier, 1976; Coney, 1980). Horizontal systems (Collier, 1976) were found to perform similarly to single junctions, with the gas being preferentially diverted with an accumulation of liquid in the exit pipe furthest away from the inlet. Vertical systems (Coney, 1980) behaved in a similar manner but under the conditions studied a plug of frothy liquid was seen to be oscillating in the main tube forcing liquid into the junctions adjacent to it.

Although the installation of manifolds is routine, the use of them as small, low inventory, economical to produce, easy to install phase separators has not been investigated thoroughly. One very recent report, Bevilacqua *et al.* (2000) has gone some way to address this.

Various “comb configurations”, simple T- and Y-junctions arranged with vertical side arms in ascending and descending orientations have been considered. The efficiency of each arrangement was considered as the number of vertical branches, their height and the liquid capacity was altered. The good separation characteristics of vertically orientated side arms and the positive effect of the number of junctions led to tests to optimise the geometrical configuration of the comb structure, see Figure 2-11.

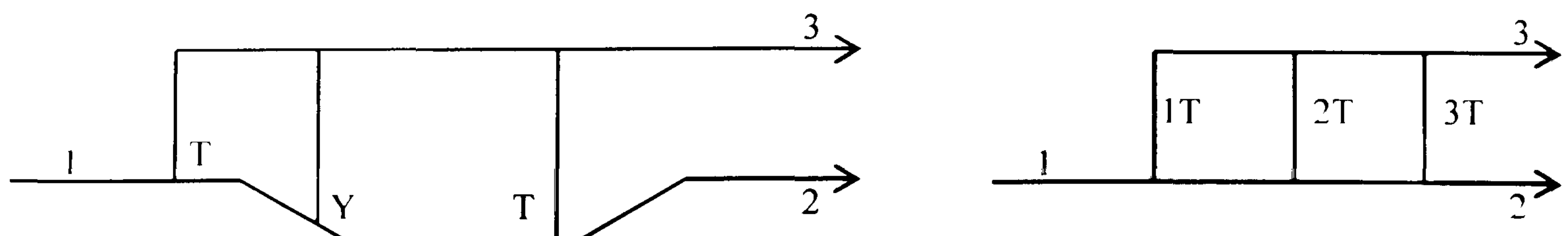


**Figure 2-11: T- and Y- configurations investigated by Beveilacqua *et al.* (2000)**



A comparison of the performance of the different configurations shows that the choice of the best configuration is closely linked to the separation performance required by the system. To guarantee high values of void fraction in the combined branch arm a combination of T- and Y-junctions proves to be most effective. Using three T-junctions together reduces the overall void fraction within the main run branch. Management of the system also has to be considered. As downstream pressures can significantly alter the phase separation characteristics of a T-junction reducing the pressure in the combined branch arm draws practically all the gas flow off, leaving a very liquid rich stream in the main pipeline, except at the highest flowrates investigated.

To date, investigations have dealt with manifolds with all branch arms lying in the same orientation. The effect on phase split of a vertically upwards branch arm followed by a vertically downwards branch arm have been investigated with a large diameter T-junction and the results can be seen in Chapter 6.



## **CHAPTER 3**

### **Experimental Arrangement**

Chapters 1 and 2 have introduced the complexities of gas-liquid two-phase flow and how it is divided at a T-junction. Experimental investigations were performed which investigate phase split in a regular 0.127m (i.d.) diameter T-junction and a reduced 0.076 / 0.127m T-junction. Large diameter pipework was used to bridge the gap between laboratory scale experiments and the actual pipe diameters used within industry. Air-water flows were investigated allowing easy comparison with previously published data with authors who have used much smaller diameter pipes, see Chapters 4, 5, 6 and 7.

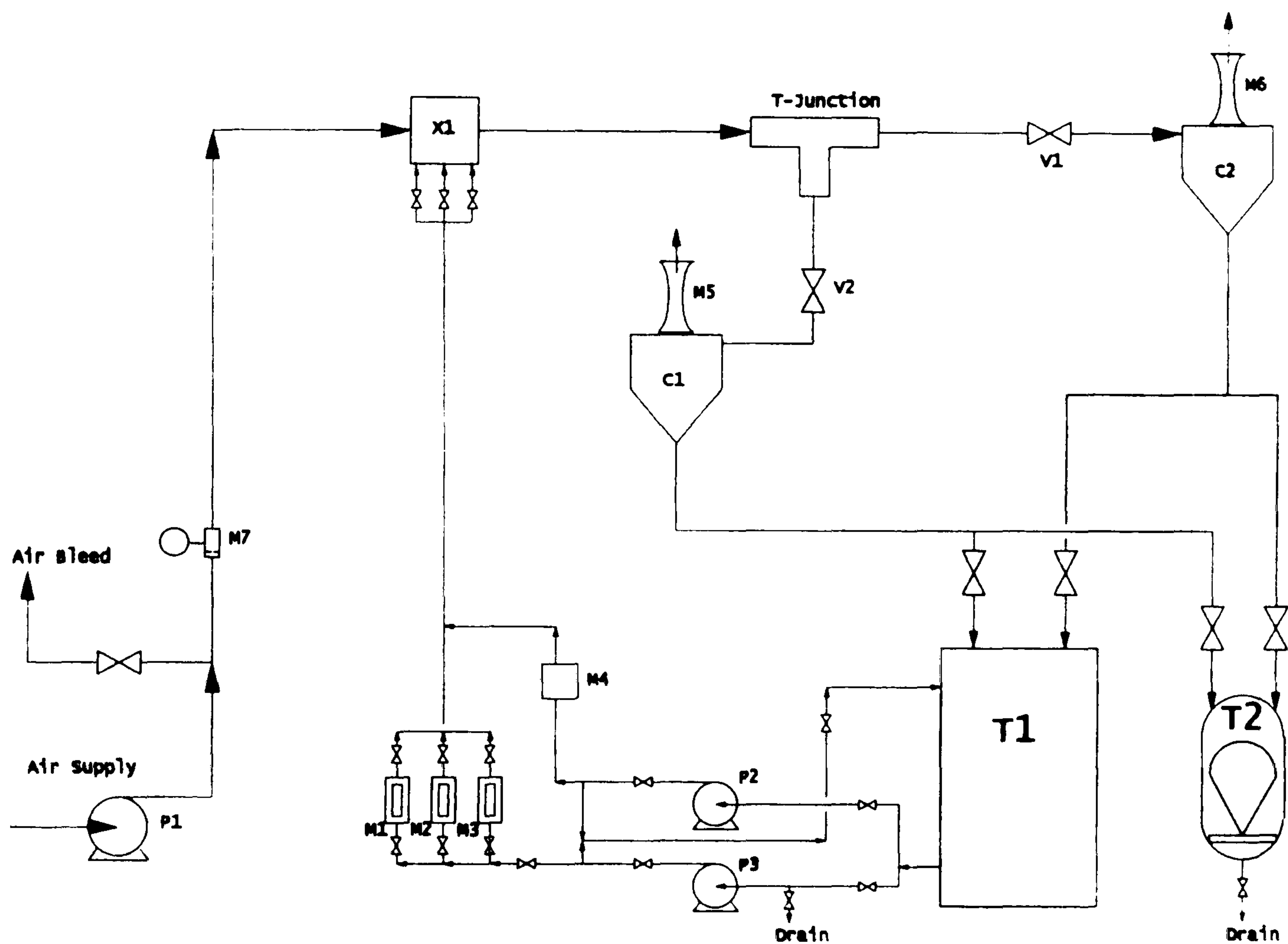
The side arms of both the 0.127m and reduced 0.076m junctions could be positioned horizontally ( $0^\circ$ ), vertically upwards ( $+90^\circ$ ) or vertically downwards ( $-90^\circ$ ). In addition, the influence of inserts at the junction, the effect of a U-bend placed on the down arm and the interaction of two junctions on the phase split were investigated. This chapter provides detailed descriptions of the apparatus used and the experimental procedure followed. The data resulting from all the experiments were used to determine the fraction of inlet gas and liquid entering the side arm. From these results the locus of phase split can be plotted on the  $G'$  vs  $L'$  graphs, as previously discussed in section 2.1.3. If this locus can be determined and then accurately predicted then the closure of the T-junction problem is complete.

### ***3.1 The Flow Facility***

The flow facility employed was a modified form of that used by Roberts (1995) and Rea (1998). It was initially configured to accommodate a 0.127m diameter T-junction where the side arm could be mounted either horizontally or vertically upwards.



Alterations were made allowing investigation of phase split at a T-junction with a reduced 0.076m side arm (with and without inserts) and with a vertically downwards side arm (with and without a U-bend). In addition further modification allowed two T-junctions placed in series at two set distances apart. A schematic flowsheet of the facility can be seen in Figure 3-1.



C1, C2	Air-water separating cyclones	P2, P3	Water pumps
M1, M2, M3	Bank of rotameters for low water flowrates	T1	Water storage tank
M4	Turbine meter for large water flowrates	T2	Water measuring tank on load cell
M5, M6	Venturi / orifice plate meters to measure exiting air flowrate	X1	Air-water mixing unit
M7	Orifice plate to measure inlet air flowrate	V1	Butterfly valve on run arm
P1	Air blower	V2	Butterfly valve on branch arm

Figure 3-1: Schematic flow diagram of the T-junction rig



In all experiments a centrifugal blower (P1) draws air from the laboratory, thus the air was at room temperature and at atmospheric pressure. The air flowrate is adjusted by use of an air bleed and measured further downstream by an orifice plate (M7). Different sized orifice plates (0.04m, 0.06m and 0.105m orifice diameter mounted in a 0.2m diameter pipe) could be used depending on the superficial air velocity required. All orifice plates used within this investigation were machined to the dimensions detailed in BS1042 and operated within the guidelines stated.

Water is drawn from the large storage tank (T1), which was constantly filled by mains tap water, by one of two centrifugal pumps (P2, P3) and the correct water flowrate is attained by bypassing part of the flow which allows a full range of flowrates to be achieved. For smaller flowrates the water is monitored by one of three calibrated rotameters (M1, M2, M3). For larger flowrates a turbine meter (M4) is used. The water then enters the main flow pipe via a porous wall mixing unit (X1). Prior to being mixed with the air the water is split into three so that it can be fed uniformly into the mixing section. The three pipes enter the mixing unit at equally spaced intervals around the circumference. The air, drawn from the blower, passes around an inverted U-bend just before it is mixed with the water. This is to reduce the risk of back pressure in the rig forcing water down the air line.

The T-junctions were placed 4m downstream of the mixer. There is a further 3.5m of 0.127m diameter run arm pipe at the end of which is a butterfly valve. Beyond the valve is a 120° bend leading to a cyclone, used to separate the air and water for measurement. All pipework downstream of the mixer are made of clear acrylic resin to aid visibility of the two-phase flow.

The air-water flow in the run arm is separated by a cyclone (C2). Either a calibrated venturi meter or orifice plates placed on top of the cyclone (M6) are used to measure the air flowrate as it is vented to the atmosphere. The venturi meter was calibrated by forcing all inlet air from the blower to exit via the venturi. With the butterfly valve in the run arm (V1) initially fully open, and the butterfly valve in the branch arm (V2) fully closed, the pressure drops across the orifice plate in the inlet stream, and across

---



the venturi, were measured in millimetres of water. The butterfly valve (V1) was systematically closed and the corresponding pressure drops measured. A calibration chart on inlet superficial velocity against the square root of the pressure drop across the venturi could be constructed to calculate the air flowrate exiting through the venturi. The venturi was initially calibrated using the density of air at atmospheric conditions. However, during experimentation the air would be fully saturated but the calculated difference between the two air densities was found to be negligible. The venturi meter was used to measure air flowrates above 15m/s; below this flowrate a suitable choice of orifice plate was made. The flowrate of water leaving the bottom of the cyclone was calculated by diverting it to a weigh tank (T2) on a calibrated load cell. A timed discharge could then be measured. When measurement was not required, the water was returned to the main feed tank. The load cell had an upper limit of 120kg and so at high water flowrates timed weighing could only be very short.

Two T-junctions have been used during this investigation. A “regular” T-junction with the main bore and side arm both 0.127m in diameter and a “reduced” T-junction, which has a main bore of 0.127m and a side arm of 0.076m. Both T-junctions are machined from an acrylic resin block with the outside machined to a square cross-section (0.2 x 0.2 m) to minimise refraction problems during observation. Both have carefully machined sharp corners to eliminate the radius of curvature as a possible variable in the experiments. Both T-junctions have flanges at the three ends to mate with the rest of the test section pipework.

Butterfly valves (V1, V2) are used to control the pressure drops occurring in the two pipelines downstream of the T-junction, and hence are a way of regulating the flow split. Each butterfly valve has been positioned as far as possible from the T-junction and just before the air-water separating units.

Brief descriptions of the pipe arrangements for the differing geometries studied are given in the following sections. The diagrams presented are to aid visual conception and have not been drawn to scale. All major pipe lengths and diameters ( $\phi$ ) have been shown.

---



### 3.1.1 Altering side arm orientation

With the run and side arm both lying in the horizontal plane, see Figure 3-2, the regular and reduced T-junctions were used to investigate phase split. The centre of either T-junction was 4m (31D) downstream of the air-water mixing unit. The air-water mixture passing down the side arm is separated in a cyclone with the air being metered by orifice plates before being vented to the atmosphere and the water being diverted to the weigh tank when measurement is required.

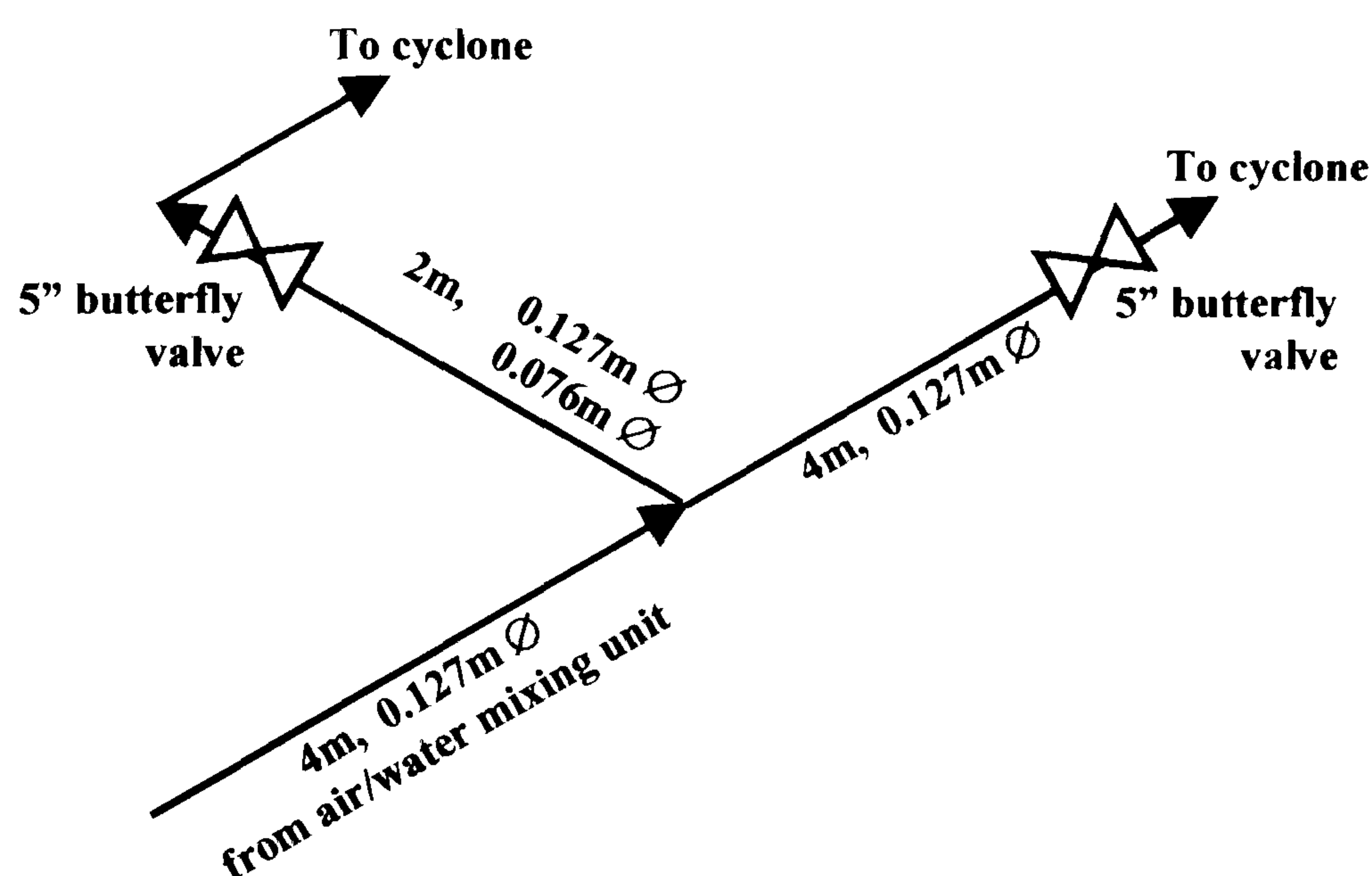


Figure 3-2: Horizontal side arm



With the side arm vertically upwards (+90°), see Figure 3-3, the T-junction remains 4m from the air-water mixing unit. Due to the fixed location of the separating cyclone, the vertically upwards side arm is followed by two 90° bends before the butterfly valve.

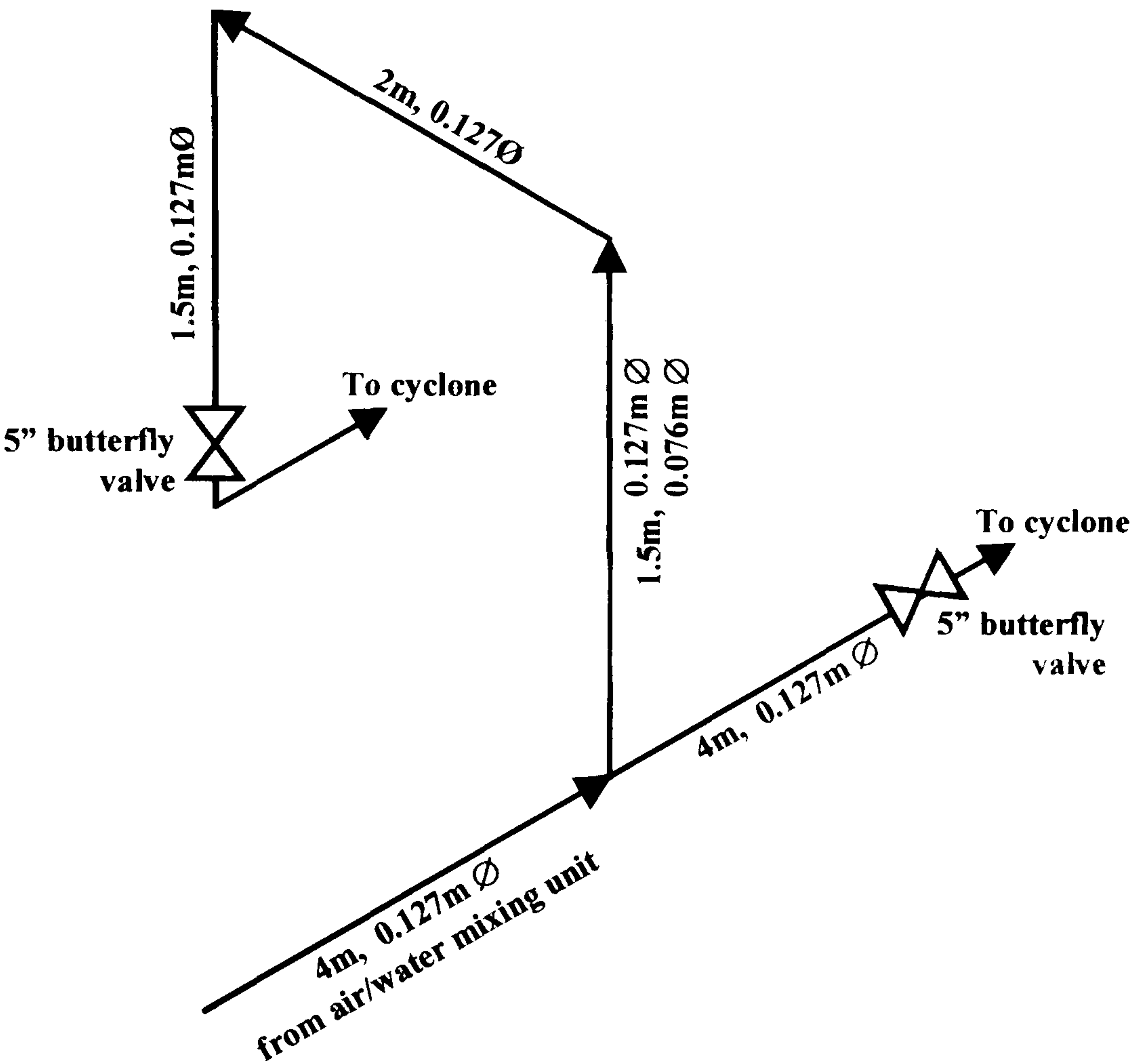


Figure 3-3: Vertically upwards side arm



With the side arm vertically downwards ( $-90^\circ$ ), see Figure 3-4, the T-junction was moved 0.5m downstream to accommodate the new pipework. Both the regular and reduced T-junctions could be placed at the new location. The vertically downwards side arm consists of 1.6m of straight piping ending at a butterfly valve before a  $90^\circ$  bend leading to an additional separating tank. The tank is of sufficient volume to allow the air and water to separate with the air being metered from the top of the tank using calibrated orifice plates. A sight glass on the tank was used to note the increase in volume over a measured time period. When the separating tank was full the experiments had to be stopped and the tank emptied and the main feed tank re-filled.

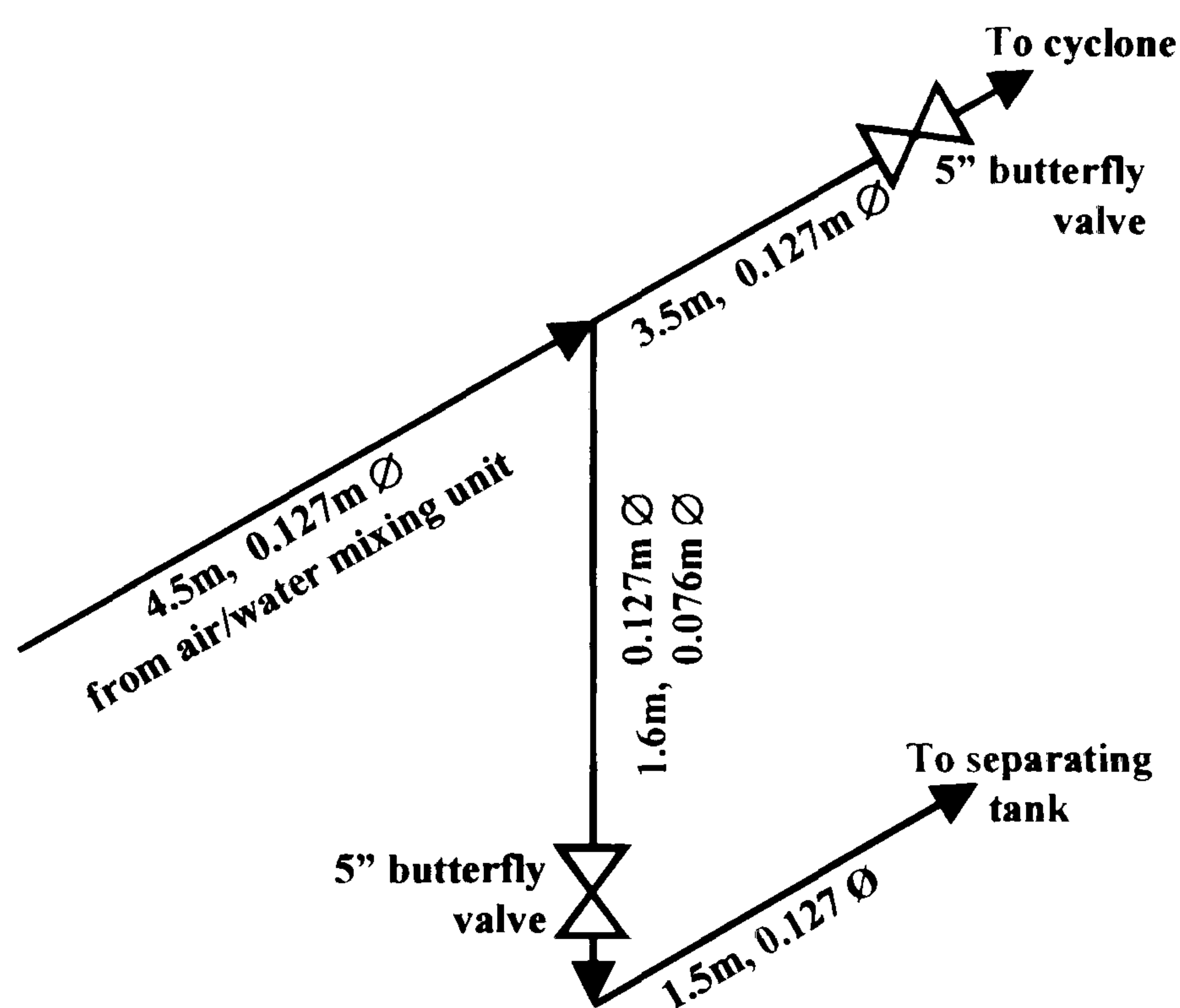


Figure 3-4: Vertically downwards side arm without U-bend



### 3.1.2 Downwards side arm with U-bend

For these experiments a U-bend, of 0.127m diameter pipe, was placed between the 90° bend at the bottom of the downwards side arm and the additional separating tank, see Figure 3-5. The U-bend was 0.88m high and 0.4m wide and a valve at the bottom of the U was provided to empty water collected between each run. The air-water mixture was separated and measured in the separating tank as for the vertically downwards side arm orientation.

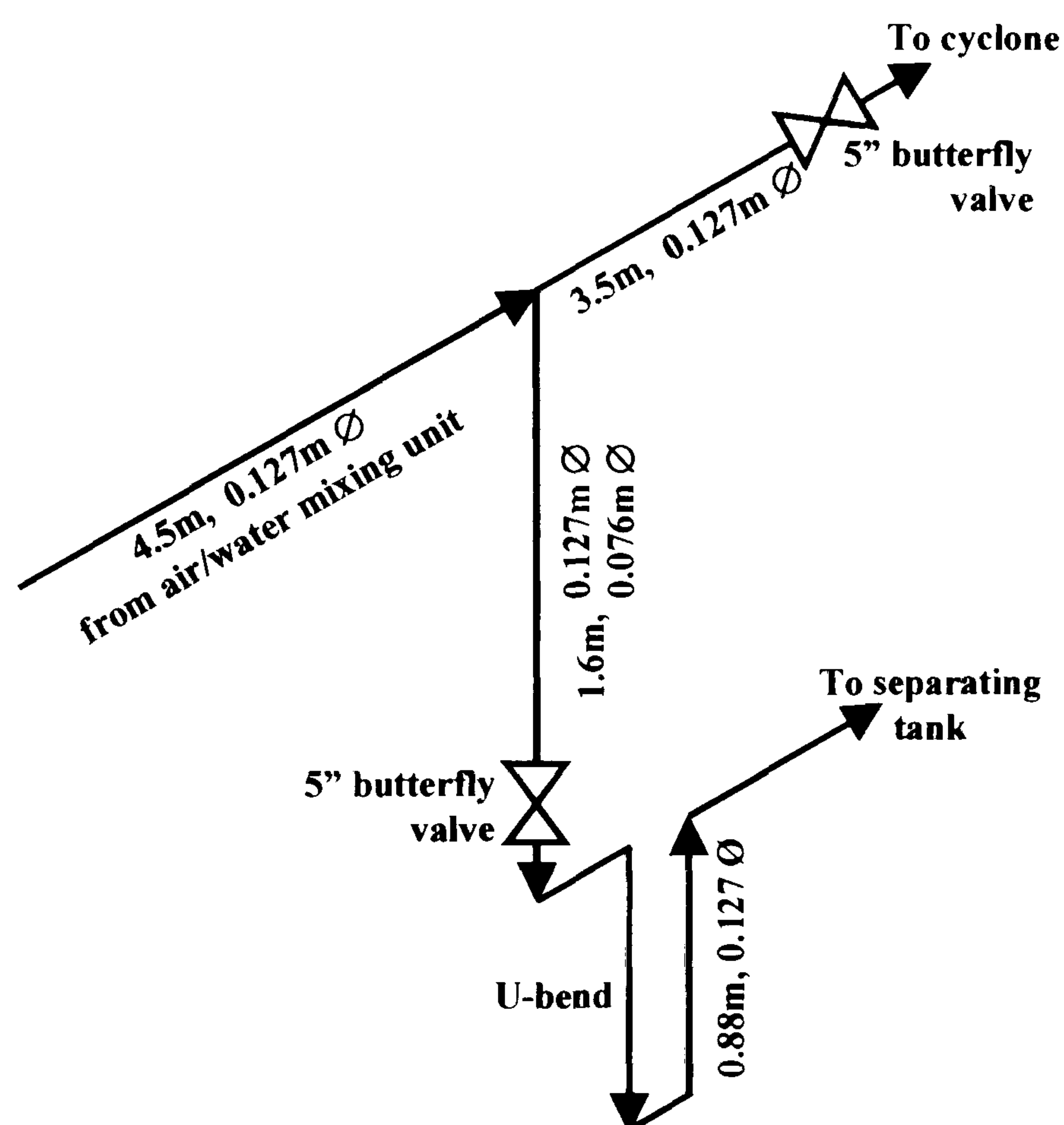


Figure 3-5: Vertically downwards side arm with U-bend



### 3.1.3 Two T-junctions in series

The effects on phase separation of two T-junctions in series were investigated. The first T-junction was positioned 4m downstream of the air-water mixing unit with the side arm positioned vertically upwards. The second T-junction could either be placed 0.5m or 1.2m downstream of the first with a vertically downwards side arm, as shown in Figure 3-6. Both the regular and reduced T-junctions could be placed in either location. The air-water flows from the three outlets (vertically upwards side arm, vertically downwards side arm and the horizontal run arm) were separated in either the cyclones or the additional separating tank and the respective flowrates measured as described above.

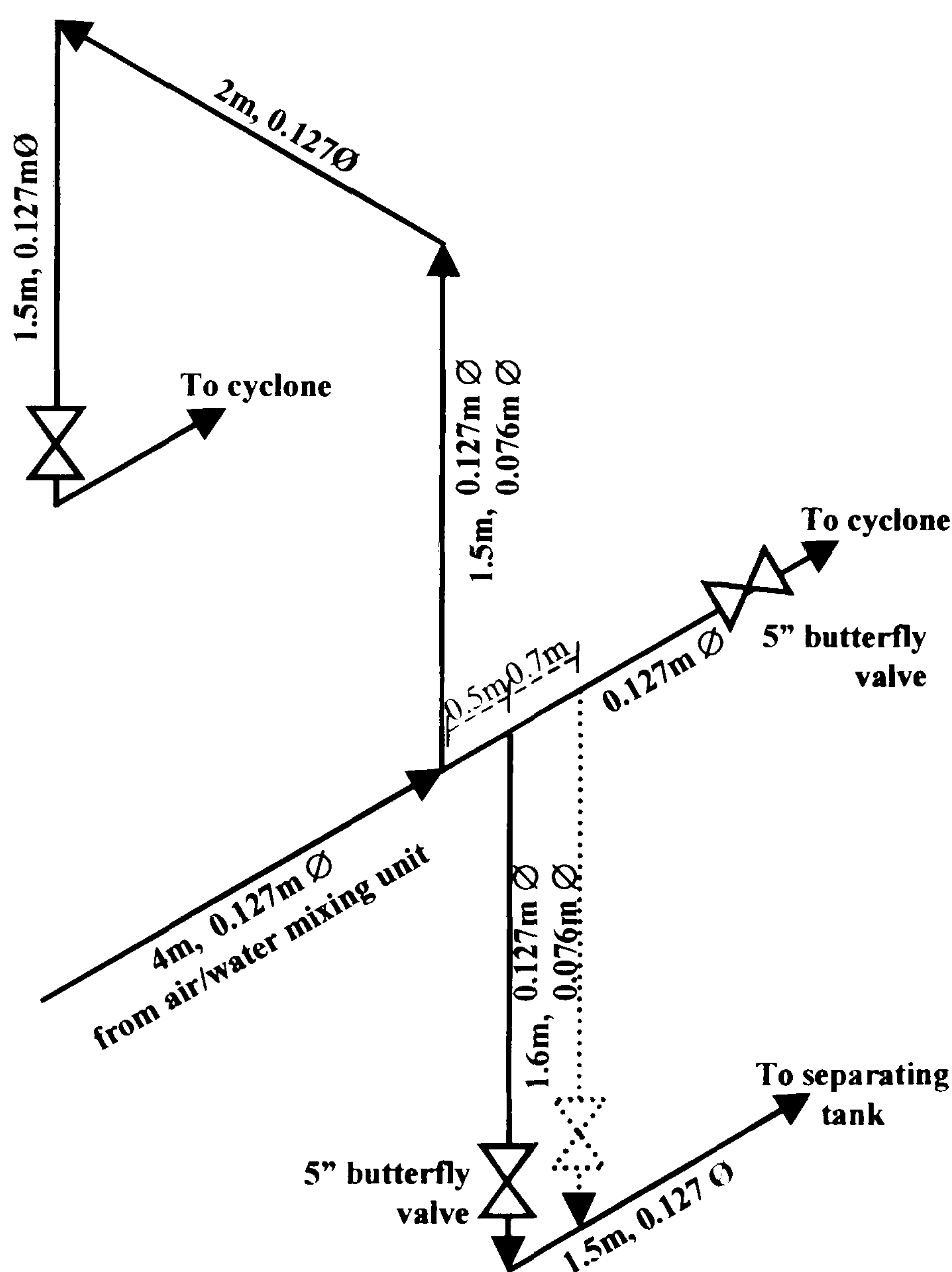


Figure 3-6: Two T-junctions in series



### 3.1.4 The T-junctions and inserts

Inserts were tested in both the regular and reduced T-junctions. In all cases the inserts were tested with the side arm in the horizontal configuration. The inserts were designed to be a tight fit within their respective side arms and were machined with walls as thin as possible so that the internal diameter of the T-junction remained essentially unaltered. Both inserts were manufactured from a clear plastic so that visual observations of the flow split occurring at either junction were not impaired. The protruding tip of the insert was cut to an angle of either  $30^\circ$  or  $45^\circ$ . In Figure 3-7 the insert on the left is for the regular T-junction with the top cut to  $30^\circ$ ; the insert on the right is for the reduced T-junction and has the top cut to  $45^\circ$ . All inserts were made long enough so they could be fixed at different protrusion depths.

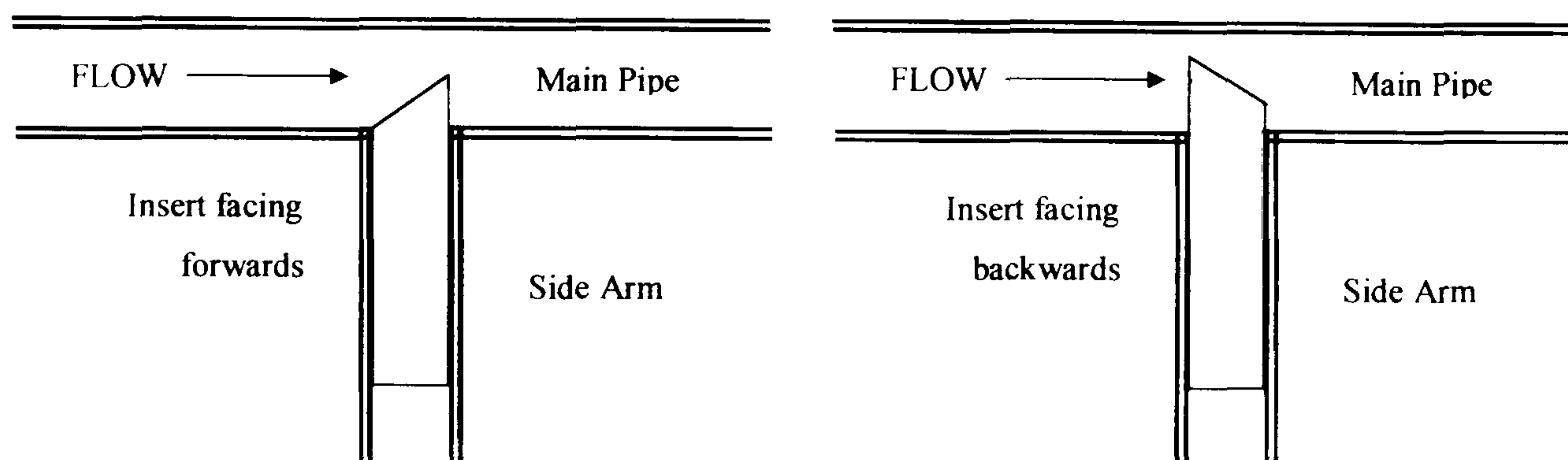


Figure 3-7: Inserts placed in the side arm of both T-junctions

Protrusion depths were measured from the side of the main pipe to the tip of the insert and were reported in the form of the fraction of the main pipe obstructed. Two protrusion depths were investigated. The first was a protrusion depth of  $\frac{1}{2}D$  which corresponded to the tip of the insert lying halfway across the diameter of the main pipe ( $\frac{1}{2} \times 0.127\text{m} = 0.064\text{m}$ ) the second protrusion depth of  $\frac{3}{4}D$  corresponded to the tip of the insert lying three-quarters of the way across the main pipe ( $\frac{3}{4} \times 0.127\text{m} =$



0.095m). At all protrusion depths, the insert could be rotated through at least  $180^\circ$  so that the effects of the scooped section facing forwards and backwards could be studied. Figure 3-8 shows schematically the insert positioned at a protrusion depth of  $\frac{1}{2}D$ , facing forwards and at a protrusion depth of  $\frac{3}{4}D$  facing backwards.



**Figure 3-8: Inserts facing forwards at protrusion depth  $\frac{1}{2}D$  and backwards at protrusion depth  $\frac{3}{4}D$**

### 3.2 Experimental Procedure for a Single T-junction

The following operating procedure was followed for all experiments investigating the phase split at a single T-junction.

The split characteristics of each of the geometrical arrangements shown from Figure 3-3 to Figure 3-5 with a single T-junction were obtained by changing the relative resistances in the side arms and run arm by using the butterfly valves. By altering the valves in a methodical manner, points from (0,0) to (1,1) can be obtained and used to plot the locus of the fraction of inlet gas drawn off versus the fraction of inlet liquid drawn off down the side arm, as previously mentioned in Chapter 2. Point (0,0) refers to no liquid or gas entering the side arm, i.e. the side arm butterfly valve is fully closed and the run arm valve is fully open. The point (1,1) refers to all the inlet flow being diverted down the side arm, i.e. the side arm butterfly valve is fully open and the run arm valve is fully closed. All butterfly valves are initially open and then readings taken for the run arm valves being slowly closed with the side arm valve



fully open. The side arm valve was then slowly closed with the run arm fully open. A typical set of flow split results are given in the following sections for each of the different geometries studied.

Prior to each set of flow split data being recorded, an air balance was performed across the rig. This served two purposes. The first was to check for air leaks. The inlet air and the air flow from the two cyclones were measured using the orifice plates. The second purpose of performing an air balance was to calibrate the venturi meters on top of the cyclones as previously described in section 3.1. The venturi meters were only used to measure air flowrates above 15m/s.

### **3.2.1 Operation with the side arm lying horizontally ( $0^\circ$ ) and vertically upwards ( $+90^\circ$ )**

For the side arm lying horizontally or vertically upwards results were obtained for each set of inlet conditions in the following manner. Firstly, air was drawn through the rig by turning on the blower with the air bleed fully open; correct air flow was obtained by selecting the appropriate orifice plate and partially closing the air bleed. Depending on the flow of water required, the relevant pump was selected, the smaller pump only being able to provide flowrates corresponding to superficial water velocities up to 0.1m/s, and the appropriate valve was used to adjust the water flowrate. Flowrates were measured by either the bank of rotameters (for smaller flows) or by the turbine meter (for larger flowrates).

Once the two-phase mixture flowed in a stable fashion through the rig, with the butterfly valves in both the run and side arms fully open, measurements could be made. A pool of water was maintained in the bottom of the cyclones to form a plug thus ensuring no air exited with the water. The orifice plates or the venturi meters measured the exiting air. Water was diverted to a weigh tank on a load cell which, as previously stated, had an upper limit of 120kg. At high liquid flowrates, above 0.31m/s, timed discharge could therefore last no longer than 20 seconds. Once the



readings at the initial open valve settings were recorded, the butterfly valve in the run arm was slowly closed, leaving the side arm valve open and readings were taken at each setting. The run arm valve was then left open whilst readings were taken as the butterfly valve in the side arm was slowly closed. Measurements for each butterfly valve setting were noted when the error in the mass balance on the water side was less than 5% and on the air less than 10%. These readings formed the points (0,0) to (1,1) on the fraction of liquid drawn off against the fraction of gas drawn off down the side arm graphs. Procedure is identical whether the side arm is horizontally or vertically upwards as both orientations use the cyclones to separate the air and water mixture and a typical set of results is given in Figure 3-9 for annular flow. As can be seen, the phases have split at the junction, with the flow down the side arm for both side arm orientations being typically richer in gas than liquid. These results are expanded in Chapter 4 where the effect on phase split with a reduced T-junction is also considered.

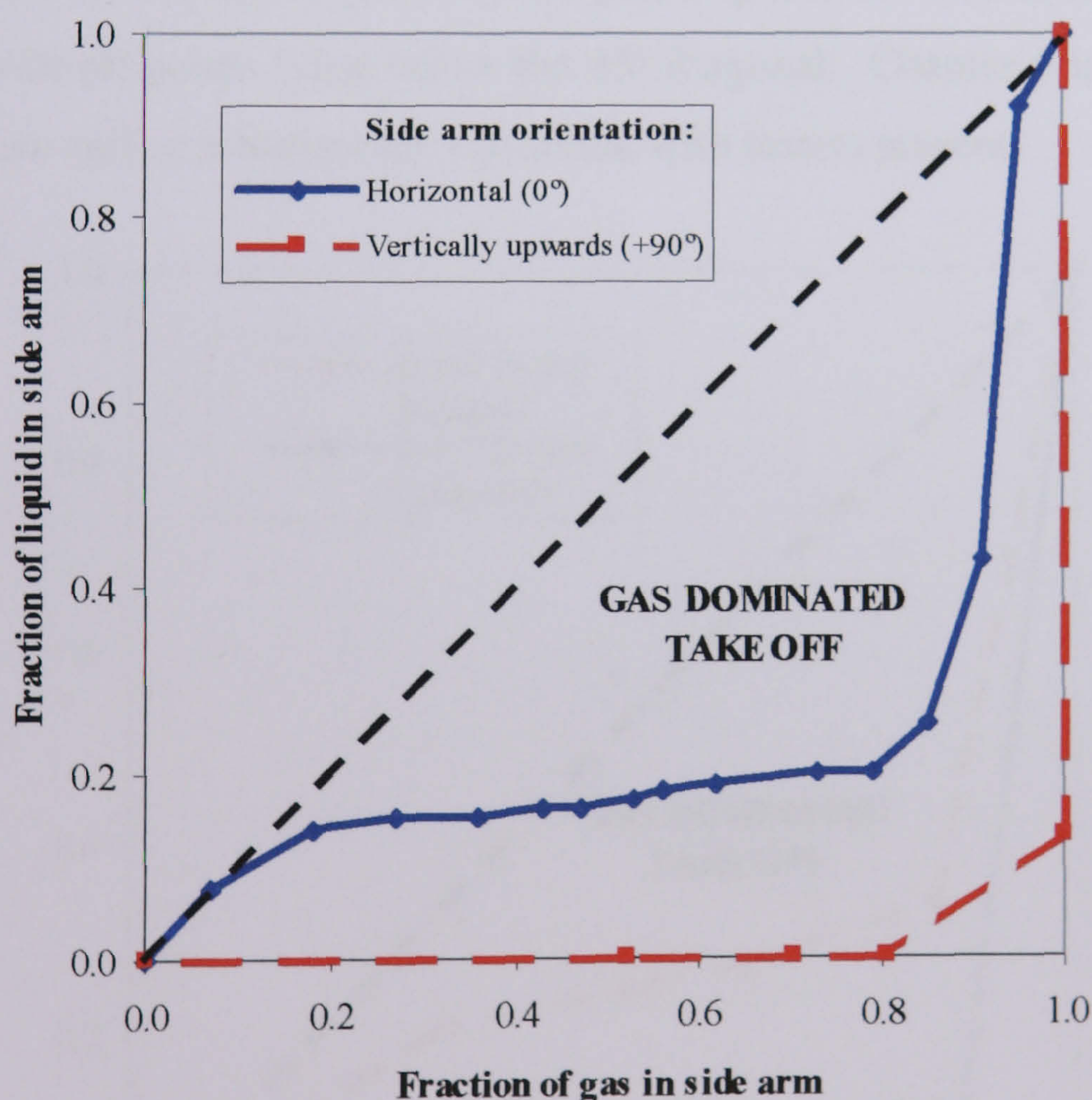


Figure 3-9: Typical flow split results for annular flow with the side arm positioned horizontally and vertically upwards



### 3.2.2 Operation with the inserts

With an insert present within the T-junction, the inlet air and water superficial velocities were set as described in the previous section. The insert was held in position by the friction generated between itself and the inside pipe wall as it was machined to be a close fit. Flow split results were obtained in the above manner by altering the position of the run arm and side arm butterfly valves, the air and water flowrates being measured by orifice plates or the load cell respectively. Experiments were repeated with the insert set at the different protrusion depths ( $\frac{1}{2}D$ ,  $\frac{3}{4}D$ ) and for different orientations of the scooped section (facing forwards or backwards) as previously described in section 3.1.4. A typical set of flow split results can be seen in Figure 3-10 for phase split at a regular T-junction with stratified flow. As expected, since the side arm is lying horizontally the phase split in the side arm is typically gas dominated with all points lying below the 45° diagonal. Chapter 5 is devoted to the effect on phase split at a horizontal T-junction with inserts present.

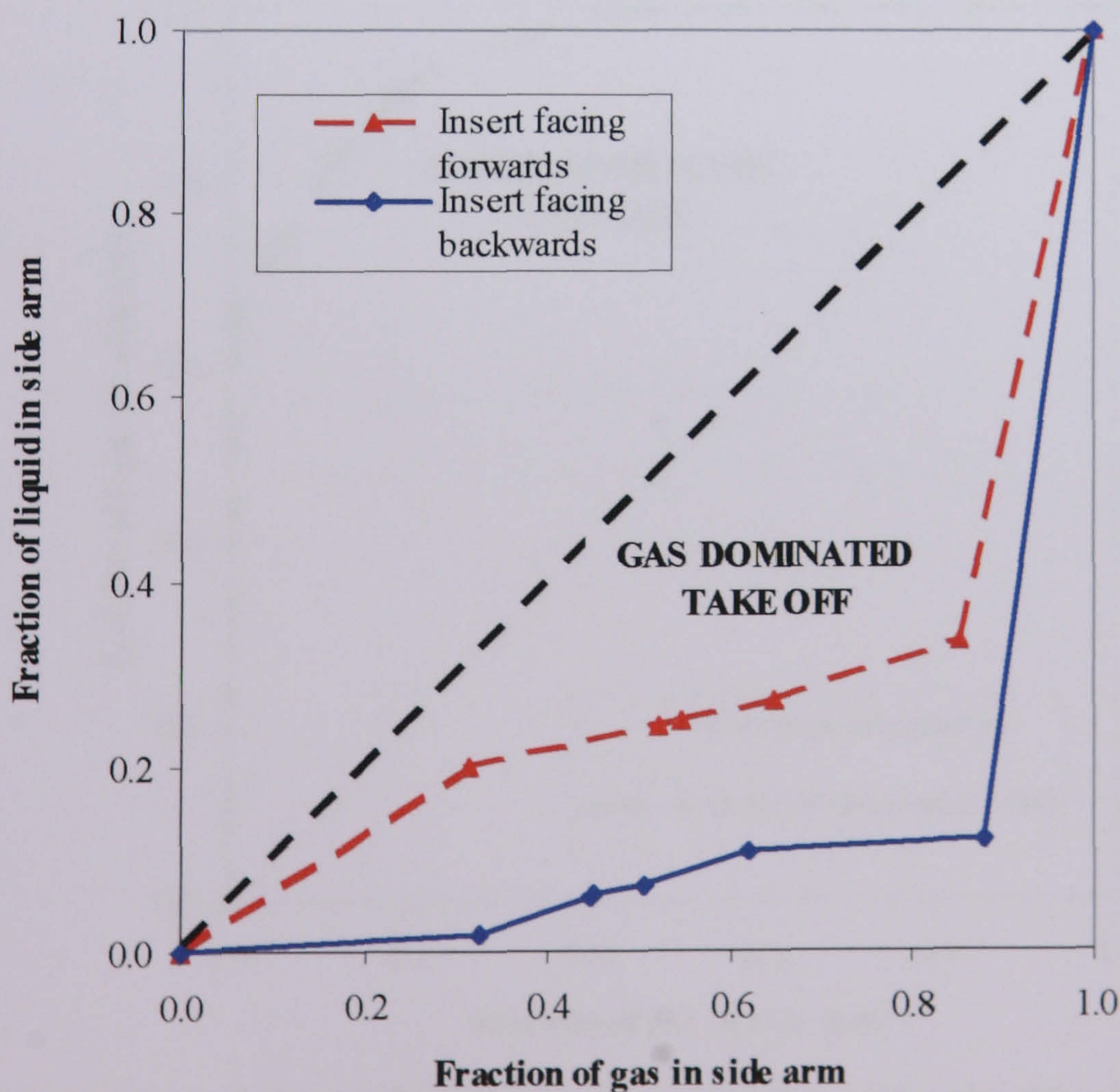


Figure 3-10: Typical phase split for stratified flow with the 45° insert facing forwards and backwards at a protrusion depth of  $\frac{1}{2}D$



### 3.2.3 Operation with the side arm vertically downwards ( $-90^\circ$ ) with and without a U-bend

With the downwards side arm an additional separating tank was used instead of a cyclone to determine the air and water flowing down the side arm. The air was measured using an orifice plate and the water by an increase in volume of the tank over a known period of time, by use of a sight glass. A complete set of results is again obtained by gradually closing the butterfly valve in the downwards side arm and then the valve in the run arm and noted when the error in the air and water mass balances were less than 10% and 5% respectively. A brief error analysis for a typical data point can be found in Appendix A and a set of results can be seen in Figure 3-11. Unlike all the previous results, phase split for this orientation of side arm is typically liquid dominated, as all points lie above the  $45^\circ$  diagonal representing equal split between the two junction outlets. Detailed discussions can be found in Chapter 4.

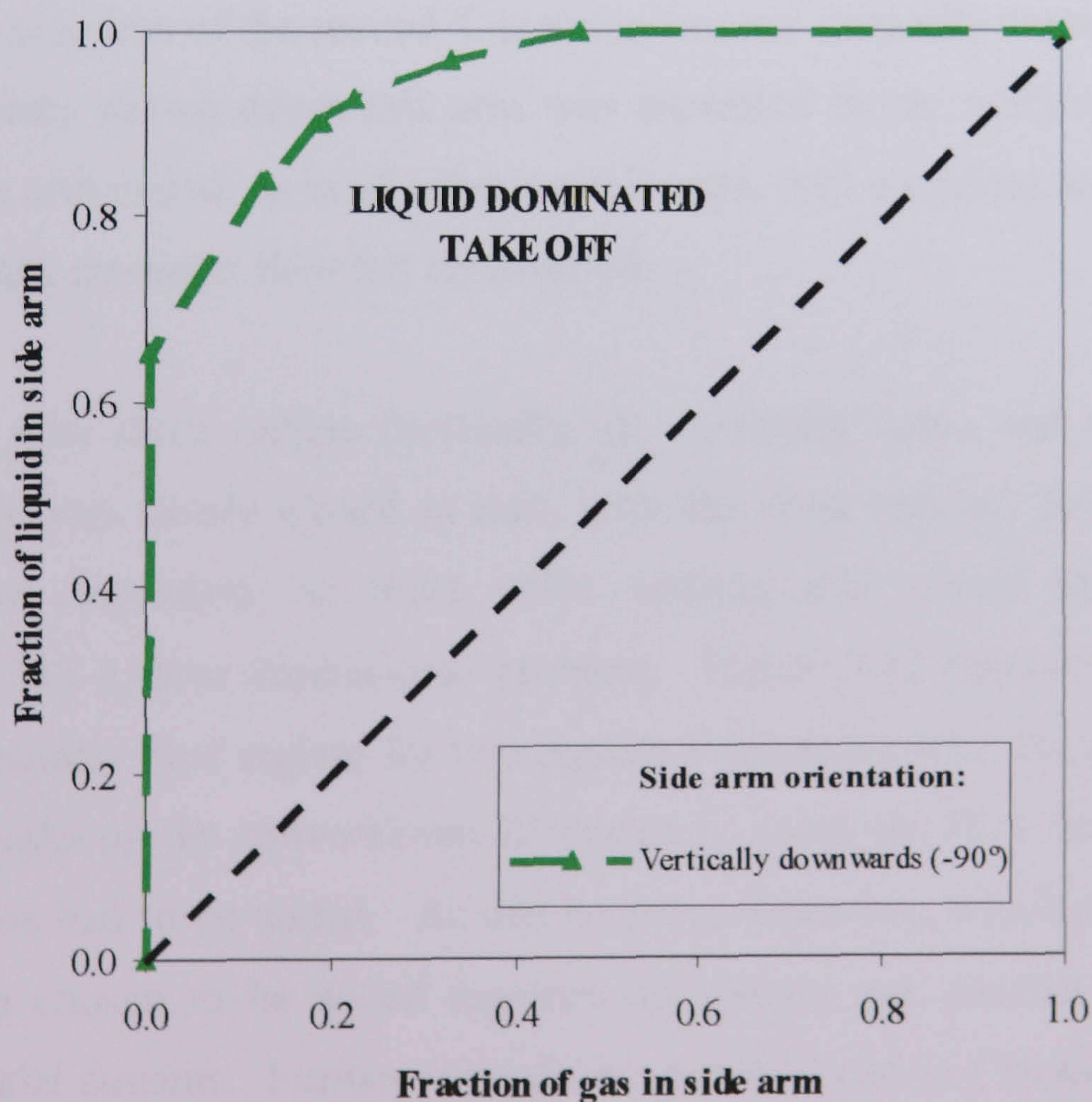


Figure 3-11: Typical phase split results for stratified flow with a the side arm positioned vertically downwards



With the U-bend on the downwards side arm, the initial inlet flowrates of the air and water were set and the rig was left to run for approximately 3 minutes, depending on water flowrate, prior to any readings being taken. This was to allow the water to accumulate within the U-bend at the level specific to the set inlet conditions. Flow split data was then recorded in the above manner and the U-bend drained before setting new inlet flow conditions. Typical results again show liquid dominated take off down the side arm and have been discussed in full within Chapter 4.

### ***3.3 Experimental Procedure with Two T-junctions in Series***

Two T-junctions could be placed within the rig with the centres of the junctions either 0.5m or 1.2m apart and the air-water flow set as described for all previous geometrical arrangements. The side arm of the first T-junction was positioned vertically upwards and the air-water mixture drawn up this arm was separated and measured using a cyclone. The side arm of the second T-junction was set vertically downwards and the air-water mixture drawn down this arm was separated in the additional separating tank. The run arm ended, as in all other experiments, with a cyclone used to separate and measure any air-water flow left un-diverted.

As there are now three outlets (vertically up, vertically down and run arm) each butterfly valve was slowly closed in turn, with the other two left fully open. This produced data dependant on three valve settings and turned the phase split phenomenon into a three dimensional problem. Figure 3-12 shows a set of results taken in the annular flow regime for two regular T-junctions set 1.2m apart. In order to plot the results on the conventional  $G'$  versus  $L'$  plots, the flow down two of the three side arms had to be added. As can be seen, depending which combination of side arms are chosen to be added together the system can produce gas or liquid dominated outlet streams. Further explanation can be found in Chapter 6 where two T-junctions in series are discussed in greater detail.



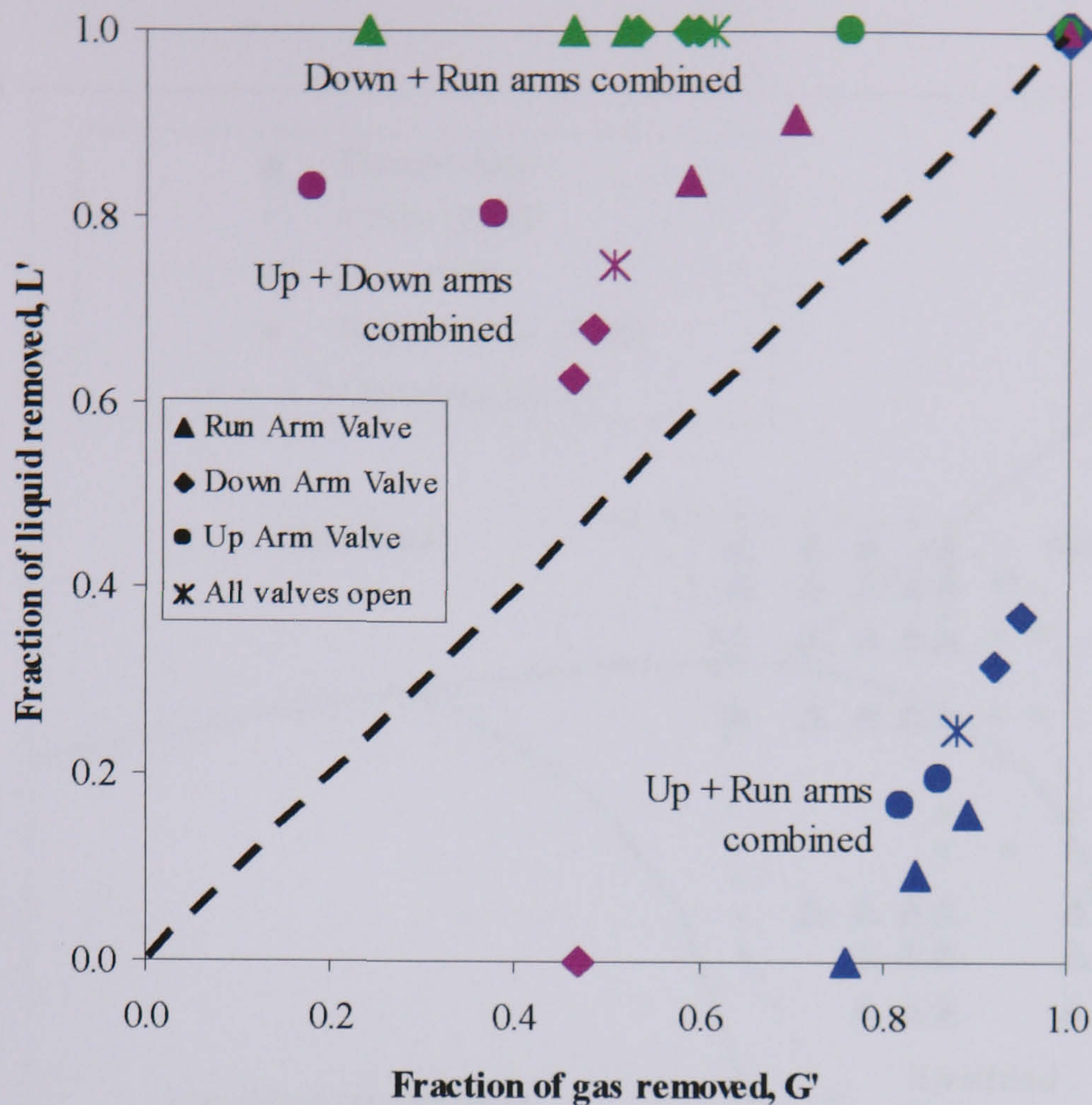


Figure 3-12: Phase split results annular flow with two regular T-junctions in series

### 3.4 The Flow Patterns Investigated

Three series of experiments were performed to investigate two phase flow split at a T-junction. The first investigated the effect of side arm orientation; the second explored the effect on phase split in the presence of inserts protruding from the side arm into the main pipe and diameter and the third examined the consequences of placing two T-junctions in series. The effect on phase split at a T-junction of each of the above has been studied in depth in the following chapters.

Experiments for all geometrical arrangements were generally performed in the stratified and annular flow regimes. As can be seen in Figure 3-13 the visual observations of the flow agreed favourably with those predicted by the Taitel and Dukler (1976) flow pattern map for the facility, described in Chapter 2, except at high



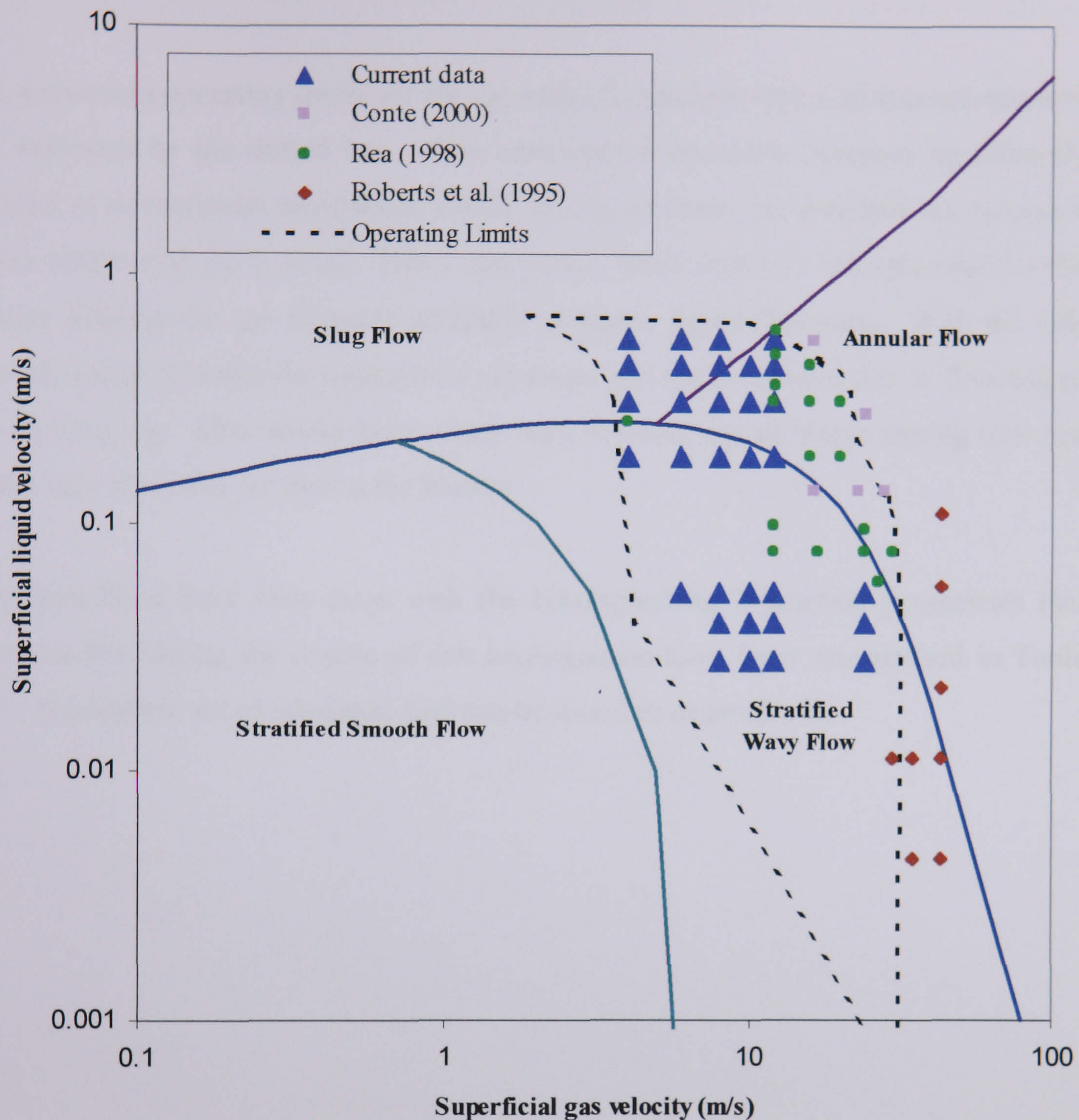


**Figure 3-13: Flow pattern map from predictions of Taitel and Dukler for a 0.127m diameter horizontal pipe compared with experimental inlet flow conditions**

liquid flowrates which were predicted to be in the slug flow regime but were observed to be in the stratified flow regime.

This could be due to the distance between the inlet air-water mixing unit and the T-junction being relatively short. Currently this distance is 31D but Penmatcha *et al.* (1996) claim that 600D of straight pipe is required before steady state two-phase flow



is achieved. However, as is shown in the following chapters, the flow split data agrees favourably with previously published results.

The maximum operating limits for the rig with a T-junction with a horizontal side arm are indicated by the dotted line. This envelope of operation becomes significantly smaller as downstream resistances within the rig increase, for example the inclusion of the inserts and the U-bend. This is due to the small head (0.1 bar) provided by the blower limiting the gas flowrate available at higher liquid flowrates. With the side arm vertically upwards the operational envelope was again reduced due to flooding of the vertical leg. This would force water back towards the air-water mixing unit and potentially down the air line to the blower.

The superficial inlet flow rates with the corresponding T-junction geometries that were studied during the course of this investigation have been summarised in Table 3-1. A complete set of tabulated data can be found in Appendix B.



Table 3-1: Summary of all experiments performed with corresponding T-junction geometry

● - Regular 0.127m T-junction                      ○ - Reduced 0.127/0.076m T-junction  
◆ - Horizontal data published by Rea (1998)

Inlet Gas Velocity (m/s)	Inlet Liquid Velocity (m/s)	Horizontal Side Arm	Vertically Up Side Arm	Vertically Down Side Arm	Inserts	U-Bend	2 Ts
4	0.186	◆	●	●   ○			✓
	0.310	◆   ○	●	●   ○		●   ○	✓
	0.434	◆   ○	●   ○	●   ○			✓
	0.558	◆   ○	●   ○	●   ○		●   ○	✓
6	0.0535			○			
	0.186			●   ○			
	0.310			●   ○			
	0.434			●   ○			
	0.558			●   ○			
8	0.0283			●			
	0.0401			●			
	0.0535			●   ○			
	0.186	◆		●   ○			✓
	0.31	◆	●	●   ○			✓
	0.434	◆		●   ○			
	0.558	◆		●   ○			
10	0.0401			○			
	0.0535			○			
	0.186			●   ○			
	0.310			●   ○			
	0.434			●   ○			
12	0.0283		●   ○	○		○	
	0.0401	◆   ○	●   ○	○		○	
	0.0535	◆   ○	●   ○	○		○	
	0.186	◆		●   ○		●   ○	✓
	0.310	◆   ○		●   ○	●   ○	○	✓
	0.434	◆		●   ○			✓
	0.558	◆					
24	0.0283	◆   ○	●   ○		●		
	0.0401	◆   ○	●   ○				
	0.0535	◆   ○	●   ○		●		



### ***3.5 Visual Observations and High Speed Camera Footage***

Both Rea (1998) and Conte (2000) demonstrated that the phenomena of film stop and hydraulic jumps, respectively, could occur in large diameter pipes and captured these phenomena on film. Both authors described these phenomena in detail. With the different side arm orientations studied in this investigation, film stop and hydraulic jumps were observed. However, more attention was applied to the physical phenomena occurring at the junction with a downwards side arm. With this orientation vortices were seen to develop within the flow and a phenomenon relating to pressure reversal at the junction was also observed. Both of these phenomena were captured on film and the video footage analysed to gain a better understanding of why these features develop. Section 4.3.2 in Chapter 4 explains these phenomena in greater detail.

To capture these images on film a high speed video system, KODAK HS 4540, was used. This has the ability to record between 4,500 full and 40,500 partial frames per second, which are recorded directly to solid state memory and not to tape. The digital images can be replayed from the memory for instant viewing or for a permanent copy can be downloaded and recorded onto tape.



## **CHAPTER 4**

### **Effect of Geometry on Phase Split at a Single T-Junction**

The effect of geometry on phase split at a single T-junction was introduced in Chapter 2, where published work relating to different side arm diameters, orientation and the affects of including baffles and inserts at the junction was reviewed. Virtually all preceding investigations have concentrated on the phase split at small diameter T-junctions. This chapter shows the effects different geometries have on phase split at a large diameter T-junction. The effect of inlet flowrates on branch arm orientation, branch arm diameter and the inclusion of U-bend down stream of the junction have been investigated. In all cases the use of the T-junction as a partial phase separator has been considered.

This investigation builds on the research of Rea (1998) who studied stratified flow at a large diameter horizontal T-junction. The phase separation results published by Rea have been compared with the T-junction geometries studied here. The separation performance of the large diameter T-junction has also been compared, where appropriate, with available data from literature.

The knowledge gained through the experimental investigations discussed in this chapter has also been considered within the subsequent chapters. Chapter 5 considers the placement of an insert at a T-junction with a horizontal side arm and how it alters the separation qualities and Chapter 6 reports on how two T-junctions placed in series affect the phase separation of different inlet two-phase flow patterns. Both refer to the separation performances discussed in this chapter for a single T-junction.



#### **4.1 Comparisons with Published Data**

To test the validity of the experimental data obtained using the large diameter flow facility with both a regular and reduced T-junction, comparisons have been drawn with the phase split data published by various authors. A particular difficulty in comparing data from different sources is finding sets with equivalent flow rates. Azzopardi *et al.* (1988) had previously suggested that to compare information from different system pressures, the momentum fluxes of the phases based on inlet superficial velocities could be used and showed that if the inlet gas and liquid momentum fluxes for a horizontal and a vertical T-junction were similar then the flow split results would lie approximately on the same line, as indicated by the data in Figure 2-4 in Chapter 2. Rea (1998) performed a comprehensive study comparing experimental data with a wide variety of previously published material. The aim was to find sets of data that plotted onto the same loci in order to correlate the separation performance of different T-junction systems with inlet conditions. Inlet quality, void fraction and momentum were used as the different bases of comparison. Rea's thorough investigations concluded that the flow regime approaching the junction still has the most significant influence on the phase split. Meaningful comparisons can then be drawn between data of two different systems with similar void fractions or inlet momentums.

The current phase split results have been compared, where appropriate, with published data based on inlet void fractions and the gas-liquid momentum fluxes. Specific attention was drawn to previous studies investigating the phase split at both regular and reduced T-junctions. It should be stated that, due to the number of methods that are available within literature for calculating void fractions, all void fractions quoted have been calculated using the CISE correlation, Premoli *et al.* (1970). The reader is referred to the detailed investigation by Holt (1996) for any further information on void fraction equations.



## **4.2 Effect of Side Arm Diameter**

In the present work the effect of branch diameter was studied using a regular, 0.127m-0.127m diameter T-junction and a reduced branch arm diameter, 0.127m-0.076m, T-junction. This gives two branch-to-inlet ( $D_3/D_1$ ) ratios of 1 and 0.6. The effect of altering the side arm diameter on gas and liquid take off was considered for the side arm lying horizontally ( $0^\circ$ ), vertically upwards ( $+90^\circ$ ) and vertically downwards ( $-90^\circ$ ). Experiments were performed predominantly with stratified flow approaching the junction. At higher inlet gas velocities a film was seen to flow along the top of the pipe and droplets were carried within the central gas core indicating annular flow, as predicted by the flow pattern map.

### **4.2.1 Horizontal side arm ( $0^\circ$ )**

The results of the experimental investigation can be split into the two inlet flow patterns – stratified and annular. Previous methodical investigations (Azzopardi *et al.*, 1988, Reimann *et al.*, 1988, Shoham *et al.*, 1989) have shown that inlet flow regimes are significant in determining the degree of separation that occurs at the junction due to the different characteristics they exhibit, as described in Chapter 1. Figure 4-1 confirms this point; data from annular and stratified flow patterns with the branch arm lying horizontally ( $0^\circ$ ) (denoted by the letter ‘h’ in the legend) can be seen to follow different trends. The phase split results presented below have therefore been classified into the two different inlet flow patterns studied and the phase split results for the regular and reduced T-junctions compared.

The main difference between the regular and reduced T-junction is the pressure difference in the branch arm. For the same inlet conditions, a higher pressure drop can be measured in the reduced side arm compared to the regular T-junction. This is because for the same fraction of gas taken off down the reduced diameter side arm,



the gas velocity is faster and therefore, by Bernoulli, results in a higher pressure drop. For the inlet and the run arms the pressure distributions for both the regular and reduced T-junctions, under the same inlet flow conditions, are approximately the same, as previously described in Chapter 2.

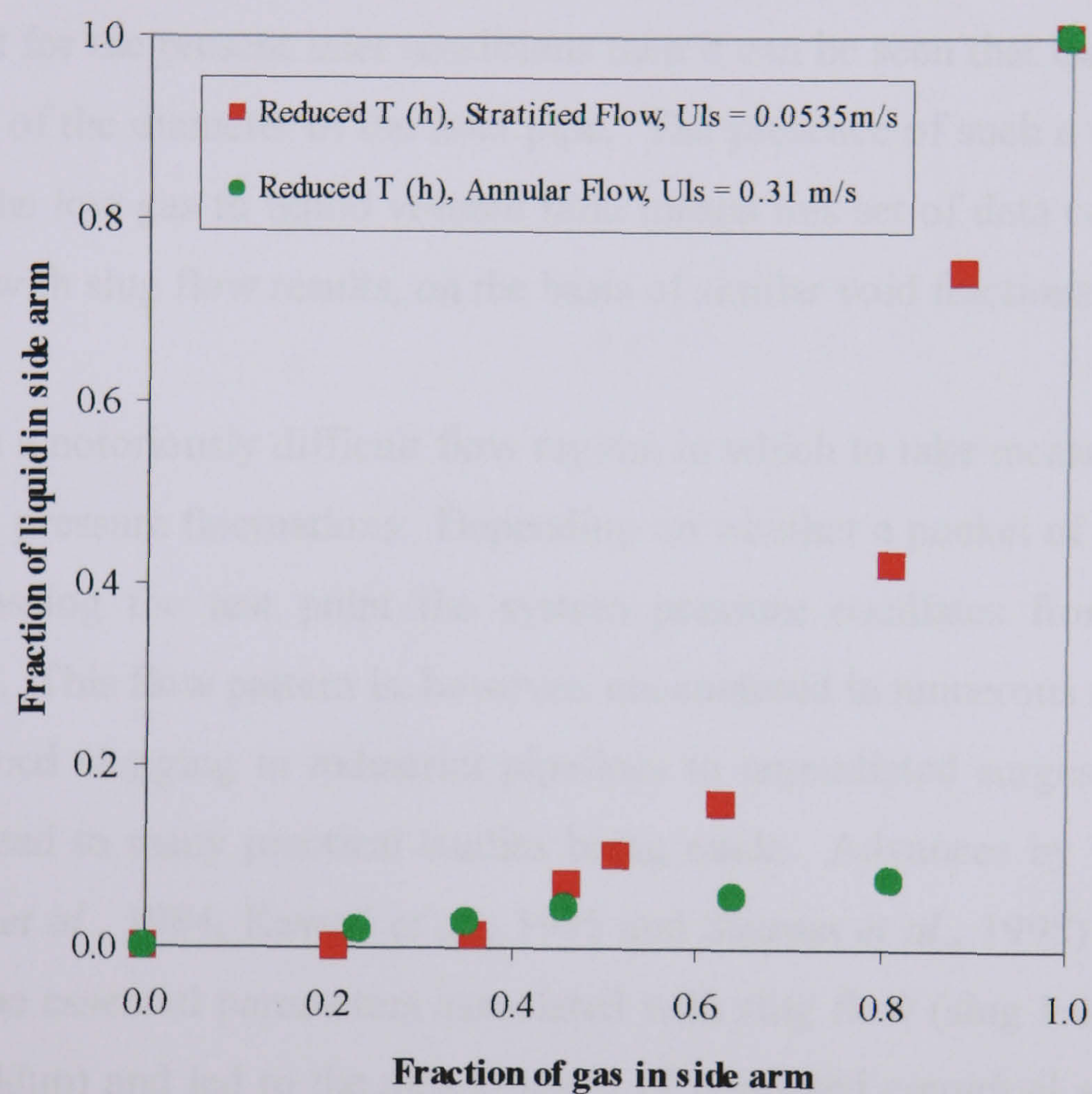


**Figure 4-1: The effects of inlet flow pattern on a horizontal reduced T-junction,  $U_{gs} = 12 \text{ m/s}$**



### ***Stratified Flow***

Experiments within this flow regime can fall into two categories – those with a high liquid but low gas inlet flowrate and those with a low liquid but high gas inlet flowrate. For the first set of conditions, high liquid ( $U_{ls}$  from 0.31 to 0.558m/s) but low gas ( $U_{gs} = 4\text{m/s}$ ) inlet flowrates, the liquid layer flowing along the bottom of the pipe was seen to be quite a substantial depth. Rea (1998) measured the film thickness for various inlet conditions using conductance probes. If these results are extrapolated for the present inlet conditions then it can be seen that the liquid depth is over a third of the diameter of the inlet pipe. The presence of such a large volume of liquid and the low gas to liquid volume ratio means this set of data can be compared favourably with slug flow results, on the basis of similar void fractions.

Slug flow is a notoriously difficult flow regime in which to take measurements due to the constant pressure fluctuations. Depending on whether a pocket of gas or a slug of liquid is passing the test point the system pressure oscillates from high to low respectively. This flow pattern is, however, encountered in numerous situations, from terrain induced slugging in industrial pipelines to unpredicted surges in production, which has lead to many practical studies being made. Advances by various authors (Kvernfold *et al.*, 1984, Kawaji *et al.*, 1995 and Sharma *et al.*, 1998) have helped to determine the essential parameters associated with slug flow (slug length, frequency, velocity, holdup) and led to the development of improved empirical and mechanistic slug flow models. Scott *et al.* (1987) developed a mechanistic model for slug flow in large diameter pipelines, taking into account the longer development lengths required compared with fully developed slug flow in small diameter pipelines.

For the flow split results for the horizontal regular T-junction taken by Rea (1998) it can be seen, in Figure 4-2, that as inlet superficial liquid velocity is increased then the fraction of liquid taken off through the side arm is reduced. This is due to the increased momentum of the liquid phase increasing its inertia and hence its reluctance to be drawn off down the side arm and the data of Hong (1978), Shoham *et al.* (1989) and Walters *et al.* (1998) all exhibit similar trends. It can also be seen that the



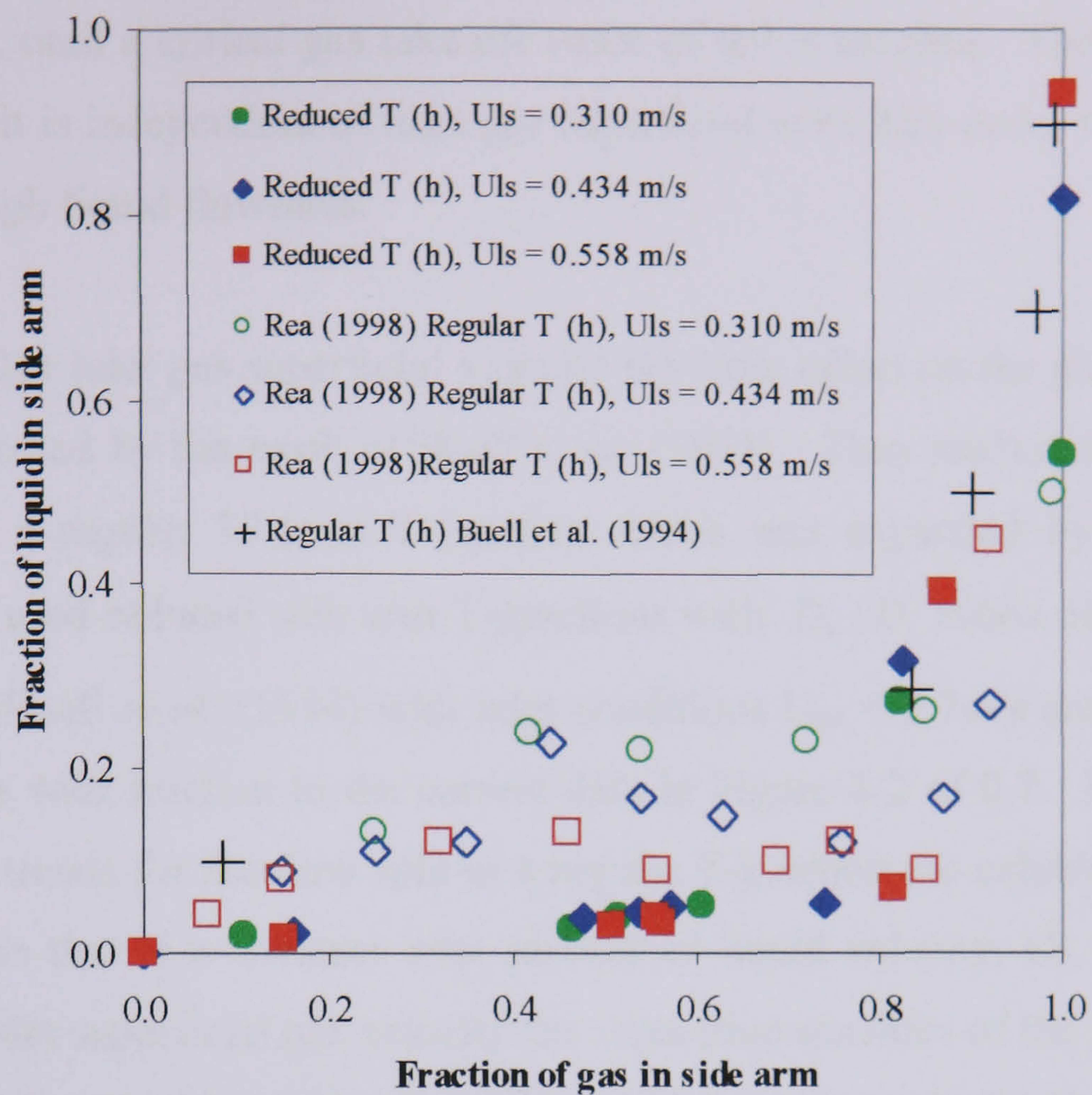


Figure 4-2: Phase split for stratified flow at a horizontal regular and reduced T-junctions,  $U_{gs} = 4\text{m/s}$

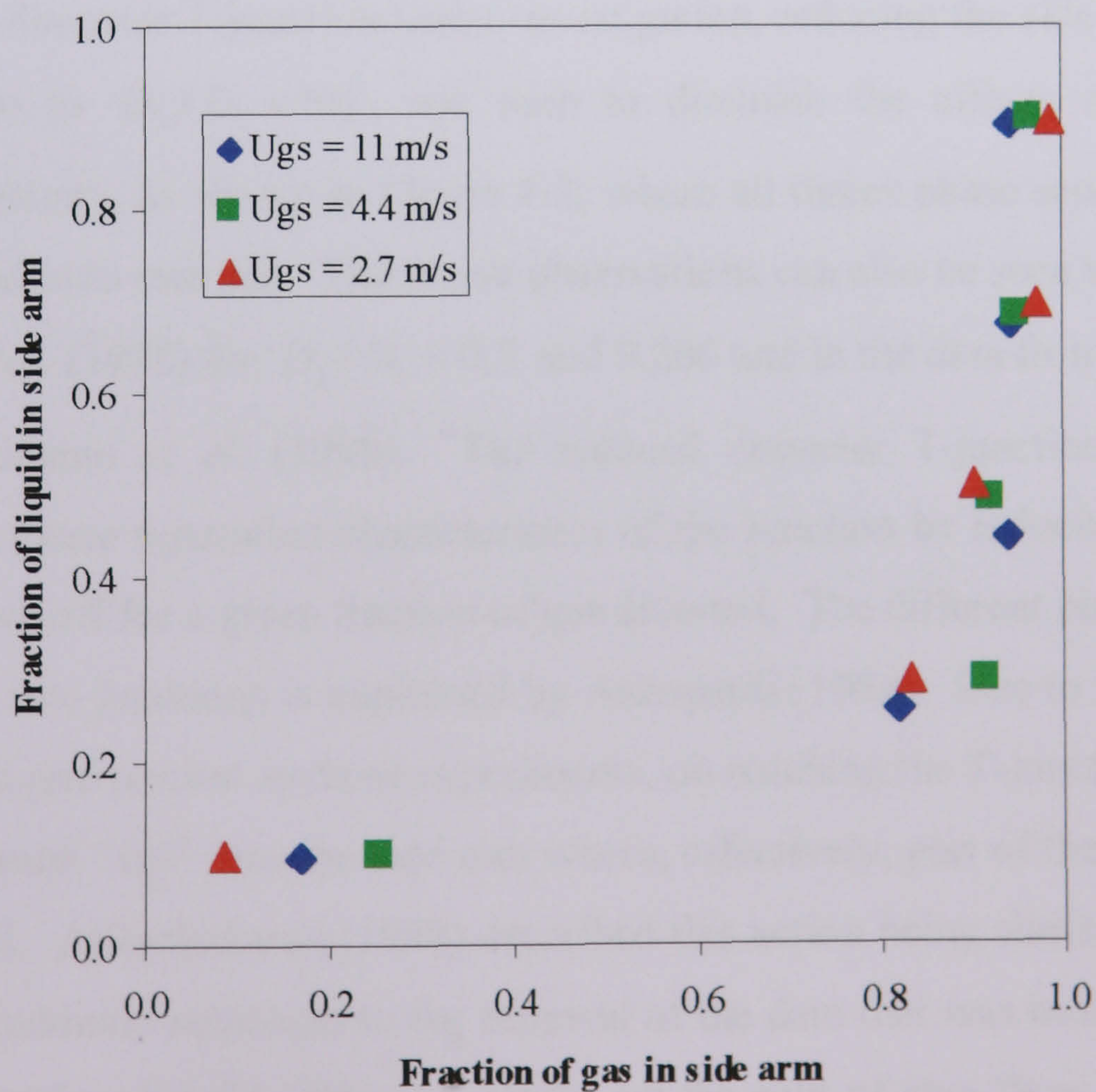


Figure 4-3: Slug flow data of Buell *et al.* (1994) with similar void fractions to the current data,  $U_{ls} = 0.18\text{m/s}$



fraction of liquid drawn off down the side arm remains independent of the fraction of gas diverted, until a critical gas take off value of 0.9 is reached. This could indicate that flow split is independent of inlet gas superficial velocities under these conditions – low gas, high liquid flowrates.

The theory that inlet gas superficial velocity has little effect on the phase split within can be supported by the work of Buell *et al.* (1994). They studied the split of slug flow within a regular 37.6mm T-junction which was expanded by Walters *et al.* (1998) who used reduced side arm T-junctions with  $D_3 / D_1$  ratios of 0.5 and 0.206. The data of Buell *et al.* (1994) with inlet conditions  $U_{gs} = 2.7\text{m/s}$  and  $U_{ls} = 0.18\text{m/s}$  has a similar void fraction to the current data in Figure 4-2 of 0.7. For both sets of data similar trends for the flow split at a regular T-junction are exhibited. Figure 4-3 clearly shows that at a constant inlet superficial liquid velocity,  $U_{ls} = 0.18\text{m/s}$ , and increasing inlet superficial gas velocity the separation qualities of the junction remain unchanged. A critical gas take off of 90% still has to be reached before any dramatic rise in the fraction of liquid drawn off.

For the large diameter T-junction under investigation, reducing the side arm to give a diameter ratio to  $D_3 / D_1 = 0.6$ , was seen to diminish the effects of inlet liquid superficial velocity, as shown in Figure 4-2, where all three phase separation curves have collapsed onto one line. The above observations can also be seen within the data of Walters *et al.* (1998) for  $D_3 / D_1 = 0.5$  and 0.206 and in the data from the extensive study by Reimann *et al.* (1988). The reduced diameter T-junction significantly improves the phase separation characteristics of the junction by reducing the fraction of liquid drawn off for a given fraction of gas diverted. The different phase separation ability of the two junctions is explained by Azzopardi (1984). Due to the significant depth of the liquid present in these experiments, on reaching the T-junction part of the liquid film would “fall” into the side arm where, effectively, part of the pipe wall had been removed. Arirachakaran (1990) described this action being similar to a body of water being suddenly subjected to the removal of the dam that was holding it in place and termed it “dam break” within his model on the split of slug flow at T-junctions. Obviously, for the smaller diameter side arm the axial distance over which take off is possible is reduced. In fact the overall area available for liquid to “fall” into the side

---



arm is three times smaller than that available with the regular T-junction. This leads to the significantly reduced liquid take off for similar fractions of gas diverted.

The above theory may go some way to explain the very similar data obtained for the three runs with the reduced T-junction with the high liquid inlet flowrates (see Figure 4-2). The reduction in side arm diameter would significantly reduce the time available for take off. The liquid flowrates are only increased by around 0.1 m/s each time. This means the time available for the liquid slug passing the reduced diameter side arm entrance to diverted is between 0.13-0.24 seconds. This is  $3/5^{th}$  of the time available for the same liquid flowrates passing the larger diameter T-junction. The time difference of 0.1 seconds between the three different flow conditions is not large enough to produce a measurable difference in readings.

For the stratified flow experiments with the low liquid ( $U_{ls}$  less than 0.0535 m/s) but high gas ( $U_{gs}$  greater than 12 m/s) inlet flowrates the depth of the liquid film was seen to be much less, Rea (1998) measured the film thickness to be around 0.015 m. The significantly reduced liquid inlet superficial velocity has reduced the momentum of the liquid phase by a factor of a hundred, which in turn had the effect of increasing the fraction of liquid drawn off down the side arm for a given fraction of gas diverted. Increasing the gas velocity from 12 to 24 m/s also increases the fraction of liquid removed for a given fraction of gas drawn off as the higher gas velocity helps overcome the liquids inertia into being taken off down the branch arm. These trends can be clearly seen if Figure 4-4 and Figure 4-5 are compared.



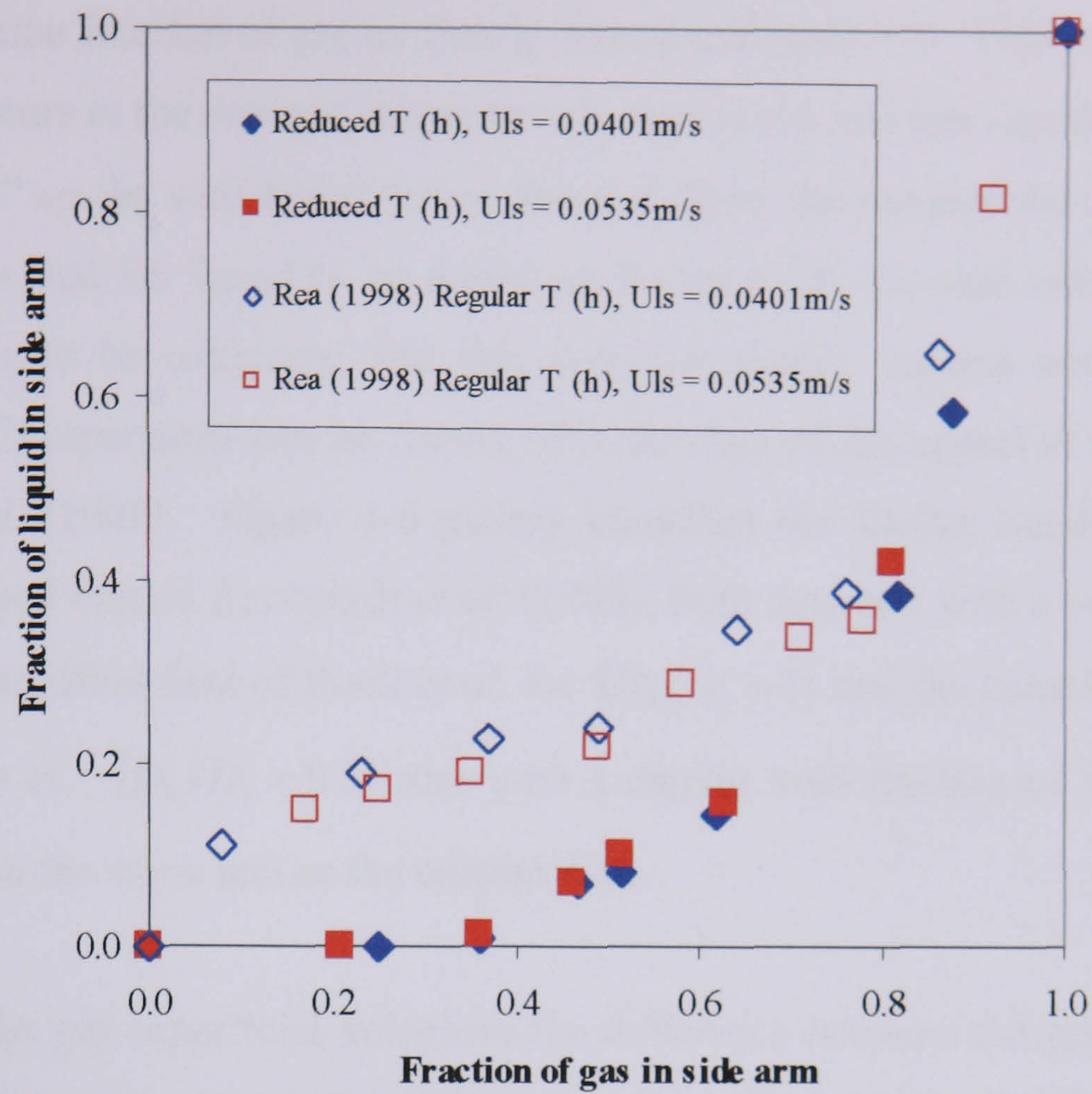


Figure 4-4: Phase split for stratified flow at a horizontal regular and reduced T-junction,  $U_{gs} = 12 \text{ m/s}$

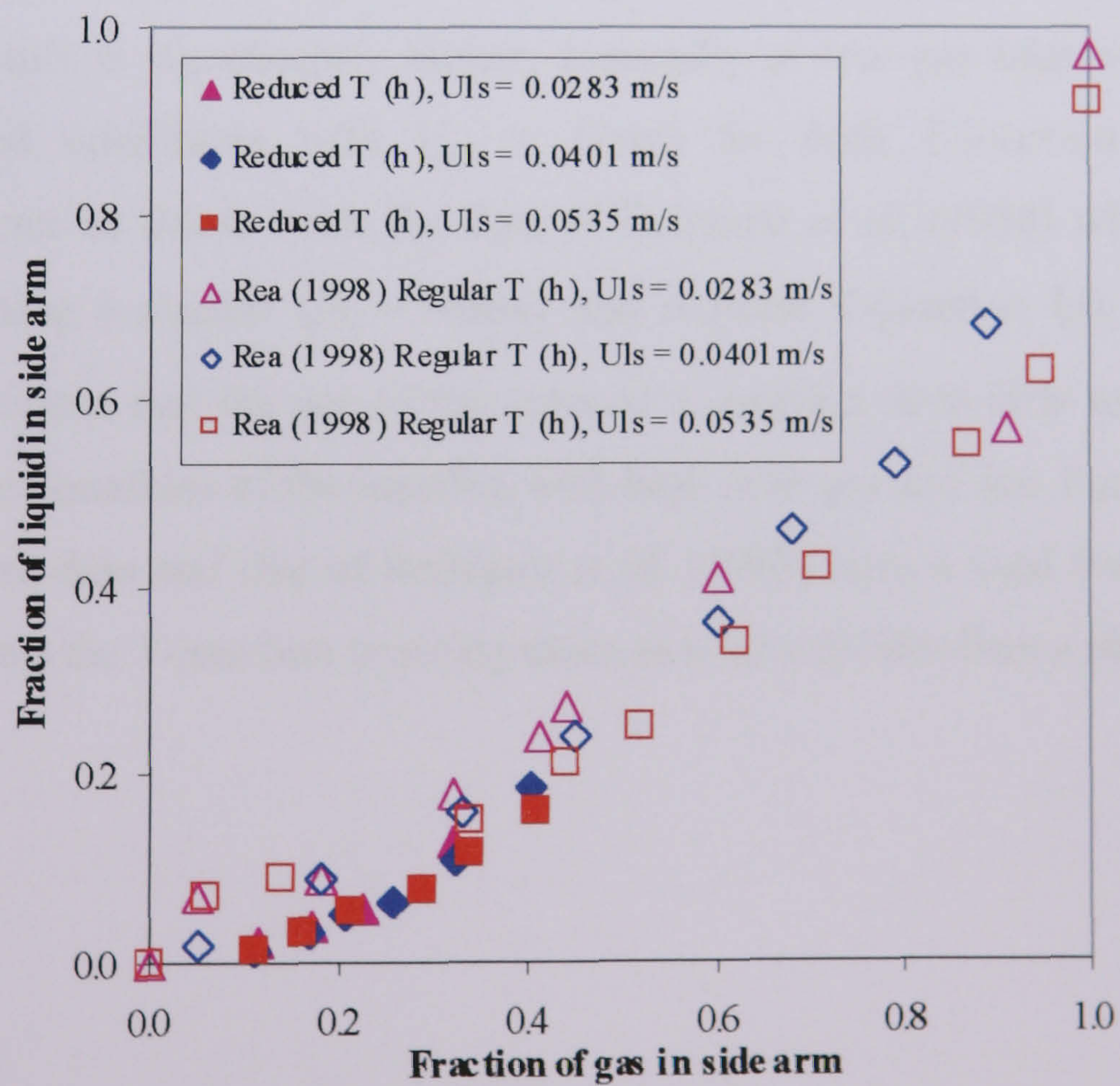


Figure 4-5: Phase split for stratified flow at a horizontal regular and reduced T-junction,  $U_{gs} = 24 \text{ m/s}$



Reducing the side arm diameter decreases the fraction of liquid drawn down the side arm for the same fraction of gas as clearly shown in Figure 4-4. This improved phase separation occurs at the reduced diameter side arm as the low gas-liquid interface now has to “climb” up the wall before being diverted down the reduced diameter side arm. This indicates that for liquid to be drawn up the step into the side arm the inertia of the phase has to be overcome and this does not readily happen under these inlet conditions. Comparisons can be drawn with the data of Azzopardi *et al.* (1988) and Shoham *et al.* (1989). Figure 4-6 plainly identifies the similar trends between the current data and that of Azzopardi *et al.* (1988), both data sets with a void fraction of 0.934. The stratified data of Buell *et al.* for  $(D_3/D_1 = 1)$  and the complementary data by Walters *et al.*  $(D_3/D_1 = 0.5)$  also with a similar void fraction of 0.93 were also found to lie on the same loci as the current data.

At higher inlet gas superficial velocities the difference between the phase separation qualities of the regular and reduced T-junctions are diminished, see Figure 4-5. The combination of the higher gas momentum and reduced diameter side arm overrides the inertia forces of the liquid phase meaning the fraction of liquid being drawn off with  $U_{gs} = 24\text{m/s}$  is significantly higher, especially at low gas take off rates, than under stratified conditions with  $U_{gs} = 12\text{m/s}$  for both T-junction geometries. Comparisons can be drawn with the data of Reimann *et al.* (1988) who performed experiments using a regular  $(D_1 = 50\text{mm})$  and reduced T-junction  $(D_3/D_1 = 0.52)$ . Figure 4-7 indicates that the use of the reduced T-junction does little to enhance the phase separation qualities of the junction with high inlet gas and low liquid flowrates. Both the current data and that of Reimann *et al.* (1988) have a void fraction of 0.96 and in both cases the T-junction is acting more as a flow divider than a phase splitter.



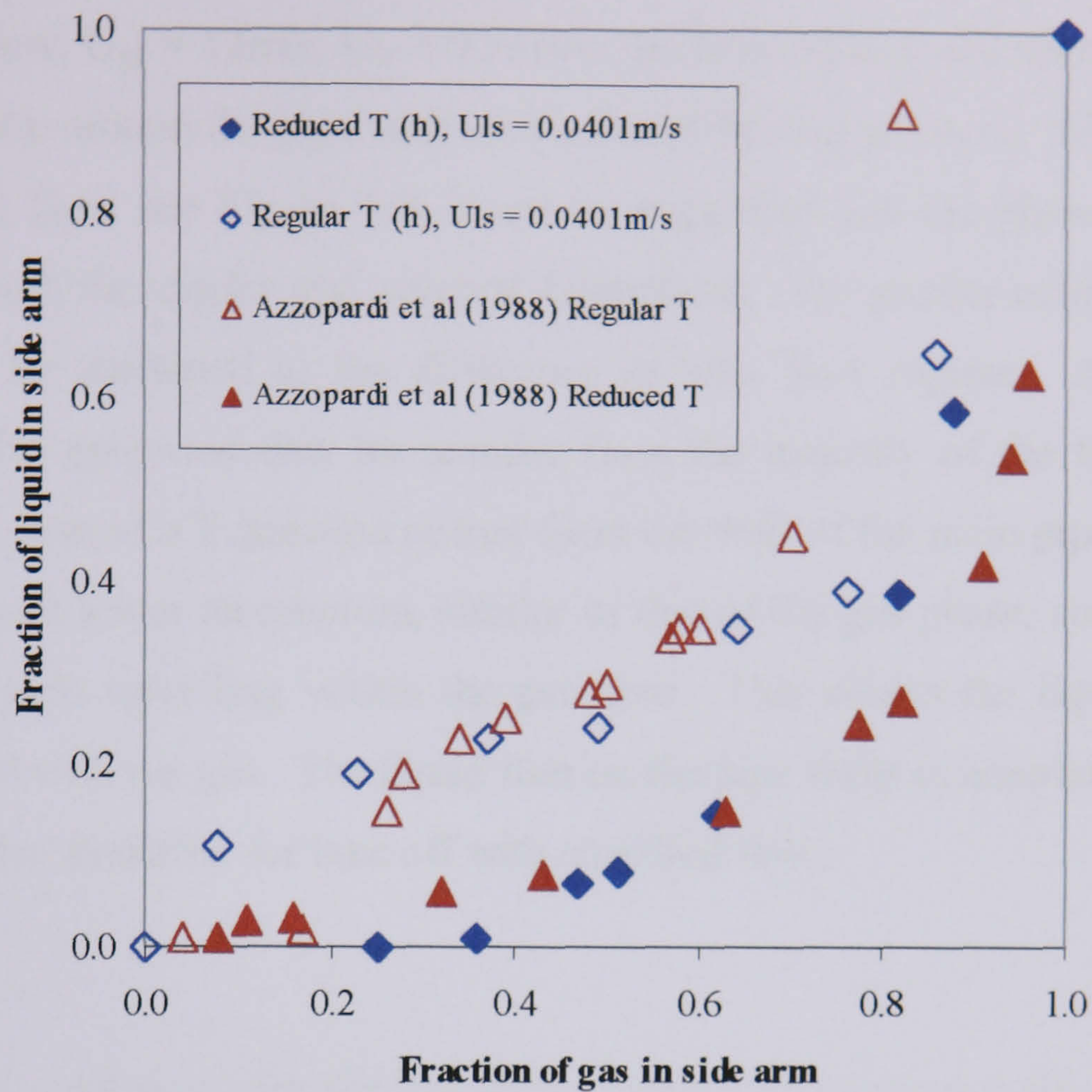


Figure 4-6: Comparison of current stratified flow data ( $U_{gs} = 12 \text{ m/s}$ ) with that of Azzopardi *et al.* (1988) based on CISE void fraction of 0.934

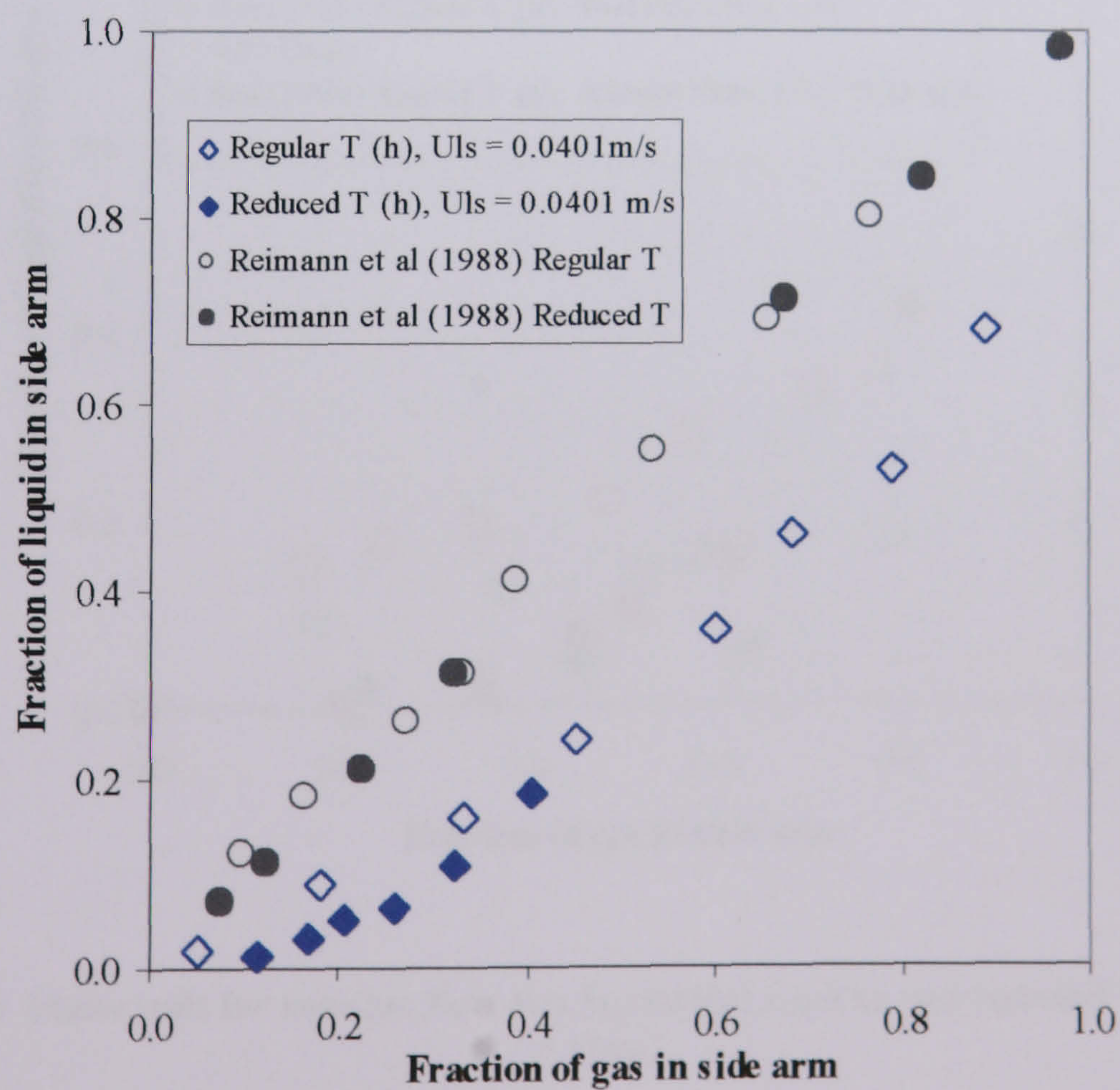


Figure 4-7: Comparison of current stratified flow data ( $U_{gs} = 24 \text{ m/s}$ ) with that of Reimann *et al.* (1988) based on CISE void fraction of 0.96



### Annular Flow

For annular flow,  $U_{gs} = 12\text{m/s}$ ,  $U_{ls} = 0.31\text{m/s}$ , the liquid phase was seen to flow as an asymmetric film around the pipe wall with a faster flowing gas core. When compared with stratified flow, see Figure 4-8, it can be suggested that the phase separation is increased at both the regular and reduced T-junctions. The greater reduction in liquid take off can be attributed to the difference in inlet flow regime. Azzopardi and Whalley (1982) proposed that for annular flow the majority of the liquid diverted down the side arm of a T-junction comes from the wall of the main pipe. This liquid flow has a much lower momentum, similar to that of the gas phase, compared to the entrained droplets travelling within the gas core. This allows the liquid film to be easily diverted with the gas. The liquid film on the pipe walls in annular flow is much thinner than that available for take off with stratified flow.

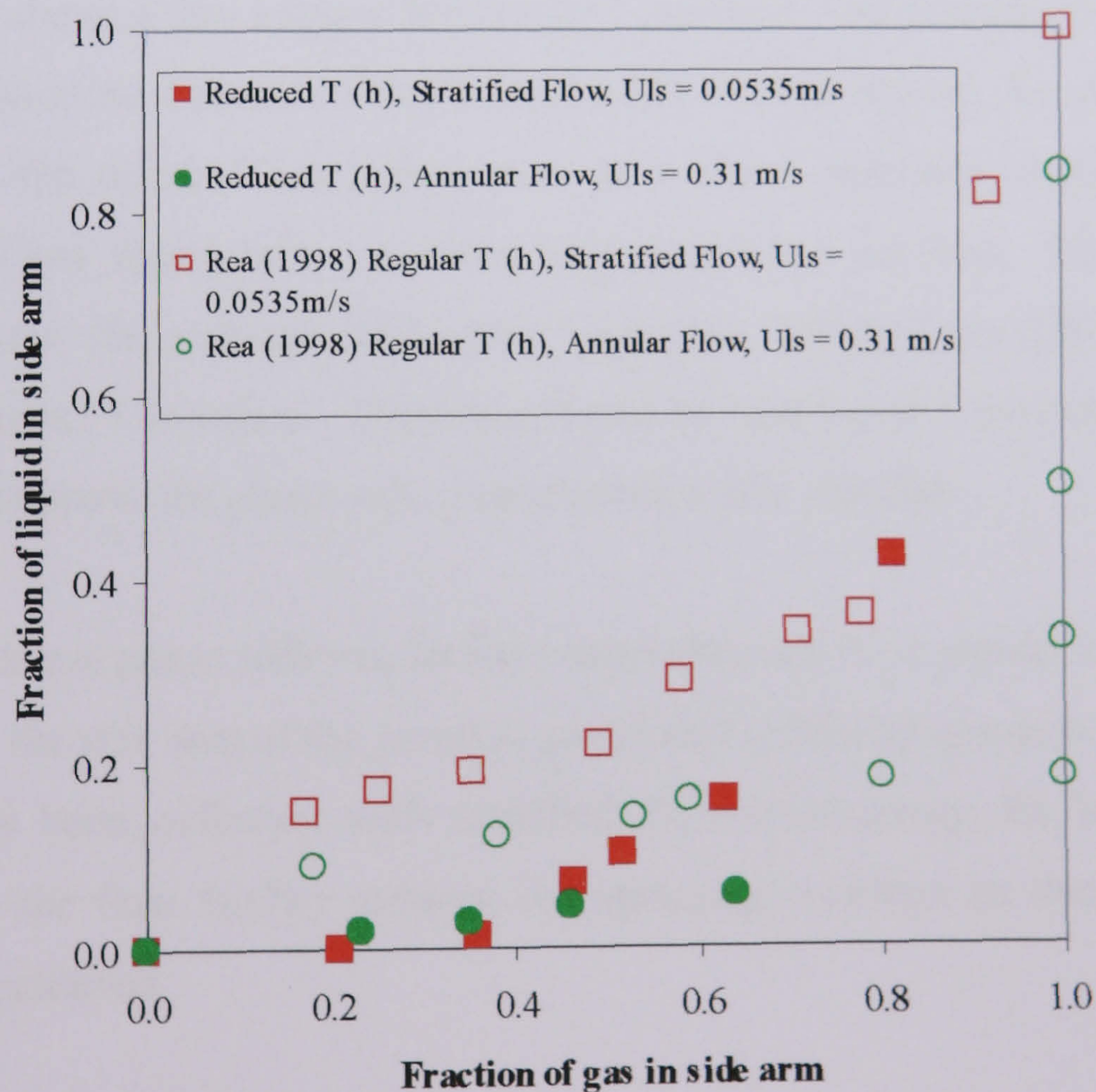


Figure 4-8: Phase split for annular flow at a horizontal regular and reduced T-junction,  $U_{gs} = 12\text{m/s}$



So although the liquid film is easily diverted, the fraction of liquid taken off down the side arm, with increasing gas take, is reduced for annular flow. The plateau present in the separation curves for both the regular and reduced T-junctions easily identifies this. The easily removed liquid film has been diverted but the faster flowing droplets entrained in the gas core can not be separated down the side arm until over 90% of the inlet gas has been diverted. After this critical value the fraction of liquid drawn off down the side arm dramatically increases with increasing gas take off. The phase split results for both the regular and reduced T-junction follow similar trends with the reduced junction drawing less liquid down the side arm. This is again due to the reduced area available for film take off, as previously described for stratified flow.

#### **4.2.2 Vertically upwards side arm (+90°)**

Section 4.2.1 showed that using a horizontal T-junction with a reduced diameter side arm could reduce the fraction of liquid drawn off. As was shown, for all approaching flow regimes the reduced T-junction acted as a phase separator, except when very high gas and low liquid inlet velocities approached the junction. However, under these conditions the reduced horizontal T-junction behaved no differently to the regular horizontal T-junction. Therefore it can be concluded a horizontal reduce T-junction can improve the phase split characteristics of a junction.

Within this section phase split results have been obtained for a regular and reduced T-junction with the side arm of the junction positioned vertically upwards (+90 °). Flow split data has been collected with stratified flow approaching the junction. The alterations to the flow facility reduced the operating envelope so that annular flow could not be achieved.

Previous authors have compared the phase split characteristics of a T-junction where the orientation of the side arm altered from the horizontal. Such investigations have been summarised Table 2-2, but close inspection of the table shows these are mainly confined to small diameter T-junctions. Those who have investigated the phase split



with larger diameter pipelines were mainly interested in answering a specific problem rather than collecting a range of data.

As previously stated in Chapter 2, main influences affecting the phase separation at a T-junction are due to gravity and the inertia of the phases. For horizontal flow a pressure gradient exists perpendicular to the direction of flow. If a homogeneous gas-liquid mixture flows into a region where a pressure gradient exists, like at a T-junction, then the gas phase is better able to follow the direction of the low pressure, due to its lower inertia, compared to the liquid phase. However, if the two phases have different phase velocities, as is often the case, the liquid phase may preferably enter the branch depending on the local values of the momentum fluxes of the phases,  $(\rho v^2)_l$  and  $(\rho v^2)_g$ , around the branch inlet and the branch arm orientation.

The influence of gravity on phase separation is visible in two ways. Firstly, within the horizontal inlet the denser liquid phase preferentially flows nearer the bottom and the gas phase nearer the top of the pipe. Secondly, in the branch arm it can be easily seen that gravity forces have a strong effect on the flow split at the T-junction and flow reversal of one phase into the main horizontal pipe often occurs when the branch axis is inclined with respect to the horizontal. More liquid is diverted into the side arm when it is inclined downwards and conversely a significant amount of inlet gas has to be diverted with the side arm inclined vertically upwards before any liquid is drawn off. These observations hold for all main pipe diameters and are accentuated with reduced side arm ratios.

By adapting the orientation of the junction, the effects of inertia and gravity may enhance the phase separation that already occurs at a simple horizontal T-junction, as described in Section 4.2.1. Both the regular and reduced T-junctions were used to study the split of stratified flow approaching a T-junction with the branch arm inclined vertically upwards.

As with the branch arm of the junction lying horizontally, the phase split results for stratified flow approaching the junction may be considered in two groups. The first



with low gas and high liquid flowrates approaching the junction and the second with high gas but low liquid inlet liquid flowrates.

For the first set of conditions, low gas and high liquid inlet flowrates, with the side arm vertically upwards the phase separation abilities of both the regular and reduced T-junctions were found to be practically identical, see Figure 4-9. In both cases the limit of all gas take off was 90% and beyond this critical value less than 20% of the liquid was diverted. The similarity of phase split for both junctions can be attributed to the very high momentum of the liquid phase.

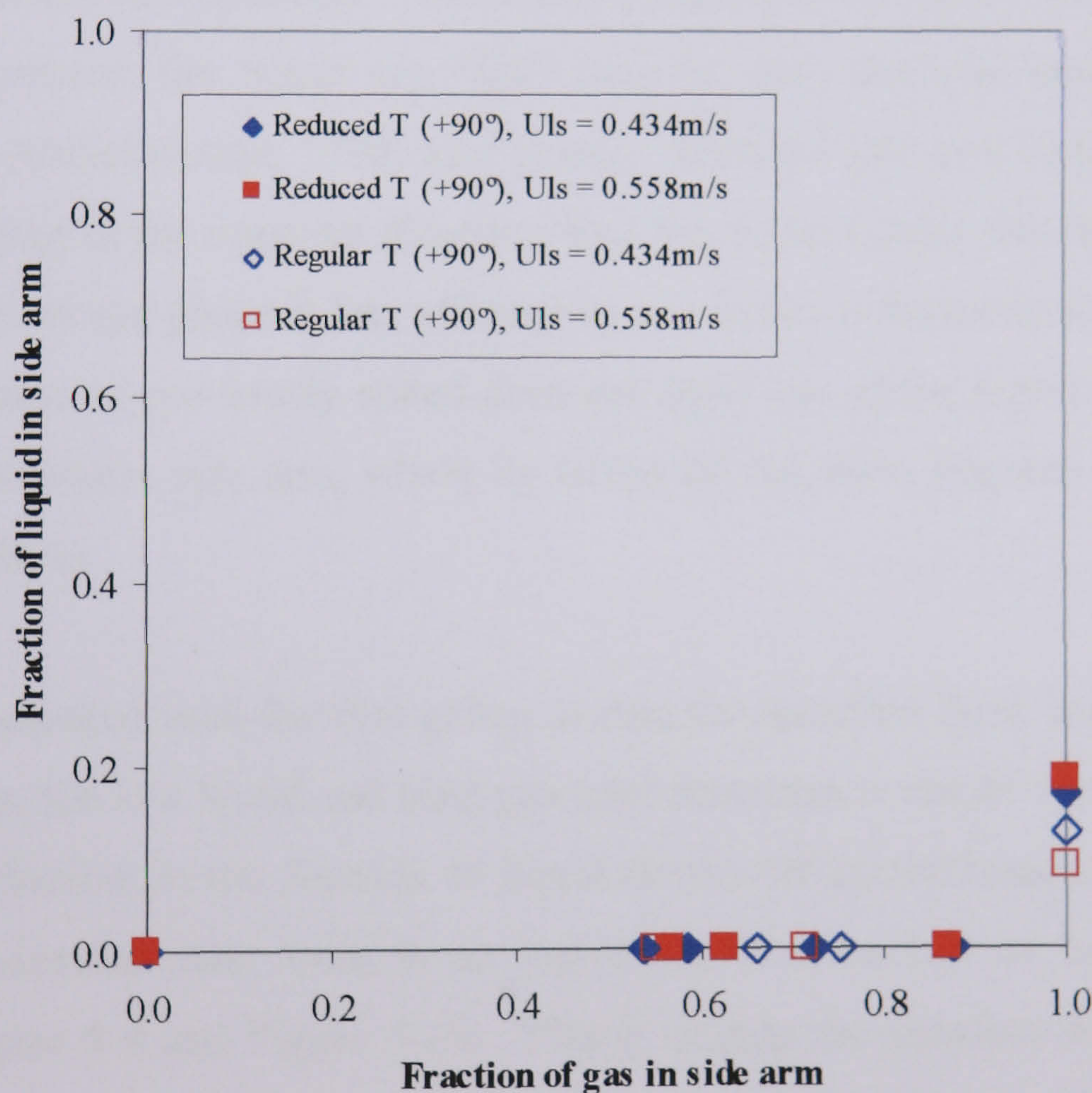


**Figure 4-9: Phase split for stratified flow at a regular and reduced T-junction with a vertically upwards branch arm,  $U_{gs} = 4\text{m/s}$**

Unlike the horizontally orientated junction the liquid can not “fall” into the side arm. With a vertically upwards side arm the liquid must be drawn up by the gas stream but with the very low gas velocities present, the fraction of gas drawn up the side arm has



insufficient velocity to overcome the inertia of the higher momentum liquid phase despite the water travelling close to the top of the pipe. Thus, no liquid is drawn up with the gas. This is a similar trend exhibited by the slug flow data of Reimann and Smoglie (1983) which showed that even with a very small diameter branch arm, the oscillatory behaviour of slug flow, i.e. gas then liquid passing under the entrance to the branch arm, was not indicative of a large liquid take off but the gas was drawn up the branch arm by the pressure drop across the junction.

Considering the geometry of the two T-junctions, one with a horizontal and one with a vertically upwards side arm the noticeable reduction of liquid in the branch arm in the latter case can be explained. With the T-junction lying horizontally and the deep liquid film present, the liquid can “fall” into the side arm (the dam break theory proposed by Arirachakaran, 1990) as it passes. With the side arm vertically upwards, gravity is acting in the opposite direction thus the liquid cannot just fall into the side arm. The lighter gas phase is less affected by gravity so is drawn up the side arm. Its low momentum, as previously stated does not draw any of the liquid with it even in the smaller diameter side arm, where by Bernoulli the same fraction of gas diverted would flow faster.

However, compared with the first group of data for stratified flow, data taken for the second group, the low liquid and high gas inlet flowrates, it can be seen that although there is a reduction in the fraction of liquid drawn off up the branch arm compared with the horizontal case, there is an increase in the fraction of liquid taken off, compare Figure 4-9 and Figure 4-10. This is despite the interface between the two phases being lower for the conditions in Figure 4-10 and hence further from the entrance of the branch arm.



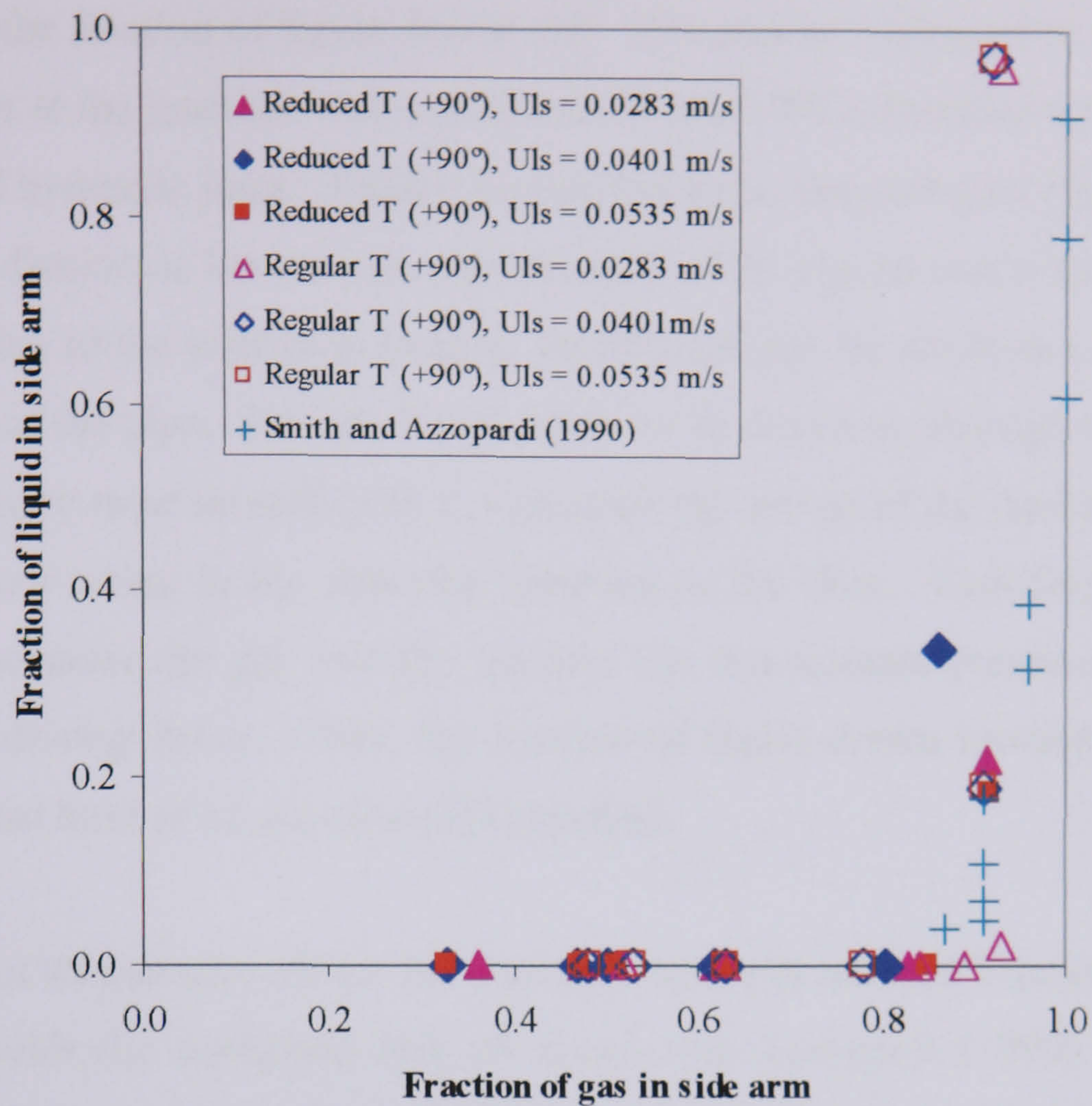


Figure 4-10: Phase split for stratified flow at a regular and reduced T-junction with a vertically upwards branch arm,  $U_{gs} = 12\text{m/s}$

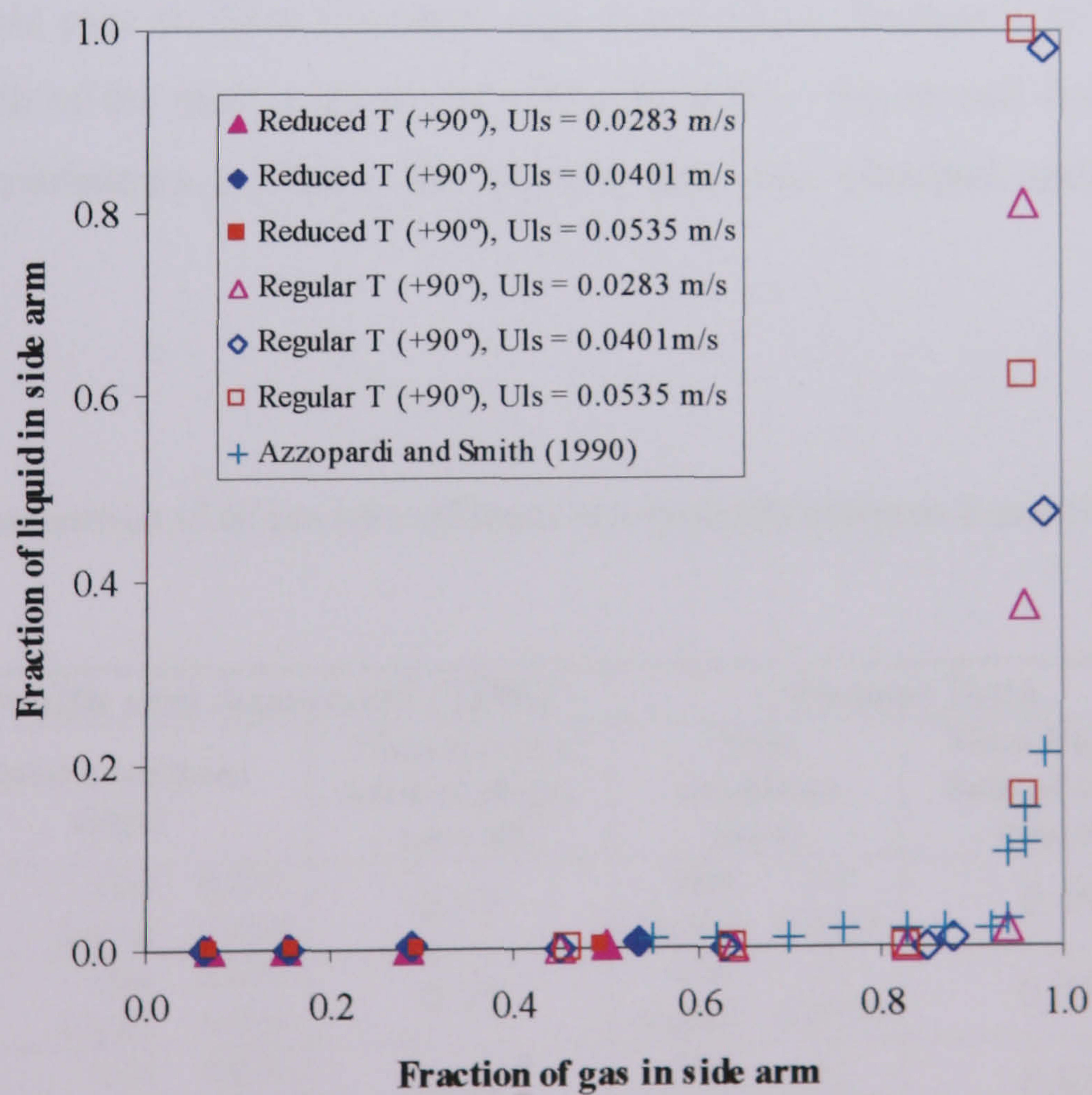


Figure 4-11: Phase split for stratified flow at a regular and reduced T-junction with a vertically upwards branch arm,  $U_{gs} = 24\text{m/s}$



Both Figure 4-10 and Figure 4-11 show that at a critical gas take off there is a rapid increase in the fraction of liquid drawn off. This can be attributed to the increase in liquid height at the junction. Azzopardi and Smith (1992) identified this phenomenon as a form of hydraulic jump. Unlike for the horizontal side arm (see Figure 4-4), there is a lack of distinction between the performance of the regular and reduced T-junction but this is due to the inlet flow pattern. In all cases the liquid flows as a layer along the bottom of the pipe. For any liquid phase to be drawn up through the branch arm the gas velocity must be sufficient to overcome the inertia of the liquid phase and the gravity forces acting in the opposite direction to the flow. Reducing the side arm diameter increases the gas velocity initially but downstream pressure losses would reduce the driving force. Thus, the fraction of liquid drawn upwards is negligible until a critical limit of all gas take off is reached.

The limits of all gas take off for the vertically upwards reduced T-junction have been compared with the published data of Smith and Azzopardi (1990) in Table 4-1. Comparisons were drawn where the two phases of the new and published data had similar momentums. Smith and Azzopardi (1990) used a much smaller scale T-junction, main pipe 0.038m diameter, side arm 0.025m diameter. In both cases the diameter ratio of the main pipe to the side arm of 0.6. Smith and Azzopardi carried out their experiments at 3bara, the present data was obtained under atmospheric conditions.

**Table 4-1: Comparison of all gas take off limits in a vertically upwards T-junction ( $D_3/D_1 = 0.6$ )**

Smith and Azzopardi (1990)		Present Data	
Inlet conditions (kg/s)	Mass fraction limit of all gas take off	Inlet conditions (m/s)	Mass fraction limit of all gas take off
Gas 0.053 Liquid 0.064	0.55	Gas 24 Liquid 0.0535	0.46
Gas 0.016 Liquid 0.066	0.79	Gas 12 Liquid 0.0535	0.85
Gas 0.023 Liquid 0.012	0.74	Gas 12 Liquid 0.0283	0.83



These results, all taken from the stratified flow regime, indicate that the limit of all gas take off is similar despite the difference in scale of the two systems. This is perhaps not surprising since the momentum of each of the fluids were similar so proportionally the same amount of gas would be required to draw off the liquid. The limit for the present data may be higher due to the larger distance the liquid has to travel before being drawn off the reduced side arm, thus the slightly greater amount of gas taken off before liquid entrainment. The data of Penmatcha *et al.* (1996) also indicated that the limit of all gas take off was 0.8 for inclinations over 35°. Using a regular T-junction they also noted that the phase split become independent of inlet liquid velocities, a similar trend is exhibited by the current data, with all phase separation curves lying together. Hence, the inclination angle of the side arm and gas splitting ratios are the major factors governing phase split.

As for the horizontal T-junction, by significantly increasing the inlet gas phase velocity the inertia of the liquid phase can be overcome. This is highlighted in Table 4-1, where for both data sets doubling the inlet gas velocity halves the limit of all gas take off for the same inlet liquid velocity.

#### **4.2.3 Vertically downwards side arm (-90°)**

The affects of moving the side arm of the T-junction from the horizontal to vertically upwards (+90°) was discussed in the previous section. It was found that a T-junction with a vertically upwards side arm performed as a partial phase separator that could be relied upon with stratified flow approaching the junction to produce a gas rich stream in the branch arm from a multiphase inlet. The horizontal (0°) T-junction did not perform as well but a significant increase in the phase separation ability of the junction, for all approaching flow patterns, was seen if the side arm diameter was reduced. The final side arm orientation studied was vertically downwards (-90°).

A comprehensive investigation considered stratified and annular inlet flow patterns approaching both the regular and reduced T-junctions with a vertically downwards

---



side arm. A series of experiments were performed to investigate the effect of inlet gas and liquid superficial velocities on the phase split. Visual observations were noted as well as phase split data recorded.

Generally, the effect of the different inlet momentum fluxes of the two phases favours the gas phase to enter the branch arm, however, with vertically downwards side arms, the effects of gravity have a much stronger influence. Under these conditions liquid is preferentially extracted through the branch arm as opposed to gas for the vertically upwards side arm.

As with other side arm orientations research has previously been confined to smaller diameter pipes, both with very small diameter side arm, simulating breaks in the horizontal coolant pipes of nuclear reactors by Smoglie, Reimann and Müller (1985) and Anderson (1987), and with larger side arm diameters, more representative of the junctions found within piping networks, Reimann *et al.* (1988), Azzopardi and Whalley (1982).

A more recent study by Penmatcha *et al.* (1996) performed a thorough investigation of a range of angles from the horizontal,  $0^\circ$ , to  $-60^\circ$ , downwards. As expected the more inclined downward the branch the more liquid is diverted and for their system complete separation of the liquid phase was achieved at inclinations beyond  $-60^\circ$ . Although no visual observations were noted within their publication a mechanistic model based on the momentum equations applied to the separation streamlines of the gas and liquid phases, originally developed by Shoham *et al.* (1987), showed promise of being able to predict phase split at a downwards T-junction although deviation of the model from the experimental results worsened the more vertical the side arm became.

Seeger *et al.* (1985) approached the phase split at a T-junction from a fairly unconventional point of view, by slowly reducing the resistance within the downwards branch arm, rather than slowly increasing it. Initially the branch arm valve was closed ( $G_3/G_1 = 0$ ) and the arm filled with water. A small fraction of the homogeneously mixed fluid at the inlet flowing over the top of the branch arm created



a recirculation zone where bubbles were seen to rise up the branch arm and re-enter the main run arm. Similar observational results were seen at both the large diameter regular and reduced T-junctions at the inlet flowrates investigated within this thesis when the branch arm butterfly valve was practically closed. Seeger *et al.* noticed a change at higher mass flux ratios ( $G_3/G_1 \geq 0.065$ ) where the recirculation zone first filled with air and then the gas-liquid interface descended until the branch arm was filled with air except for a thin liquid film flowing down the pipe walls. This was similar to the flow observed down the branch arm with low side arm resistances with the T-junction currently being studied.

Studying the data obtained for the downward inclined branch arm, it is immediately apparent that the liquid is easily diverted into the branch arm compared with either the horizontal or the vertically upwards case, see Figure 4-12. For all cases with a vertically downward orientated side arm, the phase split curves lie above the line of equal split indicating liquid dominated phase split. This is due to the physical phenomenon involved in the phase splitting process. If the dominant forces that control the motion of the fluid at the T-junction, namely gravity, inertia and pressure drop, are considered then the mechanisms involved can be understood. For downwards side arms the inertia and the gravity forces are effectively acting in opposite directions with inertia favouring the gas and gravity forces favouring the liquid phase to flow preferentially into the branch arm. The gravity forces acting on the liquid phase are generally much stronger than the effects of pressure drop across the T-junction but both act in favour of the liquid to be drawn down the side arm.



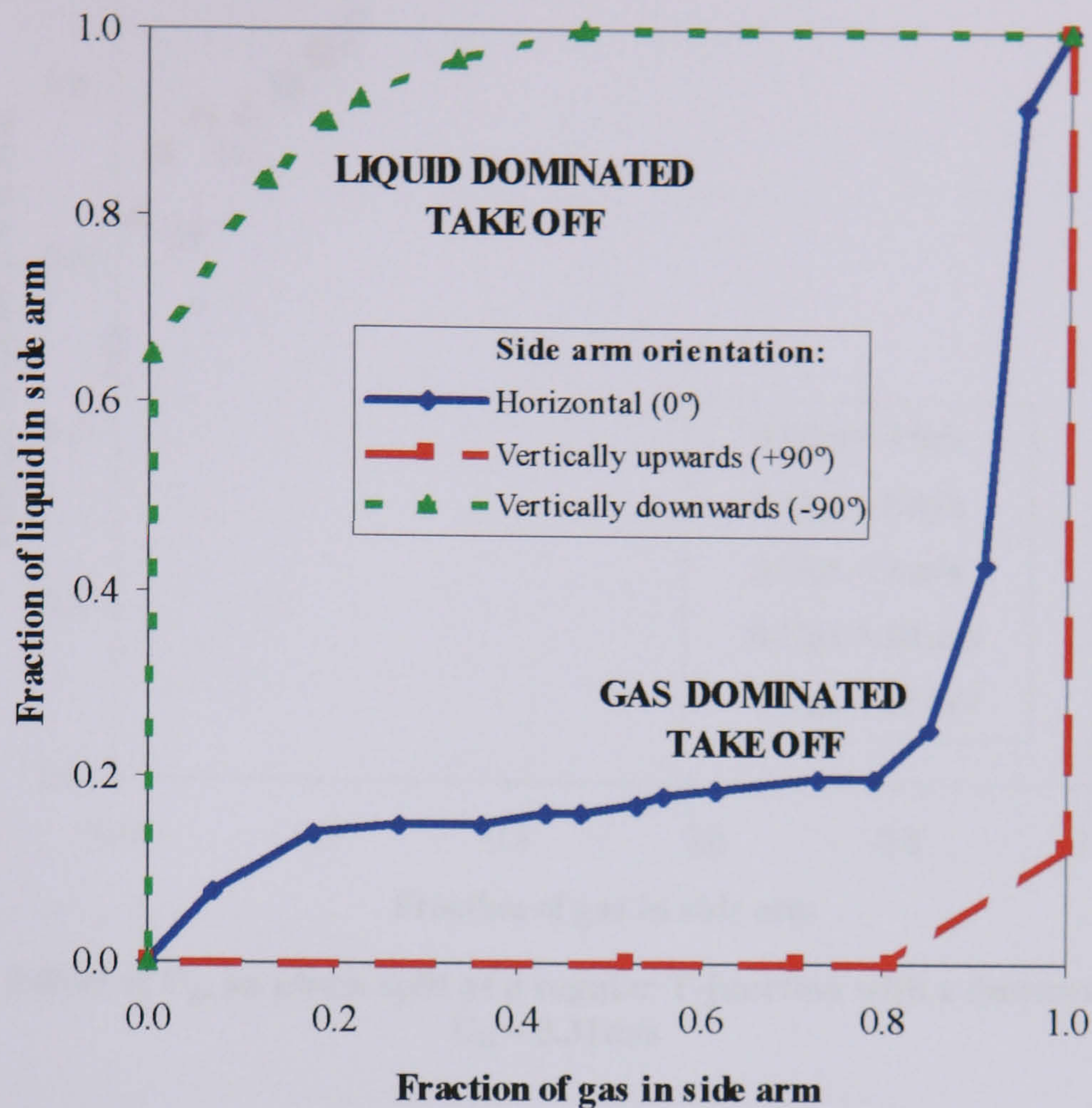


Figure 4-12: Phase split comparison of different side arm orientations,  $U_{gs} = 8\text{m/s}$ ,  $U_{ls} = 0.31\text{m/s}$

As with the side arm lying horizontally the general observation can be made - increasing inlet gas superficial velocity,  $U_{gs}$ , at constant inlet liquid superficial velocity,  $U_{ls}$ , has a nominal effect on the side arm quality, see Figure 4-13. Conversely, increasing  $U_{ls}$ , whilst  $U_{gs}$  remains constant, dramatically increases the fraction of liquid drawn off down the side arm, see Figure 4-14. This is due to the higher momentum of the liquid phase exerting a much greater influence over the phase separation characteristics of the junction and dominating the any changes increasing the gas velocity may have on the system. The phase split occurring at the junction has been discussed for both stratified and annular flow approaching the junction.



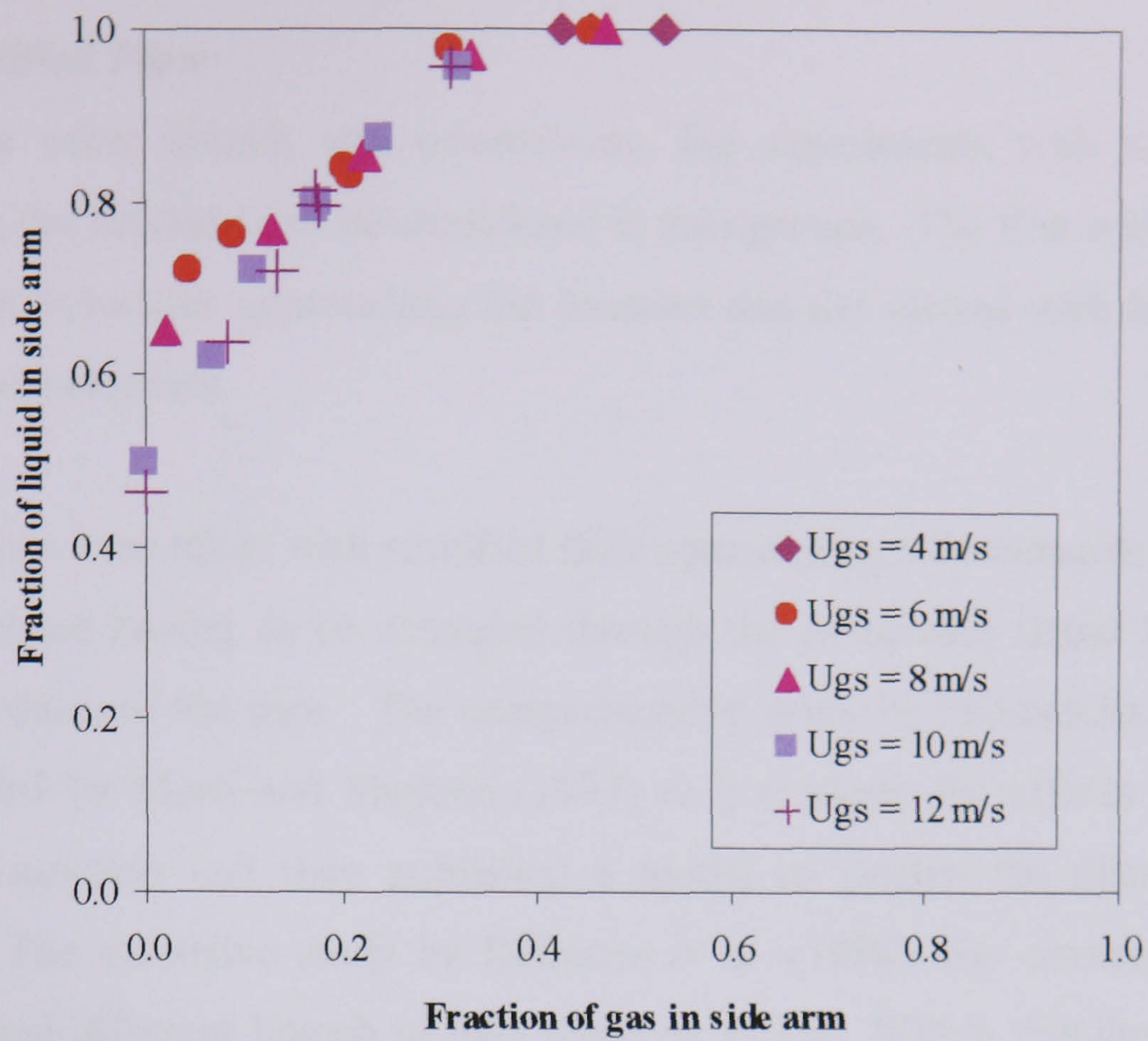


Figure 4-13: Effect of  $U_{gs}$  on phase split at a regular T-junction with a downwards side arm,  $U_{ls} = 0.31$  m/s

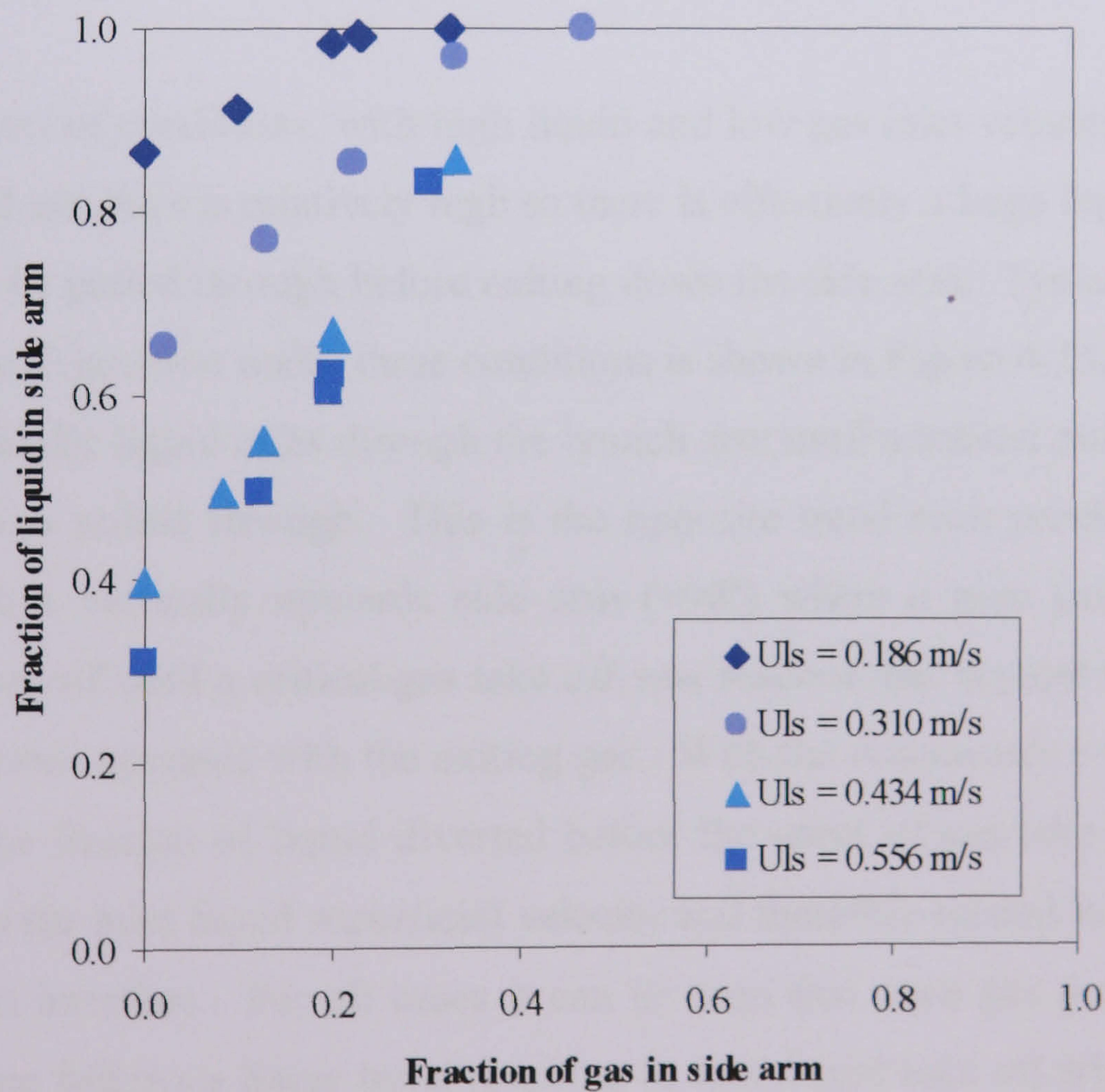


Figure 4-14: Effect of  $U_{ls}$  on phase split at a regular T-junction with a downwards side arm,  $U_{gs} = 8$  m/s



### ***Stratified Flow***

As with the other branch arm orientations, the experiments with stratified flow approaching the junction can be considered in two groups. The first with high liquid, low gas inlet velocities approaching the junction and the second with low liquid but high gas inlet velocities.

An interest has been taken with stratified flow approaching a downwards side arm due to the gas phase having to be extracted through the permanent liquid layer flowing along the bottom of the pipe. The comprehensive study by Penmatcha *et al.* (1996) was expanded by Marti and Shoham (1997) to investigate the affects of a reduced diameter T-junction and they published a model to predict the phase separation occurring. The extensive study by Reimann *et al.* (1988) also covered many inlet conditions and different branch to inlet diameter ratios. Within this thesis the phase separation occurring at a large diameter T-junction was investigated with both the regular and reduced T-junction with stratified flow.

For the first set of conditions, with high liquid and low gas inlet velocities mean that the gas-liquid interface is relatively high so there is effectively a large liquid layer that the gas must be pulled through before exiting down the side arm. Typical phase split results for the T-junction under these conditions is shown in Figure 4-15. For both T-junctions, initially liquid exits through the branch arm until a critical point is reached and then gas is pulled through. This is the opposite trend seen previously for the junction with a vertically upwards side arm (+90°) where a pure gas stream was initially drawn off until a critical gas take off was reached and beyond that point the liquid was drawn upwards with the exiting gas. With the downwards (-90°) side arm orientation the fraction of liquid diverted before the onset of gas take off occurs is dependant on the inlet liquid superficial velocity and therefore related to the height of the gas-liquid interface. For all cases it can be seen that once gas pull though has started the data follows a linear trend resulting in total liquid take off with 40% of the gas extracted.



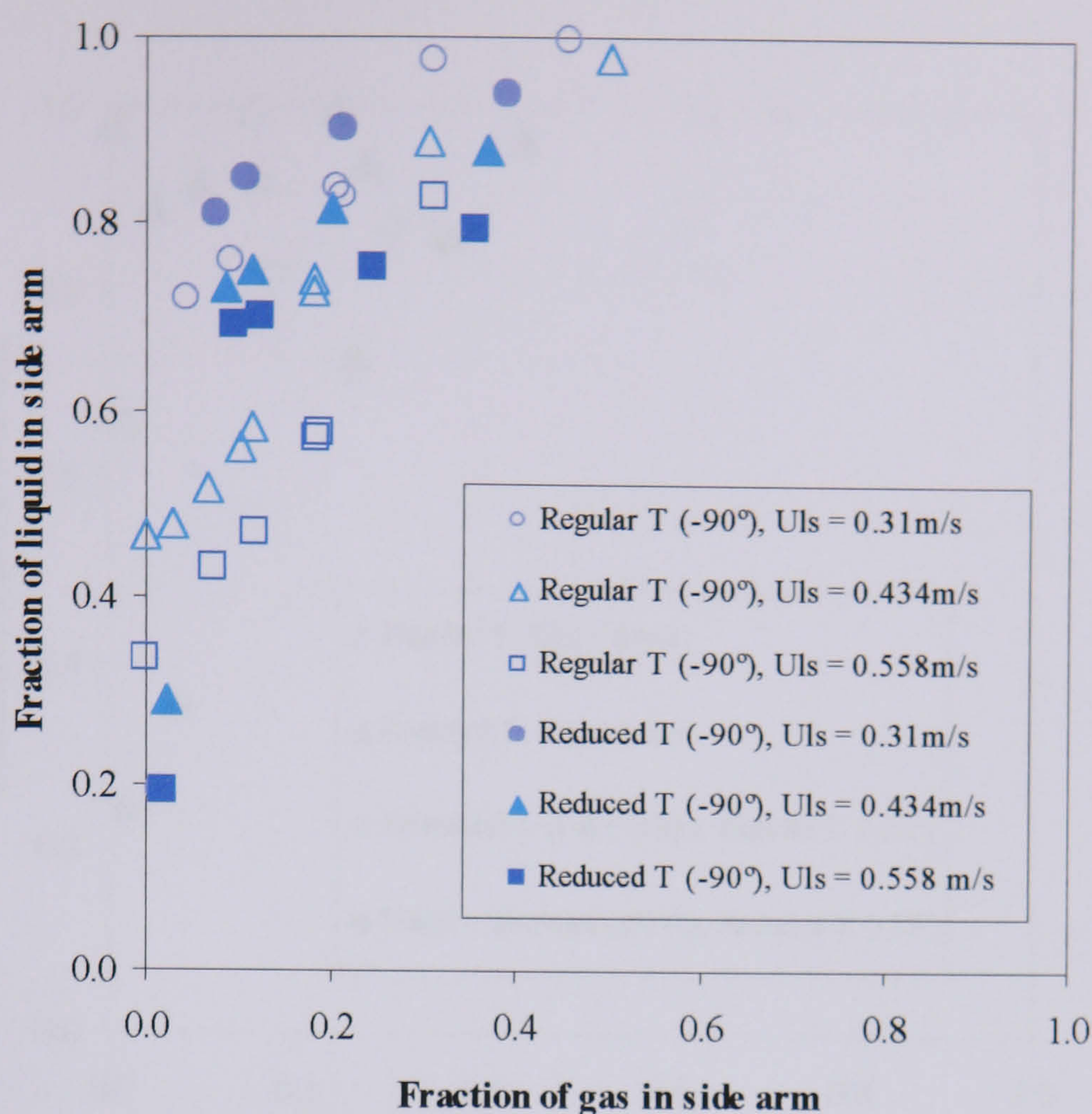


**Figure 4-15: Phase split for stratified flow at a regular and reduced T-junction with a vertically downwards side arm,  $U_{gs} = 6\text{m/s}$**

For the high liquid, low gas inlet flowrate experiments it can be seen in Figure 4-15 that reducing the side arm diameter increases fraction of liquid that can be diverted down the side arm before the onset of gas take off is reached. This could be related to the arguments previously presented where by reducing the diameter of the side arm the area of take off is reduced and therefore the time available of the liquid extracted to effect the gas stream flowing above it is reduced. The data of Penmatcha *et al.* (1996) and the complementary work of Marti and Shoham (1997) with a reduced T-junction can also be seen to show similar tendencies, as shown in Figure 4-16. Although within their high pressure system they found complete gas-liquid separation to occur with orientations below  $-60^\circ$ . The data of Reimann *et al.* (1988) also exhibits the same correlation with reducing side arm diameter.



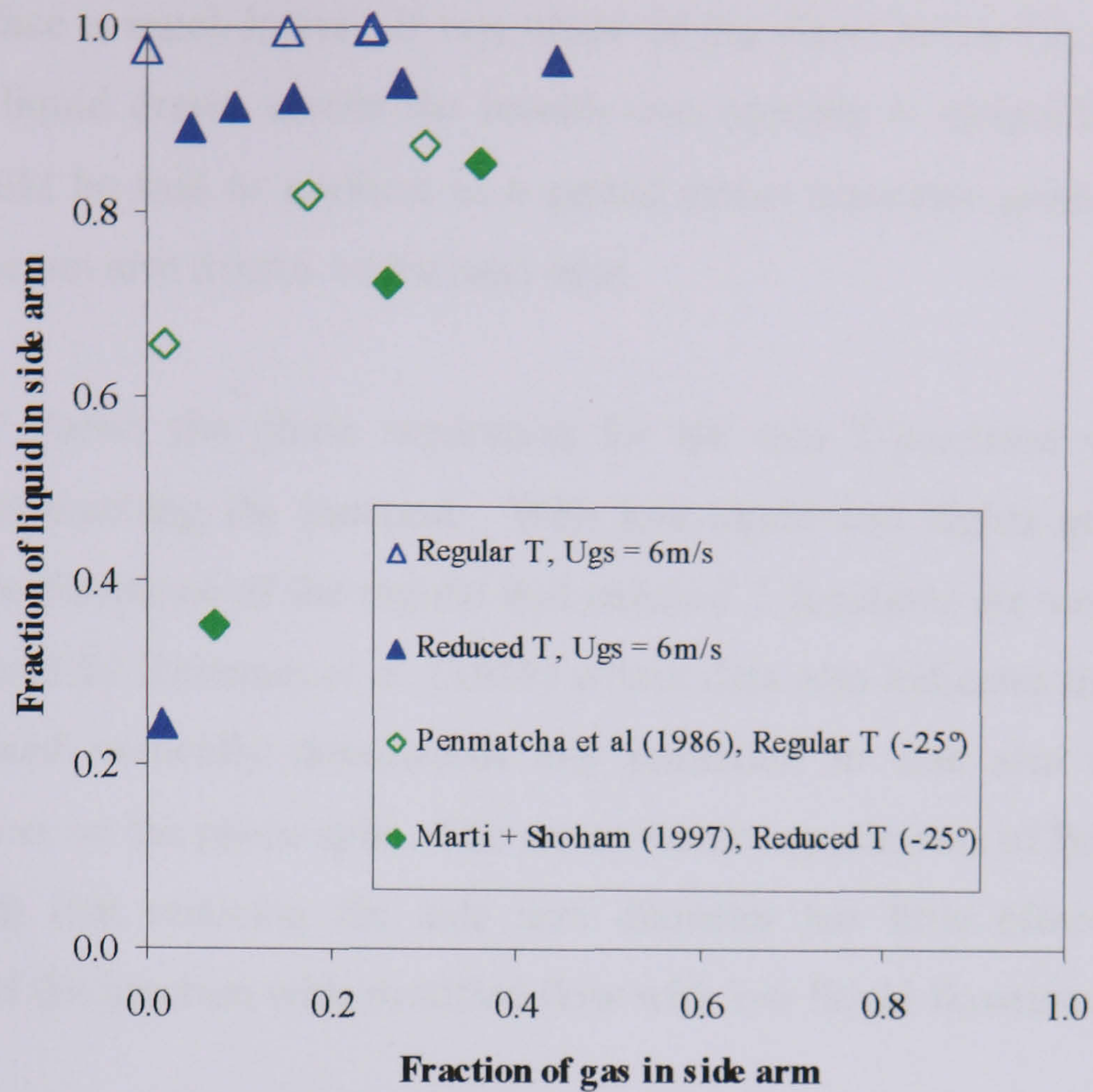


Figure 4-16: Comparison of current stratified flow data ( $U_{ls} = 0.186 \text{ m/s}$ ) with published data, CISE void fraction of 0.837

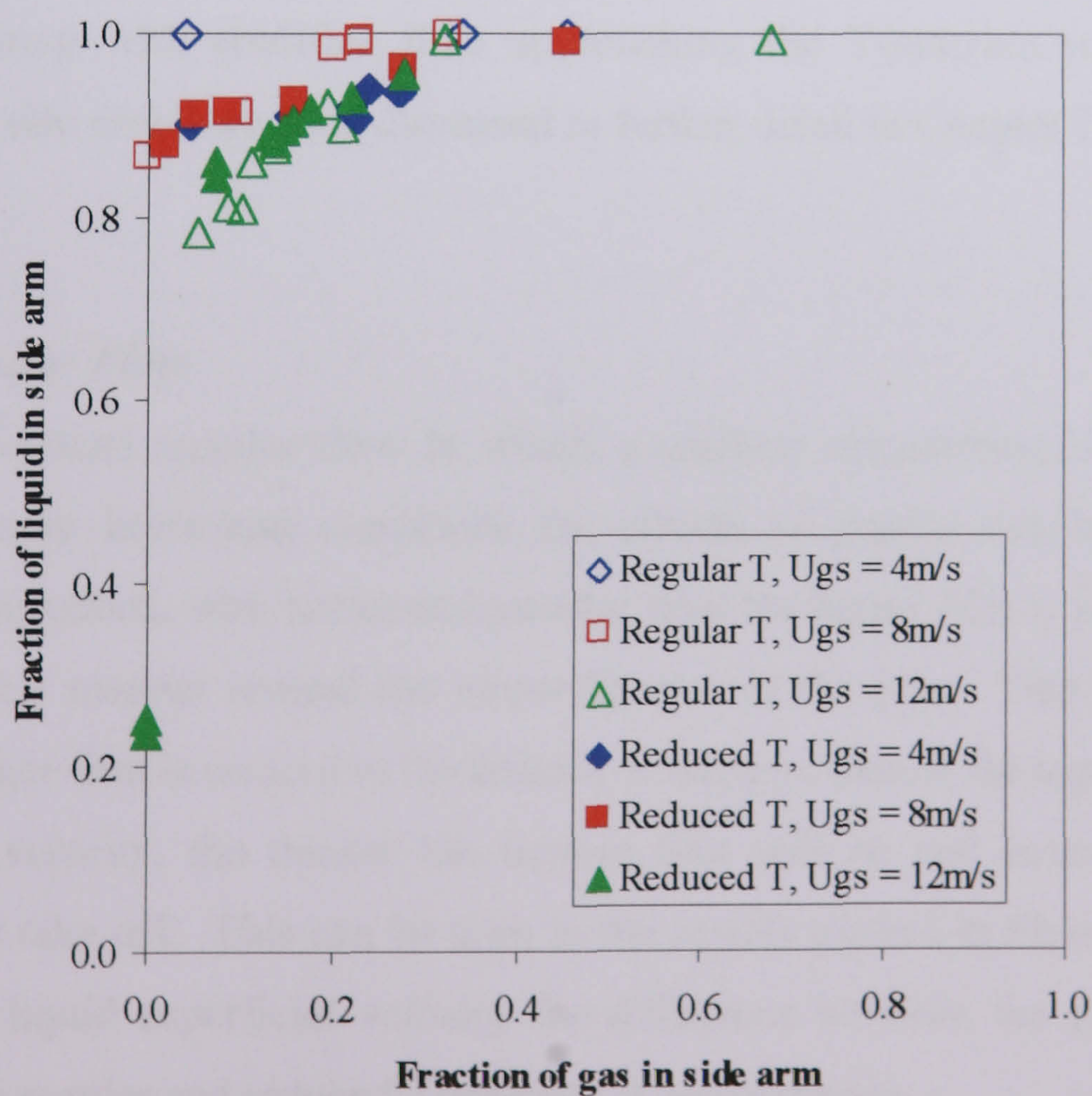


Figure 4-17: Phase split for stratified flow at a regular and reduced T-junction with a downwards side arm,  $U_{ls} = 0.186 \text{ m/s}$



For the experiments performed with the low liquid, high gas inlet flowrates the gas-liquid interface is much lower. It was observed for flows below  $U_{ls} = 0.0535\text{m/s}$  the fraction of liquid drawn across the branch arm opening is insignificant and the T-junction could be said to perform as a partial phase separator producing a gas rich stream in the run arm from a multiphase inlet.

Figure 4-17 shows the phase separation for the two T-junctions with low liquid flowrates approaching the junction. With low liquid and higher gas flowrates the separation performance of the regular and reduced T-junctions are very similar. This was also found by Reimann *et al.* (1988) whose data also indicates that with the side arm orientated vertically downwards any reduction in side arm diameter has a minimal effect on the phase split. The steam-water experiments of Peng *et al.* (1988) also confirm that reducing the side arm diameter has little effect on the phase separation of the junction with stratified flow with low liquid flowrates.

With stratified flow approaching the junction several visual phenomena were seen as the flow passed over the T-junction. These visual observations noted during experimentation have been discussed within Section 4.3 and the mechanisms though to be occurring with stratified flow approaching the T-junction with a vertically downwards side arm have been discussed in further detail in Chapter 7.

### ***Annular Flow***

Unlike for vertical annular flow in which a uniform circumferential liquid film is expected, under horizontal conditions the effects of gravity can be noticed. As previously described, with horizontal annular flow the liquid film is forced to flow in an asymmetric manner around the circumference of the pipe. Due to gravitational forces a thicker film is noticed at the bottom of the pipe than at the top. The faster the inlet liquid velocity, the thicker the bottom film will be and hence more will be available for take off. This can be seen in the results plotted in Figure 4-18. At the higher inlet liquid superficial velocity the difference between the phase separation curves of the regular and reduced T-junction is much greater.



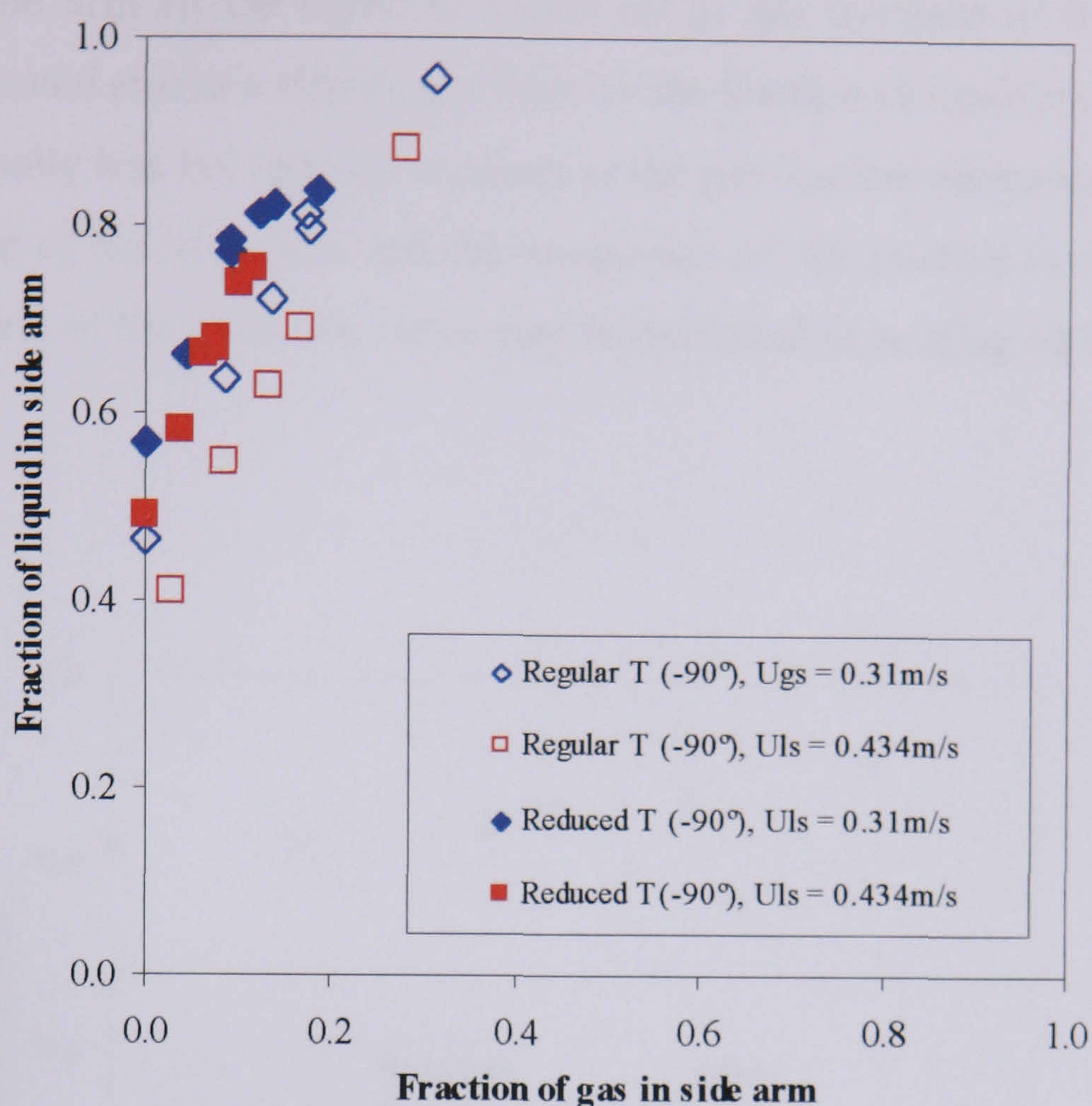


**Figure 4-18: Phase split for annular flow at a regular and reduced T-junction with vertically downwards side arm,  $U_{gs} = 12\text{m/s}$**

This is because the film flowing along the bottom of the pipe is thicker; hence reducing the area of take off, by reducing the side arm diameter, causes a much greater difference in the fraction of liquid entrained. Peng *et al.* (1993) reported similar trends with increasing inlet quality. Within the experimental range of the current data only a very slight reduction in the fraction of liquid removed for low gas fractions taken off was noticed as inlet gas velocity increased but was not as pronounced as in Peng *et al.*'s data.

For interest, Figure 4-19 shows the phase split data for horizontal annular flow ( $U_{gs} = 12\text{m/s}$ ,  $U_{ls} = 0.31\text{m/s}$ ) at a regular T-junction by Rea (1998). Plotted is the fraction of gas and liquid left in the run arm and not that taken off down the side arm. This shows that for annular flow the fraction of inlet flow taken off in the downwards side arm can exhibit similar features to that left in the run arm for a horizontal T-junction,



compare Figure 4-18 and Figure 4-19. One significant characteristic is that with a downwards side arm all the liquid is drawn off at gas fractions of 0.4 and above. With the horizontal arm at a similar gas fraction the fraction of liquid remaining in the run arm is initially less but remains constant as the gas fraction increases. This shows that knowledge of the inlet flow and the orientation of the junction is significant and different features of the phase split curve may be exploited depending on the situation.

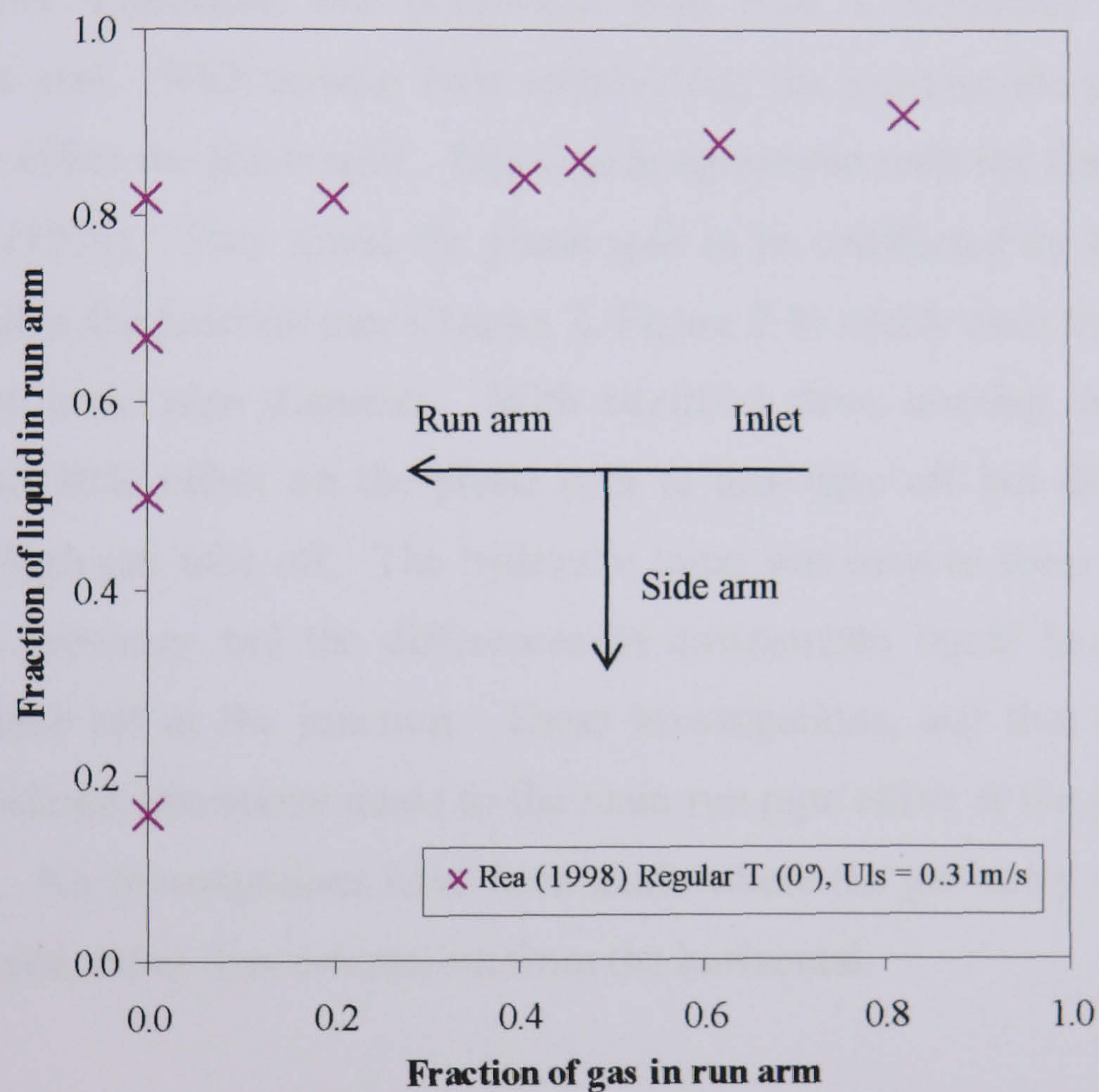


Figure 4-19: Phase split for annular flow at a regular horizontal T-junction,  $U_{gs} = 12\text{m/s}$



#### **4.2.4 Downwards side arm with U-bend**

The papers by Fouda and Rhodes (1974), Butterworth (1980) and Azzopardi and Smith (1992) are a few of the published works that consider altering the geometry around the T-junction. As mentioned in Chapter 2 the work of Azzopardi and Smith (1992) investigated the split of annular and stratified flow at a reduced T-junction ( $D_3/D_1 = 0.67$ ) with and without a 90° bend in the run arm downstream of the junction. The T-junction was positioned with both a horizontal and vertically upwards side arm. With annular flow approaching the junction the presence of the bend did not effect the phase split. This was in agreement with the findings of Fouda and Rhodes (1974). They found the phase split to be unaffected by the presence of baffles placed at the junction (see Chapter 2, Figure 2-8) which were less than half the height of the main pipe diameter. With stratified flow, altering the downstream geometry had little effect on the phase split at low take off but differences were observed at high gas take off. The hydraulic jump was seen to form irrespective of downstream geometry and the differences in downstream liquid height forced the changes in take off at the junction. These investigations, and that of Butterworth (1980), considered alterations made to the main run pipe either at the junction or just downstream. No investigations have been made where the geometry of the side arm has been altered, other than orientation from the horizontal.

Here a U-bend has been placed on the downwards side arm between the junction and the separator. The aim in mind was to reduce the fraction of gas drawn off through the side arm by the formation of a large liquid plug in the side arm. As indicated in the previous section using a T-junction with a reduced diameter side arm gives an improved phase split when compared with the regular T-junction. Adding a U-bend to the reduced diameter side arm could improve this phase split further so that practically all the liquid could be drawn off down the side arm before any gas entrainment.



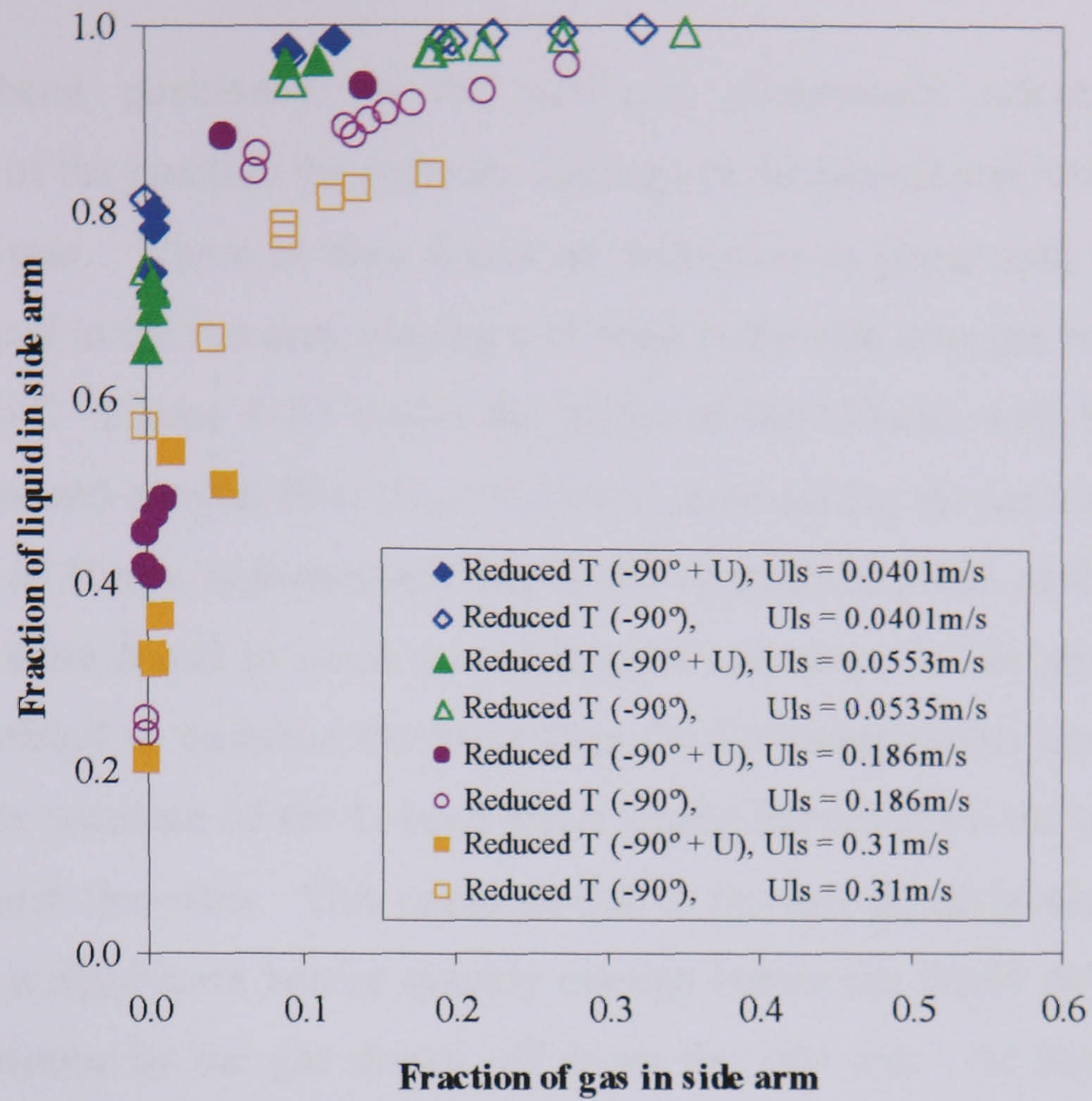


Figure 4-20: Phase split for stratified and annular flow at a reduced T-junction with and without a U-bend,  $U_{gs} = 12 \text{ m/s}$

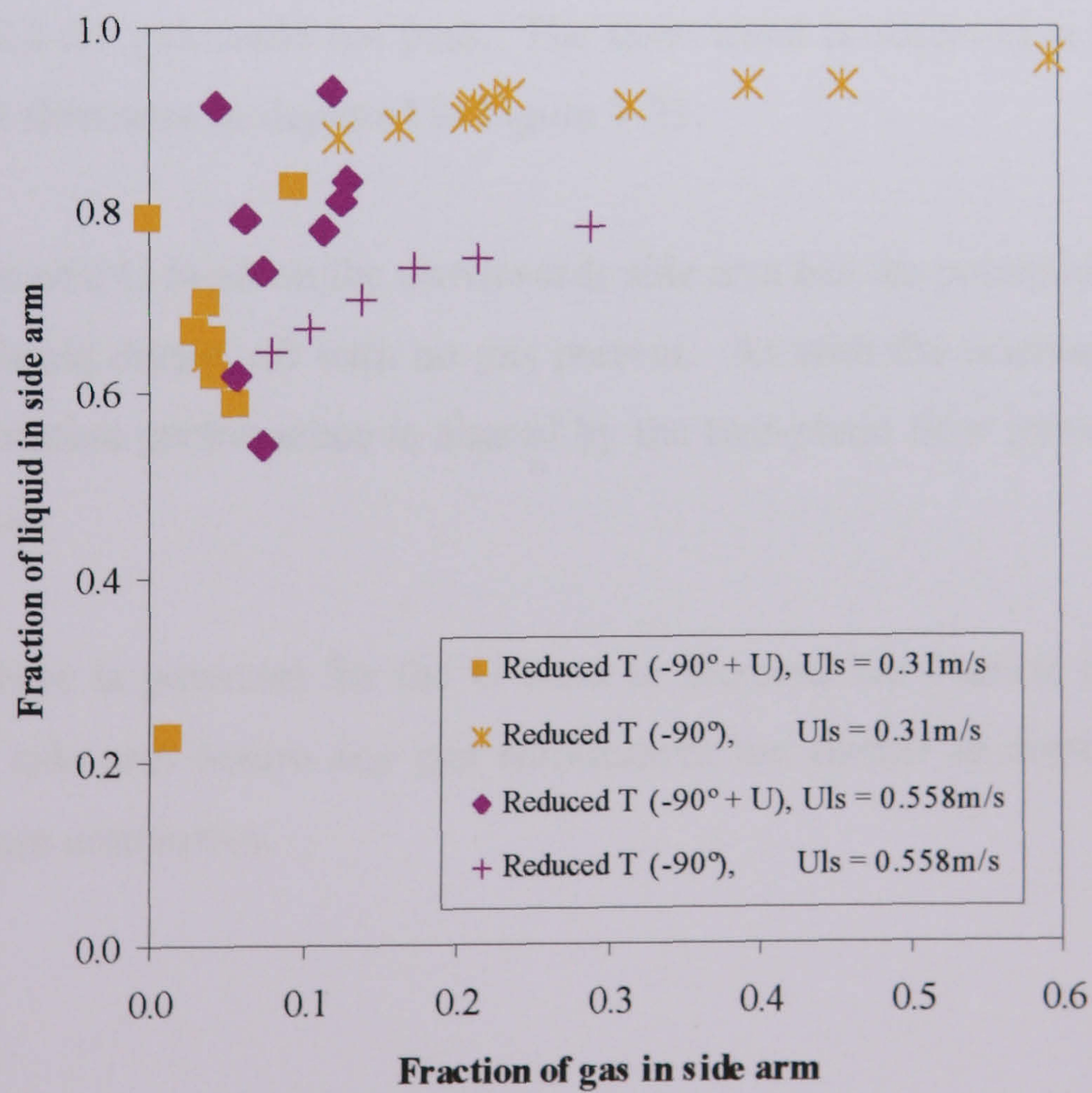


Figure 4-21: Phase split for stratified flow at reduced T-junction with and without a U-bend,  $U_{gs} = 4 \text{ m/s}$



With a U-bend positioned on the vertically downwards orientated side arm downstream of the junction the opposite findings to Azzopardi and Smith (1992) were found to be true. Where as they found no difference in phase split at a T-junction with a 90° bend in the run arm, placing a U-bend in the side arm can be seen to reduce liquid take off. Figure 4-20 shows the effect of the U-bend with low liquid inlet stratified flow and annular flow ( $U_{ls} = 0.31\text{m/s}$ ) approaching the junction at a constant gas velocity of 12m/s, unfortunately due to the operational limits of the rig the phase split results were found to reach a certain point and stop. If the phase split curves were extrapolated to continue the locus then the following points can be noted. As indicated, the presence of the U-bend has a negligible effect on the phase split with low inlet liquid flowrates. This could be due to the low liquid levels in the U-bend not forming a significant barrier quickly enough before the liquid collected is swept into the separator by the gas drawn off down the side arm. At higher inlet liquid flowrates, with the inlet flow pattern changing from stratified to annular flow, the presence of the U-bend does reduce the fraction of gas drawn through the side arm. Here the accumulation of liquid was assumed to be sufficient to form a proper barrier through which the gas could not pass. The same trend is observed at high liquid and low gas inlet flowrates as depicted in Figure 4-21.

The presence of a U-bend on the downwards side arm has the potential to increase the fraction of liquid drawn off with no gas present. As with the orientation of the side arm the separation performance is altered by the two-phase flow pattern approaching the T-junction.

As shown there is potential for the U-bend to increase the fraction of liquid drawn through the side arm before any gas entrainment but further in-depth investigations would be more conclusive.



### ***4.3 Visual Observations at the T-junction with a Downwards Side Arm***

It was observed during experimentation that some very interesting physical phenomena were occurring at the T-junction as the two phases redistributed themselves between the two outlets. These included the formation of hydraulic jumps and in some cases, especially with a vertically upwards side arm, film stop. These have not been discussed in detail within this thesis as both were given significant attention by Rea (1998) and Conte (2000). Instead, attention has been given to the phenomena occurring when the two phases split at a T-junction with a downwards side arm. Here the gas phase has to be drawn through the denser liquid phase which is flowing along the bottom of the pipe. Phenomena as vortices, and “dips” in the liquid level above the junction were noted and in some cases pressure reversal at the T-junction produced an interesting feature as described below. The various physical phenomena observed were a function of the inlet flow regime, diameter of the side arm and the fractions of both gas and liquid being diverted.

Figure 4-22 shows the split stratified flow ( $U_{gs} = 4\text{m/s}$ ,  $U_{ls} = 0.186\text{m/s}$ ) with a low liquid inlet flowrate as it passed over the regular T-junction with a downwards side arm. Flow is from right to left and the butterfly valves in the run and down arm were fully open. As with all stratified flows studied, arrow A indicates that the liquid “falls” into the branch arm until it nears the far side of the down pipe. As can be seen “fingers” of liquid, depicted by arrow B, are being drawn back up the pipe wall and into the run arm. At faster inlet liquid or gas flowrates these are seen to enter the run arm. In Chapter 7 it has been suggested that there is a stagnant gas pocket trapped in the branch arm that is supporting the liquid as it flows over the branch arm.





Figure 4-22: Stratified flow (low gas-liquid interface) at the regular T-junction

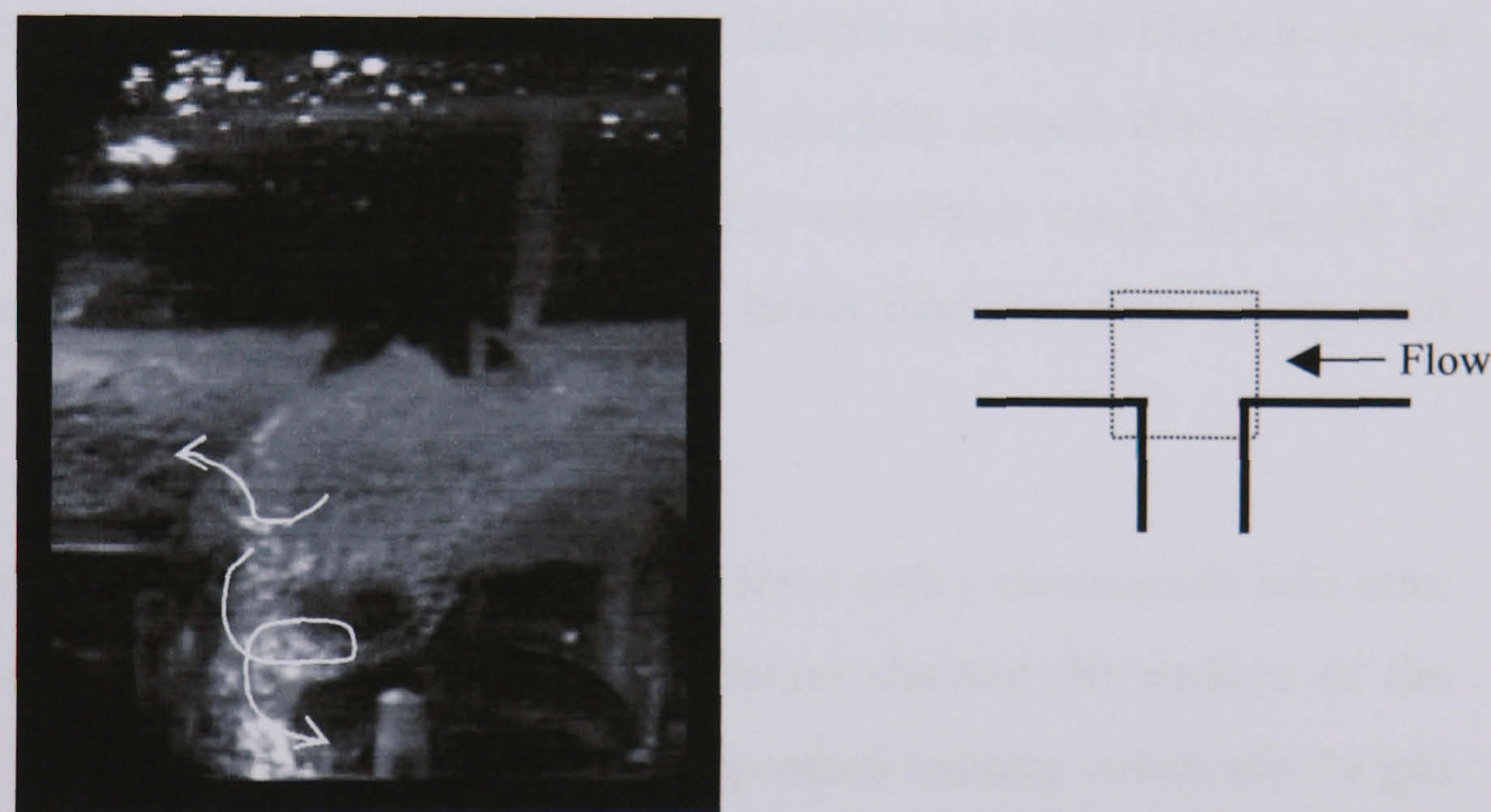


Figure 4-23: High liquid, high gas flowrates approaching the regular T-junction

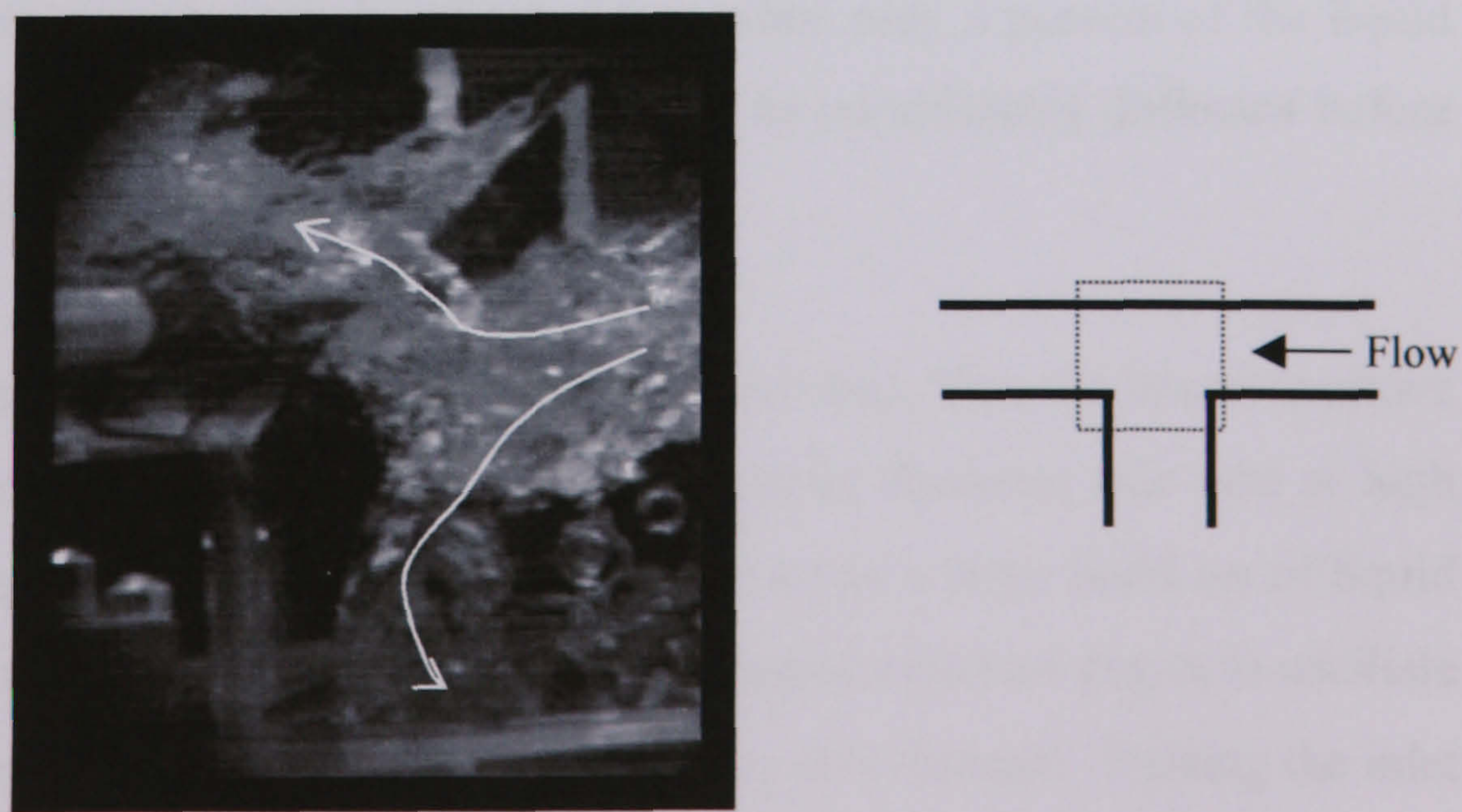


Figure 4-24: High liquid, low gas flowrates approaching the T-junction



Increasing both the gas and liquid inlet flow rates ( $U_{gs} = 10\text{m/s}$ ,  $U_{ls} = 0.558\text{m/s}$ ), see Figure 4-23, promotes the formation linked to pressure reversal at the T-junction. This occurred at the T-junction when both the run and branch arm valves were open. The liquid was seen to initially flow down the side arm, as in Figure 4-22 but before reaching the far side of the junction the liquid flowing at the edge of the stream starts to fall rotating, like water flowing down a plughole. The top part of the liquid stream is seen to be pulled back up again and flows along the run arm. The feature created by part of the liquid falling down the side arm and part of the liquid being dragged back into the run arm was hollow, and could be described as a transparent banana being continuously peeled.

The same feature can be seen more clearly at a lower gas flowrate, Figure 4-24 ( $U_{gs} = 4\text{m/s}$ ,  $U_{ls} = 0.558\text{m/s}$ ). It was also noticed that this feature was more likely to occur when the butterfly valve in the downwards arm is partially closed than when the butterfly valve in the run arm was closed. No other references could be found to support this feature so it could be a function of the larger diameter pipes being used here.

In smaller diameter pipes vortices are more likely to form with a downwards side arm. However, visual observations at the reduced T-junction showed the surface of the liquid layer above the side arm entrance became depressed leading eventually to gas being pulled down into the side arm. Such observations were also noted by Reimann and Khan (1982). Their study of stratified flow approaching small breaks within various geometrical arrangements highlighted that when only a portion of the liquid flows down the side arm the gas-liquid interface can be considerably deflected before vortex-free gas pull through is observed.

As the liquid flowrate increases and the interface level rises, then the interface above the junction becomes merely deflected. For the reduced diameter side arm at high inlet liquid flowrates, closure of the run arm valve created a large build up of liquid by the junction. Under these conditions the funnel-shaped interface began to oscillate and was intermittently sucked through, vortex-free gas pull-through. Raising the inlet



liquid flowrate further produced a continuous wispy vortex like formation which draws air into the branch arm similar to those indicated in Figure 4-25.

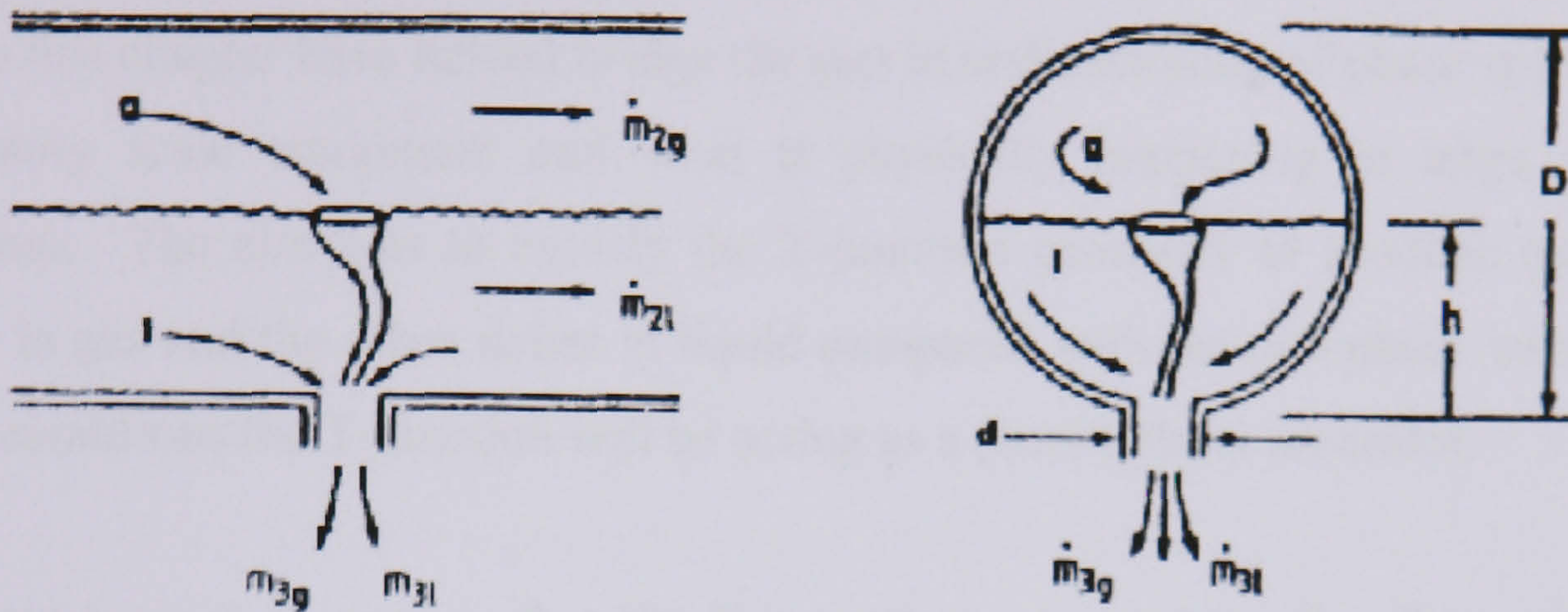


Figure 4-25: Gas pull through at a small break in a large diameter pipe, Reimann & Khan (1982)

With either T-junction in place and the branch arm valve closed and thus full of water, similar observations to Seeger *et al.* (1985) were noted. Firstly, a similar recirculation zone was seen as the gas bubbles entrained in the side arm were seen to rise up and get drawn back into the branch arm. Secondly, as the valve was opened further the gas-liquid interface descended until it was swept out of the branch arm and the liquid fell as a film of the pipe walls around a gas core.



#### **4.4 Conclusions**

The many different side arm orientations for a large diameter T-junction studied within this chapter have helped bridge the gap in understanding of phase split in small laboratory scale equipment and what is physically happening in large industrial pipelines. The aim was to modify the T-junction geometry to produce one stream richer in gas and the other richer in liquid compared with the two-phase inlet. Under these conditions the T-junction will be acting as a partial phase separator.

The major point to note is that the flow pattern approaching the T-junction has a significant affect on the phase split. Thus, methods of predicting the two-phase flow pattern likely to occur in a given pipeline are essential to efficient plant operation.

With all side arms lying in the horizontal plane ( $0^\circ$ ), a regular T-junction performs as a phase separator (less than 20% of liquid in a gas rich stream). With the low liquid and high gas flowrates (stratified flow) the junction acts more of a flow divider than phase separator.

In all cases introducing a reduced diameter T-junction significantly improved the phase separation qualities at the junction. For stratified flow with a high gas-liquid interface and annular flows the fraction of liquid in the gas rich stream is reduced to below 5%. For stratified flow the fraction of liquid was reduced but increasing the inlet gas superficial velocity reduced any appreciable affects.

Rotating the side arm vertically upwards ( $+90^\circ$ ) instantly improved the separation qualities of the T-junction. The differences in phase separation qualities of the regular and reduced junctions are diminished. For all flow regimes approaching the junction, a virtually liquid free (generally less than 1%) gas stream was created from the two-phase inlet flow. The limits of all gas take off being generally above 80%.



Rotating the side arm vertically downwards ( $-90^\circ$ ) did not produce such a gas free, liquid rich stream as described above. However industrially, a greater fraction of gas can be tolerated within a liquid rich stream, unlike fast flowing liquid droplets in a gas rich stream which can cause a lot of damage. With this orientation of side arm it was stratified flow approaching the junction that provided the best liquid rich stream, with over 80% of the liquid being diverted with minimal gas. It was noted that with increasing gas flowrate the difference in phase split qualities of the regular and reduced junction were reduced.

The addition of a U-bend on the downwards branch arm was seen to improve the phase split at the junction with high liquid flowrates approaching. The liquid build up in the U-bend reduced the fraction of gas drawn the branch arm.

For all side arm orientations and all inlet flowrates the presence of a reduced diameter T-junction ( $D_3/D_1 = 0.6$ ) can improve the phase split qualities of the junction with no detrimental effect to the system, even if the junction only works as a flow splitter rather than as a phase separator as seen with some inlet conditions. In all the cases the pipeline has not significantly been altered, merely the T-junction being exploited as a cheap, easy to maintain partial phase separator.



## CHAPTER 5

### Placing an Insert at a Single T-Junction

A study of the effect of side arm orientation on the phase split at a single T-junction was reported in depth within Chapter 4. The orientation, the significance of reducing the side arm diameter, and the effect of the approaching flow pattern were investigated but the physical geometry of the junction remained unaltered – in all cases a plain sharp edged T-junction machined from a 200mm acrylic block was used. Within this chapter the effects of an insert placed at the junction on phase split are reported.

T-junctions can be considered as partial phase separators or flow dividers. Under certain conditions (high gas and low liquid inlet flowrates as described in Chapter 4) a horizontal T-junction may behave more as a flow divider than a phase separator but rotating the side arm from the horizontal promotes the phase separation qualities of the junction. In this series of experiments inserts were placed within a horizontal T-junction to try and enhance the phase separation qualities. Both the regular and reduced T-junctions were used and their effects on phase split were studied with both annular and stratified two-phase flow patterns approaching the junction.

As will be described, the size of the insert was thought to have a major influence on the phase split and so different insert protrusion depths were studied. The shape of the top of the insert was also considered to play an important role in determining the fraction of liquid and gas diverted, so this too was investigated.



### 5.1 Previous work on T-junctions and Inserts

Little work has been published where two-phase flow at T-junctions has been studied in the presence of protrusions into the main run pipe and that which has been published is over ten years old. This could be due to the more recent trend of consolidating T-junction knowledge where comprehensive, methodical research has improved models to predict the phase split at T-junctions but the more abstract ideas of how to promote phase split, rather than just being able to model it, have been left aside after initial sparks of interest.

As reported in Chapter 2, one such case is that of Butterworth (1980). Limited tests on air and water two-phase flow through a modified horizontal T-junction were reported using a reduced 0.038 / 0.025m T-junction with a section of tubing inserted into the side arm with the end of cut off at an angle of 45°. The insert was made such that it could be turned thus allowing the orientation of the plane of the cut to be changed with respect to the flow direction, see Figure 5-1 Results were compared with the insert facing forwards (scooped section facing the direction of flow, position A), with the insert facing backwards (scooped section opposing the direction of flow, position B) and for a non-protruding case. All arms of the T-junction lay in the horizontal plane.

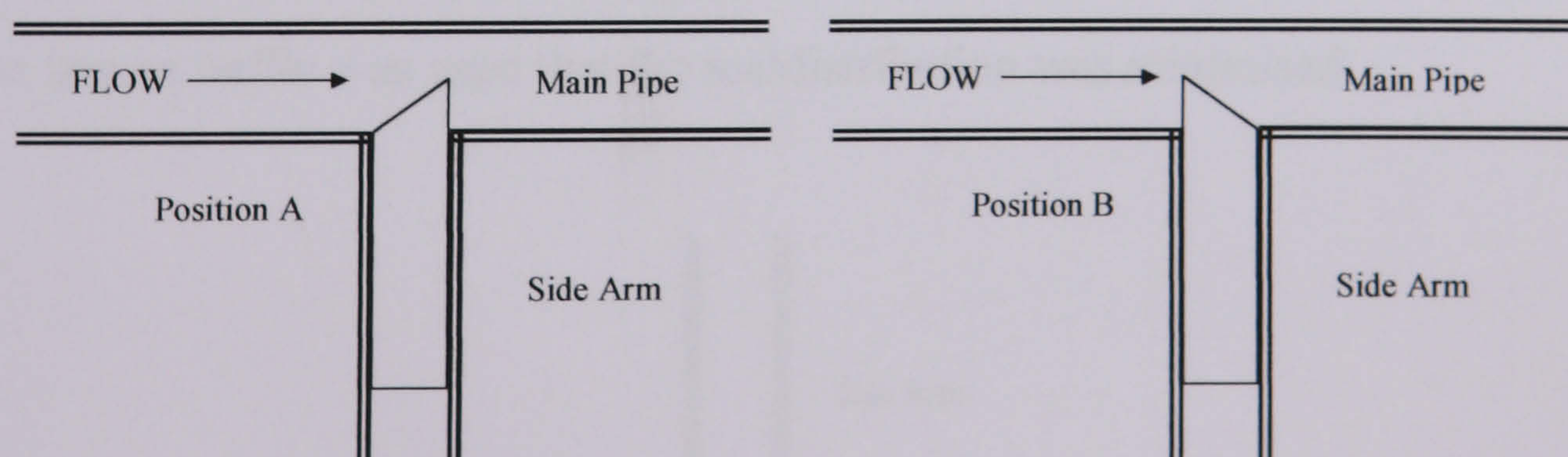


Figure 5-1: The insert positions used by Butterworth (1980)



Only three sets of experiments were performed by Butterworth, one in each of the following inlet flow regimes: annular, wavy and stratified. For each case the performance and the effect on phase split for the different insert positions was recorded. Simply, for the annular flow case, a forward facing insert decreased the maldistribution present when no insert is present, whilst the backwards facing insert increased the phase separation. In contrast, for wavy flow, the forwards facing insert can reduce the maldistribution at low gas take off but had very little effect at high gas take off. The backwards facing insert had little effect.

These experiments formed only a limited investigation and raised questions as to the effectiveness of placing inserts at a T-junction if it is to be used as a partial phase separator. These questions were considered and formed the basis of the current investigation into phase redistribution at a large diameter T-junction.

A more complete set of experiments were performed earlier by Fouada and Rhodes (1974) who studied the effects of baffles placed in a reduced 0.05 / 0.025m T-junction. Two-phase annular flow through a horizontal tee with a vertical side branch was used to study the effects of baffles and homogenisers on downstream qualities. Their aim was to produce an equal phase split between the branch and main pipe, whereas the objectives of the current research are to enhance the phase split at the junction. The baffles were a quarter, half and three quarters of the tube diameter in height and placed just at the base of the T-junction as indicated in Figure 5-2. Without the baffle present there was significant maldistribution. However, it was only when the largest baffle was used that the maldistribution was minimised.

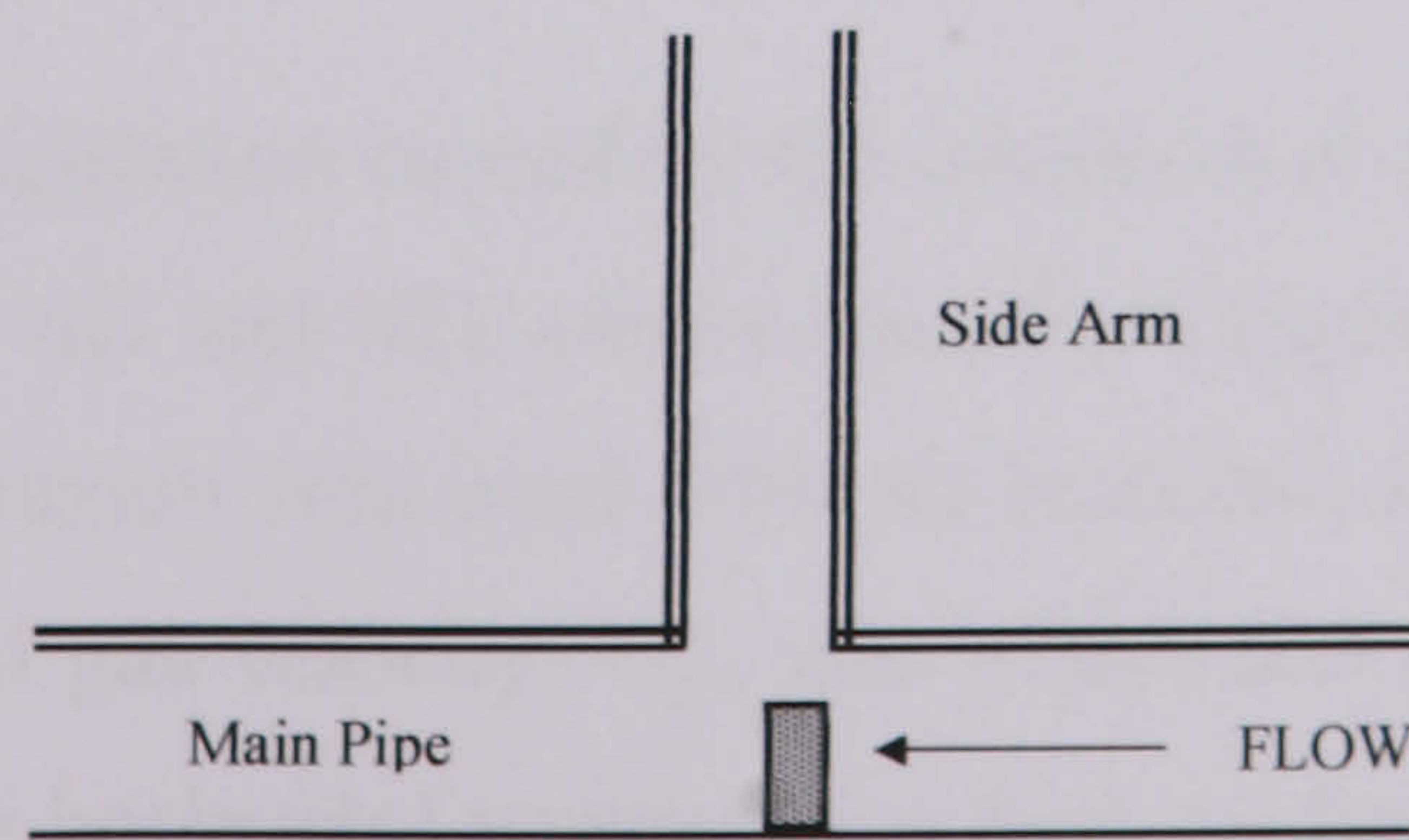


**Figure 5-2: The T-junction with baffle as used by Fouada and Rhodes (1974)**

---



## **5.2 Adding an insert at the large diameter T-junctions**

An insert was made for both the regular and reduced T-junctions as described in Chapter 3, section 3.1.4. The insert, for both cases, was machined as thin as possible so that the inside diameter of the side arm was not reduced. The inserts were able to slide up and down the side arm as well as rotate through 360°. This allowed both the protrusion depth of the insert and the direction the scooped section faced – forwards (with the flow) or backwards (against the flow) to be altered.

The initial investigation by Butterworth (1980) only considered the direction the insert was facing to affect the phase separation occurring at the junction. This was expanded on by investigating the influence of the plane of the cut at the tip of the insert, with respect to flow direction, on the degree of separation at the junction. Two angles of cut were investigated, 45° and 30°, these can be visualised in Figure 3-7, Chapter 3. Two protrusion depths,  $\frac{1}{2}D$  and  $\frac{3}{4}D$  were studied. A protrusion depth of  $\frac{1}{2}D$  indicates that the tip of the insert protruded from the side arm to half way across the diameter of the main run pipe and a protrusion depth of  $\frac{3}{4}D$  indicates that flow split data was recorded with the tip of the insert protruding three-quarters of the way across the main pipe. A series of experiments were performed within the annular, stratified-wavy flow regimes.

### **5.2.1 Altering the angle of cut of the insert**

The effects on phase separation caused by the insert cut at angles of 30° and 45° at the two protrusion depths,  $\frac{1}{2}D$  and  $\frac{3}{4}D$ , can be seen from Figure 5-3 to Figure 5-6. In all cases the regular T-junction was used with all branches lying within the horizontal plane. Inlet superficial gas velocity,  $U_{gs}$ , was 12m/s and superficial liquid velocity,  $U_{ls}$ , was 0.31m/s giving horizontal annular flow with an asymmetric liquid film.



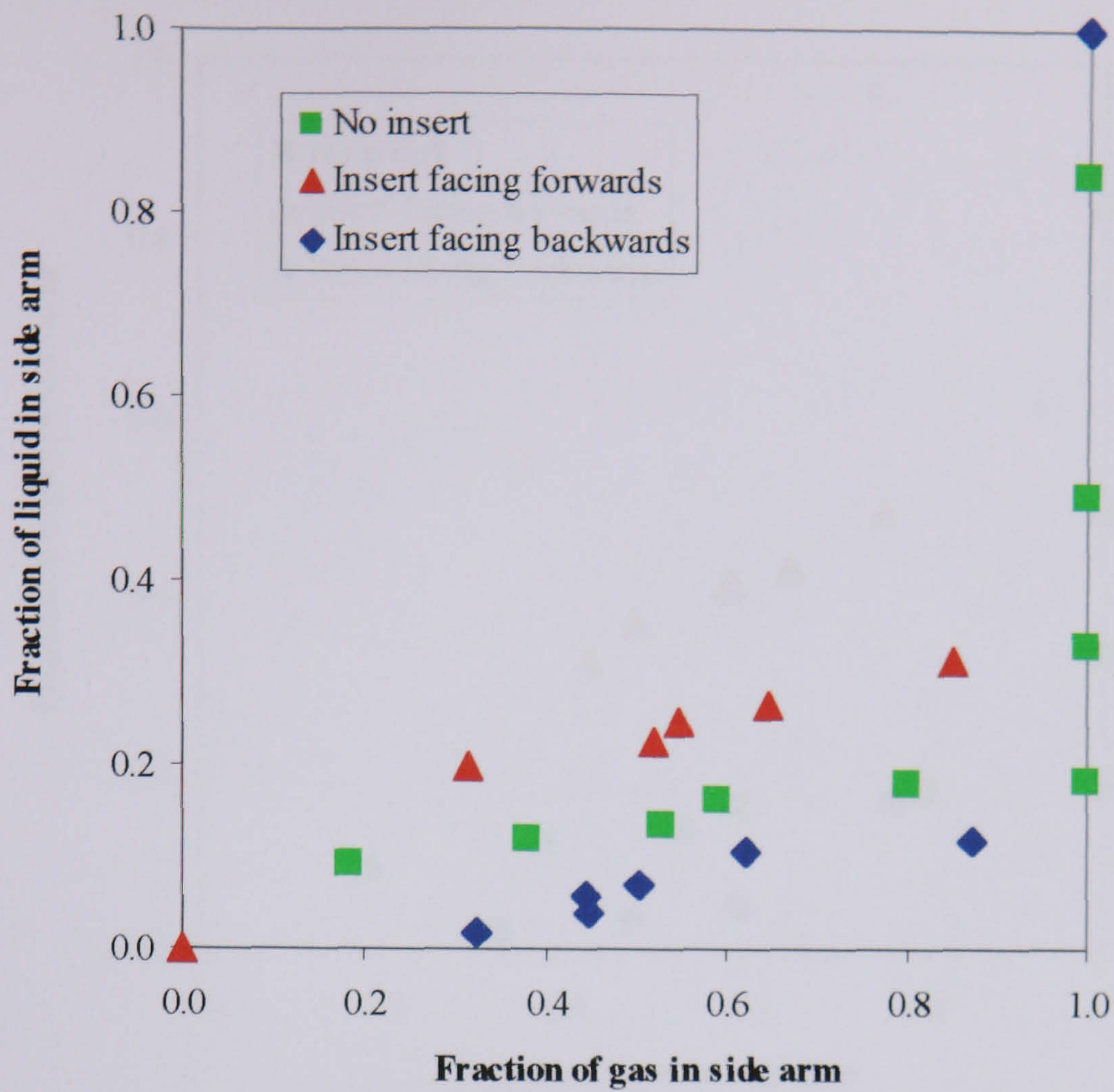


Figure 5-3: Annular flow,  $\frac{1}{2}$ D protrusion, 45° insert

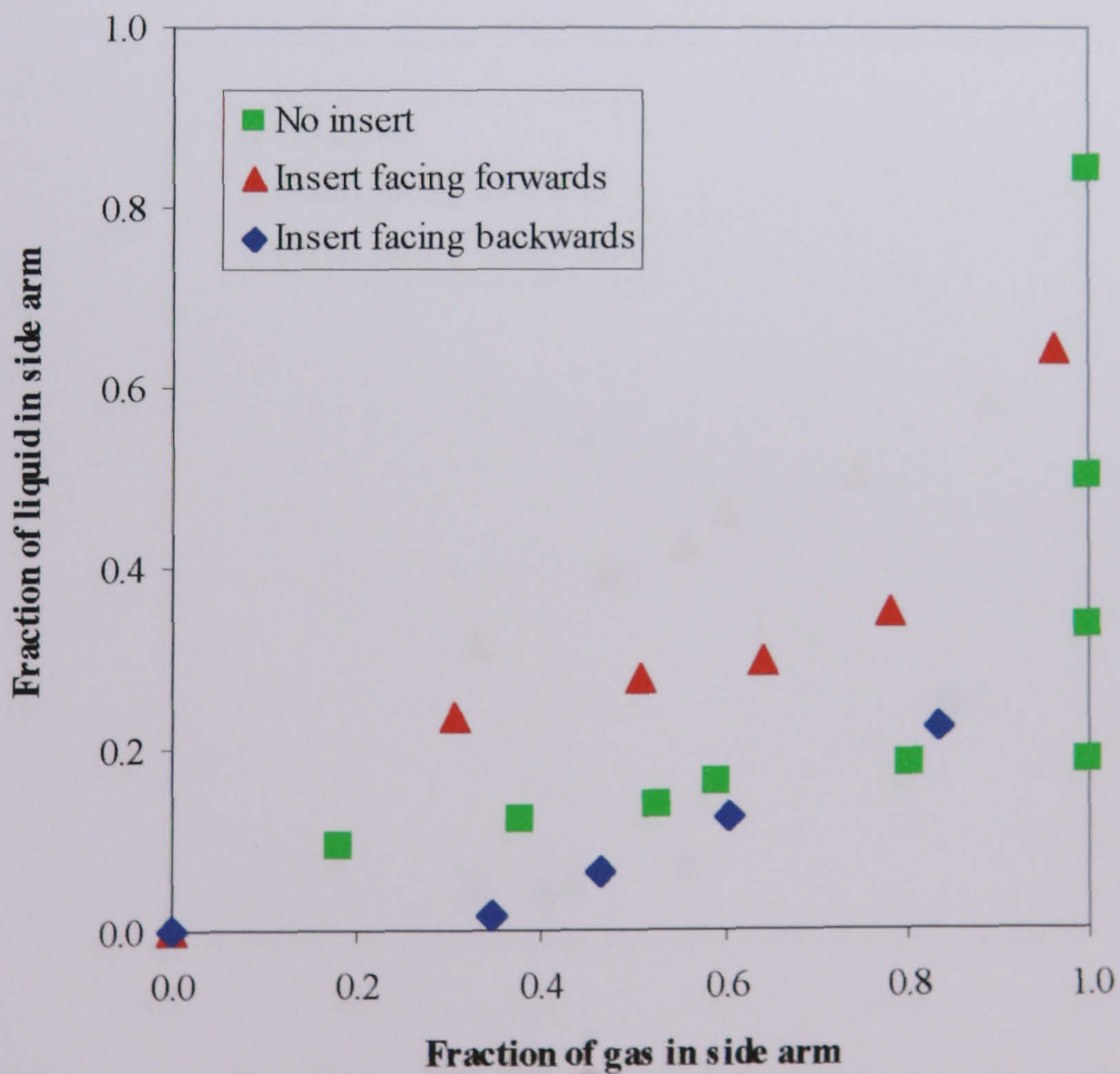


Figure 5-4: Annular flow,  $\frac{1}{2}$ D protrusion, 30° insert



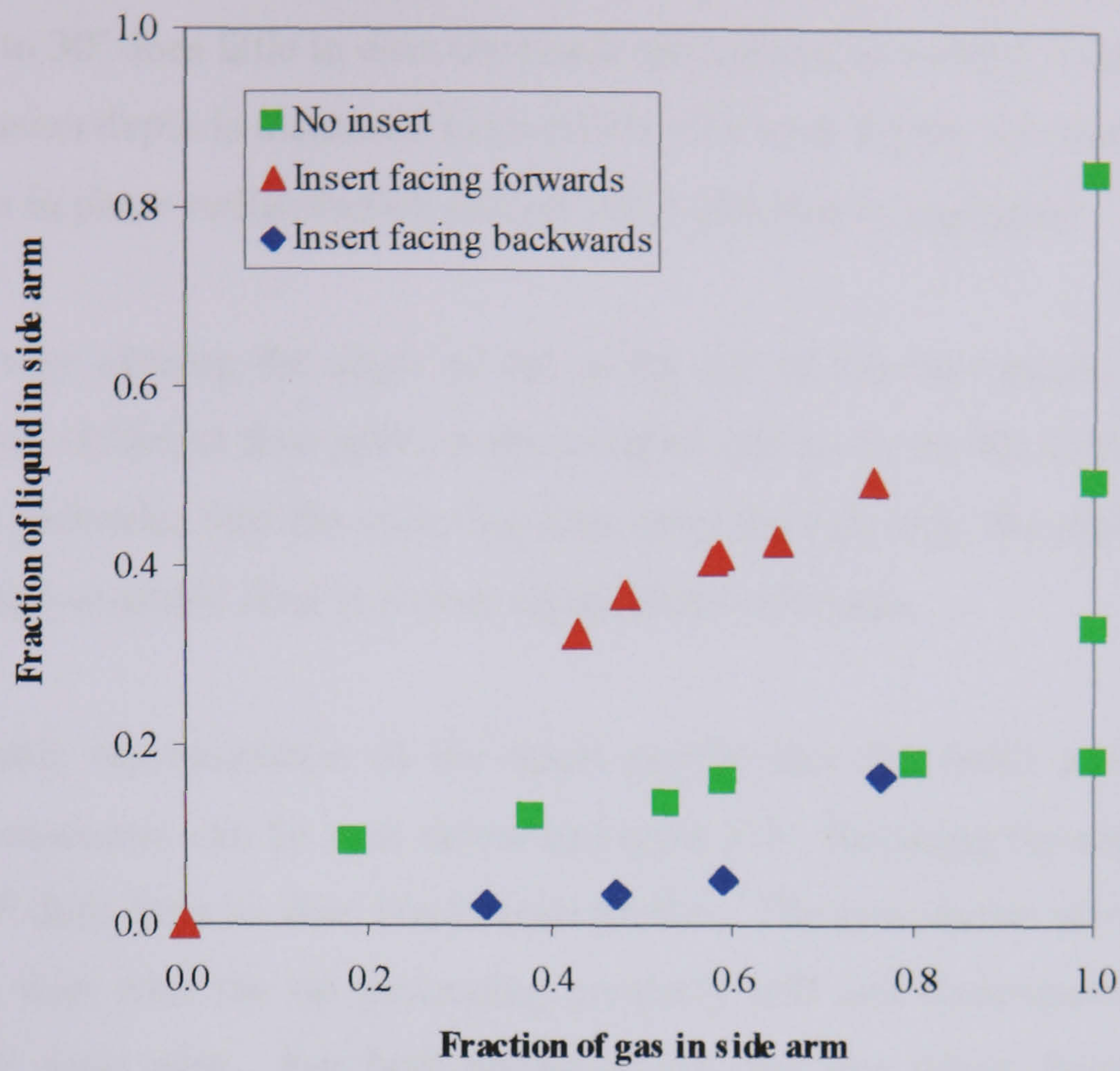


Figure 5-5: Annular flow,  $\frac{3}{4}D$  protrusion, 45° insert

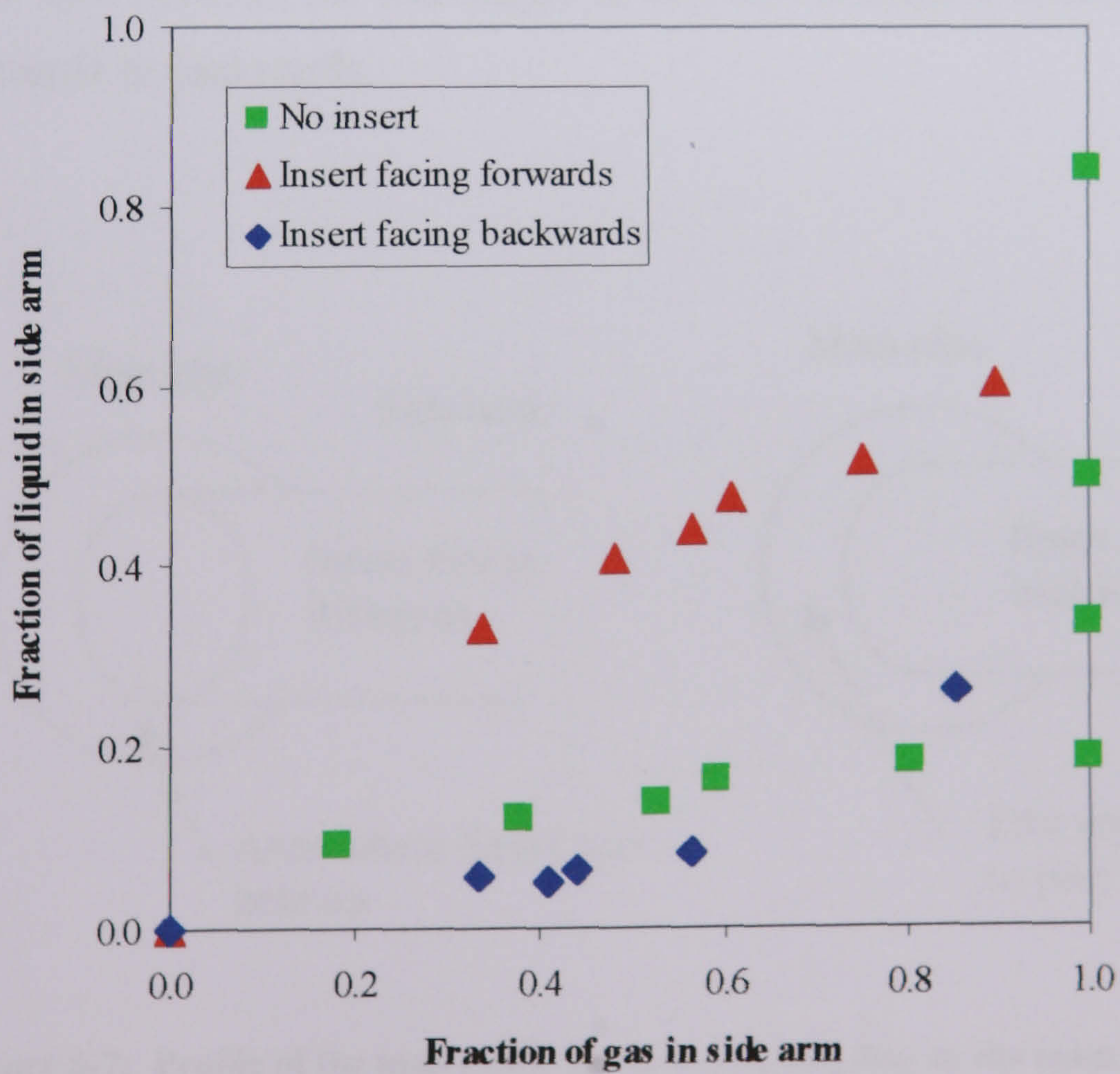


Figure 5-6: Annular flow,  $\frac{3}{4}D$  protrusion, 30° insert



Comparing Figure 5-3 and Figure 5-4, it can be seen that reducing the angle of cut from  $45^\circ$  to  $30^\circ$  does little to alter the phase split properties of the T-junction. Even if the protrusion depth is increased from  $\frac{1}{2}D$  to  $\frac{3}{4}D$ , as in Figure 5-5 and Figure 5-6, the difference in phase redistribution around the T-junction is negligible.

Reasons why altering the angle of cut at the top of the two inserts does not show significantly different flow split results could be due to the profile of the insert. When the insert protrudes into the main run arm, from the side arm, the profile seen by the on-coming two-phase flow is almost identical in both cases.

A schematic representation of the insert profile that the fluids arriving at the T-junction encounter can be seen below in Figure 5-7. Reducing the angle of cut from  $45^\circ$  to  $30^\circ$  does little to alter this overall profile. The two inserts were set in exactly the same way with the tip protruding precisely half and three-quarters of the way across the main pipe. For both angles of cut, the area where liquid was held up behind the insert and the free area for the flow to pass the insert were very similar. This meant there was little difference in flow split of the two inserts. The difference in the flow split between the two angles of cut was minimal whether the insert was facing forwards or backwards.

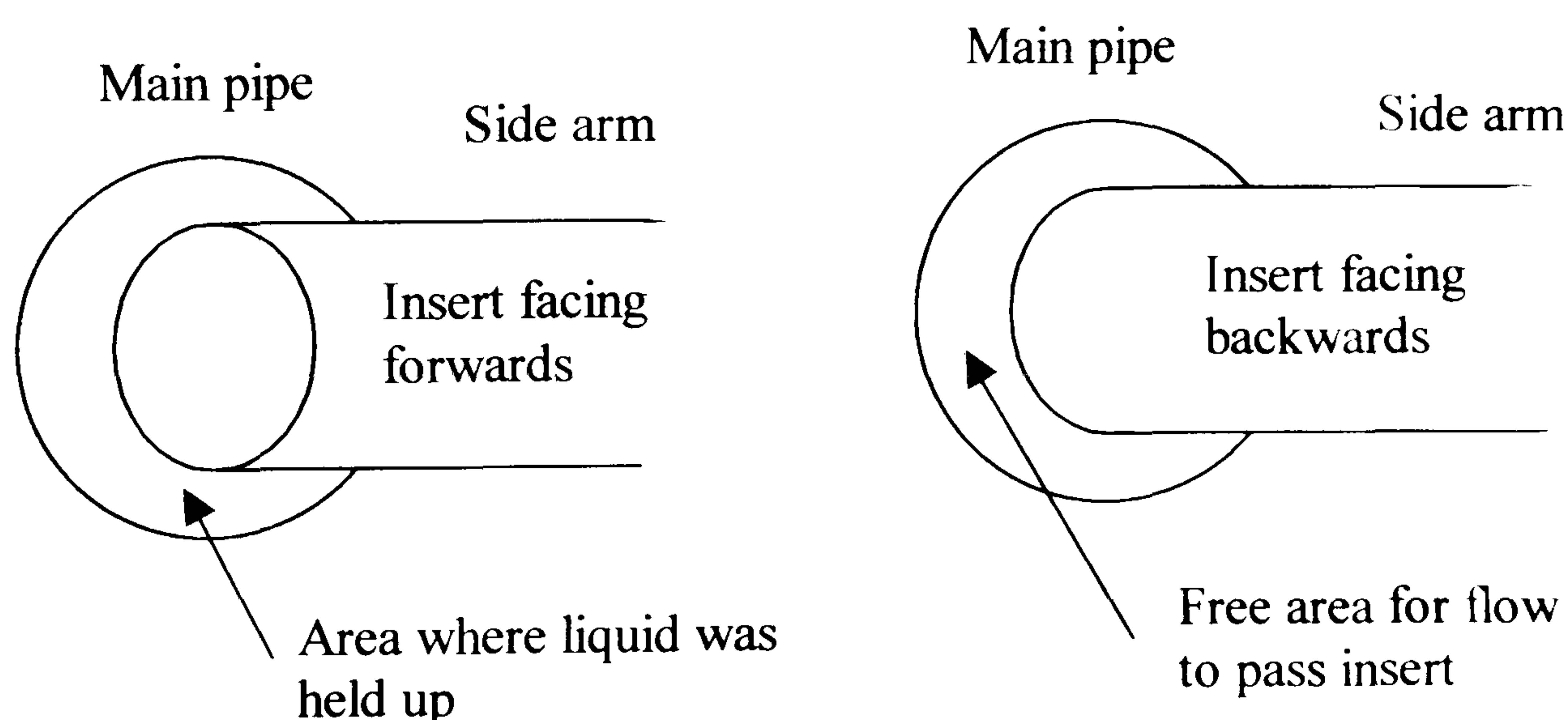


**Figure 5-7: Profile of the insert seen by the on-coming flow in the main run arm**



If the idea of profile area is extended further for other angles of cut, for example reducing it further to  $15^\circ$ , then similar arguments could be stated. The overall profile would not be affected therefore the effect on phase redistribution is thought to be almost negligible. It was originally thought that due to the  $45^\circ$  insert having the slightly more open nature – the angle of cut removing more of the side of the insert. see Figure 3-7 in Chapter 3 – a greater proportion of the liquid droplets entrained in the gas core of annular flow would be intercepted compared to the  $30^\circ$  insert. However, this was not the case and it is therefore expected that no other angle of cut would significantly alter phase split at the junction in the presence of an insert.

### **5.2.2 Altering the protrusion depth of the insert**

Protrusion depth of the insert was investigated, primarily with the  $45^\circ$  insert since the angle of cut was deemed to have little significant effect on the phase split at the T-junction. A series of experiments were performed with both annular and stratified-wavy two-phase inlet flow with the regular 0.127m T-junction and all branches lying in the horizontal plane

Comparing Figure 5-3 and Figure 5-5, the effects of protrusion depth can be clearly seen for annular flow. At  $\frac{3}{4}D$  the position of the insert, whether it is facing forwards or backwards, has more of an effect than when the insert is at a  $\frac{1}{2}D$  protrusion depth. At  $\frac{3}{4}D$  and with the insert facing backwards a greater liquid hold up behind the insert was seen. As the liquids builds up the gas is forced to pass between the insert and the wall of the main pipe, resulting in an area of low pressure, faster flowing gas around the tip of the insert. Once past the insert the gas has a greater area in which to expand into and thus a large proportion is drawn down the side arm. Under these conditions the T-junction and insert acted as a good partial phase separator. At  $\frac{3}{4}D$  and the insert facing forwards the insert acts like a large scoop and diverts a large proportion of both the liquid and gas down the side arm. Under these conditions the T-junction and insert acted more like a flow divider, with nearly an equal split between the branch



arm and the run arm. Such effects were more exaggerated with the insert at a protrusion depth of  $\frac{3}{4}D$ , as opposed to  $\frac{1}{2}D$ .

Experiments performed in the stratified-wavy flow regime, for example with inlet superficial gas velocity,  $U_{gs}$ , at 24m/s and the inlet superficial liquid velocity,  $U_{ls}$ , at 0.0535m/s, see Figure 5-8 and Figure 5-9. With the insert at a  $\frac{1}{2}D$  protrusion depth, facing forwards, only a very slight improvement in flow split was seen in the results compared with no protruding insert in place. However, with the insert at  $\frac{1}{2}D$  facing backwards the effect was to create more of an even flow splitter. These were the opposite results compared to those for annular flow where at the same protrusion depth and the insert facing backwards, the phase separation qualities of the junction were increased. Butterworth (1980) also observed similar findings for the small diameter T-junction, where the phase split results for annular and stratified flow in the presence of an insert were opposite to one another.

Under stratified-wavy flow conditions, the liquid is flowing along the bottom of the main pipe but does not form a very thick layer. This meant with the insert at  $\frac{1}{2}D$  facing forwards the liquid had to rise slightly to enter the side arm and could not just be scooped in. However, with the insert facing backwards, as the gas was forced around and over the insert the liquid also began to rise up and around the back of the insert. This reduced the momentum of the liquid phase allowing it to be diverted more easily with the gas down the side arm.

With the insert  $\frac{3}{4}D$  across the pipe there was only a narrow channel available for the fluids to flow around the insert. When the insert faced forwards the build up of liquid in front of the insert was easily forced into the side arm by the faster flowing gas. However, with the insert facing backwards the gas was forced to pass between the insert and the side wall of the main tube. As, by Bernoulli the gas would be flowing much faster through the constriction the liquid being dragged past the insert with it would therefore have a much higher momentum. This resulted in less liquid therefore being diverted down the side arm for the same fraction of gas taken off.



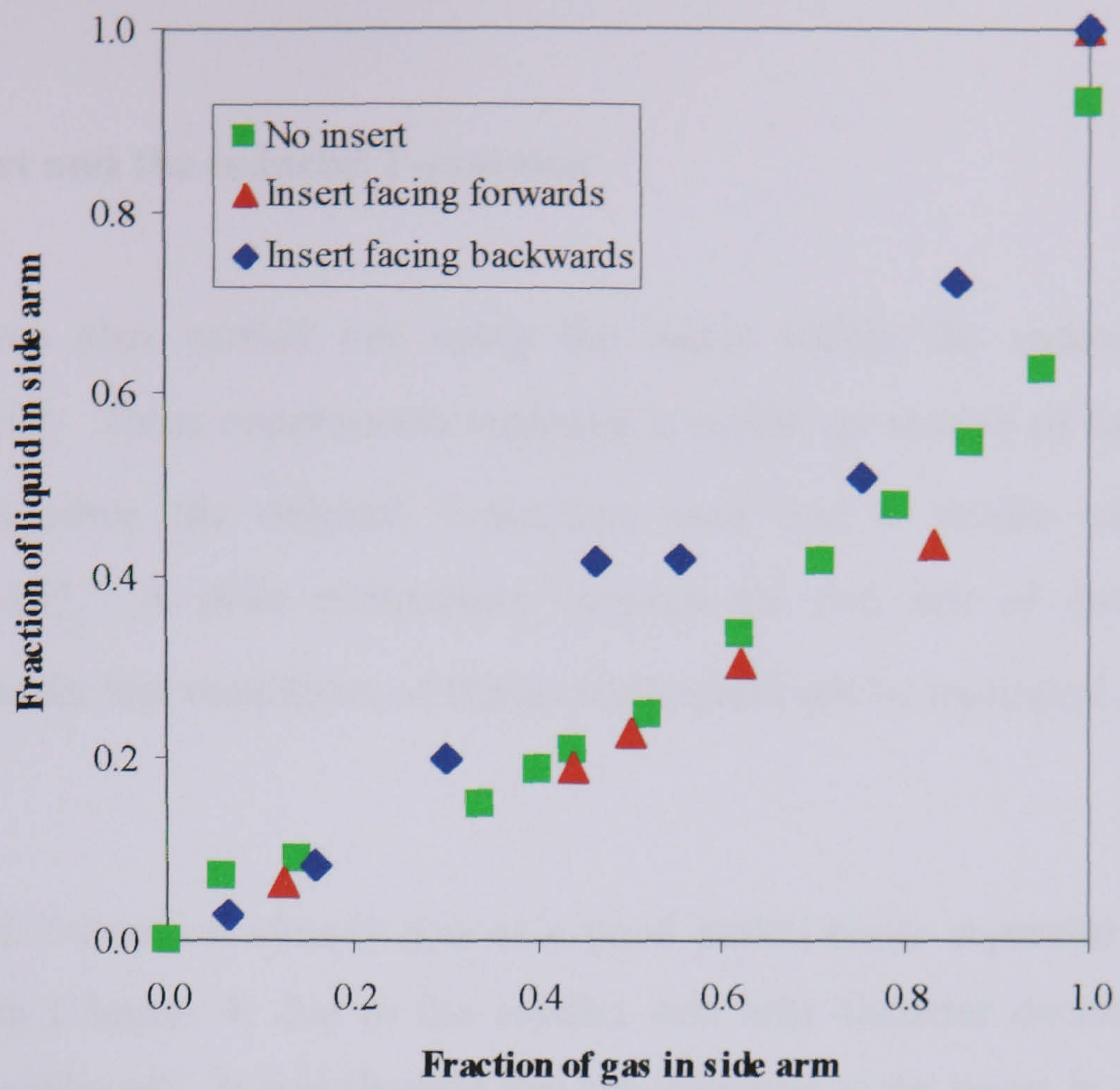


Figure 5-8: Stratified-wavy flow, 1/2D protrusion, 45° insert

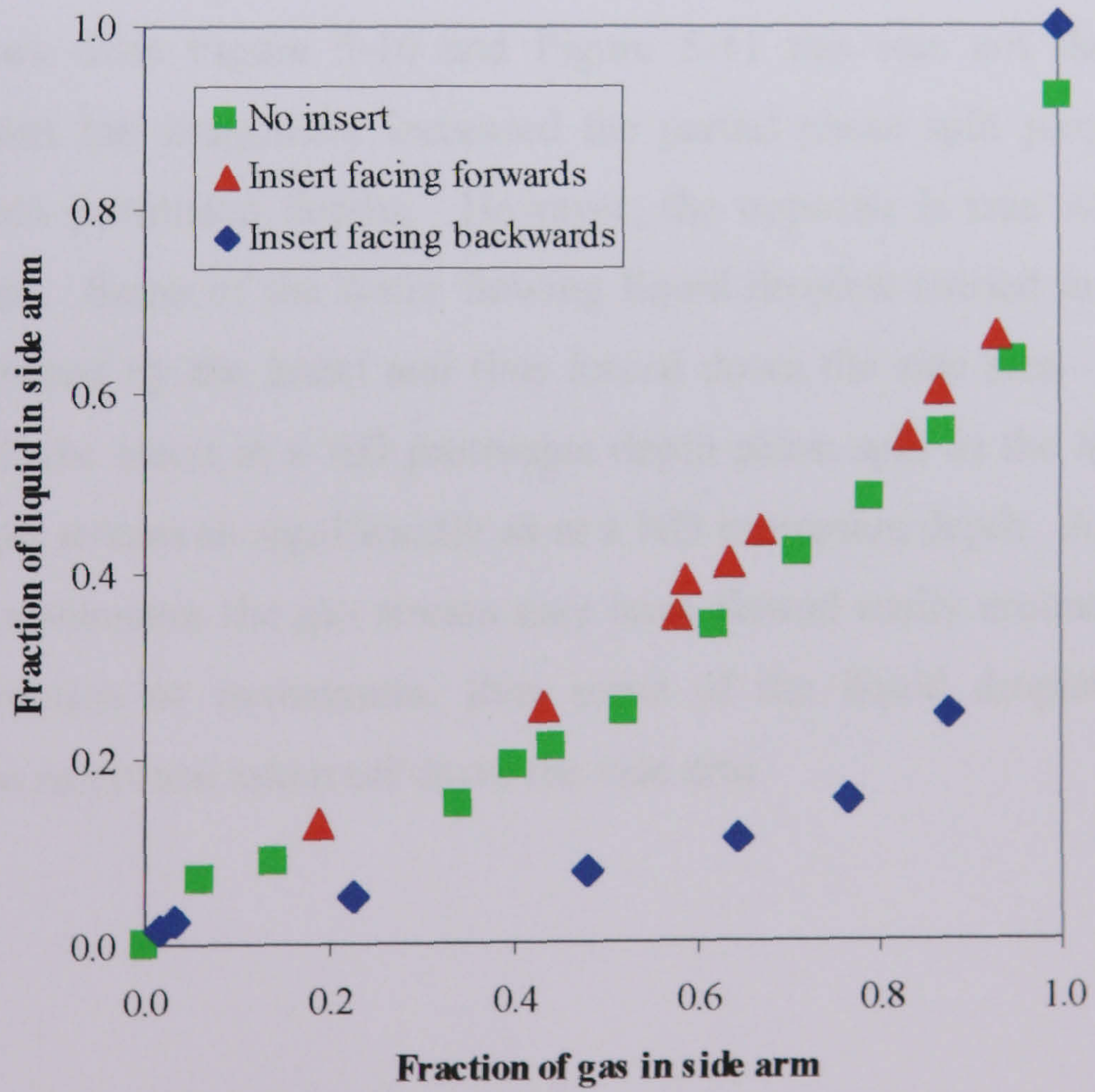


Figure 5-9: Stratified-wavy flow, 3/4D protrusion, 45° insert



### **5.2.3 Insert and the reduced T-junction**

Research was also carried out using the insert within the reduced T-junction ( $D_3/D_1 = 0.6$ ). These experiments represent a scaled up version of the Butterworth (1980) runs since the original T-junction used had a similar side arm ratio ( $D_3/D_1 = 0.65$ ). A strict comparison between the two sets of data can not be performed as the test conditions of Butterworth could not be replicated on the present rig.

The reduced T-junction already acts as a good partial phase separator, as explained previously in Chapter 4, due to the smaller side arm diameter decreasing the area available for take off. It was thought that the presence of the insert in either position would enhance the phase split as the protrusion forms a physical boundary thus preventing even the slower liquid film from being extracted into the side arm.

As can be seen from Figure 5-10 and Figure 5-11 this was not the case. The backwards insert has marginally increased the partial phase split properties of the junction at both protrusion depths. However, the opposite is true with the insert facing forwards. Some of the faster flowing liquid droplets carried in the gas core have been captured by the insert and thus forced down the side arm. This is more noticeable with the insert at a  $\frac{1}{2}D$  protrusion depth phase split as the insert may not interrupt the gas stream as significantly as at a  $\frac{3}{4}D$  protrusion depth. As the insert is only 0.076m in diameter the gas stream may have flowed easily around it with little change in direction or momentum, thus some of the liquid droplets have been captured by the insert and taken off down the side arm.



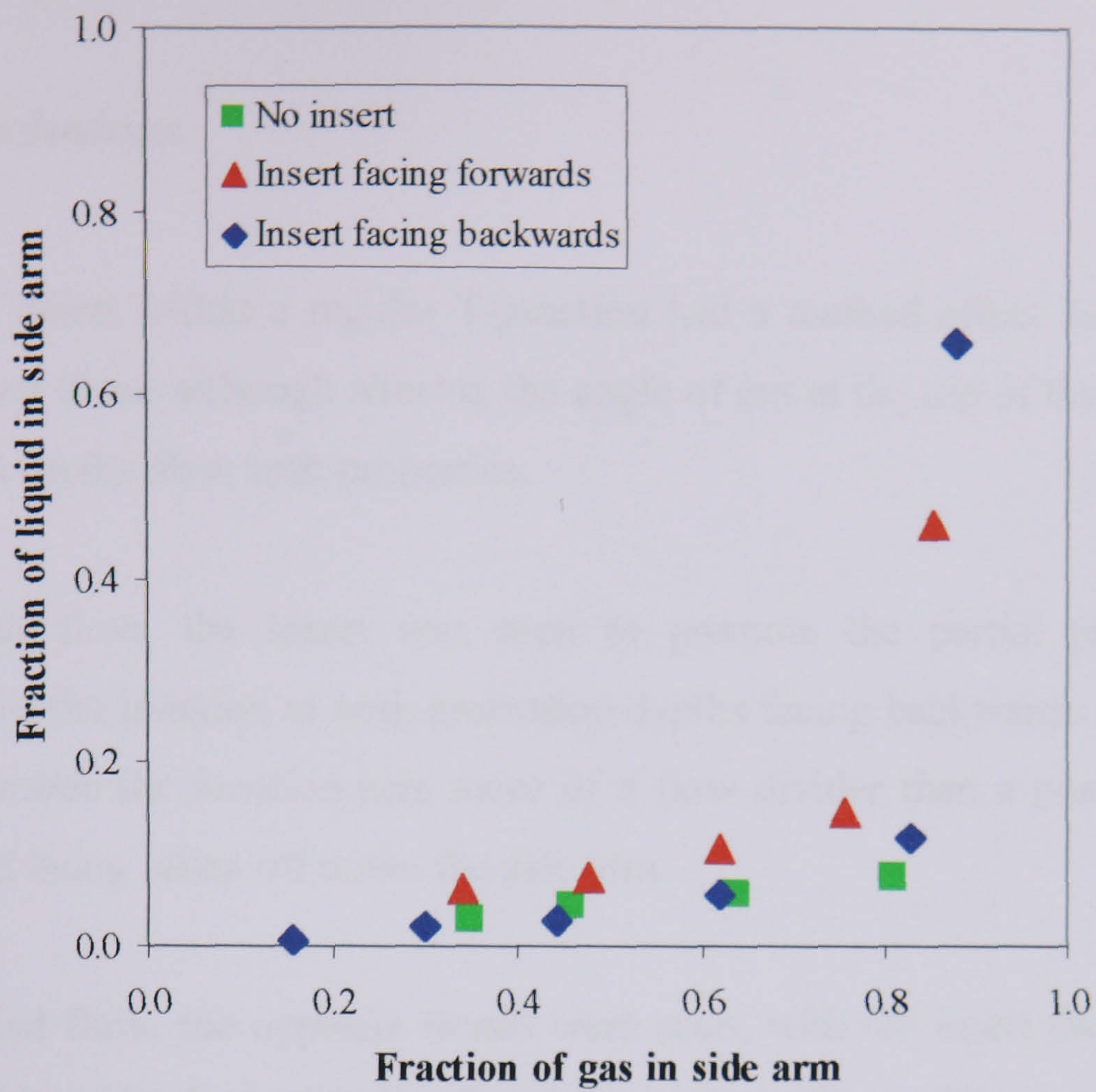


Figure 5-10: Reduced T-junction, annular flow,  $\frac{1}{2}D$  protrusion,  $45^\circ$  insert

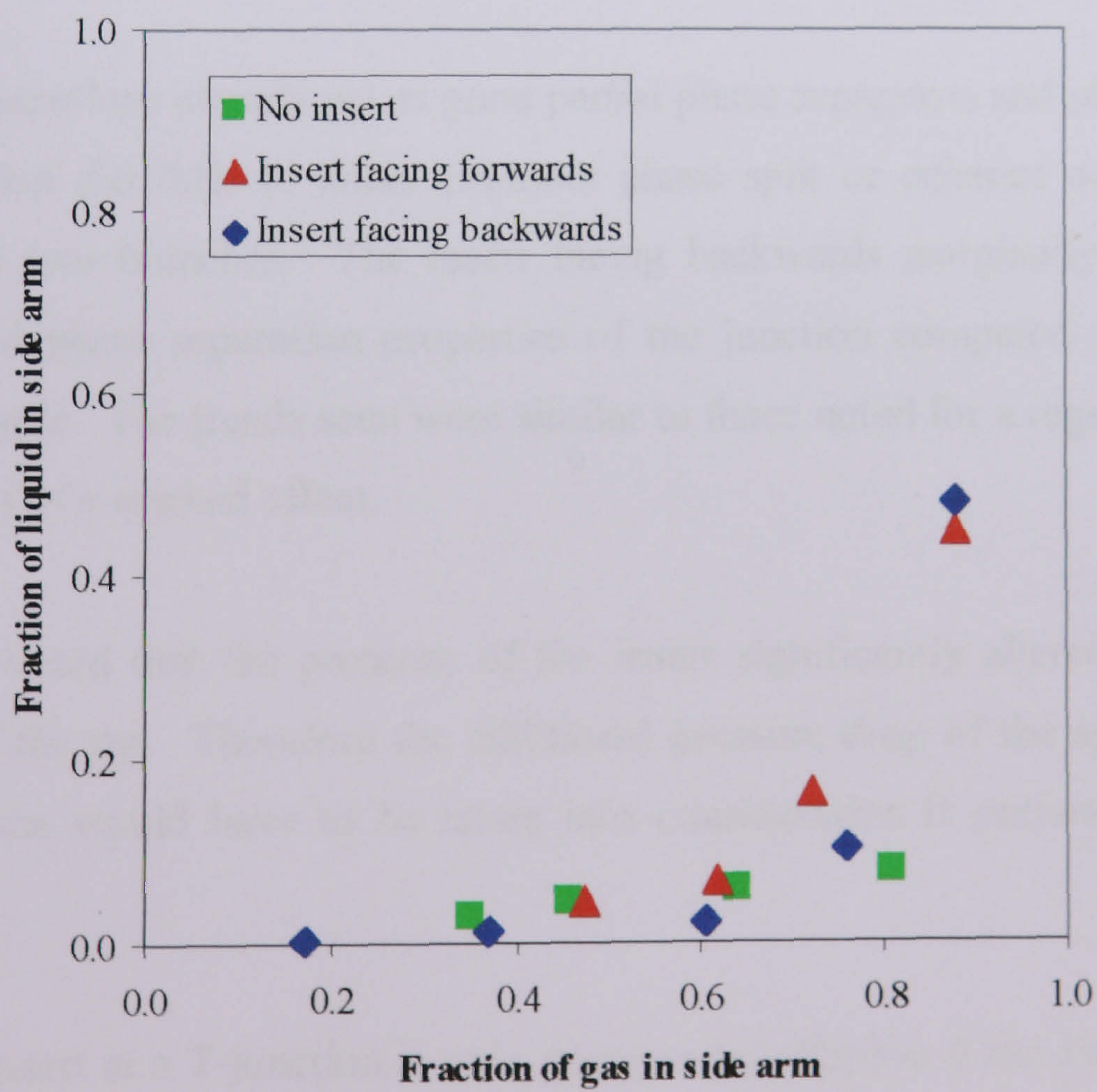


Figure 5-11: Reduced T-junction, annular flow,  $\frac{3}{4}D$  protrusion,  $45^\circ$  insert



### **5.3 Conclusions**

Placing an insert within a regular T-junction had a marked effect both with annular and stratified flows although altering the angle of cut at the top of the insert had little to no effect on the flow split properties.

For annular flow, the insert was seen to promote the partial phase separation properties of the junction at both protrusion depths facing backwards. With the insert facing forwards the junction acts more of a flow divider than a phase splitter, with more liquid being taken off down the side arm.

For stratified flow, the opposite trends were seen, with the insert facing forwards at both protrusion depths improving the phase split qualities of the junction. With the insert facing backwards, again the junction acted more as a flow divider than phase splitter.

Reduced T-junctions already act as good partial phase separators and placing an insert at the junction did little to either promote phase split or enhance equal flow split between the two branches. The insert facing backwards marginally improved the already good phase separation properties of the junction compared with the insert facing forwards. The trends seen were similar to those noted for a regular T-junction, just with less of a marked effect.

It was also noted that the presence of the insert significantly altered the operating envelope of the rig. Therefore the additional pressure drop of the system with the insert in place would have to be taken into consideration if performance is to be maintained.

Placing an insert at a T-junction is only going to be effective if the inlet flow regime is known or can be effectively predicted since the direction the insert faces in order to promote phase split is different for the various flow regimes. If the inlet flow regime



cannot be predicted with certainty then placing an insert at a junction could have the opposite of the desired effect and thus have disastrous consequences on downstream equipment.

The forcing of a scrubber through the pipe network to remove deposits from the walls and so clearing the system, known as pigging, is also an issue to consider. With the inserts protruding into the main pipe, pigging that section could obviously not be done. Pigs could be retrieved before they reached the insert and re-entered at a more suitable location down stream but this scheme would only be cost effective and practical if the presence of the insert significantly improved the operation efficiency of the plant.



## CHAPTER 6

### Two T-junctions in Series

The work presented in earlier chapters considered the phase separation of gas-liquid flows at a single T-junction. Branch arm orientation and diameter; the effect of inserts and the addition of a U-bend have all been investigated with the ultimate aim of improving the phase separation. Within this chapter the use of two T-junctions in series has been considered. The initial aim of combining two T-junctions is to produce two essentially single phase streams with minimal intervention and cost. If this could be achieved without creating a complicated system then the possibilities of using T-junctions as partial phase separators is further increased. Plus, if the creation of two essentially single phase streams can be guaranteed then the reluctance to use novel ideas within industry may be overturned.

Rea (1998) defined a good split achievable with a simple T-junction as 80% by mass of the gas exiting with less than 20% by mass of the liquid. A tighter criterion has been suggested as less than 10% by volume liquid exiting with the gas and less than 10% v/v gas in liquid. Such an approach is beyond the separation capacity of a single T-junction but is not deemed impossible for simple combinations of two junctions.

Two T-junctions were placed in series, the first with a vertically upwards (+90°) side arm, creating a gas rich stream, and the second a vertically downwards (-90°) side arm, to draw off the liquid. The remainder of the two-phase flow continues along the run arm. Movement of valves on each arm controls the phase split at each junction.



Only one other recent study has considered the effect of combining the phase separation properties of single T-junctions. The research of Bevilacqua *et al.* (2000) considered combinations of junctions where all branch arms were vertically upwards and their results related fractional gas (or liquid) take off against void fraction. Their investigations clearly show that combining junctions produces some very desirable effects and is worthy of serious consideration. They, however, studied the system as a whole whereas here the aim is to build a more complete picture by investigating specific system properties.

In order to gain a complete picture of how the system performs various aspects in particular were studied. These included altering the separation distance of the junctions to identify any interacting behaviour between the two; reducing the side arm diameter of the downwards junction to reduce the gas fraction drawn off and the effects of changing downstream resistance in each branch arm. The results have been presented in several ways to show the overall performance of the system and how the phase separation is related to its two individual junctions.

### ***6.1 Graphical representation of the phase separation***

The experimental configuration of the rig and detailed operating procedures are given in Chapter 3. The separation distance of the two junctions was measured from centre to centre and could be set at either 0.5m or 1.2m apart. For simplicity, the system can be represented schematically as indicated in Figure 6-1. The first junction was positioned with a vertically upwards (+90°) side arm and the second had a vertically downwards (-90°) side arm. Butterfly valves located on the up, down and run arms were used to control the phase split at the junctions and the air-water mixture leaving each branch was separated and measured, as in previous experiments.



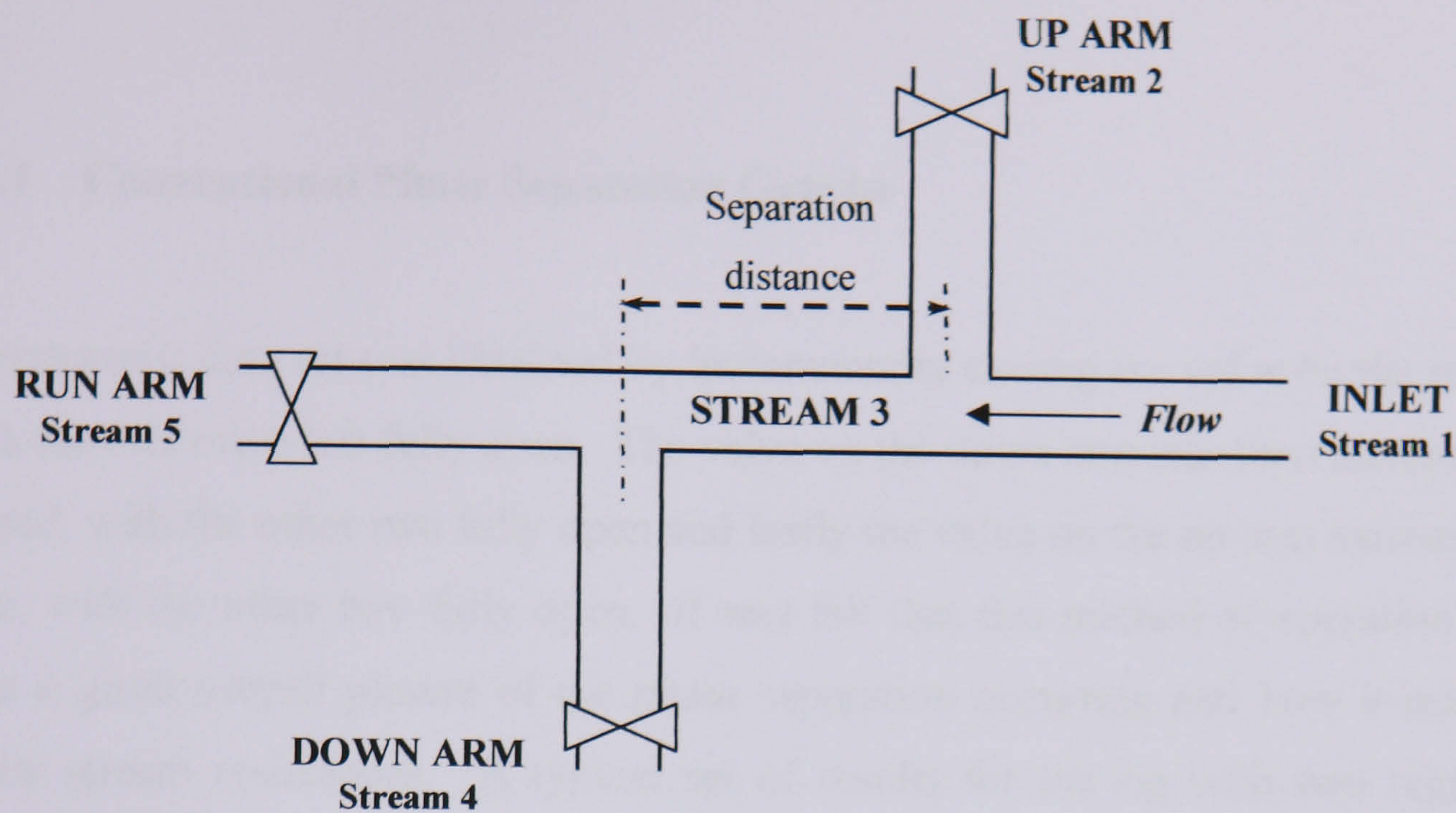


Figure 6-1: Schematic diagram of the two T-junction system

The data presented in the following graphs has used the stream numbers as indicated above, where stream 1 is the multiphase inlet and streams 2, 4 and 5 are the three system outlets. Stream 3 is the section of pipework between the two junctions and it could be seen as the new inlet conditions to the second T-junction, after gas extraction has occurred through the first. Having two active T-junctions the system now has three dynamic outlets, the composition of each dependent on the position of the butterfly valve in each outlet. This has transposed the problem into one with three dimensions as, obviously, the composition of all three outlets is related. As shown in Chapter 2 (Figure 2-11) Bevilacqua *et al.* (2000) combined the outlets of all their junctions so their comb separator still effectively had one inlet and two outlets, thus avoiding this problem. Many approaches have been considered in order to find a suitable method of presenting the separation data; some have been considered in more detail within this chapter.

As with the experiments for the single T-junction, the inlet flow rates studied fell within the annular and stratified flow regimes. As previously, the data from the stratified flow regime can be considered as high liquid, low gas inlet flows and low



liquid, high gas inlet flowrates. General trends were noticed within each flow pattern but reported here are only specific examples from each case.

### **6.1.1 Conventional Phase Separation Graphs**

A systematic data set was obtained by incrementally closing the valve on the run arm; with the other two left fully open. The valve on the down arm was then incrementally closed, with the other two fully open and lastly the valve on the up arm incrementally shut, with the other two fully open. It was felt that this method of operation would give a good overall picture of the phase separation occurring and how it related to down stream resistances. A typical set of results for the rig with two regular T-junctions being used, set 1.2m apart, can be seen in Figure 6-2 to Figure 6-5. Figure 6-2 shows the phase split curve for the up arm (stream 2). The fraction of inlet gas ( $G'$ ) drawn up the 0.127m diameter branch arm has been plotted against the fraction of inlet liquid ( $L'$ ) drawn up the same branch arm. The triangular symbols represent the phase split as the run arm butterfly valve is closed; the diamonds represent the effects of closure of the down arm valve and the circular symbols correspond to closure of the up arm valve. Data was also taken with all three valves left open. All points can be seen to lie along the x-axis, indicating that this is a pure gas stream. The fraction of the inlet gas drawn off increases to 75% as the run arm valve is closed. The close proximity to each other of the points representing movement of the down arm valve (the diamonds) indicates that little gas is taken off down this arm and what is cannot be forced back through the up arm to improve its take off. Obviously closure of the up arm valve reduces all gas drawn off and forces it through the two remaining open branch arms as indicated by the low  $G'$  values of the circular points.

Plotting the phase separation at the second T-junction with the downwards side arm, the data can be looked at from two points of view. The first considers the phase split based on the inlet two-phase flow in stream 1, see Figure 6-3. A liquid rich stream can be identified showing the fraction of gas entrained. A maximum is achieved with the run arm valve fully shut where all the liquid is being drawn off through the down leg together with about 25% of the gas. This corresponds to the maximum gas



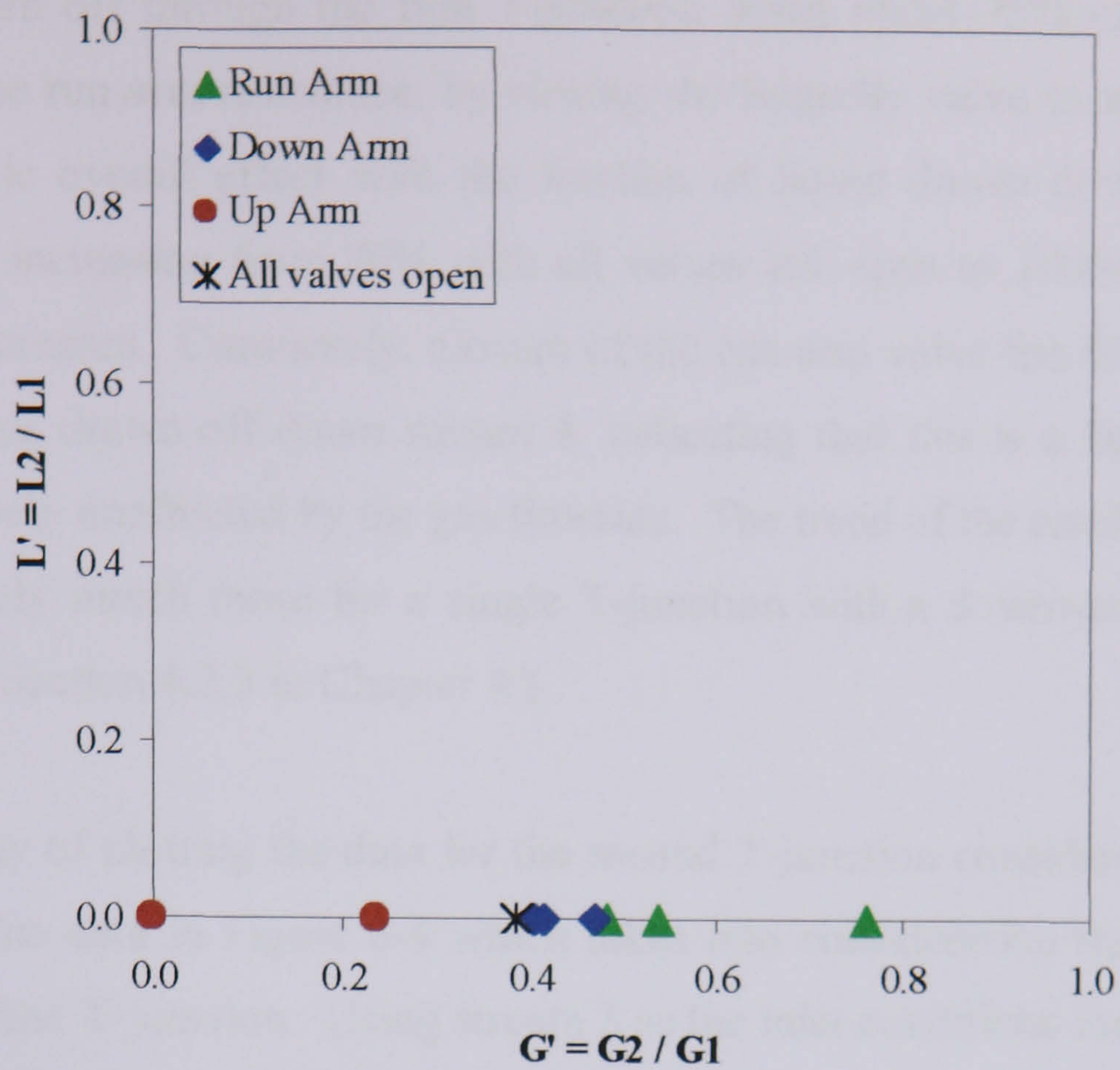


Figure 6-2: Phase split results for the up arm,  $U_{gs} = 12\text{m/s}$  and  $U_{ls} = 0.31\text{m/s}$

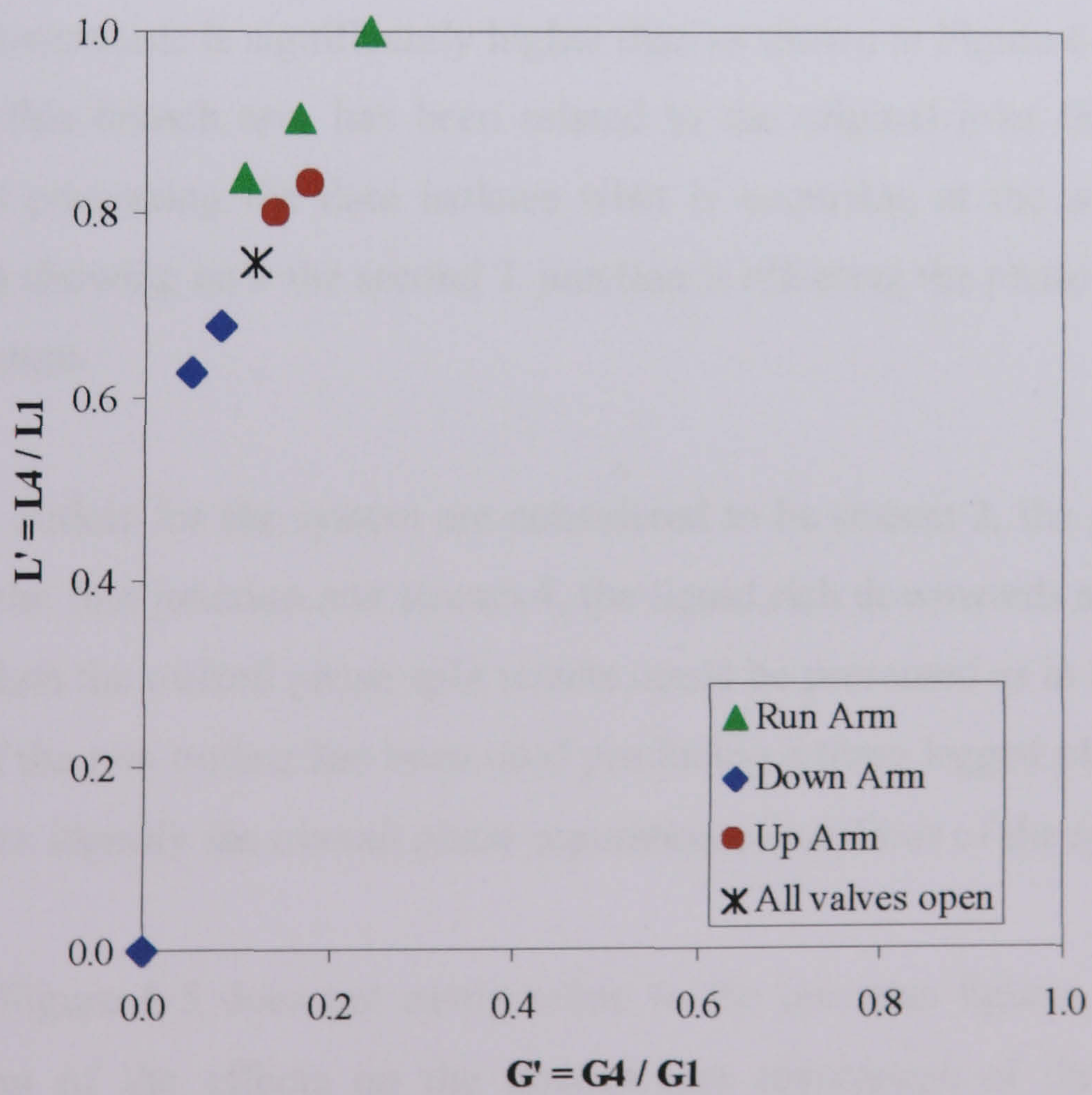


Figure 6-3: Phase split results for the down arm based on inlet,  $U_{gs} = 12\text{m/s}$  and  $U_{ls} = 0.31\text{m/s}$



fraction drawn off through the first T-junction being about 75% of the inlet flow. Increasing the run arm resistance, by closing the butterfly valve in stream 5, has the most dramatic overall effect with the fraction of liquid drawn down the stream 4 significantly increasing from 70% with all valves left open to 100% as the run arm resistance increases. Conversely, closure of the run arm valve has little effect on the fraction of gas drawn off down stream 4, indicating that this is a liquid rich stream that is relatively unaffected by the gas flowrate. The trend of the results plotted in this manner closely match those for a single T-junction with a downwards side arm (as described in Section 4.2.3 in Chapter 4.)

A second way of plotting the data for the second T-junction considers the inlet being stream 3. The data in Figure 6-4 which takes into consideration the gas drawn off through the first T-junction. Using stream 3 as the inlet conditions forces the locus of the plot to follow a more conventional phase split curve from (0,0) to (1,1). Using this method highlights the effects of downstream resistances and the general trends shown in Figure 6-3. It can still be noted that increasing the resistance in the run arm has the greatest effect on phase split but as shown here the fraction of gas in stream 3 diverted downwards is significantly higher than as shown in Figure 6-3 where the take off down this branch arm has been related to the original inlet flow. Hence, this method of presenting the data isolates what is occurring at the second T-junction rather than showing how the second T-junction is effecting the phase separation of the overall system.

If the two outlets for the system are considered to be stream 2, the gas rich upwards arm from the first junction and stream 4, the liquid rich downwards arm of the second junction, then the overall phase split results could be presented as in Figure 6-5. Here the sum of the two outlets has been used producing a three legged plot which initially does little to identify the overall phase separation capabilities of the system.

Although Figure 6-5 does not easily relate to the previous figures, a more detailed examination of the effects on the downstream resistances of the system can be achieved. Here closure of both the run and up arm butterfly valves have more of an



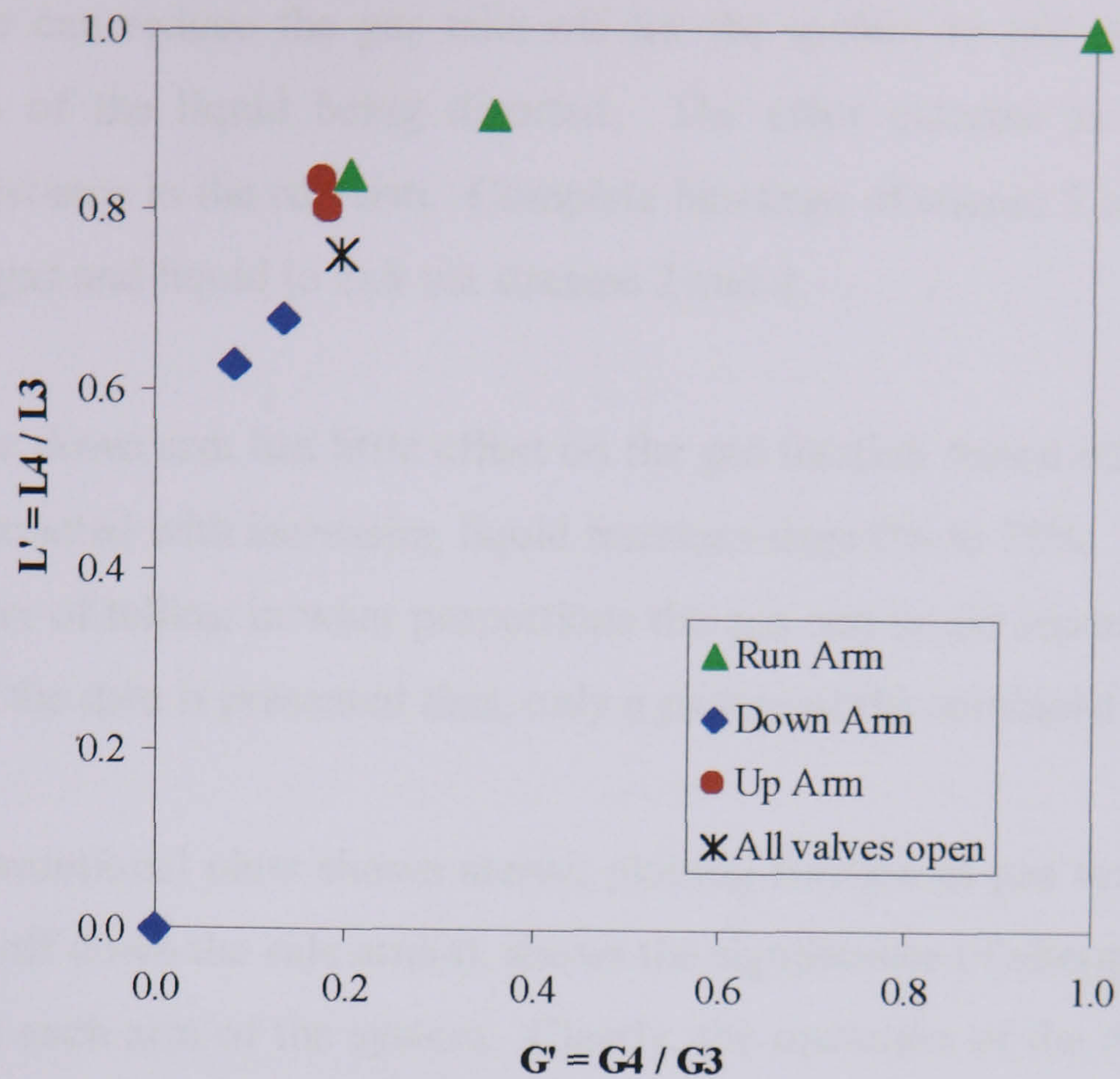


Figure 6-4: Phase split results for down arm based on stream 3,  $U_{gs} = 12\text{m/s}$  and  $U_{ls} = 0.31\text{m/s}$

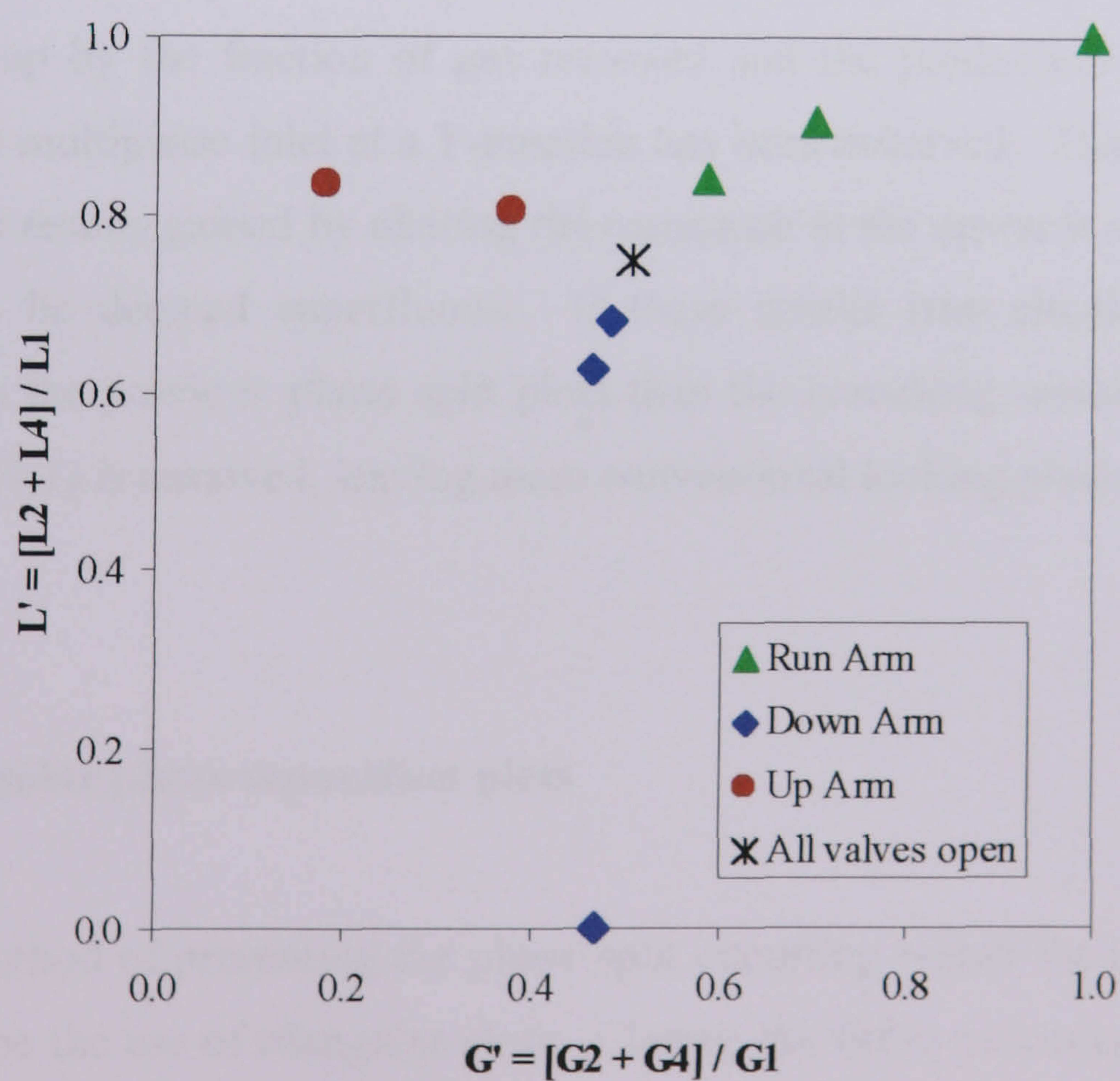


Figure 6-5: Overall phase split results for  $U_{gs} = 12\text{m/s}$  and  $U_{ls} = 0.31\text{m/s}$



effect on the fraction of gas drawn off through the system. Complete closure of the up arm valve can reduce the gas take off for the system to just under 20% with roughly 80% of the liquid being diverted. The other extreme is noted with the increased resistance in the run arm. Complete blockage of stream 5 obviously forces all incoming gas and liquid to exit via streams 2 and 4.

Closure of the down arm has little effect on the gas fraction drawn off as 50% of the gas can be extracted with increasing liquid fractions from 0% to 75%. However, there is no easy way of telling in what proportions the gas and liquid separates down each of the exits if the data is presented thus, only a picture of the combined streams given.

In all the conventional plots shown above, plotting fraction of gas versus fraction of liquid drawn off down the side arm(s), shows the significance of altering down stream resistances in each arm of the system. Clearly, the operation of the downwards side arm and the run arm butterfly valves has a more considerable effect than altering the upwards arm valve. This is because the distribution of both the gas and the liquid is effected rather than purely that of the gas. There is also little advantage gained by reducing the fraction of gas drawn up the first side arm. The liquid phase is clearly not being drawn up by the fraction of gas removed and the production of a pure gas stream from a multiphase inlet at a T-junction has been achieved. This could lead to the phase split results gained by altering the resistance in the upwards arm of the first T-junction to be deemed superfluous. If these results (the circular points) are removed from the previous phase split plots then the branching section of the locus from (0,0) to (1,1) is removed, leaving more conventional looking phase split plots.

### **6.1.2 Triangular phase separation plots**

A different method of presenting the phase split occurring within the two T-junction system could be the use of triangular plots. Clearly, the flows measured from each of the three outlets are interconnected and this is a method of representing them together on one graph.



Plotting data from the same experimental conditions as above,  $U_{gs} = 12\text{m/s}$  and  $U_{ls} = 0.31\text{m/s}$ , on a triangular diagram gives a different perspective on the results. Using the conventional  $G'$  versus  $L'$  plots, the gas fraction with its corresponding liquid fraction for each valve setting can be easily identified; with triangular diagrams the fraction of the inlet gas, liquid or the total drawn down each of the branches is shown separately.

In Figure 6-6 the fraction of gas taken off down each arm is plotted with respect to the valve position. As in the previous section, the triangular points represent movement of the run arm valve, diamond points movement of the down arm valve and circular points movement of the up arm valve and the spit with all valves open is shown by the star. This looks very similar to Figure 6-5 but here just the gas fraction leaving drawn down each of the three branches is considered. As can be seen, once again movement of the upwards arm butterfly valve forces the plot to branch off in an uncharacteristic way. Movement of this valve forces the gas, that would otherwise be drawn off, to exit with the liquid through the other two arms. This has a detrimental effect on the system by reducing its phase separation qualities and therefore would not be done in practice.

This method of plotting the phase separation characteristics was found to be fairly useful when considering the trends in the fraction of inlet gas drawn down each arm. The physical translation of these trends was however difficult to transpose to the actual two T-junction system as information on the liquid phase was lacking.



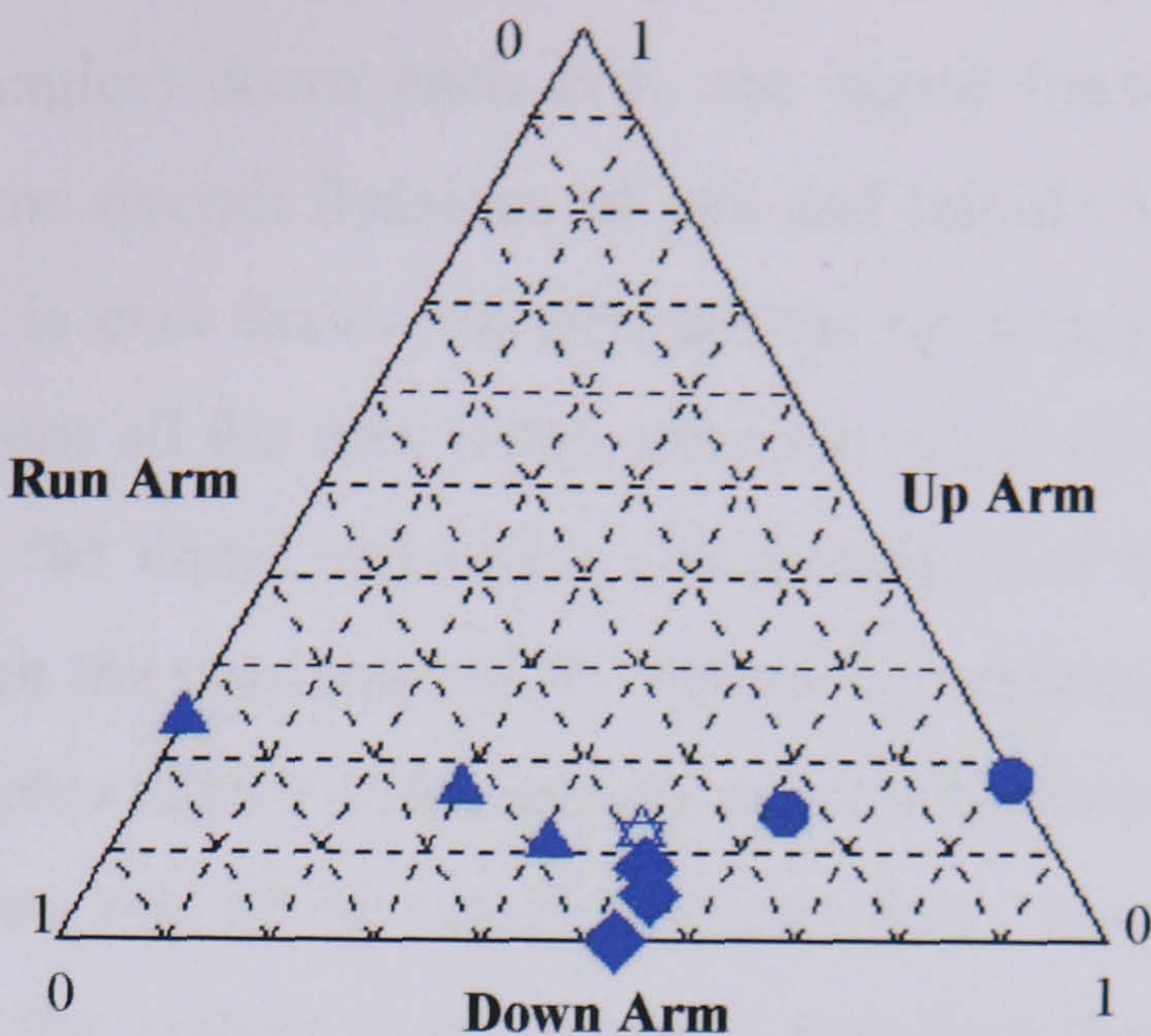


Figure 6-6: Triangular plot of gas phase split,  $U_{gs} = 12\text{m/s}$  and  $U_{ls} = 0.31\text{m/s}$

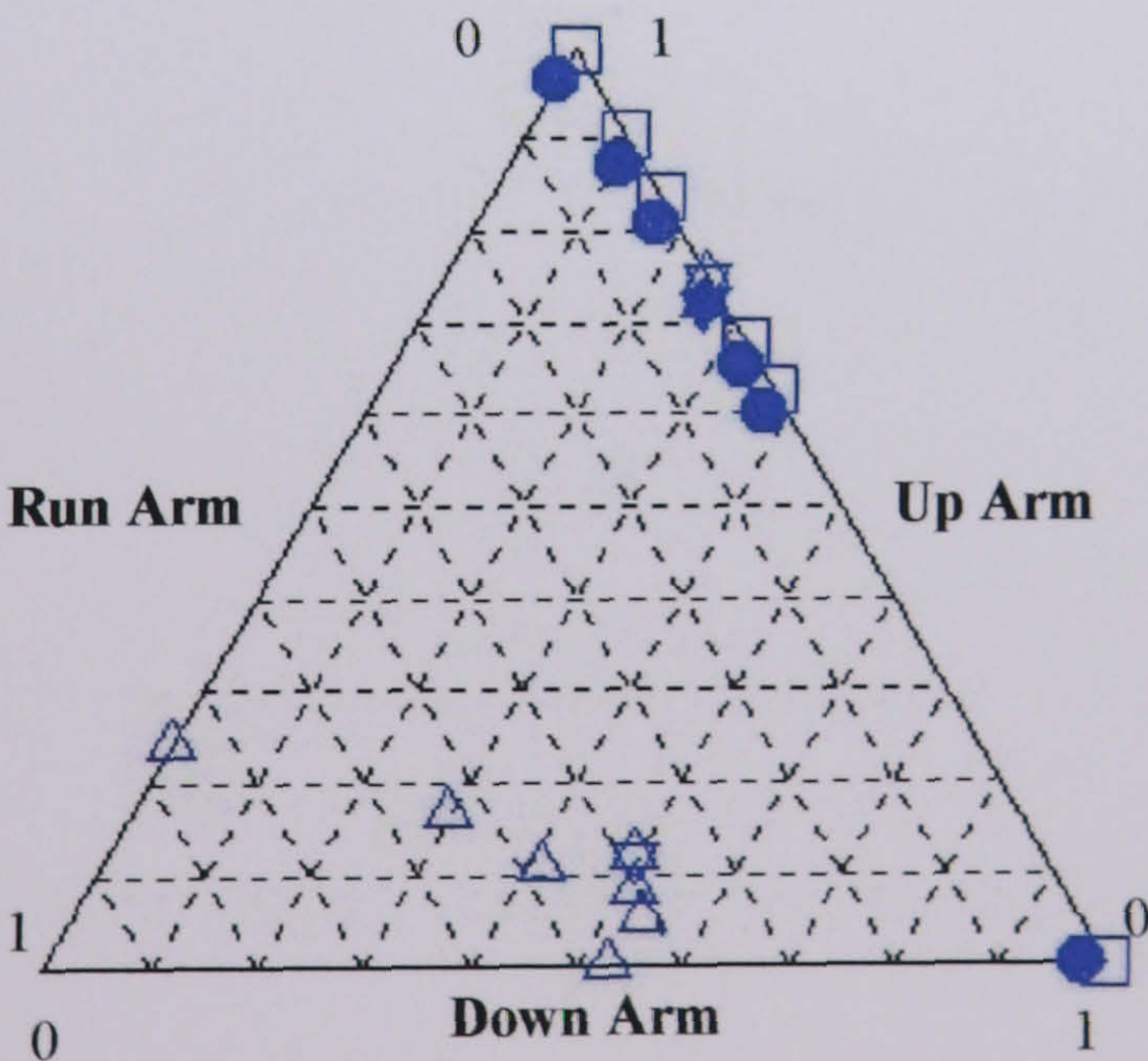


Figure 6-7: Triangular plot of the phase separation for the system,  $U_{gs} = 12\text{m/s}$  and  $U_{ls} = 0.31\text{m/s}$



Figure 6-7 represents the complete phase separation of the system based on the gas fractions (hollow triangles) down each arm, the liquid fractions (hollow squares) down each arm and the overall fractions of gas and liquid (full circles) down each arm. Since no liquid is ever drawn off through the up arm, plotting the fraction of liquid removed collapses all the data points onto the origin of the up arm axis. This method of presenting the liquid separation characteristics of the system is therefore rendered futile as were the conventional  $G'$  versus  $L'$  separation plots. Plotting the overall fractions (gas plus liquid) of the inlet flow passing down each branch shifts the trend only slightly from that of the liquid fraction curve. However, since the actual mass of gas entering the system is significantly less than that of the liquid, for all experiments, this is not surprising.

Triangular plots do not present an easy method of identifying inlet conditions leading to good separation within the two T-junction system. Whilst useful for identifying where the different phases are going, they do not produce an elegant solution. Basing the separation quality of the system on the fraction of gas drawn off through the different branches is dangerous as the liquid present is not considered.



### 6.1.3 Combining two outlets

Considering each of the three outlets individually, unlike the work of Bevilacqua *et al.* (2000), gave an insight as to how the inlet two-phase flow interacted with the two T-junction system. Knowing the composition of each stream has given the system greater flexibility and allowed a study into the effects of combining the different outlets together, as can be seen in Figure 6-8.

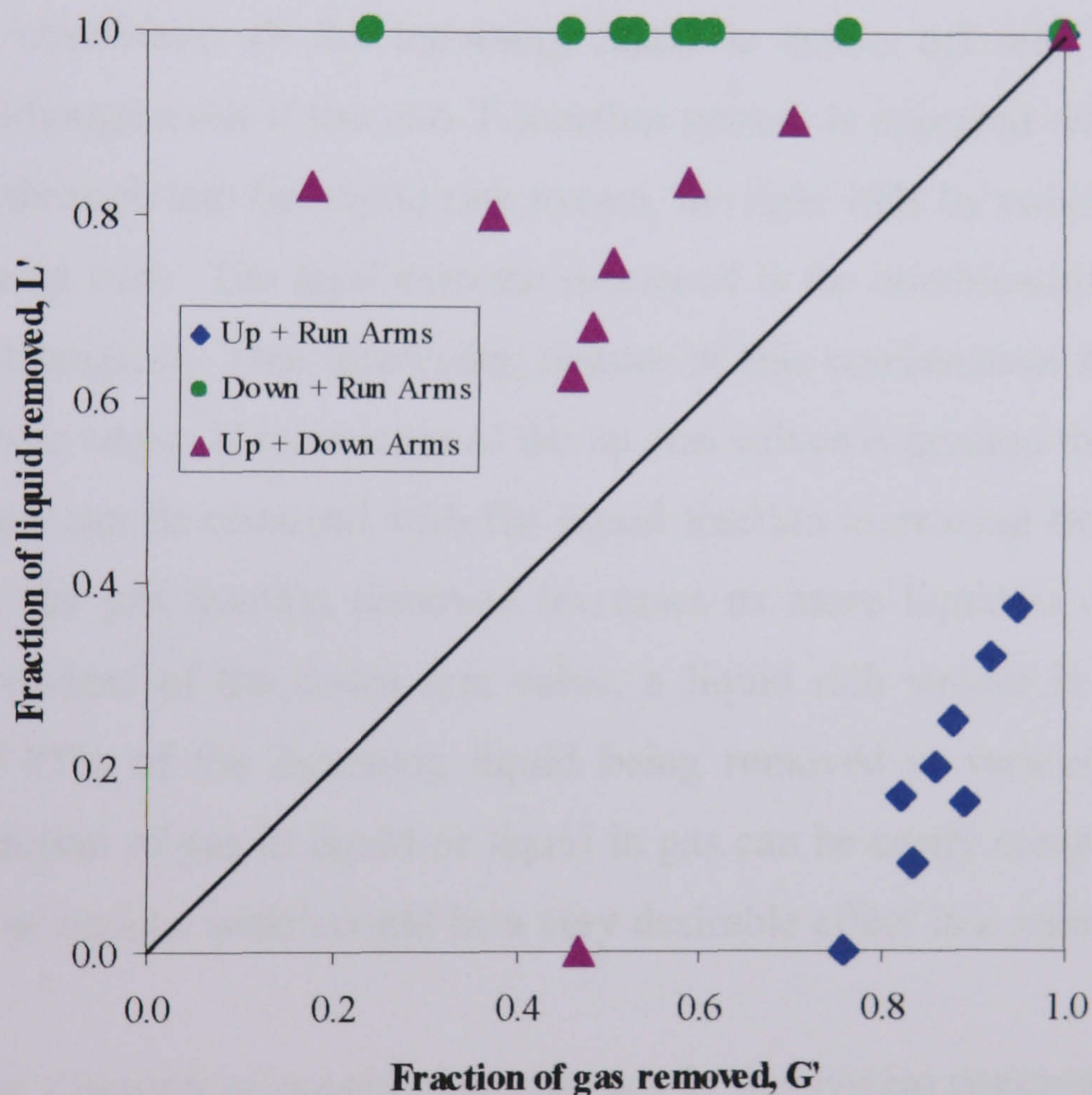


Figure 6-8: The effects of combining the different outlets.  $U_{gs} = 12\text{m/s}$  and  $U_{ls} = 0.31\text{m/s}$

Obviously, by combining two of the outlets, the system has reverted back to one with an inlet and just two outlets, which allows the use of conventional  $G'$  versus  $L'$  separation plots. The three outlets still affect the overall shape of each curve in a way not previously seen on such plots.



Depending on the separation requirements, the different junction combinations allow for various separation qualities to be achieved. Combining the up and run arms (diamonds), see Figure 6-8, gives a very gas rich separation with gas take off having a fairly low effect on the fraction of liquid drawn off. Under these conditions the minimum inlet gas extracted is 75% and this can be achieved with no liquid intake. The increase in liquid follows a fairly linear trend until the down arm valve is totally shut forcing the liquid out of the run arm but this occurs beyond a gas take off of 95%, still with less than 40% of the inlet liquid removed. This shows that the two T-junction system can achieve the 10% by volume liquid in gas separation criterion. The opposite extreme can be seen when combining the down and run arms (circles). Under these conditions all the incoming liquid is drawn off with increasing gas fractions. Although even if the two T-junction system is operated with minimal gas being drawn through into the liquid rich stream, the tight 10% by volume gas in liquid is still not being met. The least extreme measured is the combination of the up and down arms (triangles). One interesting feature of this combination is that it can be looked at in two ways. If movement of the up arm valves is ignored then around 50% of the inlet gas can be removed with the liquid fraction increasing from 0% to 75%. Beyond this, the gas fraction removed increases as more liquid is drawn off. By ignoring movement of the down arm valve, a liquid rich stream is created with a minimum of 75% of the incoming liquid being removed at various gas fractions. Hence the fraction of gas in liquid or liquid in gas can be easily controlled using this combination of outlets, which could be a very desirable effect in a separation system.

For all further discussions considering changes in the system parameters, the effects on the phase separation of the combined outlets has been presented. This method of presentation was deemed the most suitable for two reasons. Firstly, it presents a compact view of all the system features and how they interact with one another. Secondly, within an industrial setting two T-junctions mounted in series are unlikely to have three outlets. It is considered that two of the outlets would be coupled together for simplicity and to minimise piping costs.



Since all three outlets effect the overall shape of each of the curves. in all the following figures the effects of increasing the down stream resistance in each branch has been shown. The triangular symbols represent movement of the run arm valve, diamonds the down arm valve and circular for the run arm valve. The point where all valves are left open, indicating the simplest system available, is represented by a star.

## **6.2 Using a reduced T-junction**

Section 4.2.3 in Chapter 4 indicates that the use of a reduced T-junction with a downwards side arm can lower the entrained fraction of gas drawn downwards with the liquid. This concept was carried forward to the two T-junction system to further enhance the phase separation. A reduced T-junction placed with the upwards side arm would not aid gas take off, as indicated by the results in section 4.2.2 in Chapter 4. The presence of the reduced diameter side arm forces the same gas fraction drawn off to flow faster. The faster flowing gas in turn causes more of the liquid to be drawn upwards, thus lowering the quality of the gas rich stream previously created. Although this was not the case with the single T-junction, this phenomenon would reduce the quality of the gas rich stream created by the first T-junction. Hence, only the one reduced T-junction was used within the two junction system and that was with the downwards side arm.

Figure 6-9 shows the effects on the gas phase separation with the reduced T-junction in place. Comparing the combined output from the up and run arms it can be seen that the fraction of gas drawn off has increased to over 90% with reduced liquid take off. A pure gas rich stream can be achieved, leaving less than 10% of the inlet gas flow exiting within a liquid rich stream. Closer inspection of Figure 6-9 shows that, when combining the up and run arm, closure of the up arm valve increases the liquid take off for a given gas fraction thus having a detrimental effect on the separation curve. This coincides with previous discussions on the closure of the run arm valve. However, for all the following graphs the effects on phase separation of all valve positions have been shown.



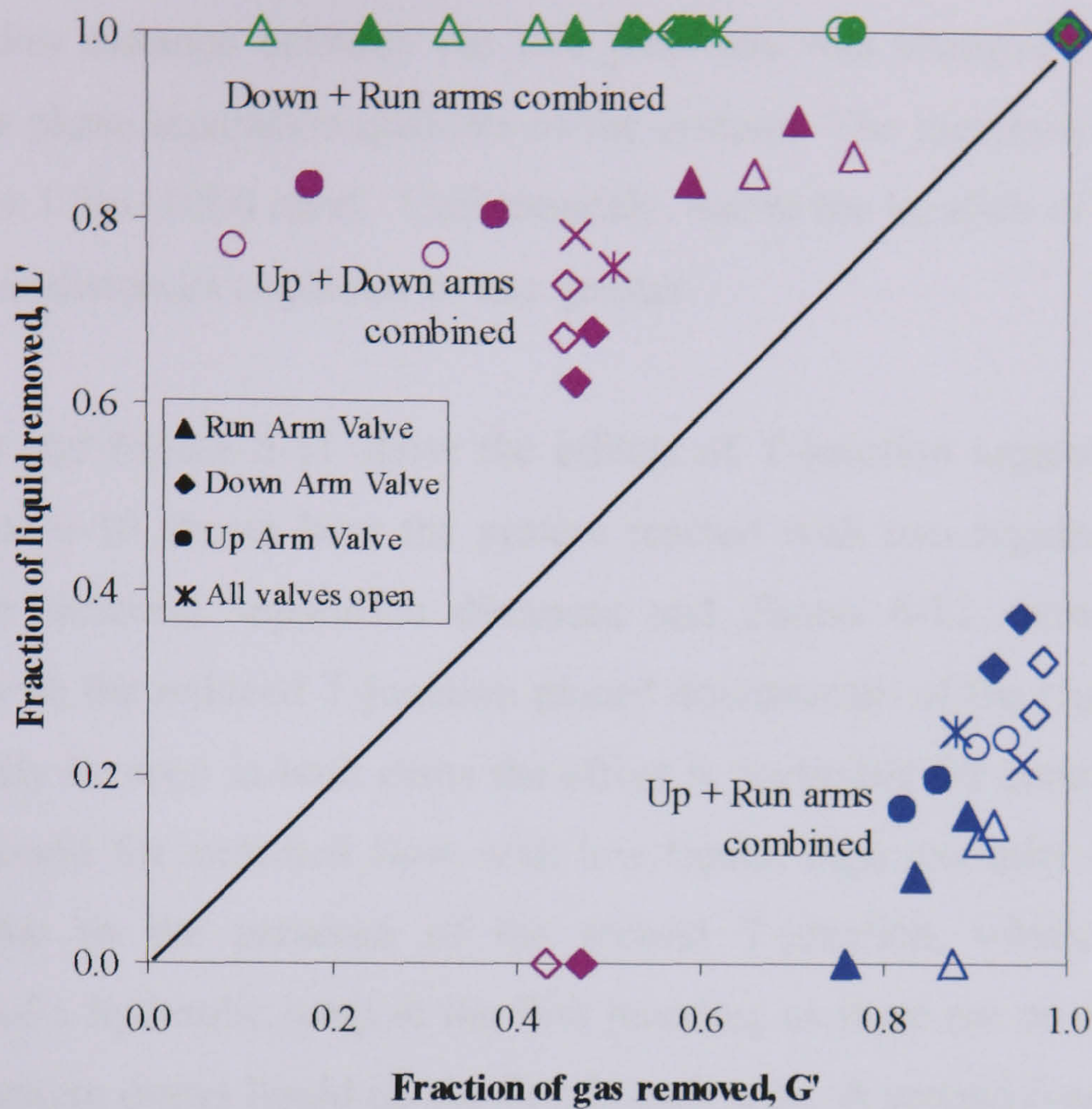


**Figure 6-9: Effects of using a reduced diameter T-junction,  $U_{gs} = 12\text{m/s}$ ,  $U_{ls} = 0.31\text{m/s}$**

**Hollow symbols represent reduced T-junction used with downwards side arm, full symbols represent two regular T-junctions within the system**

Comparing the results of the other two liquid rich combinations show that the presence of the reduced T-junction has lowered gas take off within the downwards side arm. The combined outlet of the down and run arm shows that with 100% of the inlet liquid being removed, the best separation achieved was with only 10% of the inlet gas flow being drawn off. This is a significant reduction on the fraction of gas drawn off by the two regular T-junction system and takes the two T-junction system closer to the stated 10% volume gas in liquid separation criterion. When the up and down arms are combined obviously the reduced gas take off through the down arm is almost negated by the increased gas drawn through the up arm.



### ***6.3 Altering the separation distance***

The separation distance between the two junctions was changed to investigate its effect on the phase separation qualities of the system. The junctions could be placed 0.5m (4D) or 1.2m (10D) apart. Unfortunately, due to the location of the flow facility the separation distances could not be any greater.

Figure 6-10 and Figure 6-11 show the effects of T-junction separation for annular flow. Figure 6-10 shows how the system reacted with two regular T-junctions in place at the different separation distances and Figure 6-11 shows the effect of separation with the reduced T-junction placed downstream of the regular T-junction. As can clearly be seen in both cases the effect is negligible for annular flow and the same was found for stratified flow with low liquid, high gas inlet flowrates. This could be due to the presence of the second T-junction, which eliminates the occurrence of a hydraulic jump at the first junction, as there are no conditions under which the system draws liquid up the first branch arm. A second reason why the two T-junctions seemingly do not interact could be due to the large diameter pipes involved and the relatively low gas and liquid inlet flow rates.

However, for stratified flow with high liquid, low gas inlet flowrates the effect of separation distance was negligible with the reduced junction placed down stream of the first but with the two regular junctions a variance was noted. See Figure 6-12.



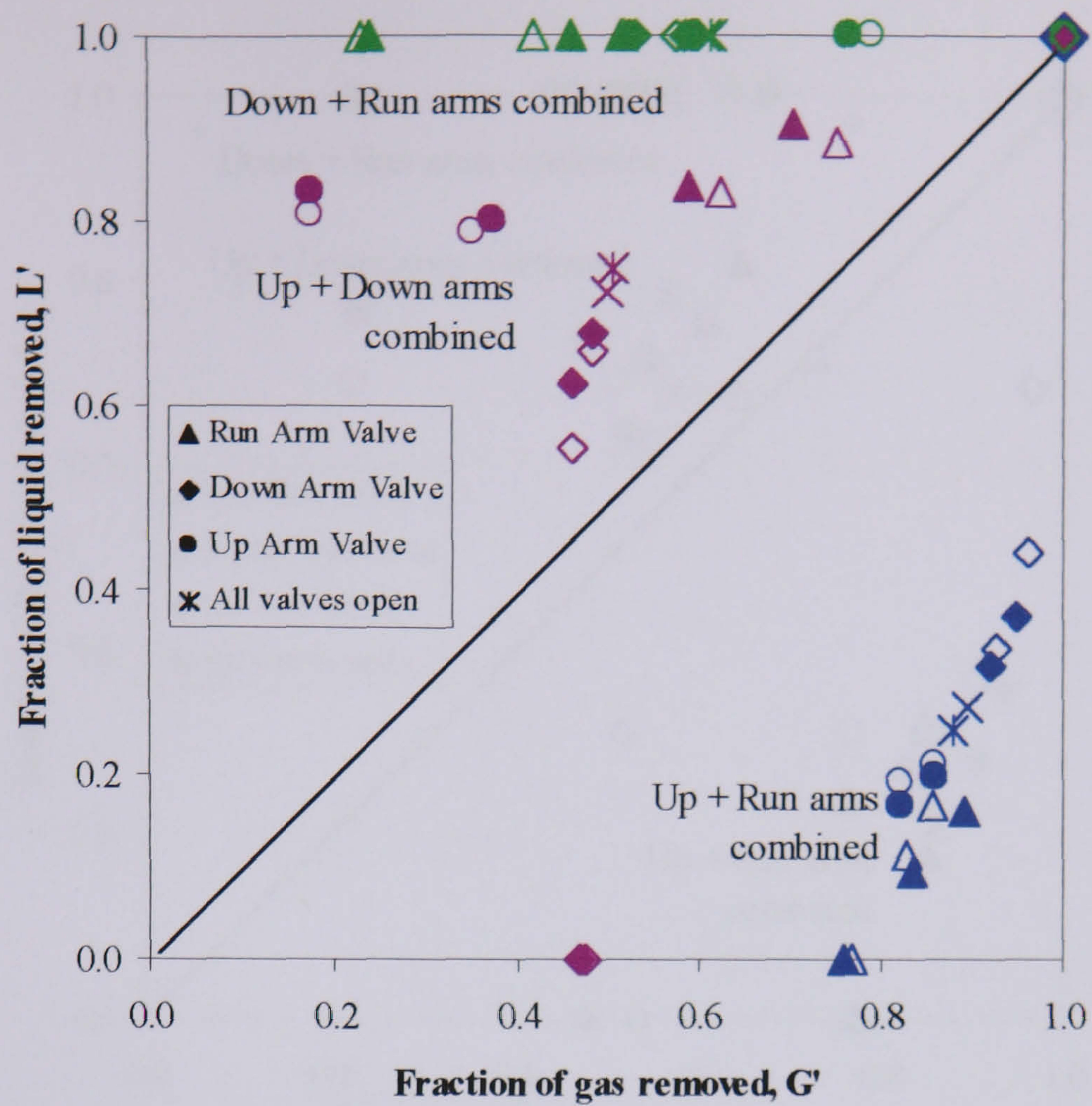


Figure 6-10: Effect on T-junction separation distance with two regular T-junctions,  $U_{gs} = 12\text{m/s}$  and  $U_{ls} = 0.31\text{m/s}$ . Hollow symbols represent separation distance 0.5m and full symbols 1.2m

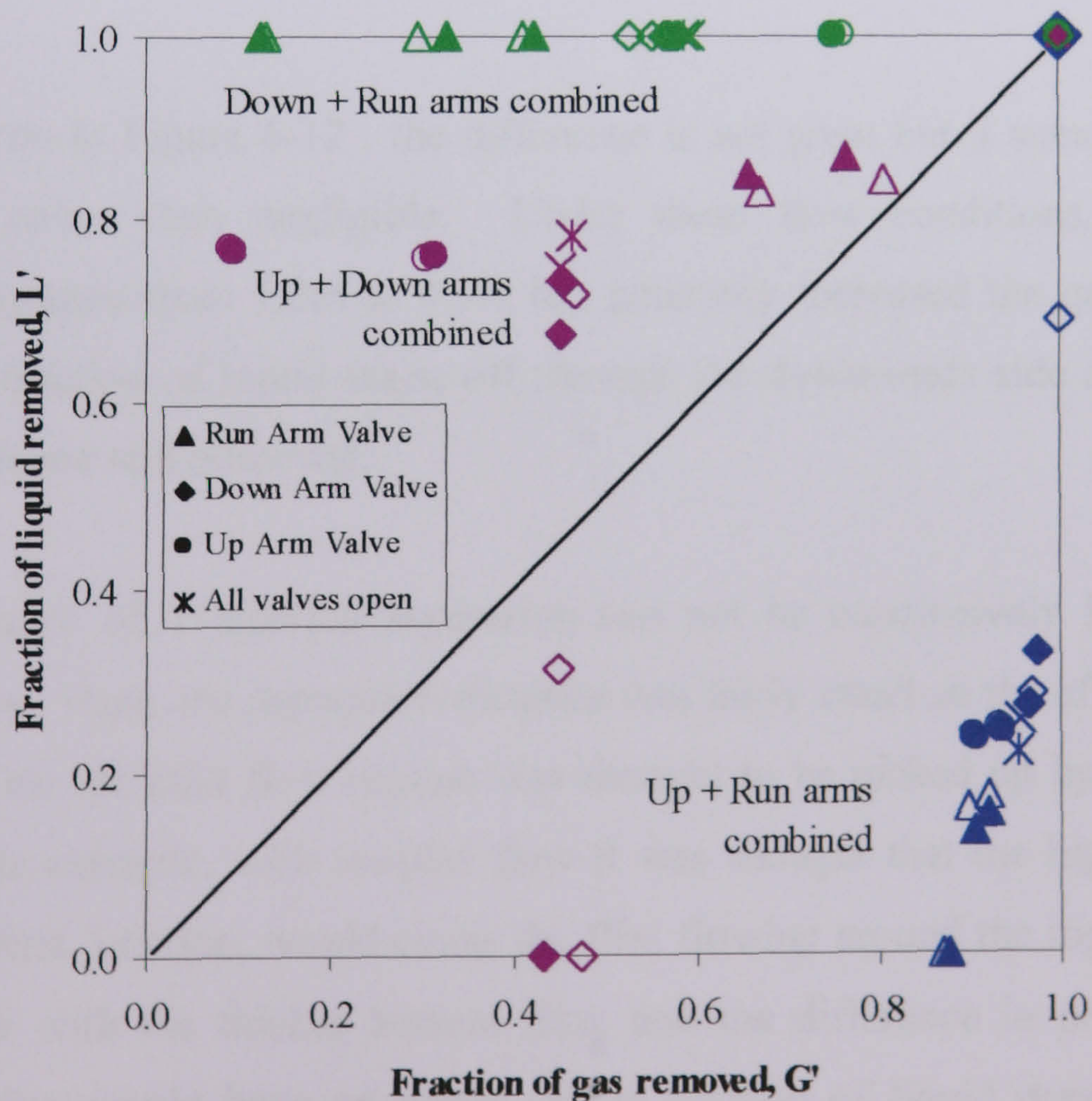
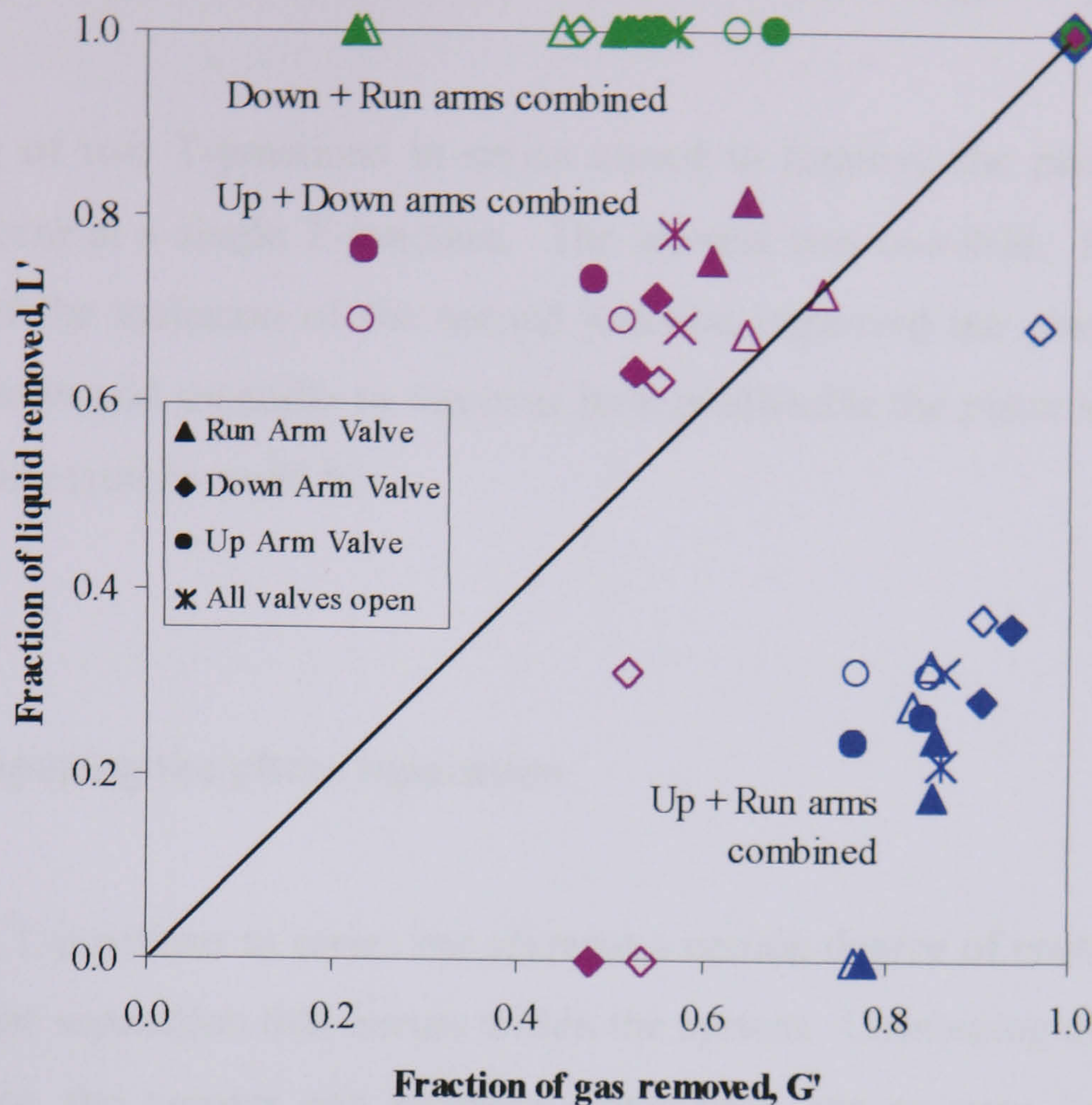


Figure 6-11: Effect of T-junction separation distance with reduced T-junction,  $U_{gs} = 12\text{m/s}$ ,  $U_{ls} = 0.31\text{m/s}$ . Hollow symbols represent separation distance 0.5m, the full symbols 1.2m





**Figure 6-12:** Effect of T-junction separation distance with two regular T-junctions,  $U_{gs} = 4\text{m/s}$ ,  $U_{ls} = 0.043\text{m/s}$ . Hollow symbols represent separation distance 0.5m, the full symbols 1.2m

As can be seen in Figure 6-12, the difference is not great but it stands out as being identifiable rather than negligible. Under these flow conditions, reducing the separation distance from 1.2m to 0.5m has generally increased the gas take off and reduced the fraction of liquid taken off through the downwards side arm. All other general trends are still observed.

The significance of T-junction separation can not be conclusively identified from these findings. Here, the separation distance was fairly small so the effect the first T-junction has on the inlet flow regime was thought to be picked up by the second T-junction. For example, with annular flow it was thought that the high gas take off through the first junction, would cause the film flowing around the top of the pipe to fall and flow with the thicker bottom film, and the difference in proximity of the second junction would have an effect of the fraction of liquid drawn through the second T-junction. Maybe this is the case but under these conditions little difference was observed.



## **6.4 Comparing Two T-junctions in series with a single T-junction**

The placing of two T-junctions in series aimed to improve the phase split already known to occur at a single T-junction. The interest was two-fold. Firstly, it was to investigate if the inclusion of the second junction improved the phase separation of two-phase flows and secondly to discover how predictable the phase separation of the two T-junction system could be.

### **6.4.1 Comparing the phase separation**

Placing two T-junctions in series has allowed a certain degree of control to be gained over the phase separation that occurs within the system. Combining different junction outlets means the system can produce either very gas or very liquid dominated streams for the same inlet flow conditions, unlike the flow split obtained with a single T-junction.

The results have been compared with those of a single junction, already investigated in detail within Chapter 4. For comparison purposes, since the phase separation of the two T-junction system can be considered in one of three ways - combining the up and run arms, the up and down arms or the down and run arms – the combination most appropriate to the results of the single junction being investigated has been considered.

The effect of the inlet flow regime has been investigated as this was one of the most significant parameters to affect the phase separation and was highlighted during the investigations on a single T-junction. The results for one particular run within the annular, stratified flow regimes have been presented to aid comparison. The results from the stratified flow regime have again been further divided into high liquid, low gas inlet flowrates and low liquid, high gas inlet flowrates. The effect on the phase separation using the reduced T-junction was also considered.



Figure 6-13 shows schematically the different branches that have been used within the following graphs to compare the phase separation at a single junction with that of the two T-junction system.

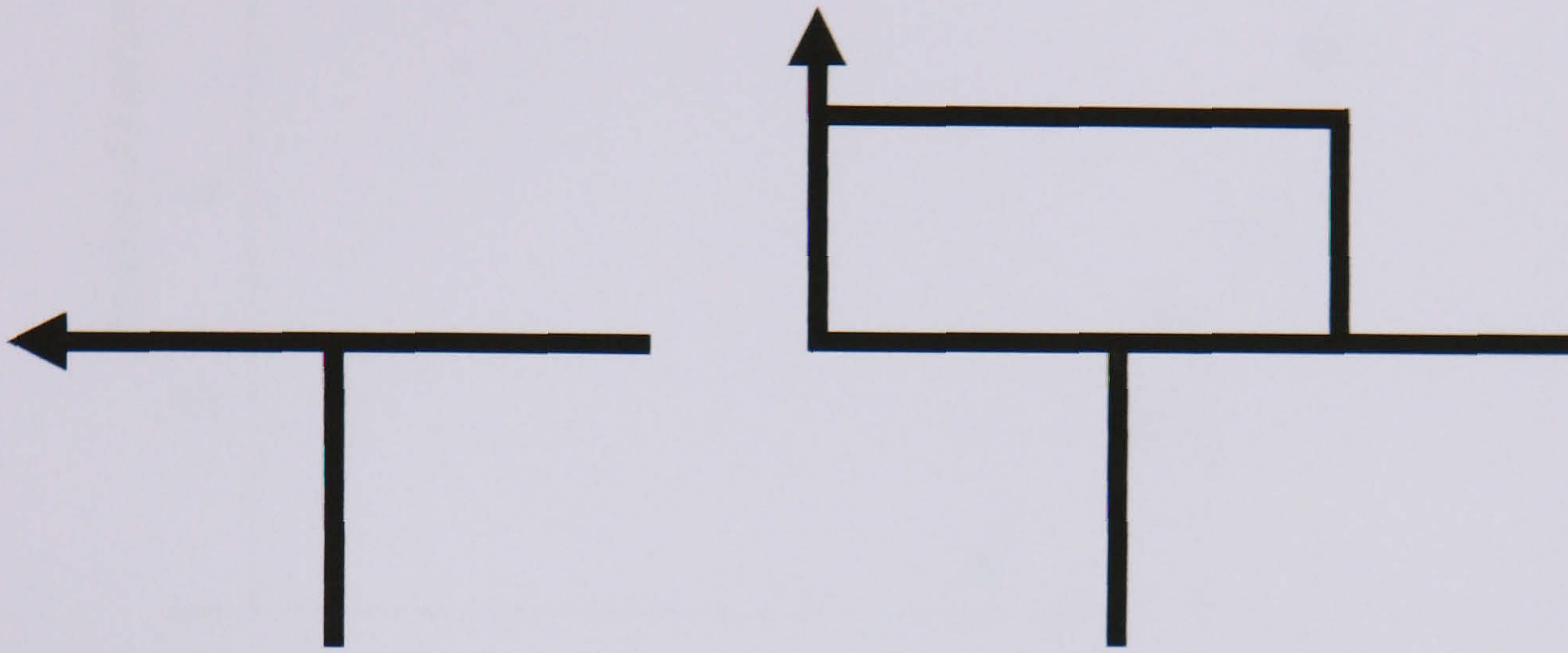


**Figure 6-13: Schematic representation of the different outlets being compared**

Figure 6-14 to Figure 6-16 show the phase separation of a single junction compared with that of the two T-junction system. In all cases the regular single T-junction was used with all branches being 0.127m in diameter and for the two T-junction system two regular junctions were set at 1m apart. As can be seen, the two T-junction system consistently performed a cleaner separation for all inlet flow rates.

Both Figure 6-14 and Figure 6-15 show movement of the up arm butterfly valve has had a detrimental effect on the phase separation. In both cases more liquid has been drawn off than otherwise achievable at the lower gas take offs. This forces the separation curve for the two T-junction system to merge with that of the single junction.



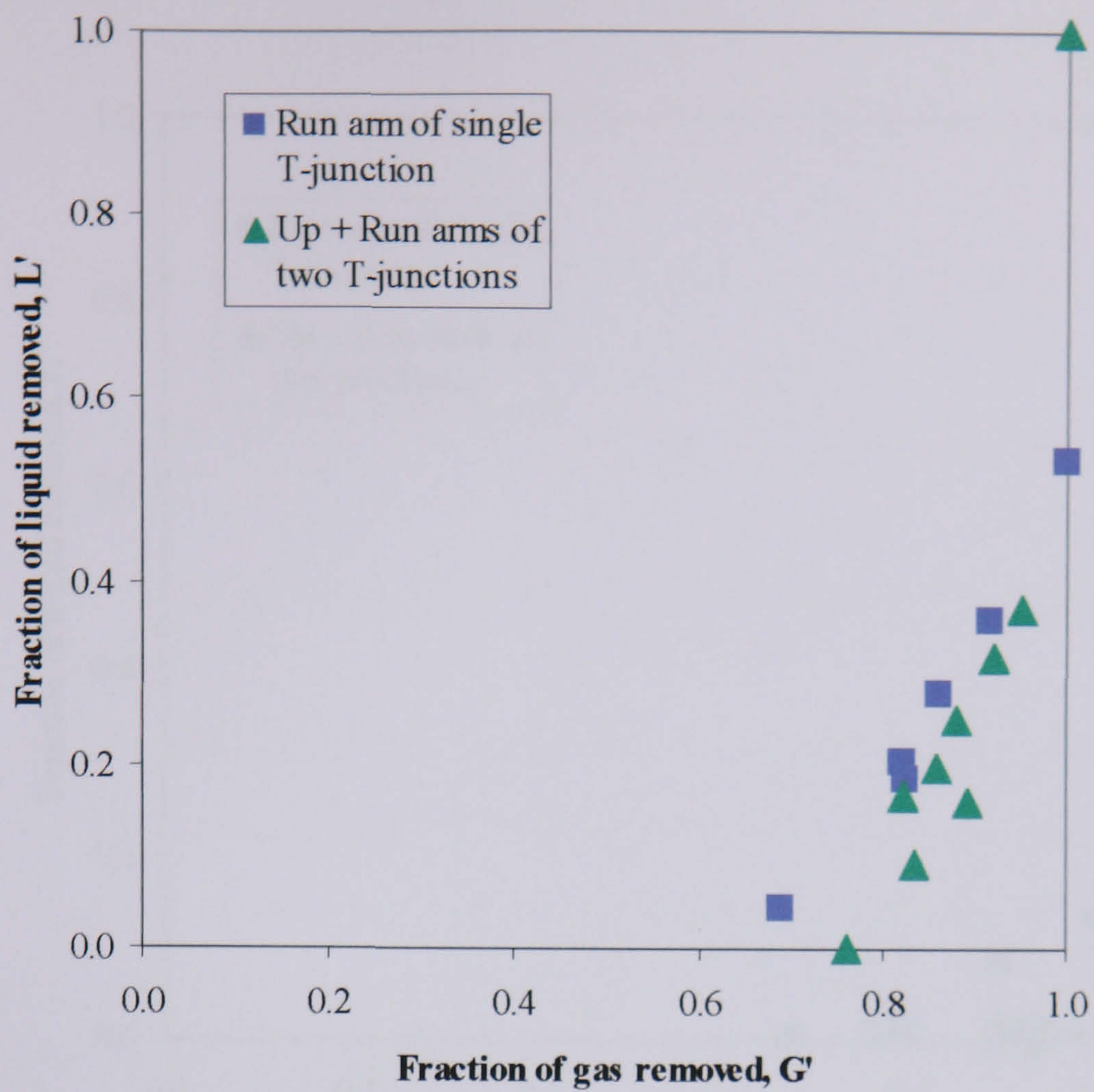


Figure 6-14: Comparison of phase split with one and two T-junctions. Annular flow,  $U_{gs} = 12\text{m/s}$  and  $U_{ls} = 0.31\text{m/s}$ .

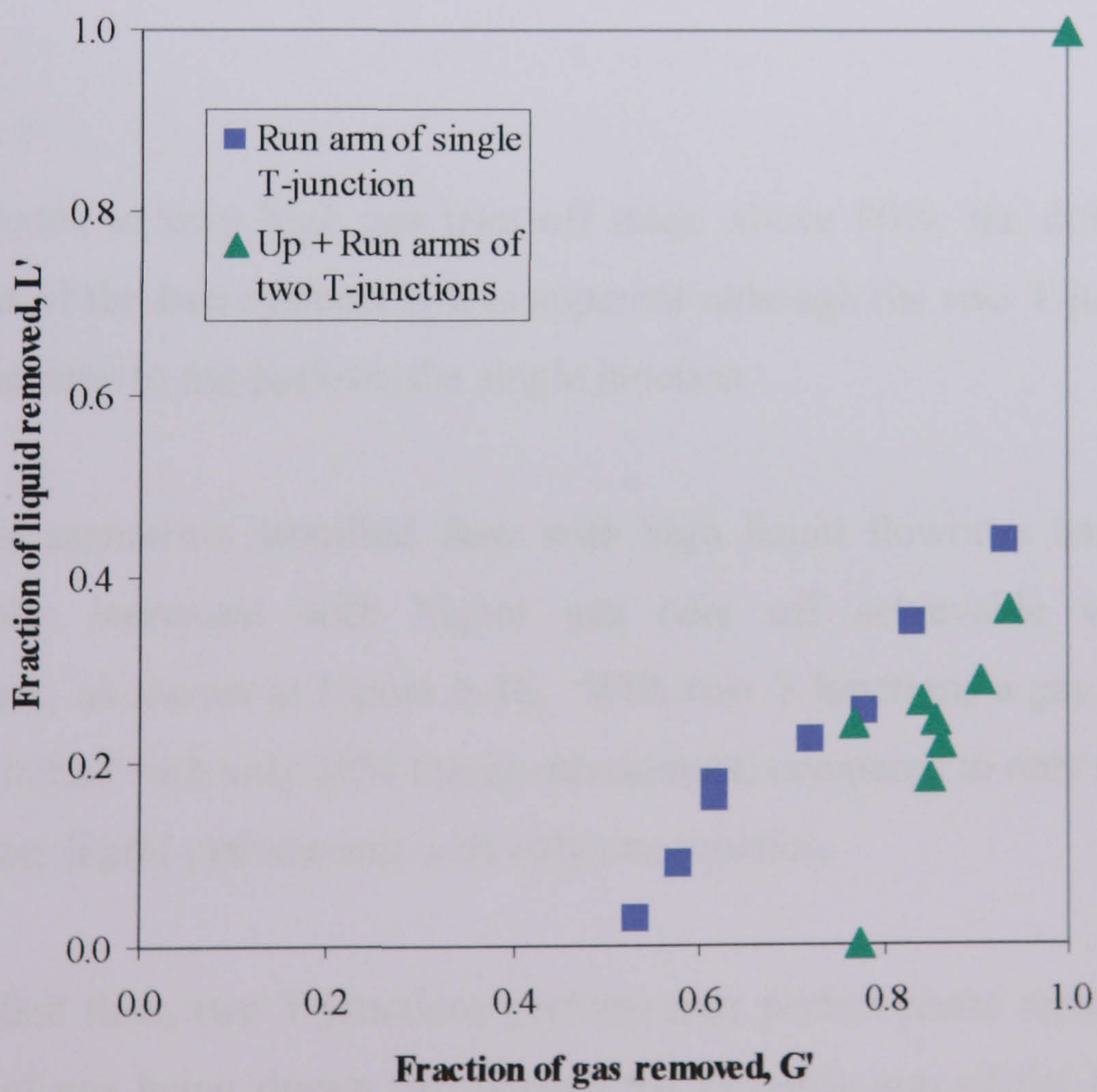
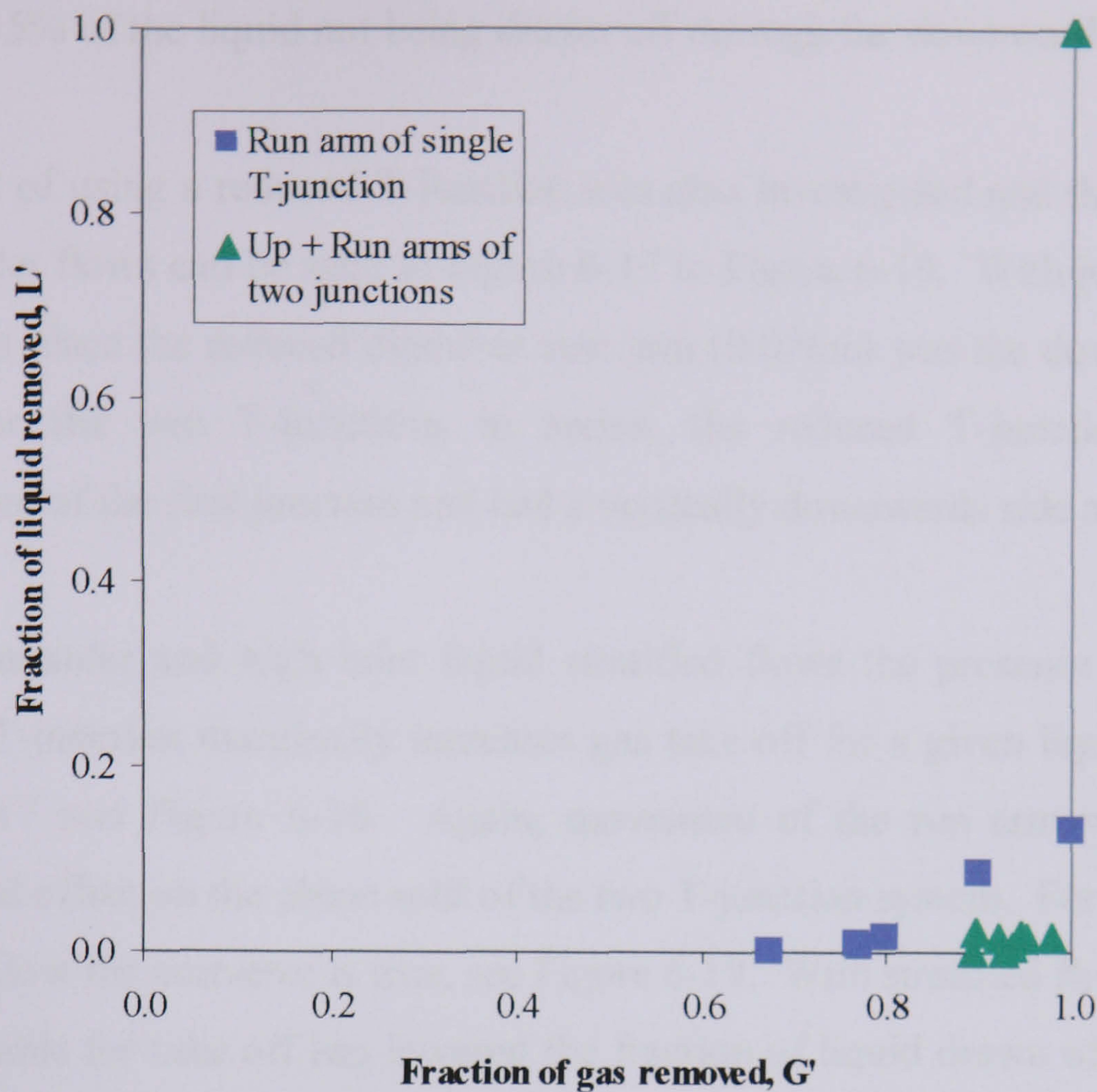


Figure 6-15: Comparison of phase split with one and two T-junctions. Stratified flow,  $U_{gs} = 4\text{m/s}$  and  $U_{ls} = 0.434\text{m/s}$ .





**Figure 6-16: Comparison of phase split with one and two T-junctions. Stratified flow,  $U_{gs} = 8\text{m/s}$  and  $U_{ls} = 0.186\text{m/s}$**

In both cases at very high gas take off rates, above 90%, the difference in phase separation of the two systems is less apparent although the two T-junctions in series can still be seen to out perform the single junction

The phase separation stratified flow with high liquid flowrates has been the most significantly increased with higher gas take off achievable with low liquid entrainment, as shown in Figure 6-16. With two T-junctions a gas take off of 85% can be obtained with only 20% liquid entrainment, compared to only 60% gas take off for the same liquid entrainment with only one junction.

For stratified flow, two T-junctions perform near perfect phase separation. With the majority of gas being drawn off through the upwards arm of the first junction the liquid has nothing to “drag” it past the opening of the downwards junction hence it is drawn off. The remaining faster flowing gas continues straight on down the run arm.



The high degree of phase separation is achievable with just a single T-junction with less than 15% of the liquid not being drawn off through the downwards arm.

The effect of using a reduced T-junction was also investigated and the results for the various inlet flows can be seen in Figure 6-17 to Figure 6-19. With just the single T-junction in place the reduced diameter side arm (0.076m) was the downwards branch arm. For the two T-junctions in series, the reduced T-junction was placed downstream of the first junction and had a vertically downwards side arm.

For both annular and high inlet liquid stratified flows the presence of the reduced diameter T-junction marginally increases gas take off for a given liquid take off, see Figure 6-17 and Figure 6-18. Again, movement of the run arm valve has had a detrimental effect on the phase split of the two T-junction system. For low inlet liquid stratified flow the converse is true, see Figure 6-19. With stratified flow, reducing the area available for take off has lowered the fraction of liquid drawn off down the side arm, forcing more to leave the exits under consideration here, especially for the case of the single junction. These results are as expected since, as discovered in section 4.2.2 in Chapter 4, the presence of a reduced diameter side arm for a T-junction with a downwards branch under these conditions has only a marginal effect on reducing the fraction of gas drawn down the branch arm for a given liquid take off.



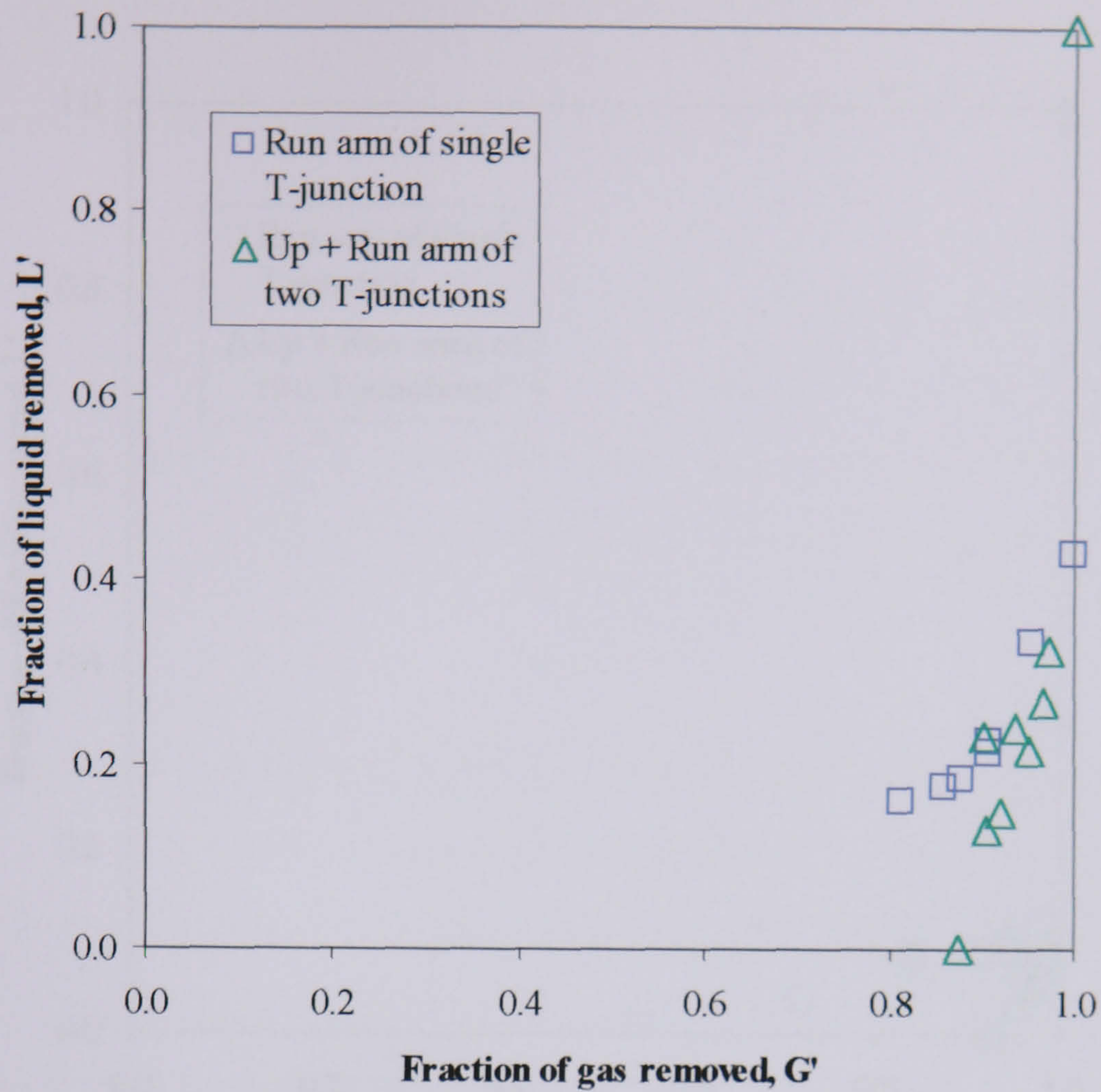


Figure 6-17: Comparison of phase separation with a reduced diameter T-junction for the one and two T-junction systems.  $U_{gs} = 12\text{m/s}$  and  $U_{ls} = 0.31\text{m/s}$

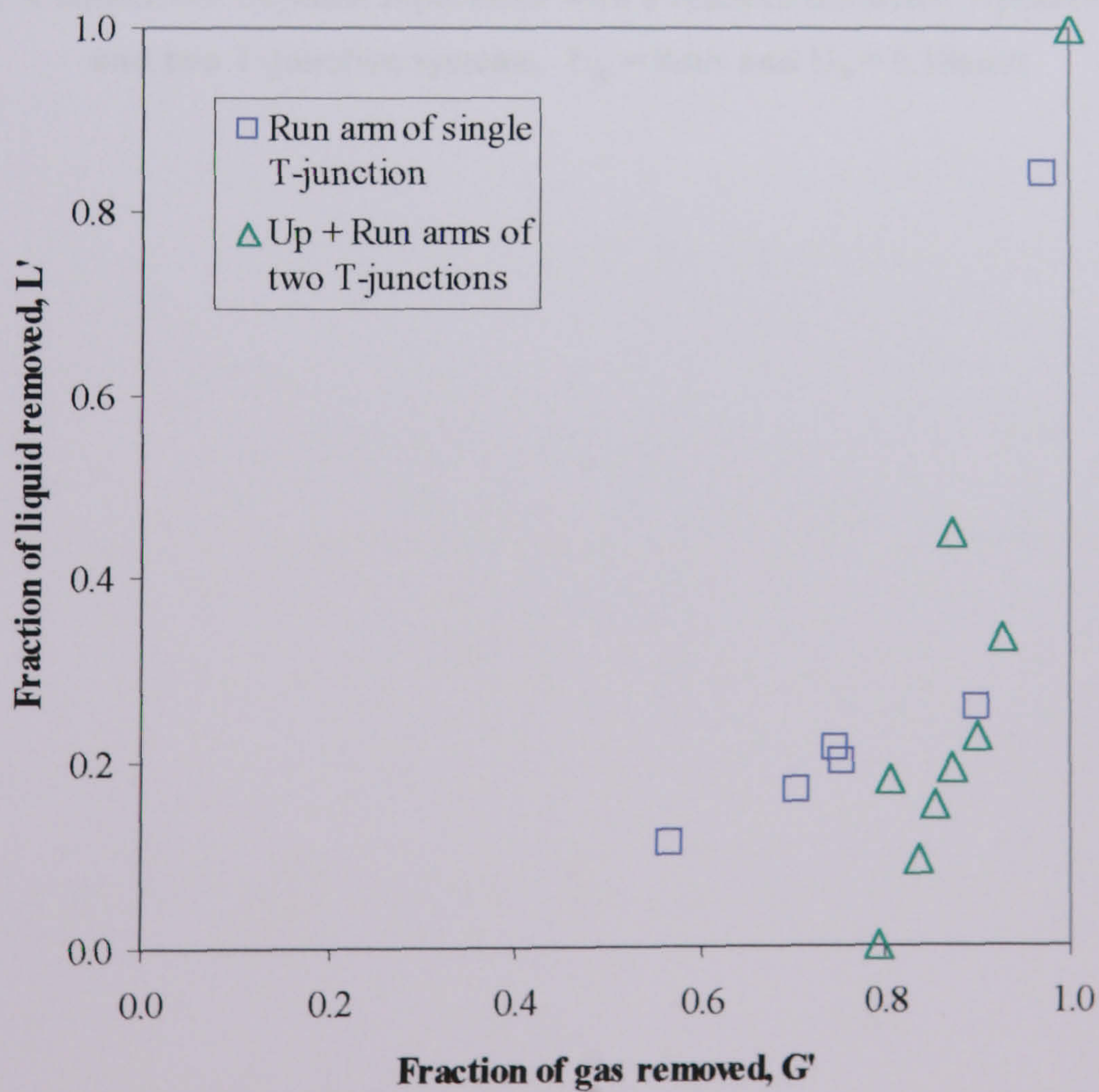
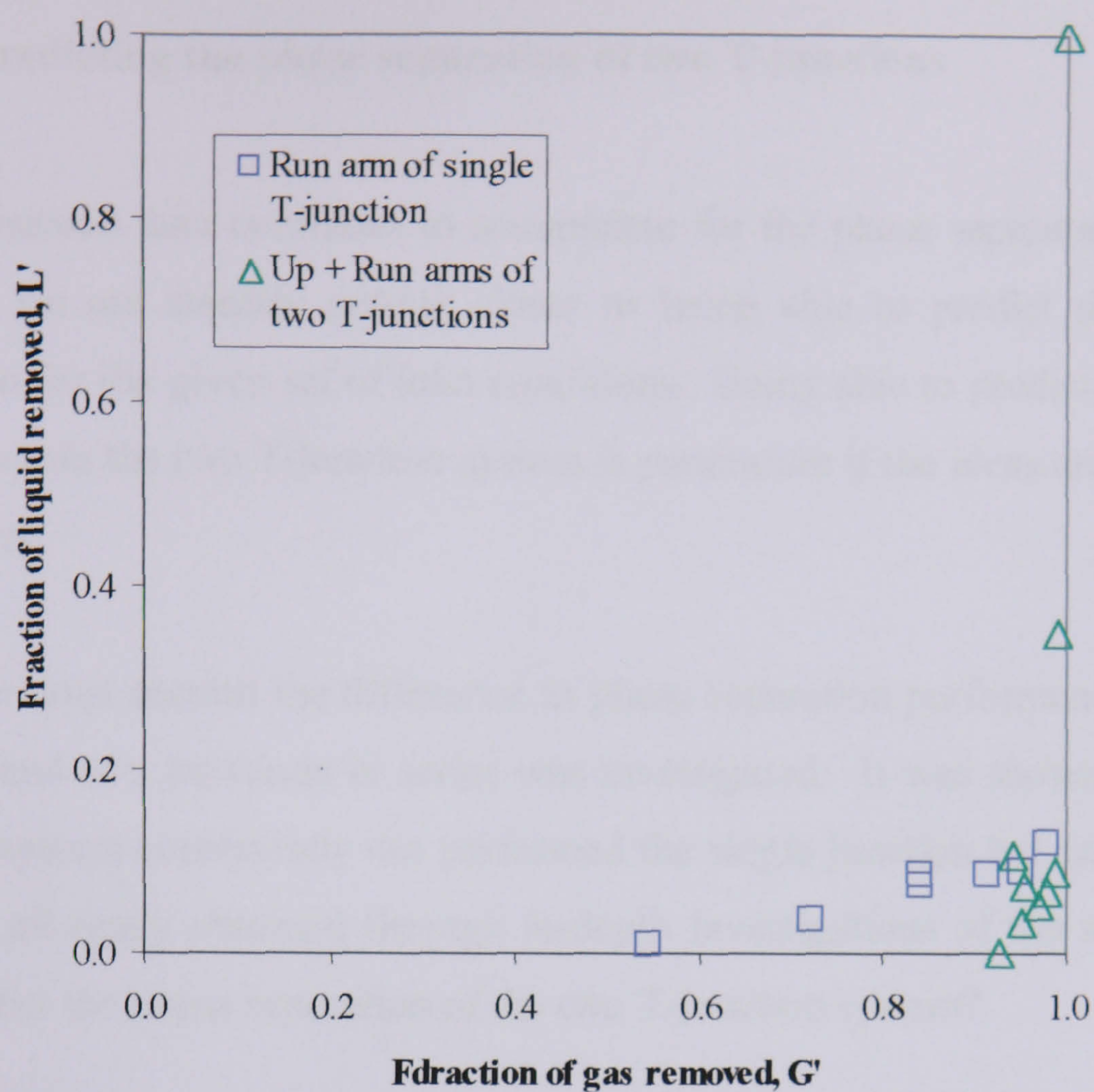


Figure 6-18: Comparison of phase separation with a reduced diameter T-junction for the one and two T-junction systems.  $U_{gs} = 4\text{m/s}$  and  $U_{ls} = 0.434\text{m/s}$





**Figure 6-19: Comparison of phase separation with a reduced diameter T-junction for the one and two T-junction systems.  $U_{gs} = 8\text{m/s}$  and  $U_{ls} = 0.186\text{m/s}$**



### 6.4.2 Predicting the phase separation of two T-junctions

As the research data continues to accumulate for the phase separation at a single T-junction, we are steadily getting closer to being able to predict the correct phase separation for the given set of inlet conditions. Being able to predict what is likely to happen within the two T-junction system is paramount if the ideas are to be embraced by industry.

In the previous section the difference in phase separation performance of a single T-junction and two junctions in series was investigated. It was shown that the two T-junction system consistently out performed the single junction but can the knowledge we have all ready obtained through in-depth investigations of the single T-junction help predict the phase separation of the two T-junction system?

The two T-junction system could be considered as two separate T-junctions, as indicated in Figure 6-20, the first with a vertically upwards side arm and the second with a vertically downwards side arm. Investigated within this section is whether the phase separation curves of the two single T-junctions, studied in isolation of each other, can be used to represent what is happening within the two T-junction system.

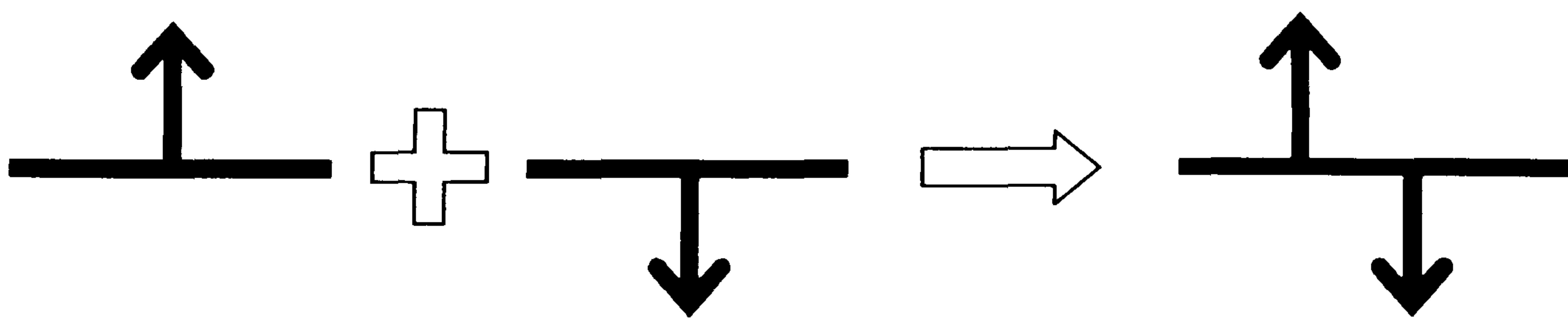


**Figure 6-20: Can the two T-junction system be represented by two individual T-junctions?**

The phase separation curves of a single T-junction, with a vertically upwards branch arm, under similar inlet conditions used within the two T-junction system can be

---



compared with the gas drawn off through the first arm of the junctions in series. A comparison can be seen in Figure 6-21 for annular inlet conditions,  $U_{gs} = 12\text{m/s}$  and  $U_{ls} = 0.31\text{m/s}$ . Similar findings were found in all cases, regardless of inlet flow regime. The presence of the second junction has eliminated liquid take off by reducing the presence of a hydraulic jump where as for a single junction there is a critical gas take off point where liquid is first drawn through the branch arm.

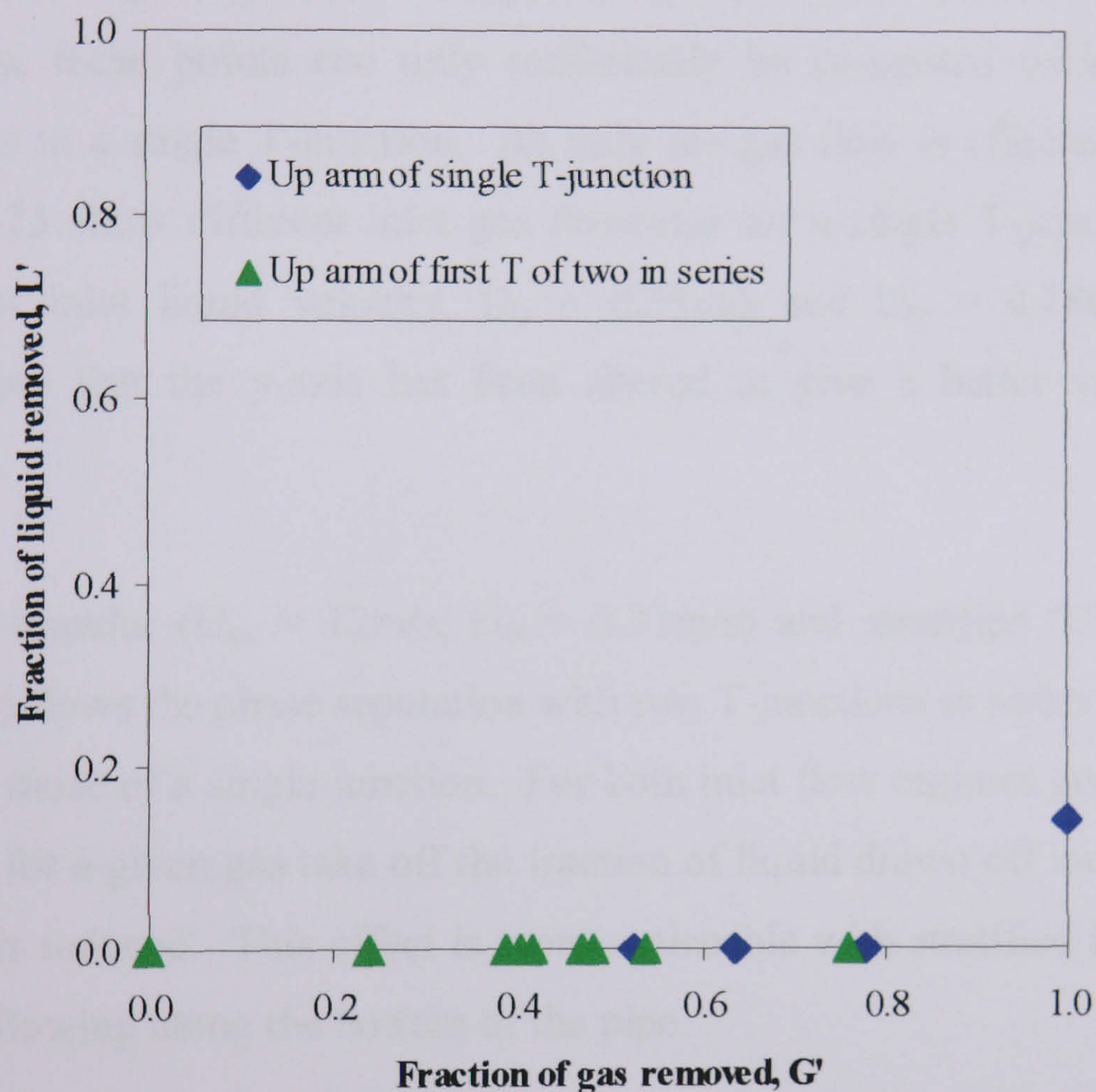


**Figure 6-21: Phase separation of a single T-junction with a vertically upwards side arm compared with the up arm of the first T of the two in series.  $U_{gs} = 12\text{m/s}$ ,  $U_{ls} = 0.31\text{m/s}$**

The maximum fraction of gas drawn off through the up arm of the two T-junction system is very similar to the critical gas take off for a single junction. This was found to be the case for all inlet conditions. The presence of the second junction ensures that the stream is 100% gas but does not increase the maximum gas take off through such an orientated junction.



The varying gas fractions drawn through the up arm of the two T-junction system means that the inlet conditions of the downwards arm keep changing. This makes comparison with a single T-junction more complicated than for the first case.

The results from two inlet flow regimes have been given in Figure 6-22 and Figure 6-23. In both figures, the phase split for the second junction of the two T-junction system is represented by the triangular points and is the phase split taking into account the fraction of gas removed through the first junction. Due to the changing inlet conditions, these points can only realistically be compared with a range of inlet conditions to a single T-junction. As only the gas flow is effected Figure 6-22 and Figure 6-23 show different inlet gas flowrates for a single T-junction at a constant superficial inlet liquid velocity,  $U_{ls} = 0.31\text{m/s}$  and  $U_{ls} = 0.186\text{m/s}$  respectively. Please note that the y-axis has been altered to give a better view of the trends observed.

For both annular ( $U_{gs} = 12\text{m/s}$ ,  $U_{ls} = 0.31\text{m/s}$ ) and stratified ( $U_{gs} = 12\text{m/s}$ ,  $U_{ls} = 0.186\text{m/s}$ ) flows the phase separation with two T-junctions in series show very similar trends to those of a single junction. For both inlet flow regimes approaching a single junction, for a given gas take off the fraction of liquid drawn off increases as inlet gas velocity is reduced. This effect is more noticeable with stratified flows when all the liquid is flowing along the bottom of the pipe.

From a visual inspection of both figures, the phase separation through the down arm of the second junction of two in series is seen to follow more closely the phase separation at a single junction with the same initial inlet gas flow into the system – in both cases  $12\text{m/s}$ . In other words, the phase separation at the second junction of two in series can be almost equated to the phase separation at a single junction without the consideration of the gas removed at the first junction.

Obviously this is merely a visual trend observed from the data. A more detailed analysis of the two T-junction trends reveals that each individual point refers to a different gas inlet flow to the junction due to the differing fractions of gas drawn through the up arm. Bearing this in mind, the data points at lower liquid take off

---



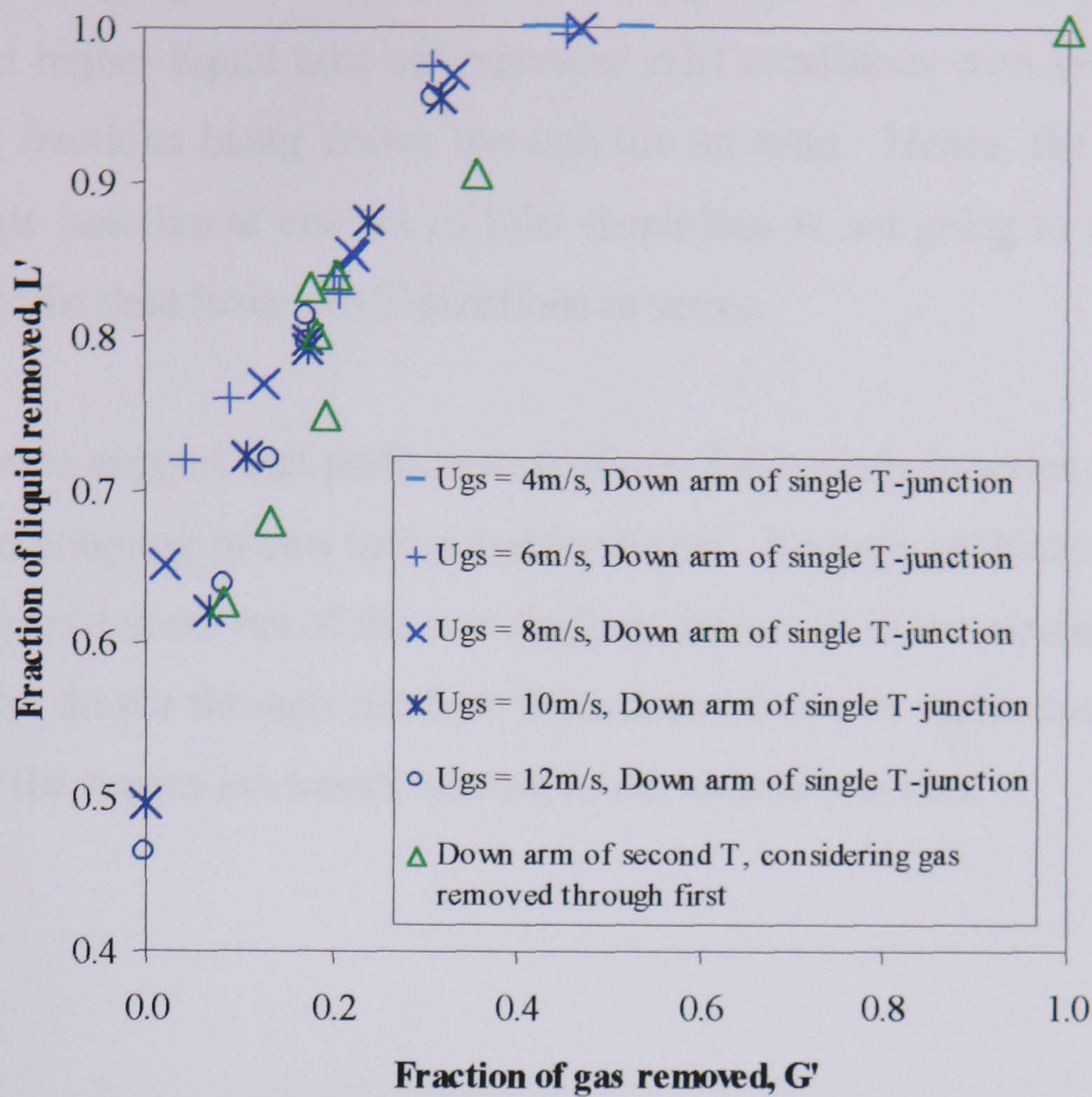


Figure 6-22: Various phase separation curves of a single T with downwards side arm compared with the down arm of the second T of the two in series.

Annular Flow,  $U_{gs} = 12\text{m/s}$ ,  $U_{ls} = 0.31\text{m/s}$

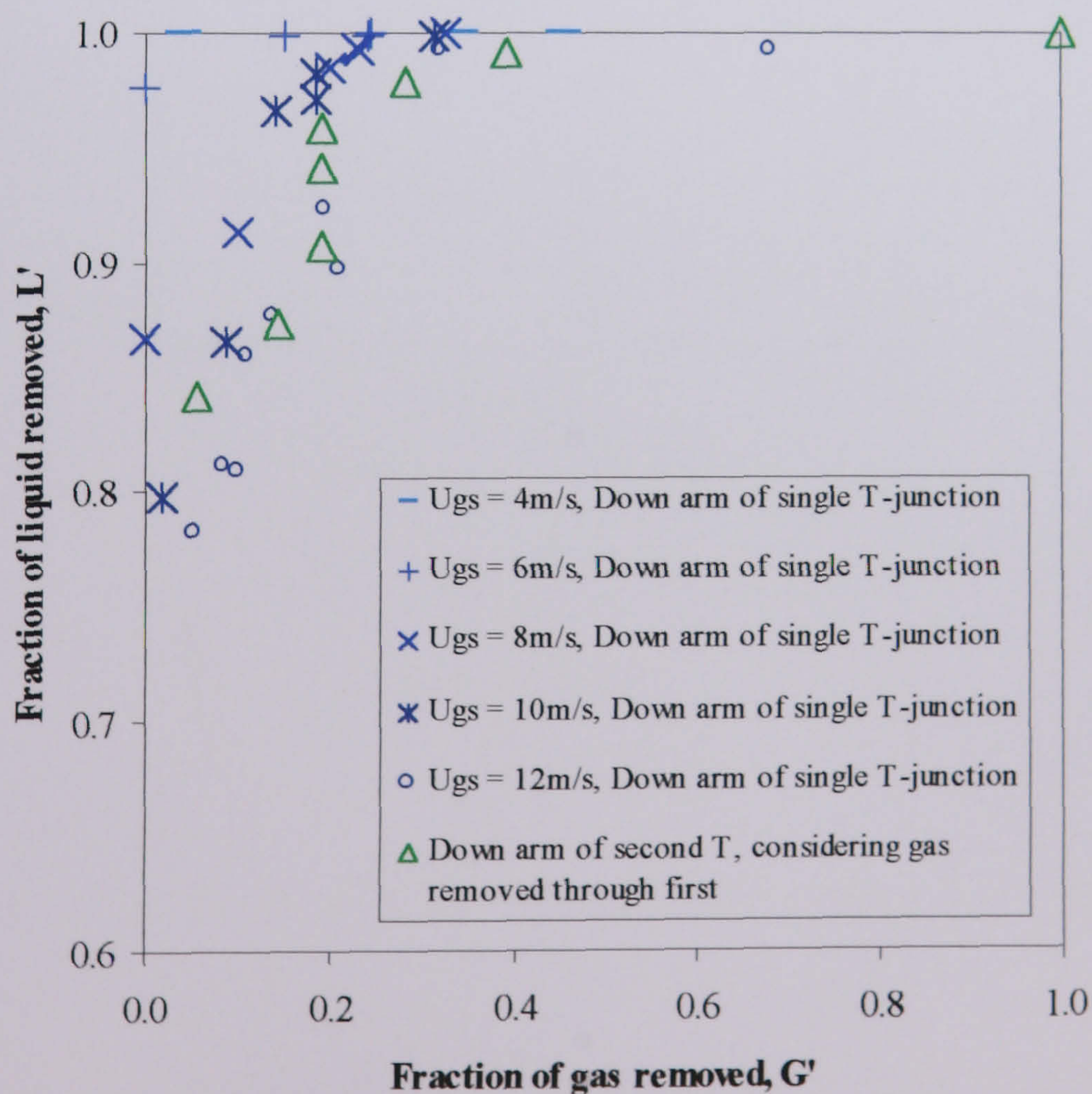


Figure 6-23: Various phase separation curves of a single T with downwards side arm compared with the down arm of the second T of the two in series.

Stratified Flow,  $U_{gs} = 12\text{m/s}$ ,  $U_{ls} = 0.186\text{m/s}$



correspond to high gas inlet flows (with little gas being drawn through the up arm) and those at higher liquid take off represent inlet conditions with low gas flow rates (higher gas fractions being drawn through the up arm). Hence, the phase split data from a single junction at one set of inlet conditions is not going to satisfy the range exhibited by the data from two T-junctions in series.

This goes on to suggest that performance of two T-junctions in series is more complex than just the coupling of two individual junctions. A rough guidance can be obtained from the separation curves of the two single junctions as to the maximum gas fraction that could be drawn through the first T-junction of two in series and an idea can be acquired of the separation trends relating to the second junction.



### 6.5 Visual Observations in the Two T-junction System

As discussed at the end of Chapter 4, the same hollow feature was seen to occur at the top of the downwards side arm. Vortices and dips in the liquid surface were also seen, as with the single junction. Since no liquid was drawn up with the gas at the first junction, no falling films were seen or areas of low pressure indicated. The inclusion of the second T-junction within the system reduced the formation of hydraulic jumps, as discussed by Conte (2000).

Within these observations the butterfly valve in the run arm was completely shut, the butterfly valve in the down arm partially closed until the liquid started being drawn up the first arm of the system by the gas. This caused the liquid in the system to build up, as if there were a blockage.

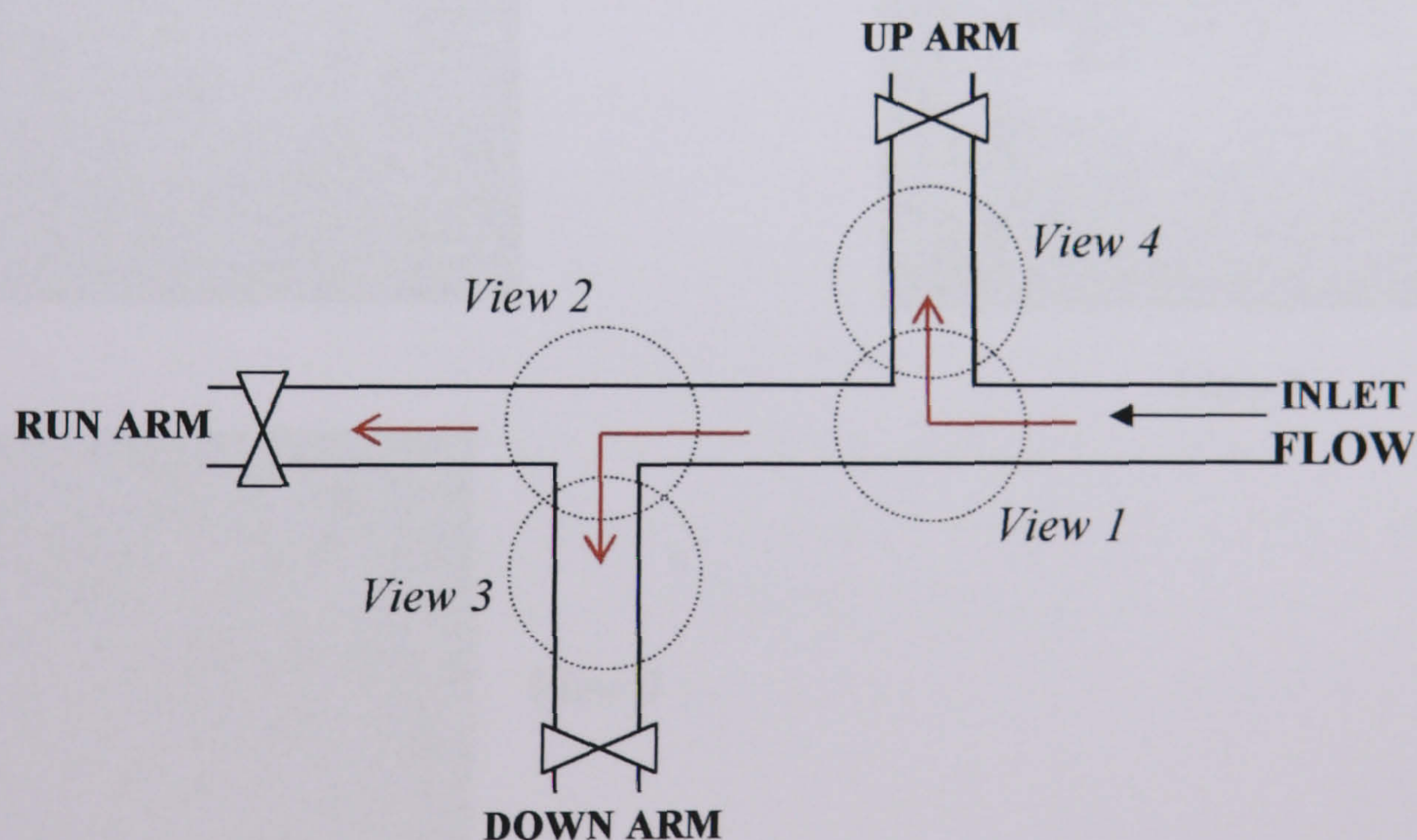


**Figure 6-24:** Schematic diagram of the two T-junction system indicating the four viewing points

Figure 6-24 is a schematic representation of the two T-junction system. In this case the first is a regular T-junction and the second is a reduced junction. Four viewing



points were used to observe the action of the liquid and gas in the heavily liquid loaded system. Views 1 and 2 show what is happening at the T-junctions and views 3 and 4 show how the phases are travelling in the down and up arms, respectively.

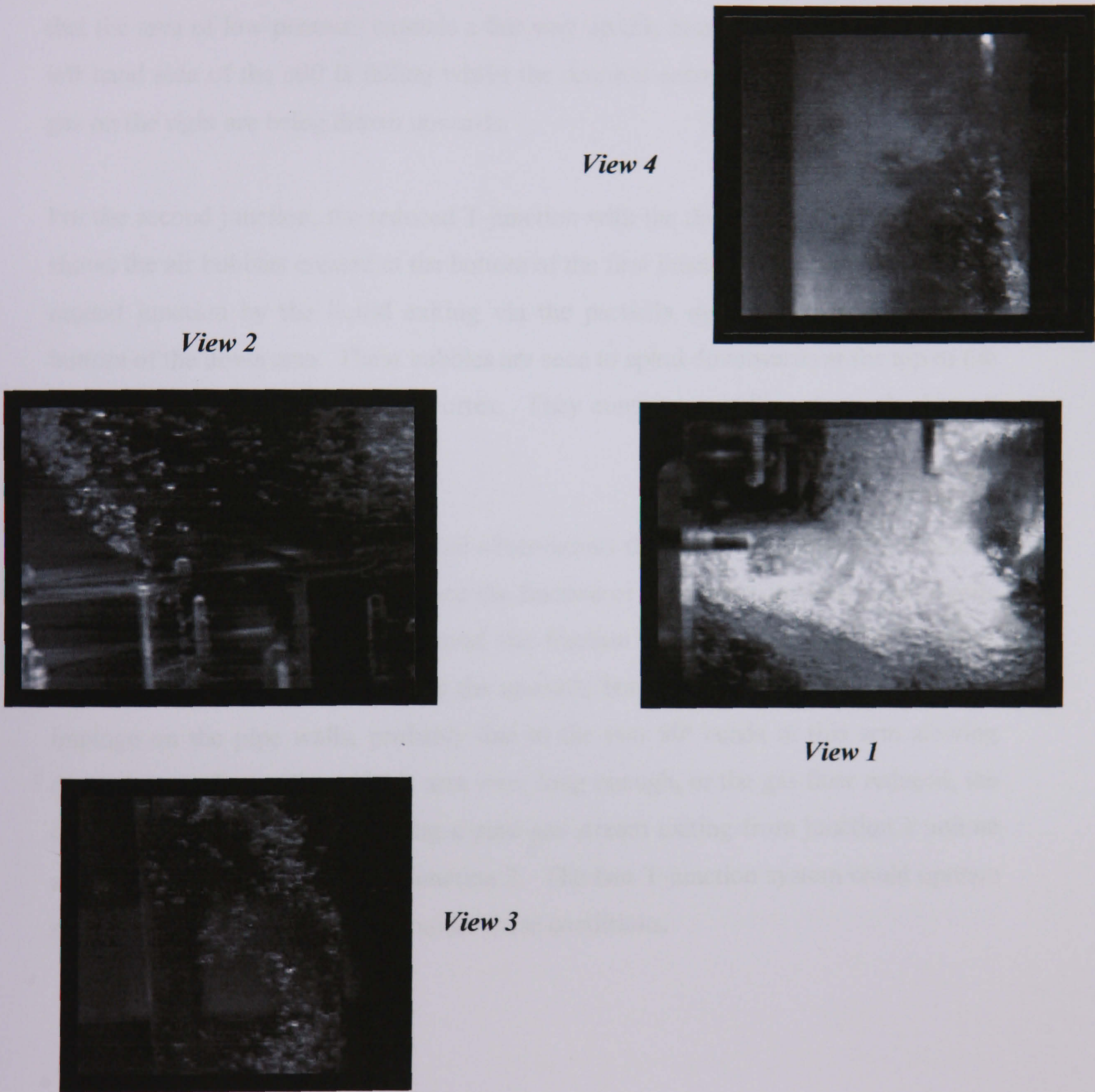


Figure 6-25: Video stills of the gas-liquid flows at a two T-junction system



Figure 6-25 shows stills taken from high speed video footage for inlet conditions  $U_{gs} = 12\text{m/s}$ ,  $U_{ls} = 0.31\text{m/s}$ . Under these conditions the hollow, peeled banana effect observed at the top of a junction with a downwards side arm does not occur. Instead, view 1 shows the liquid being drawn up the first T-junction creating a frothy mixture and an area of low pressure (on the left hand side of the picture). View 4 indicates that the area of low pressure extends a fair way up this branch arm as the film on the left hand side of the still is falling whilst the droplets entrained in the faster flowing gas on the right are being drawn upwards.

For the second junction, the reduced T-junction with the downwards side arm view 2 shows the air bubbles created at the bottom of the first junction are drawn towards the second junction by the liquid exiting via the partially open butterfly valve at the bottom of the down arm. These bubbles are seen to spiral downwards at the top of the junction, as if caught in a liquid vortex. They continue spiralling down the branch arm in an anti-clockwise fashion.

It can be concluded from these visual observations that the lagoon created by closing the run arm valve may help to reduce the fraction of gas drawn down the downwards arm, just as a U-bend reduced lowered the fraction of gas in this arm for a single junction. The droplets entrained in the upwards branch arm were seen to eventually impinge on the pipe walls, probably due to the two  $90^\circ$  bends in this arm slowing down the gas flow. Thus, if this arm were long enough, or the gas flow reduced, the droplets could be removed leaving a pure gas stream exiting from junction 1 and an almost pure liquid stream from junction 2. The two T-junction system could operate more like a total phase separator under these conditions.



## **6.6 Conclusions**

The phase split occurring at two T-junctions placed in series has been thoroughly investigated with respect to junction separation distance, effects of using a reduced diameter T-junction and how down stream resistances effect phase split for different inlet flow regimes.

The inclusion of the second T-junction produced a third outlet to the system. For plotting the fractions of inlet gas and liquid passing down each branch neither conventional  $G'$  versus  $L'$  phase split plots nor triangular diagrams were found to be totally satisfactory.

When combining the output from two junctions conventional  $G'$  versus  $L'$  plots were found to provide the best solution for presenting the data. Through different arm combinations the phase separation of a two T-junction system can be controlled to give liquid rich or gas rich streams. Being able to control the downstream resistances added a further degree of control thus allowing the system to produce a more refined split.

The physical properties of the system were found to only mildly affect the phase separation. The separation distance of the junctions had a negligible effect on most inlet flowrates. Having two T-junctions within the system prevented the formation of a hydraulic jump hence no liquid was ever drawn up the first junction thus the small junction separation distances investigated here did not produce any significant effects. The inclusion of a reduced diameter T-junction, downstream of the first junction, reduced the gas fraction drawn through the down arm of the second junction thus improving the phase separation of the system.

Having a two T-junction system has allowed greater flexibility and controllability of the phase split compared with a single T-junction. Knowledge of the phase separation

---



occurring at a single junction can be applied in part to the two T-junction system although the systems are inherently different. As yet just the trends observed from the two T-junction system can be represented but specific details are not highlighted.

It was found that the tighter phase separation criterion of less than 10% by volume of liquid exiting with the gas was achievable with the two T-junction system and a cleaner separation can be achieved than with just a single junction. However, reducing the volume of gas in liquid to less than 10% v/v was not achieved.



## CHAPTER 7

### Predicting the Phase Split at a T-junction

If T-junctions are to be used within industry as partial phase separators then it is vital to be able to predict how a two phase mixture will divide between the two outlets. Various predictive models have been published, each aiming to provide an accurate picture of what is happening at the T-junction. Some methods have provided simple solutions, based on empirical correlations whilst others are more involved and consider the problem in three dimensions. However, to date there is no one single model that can predict the phase redistribution for arbitrary inlet flow conditions and the various geometries which define the T-junction. Most experimental and theoretical studies tend to be limited to a small range of parameters, resulting in models which are to be applied within specific conditions.

This chapter starts with a brief introduction to the standard approaches of modelling the phase split at a horizontal T-junction. Junctions with downward ( $-90^\circ$ ) side arms have received little specific attention. There are few published models for this case and their predictive results are poor in comparison with those available for horizontal T-junctions. Through the analysis of the experimental results for a large diameter T-junction with a downwards side arm, given in Chapter 4, it was considered that the linear nature of the phase split results could provide a simple method of predicting the phase separation. Thus efforts in Section 7.2 are concentrated on finding a suitable correlation to predict the fraction of liquid where the onset of gas take off occurs,  $L'_{onset}$  and Section 7.3 considers the critical gas fraction,  $G'_{crit}$ , at which all the liquid is diverted down the side arm. It was hoped that the development of such an approach would provide a scheme that is easy to implement but provides realistic results. The prediction of  $L'_{onset}$  was found to be successfully related to the terminal rise velocity of a bubble through a column of liquid and the value of  $G'_{crit}$  was considered by relating the movement of the liquid to that of a particle.



## 7.1 Phase Redistribution Models

The accuracy of the predictive methods currently available for describing the phase maldistribution (phase split or flow division) at a T-junction can be very poor. Though over the last decade, these predictive models have improved significantly, due to the experimental and theoretical efforts of many researchers, but there are still many areas of this subject we do not totally understand.

### 7.1.1 The general methods for modelling two phase flow

As indicated in previous chapters the phase redistribution at a T-junction is highly complex and depends on many variables – including inlet flow regime, T-junction geometry and the pressure drops across the junction. Over the years, three general approaches have been used to describe the phase maldistribution at T-junctions -

1. Empirical Correlations – the fitting of mathematical equations to experimental data
2. Phenomenological Analysis – using simple mathematical methods to describe the fluid dynamics of the process
3. Two-fluid Numerical Simulations – highly computational models involving many numerical simulations to describe the flow redistribution

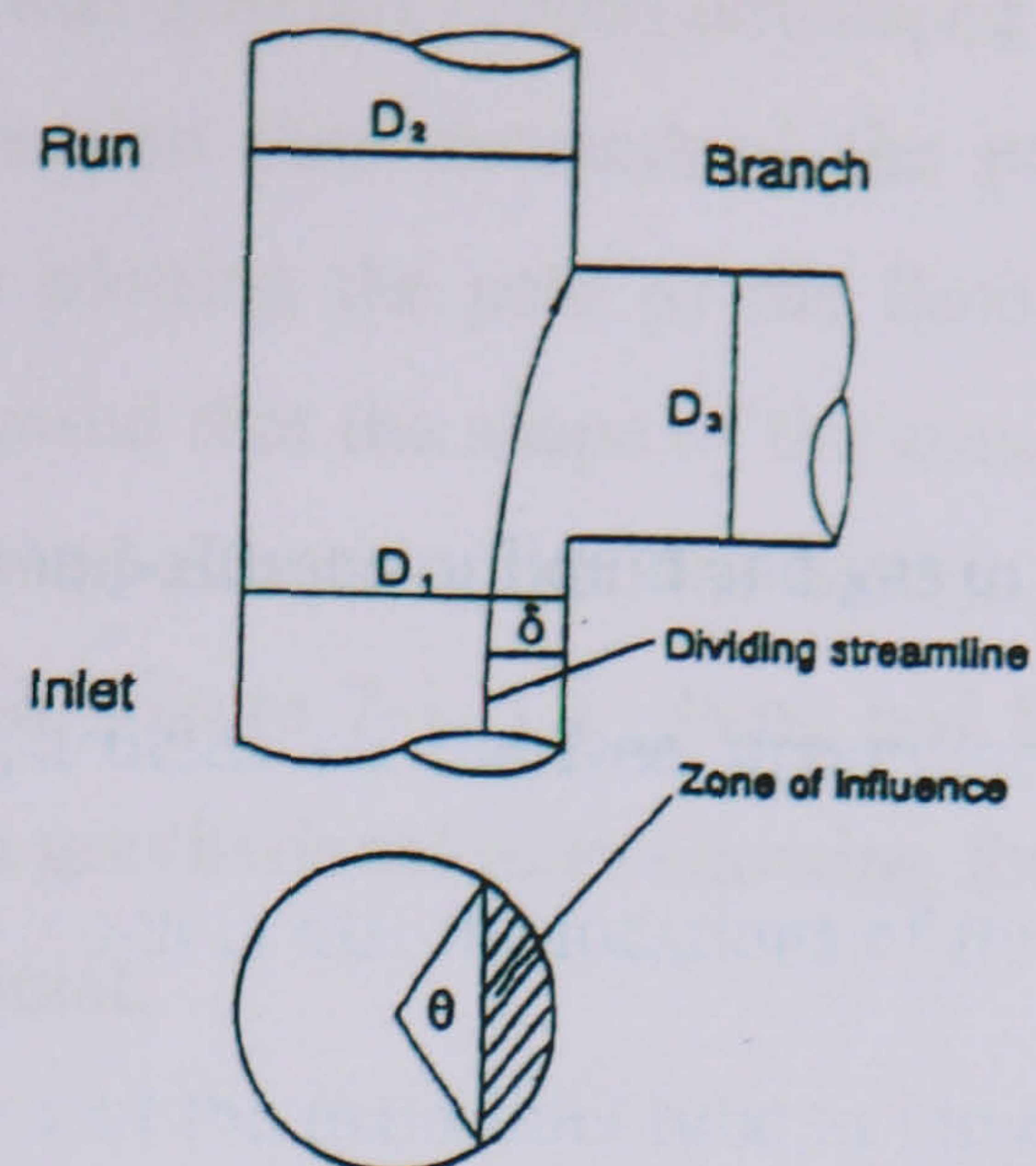
Although empirical correlations are relatively easy to formulate such models are not widely appreciated. This is because they tend only to be valid in the range of conditions bounded by the experimental data and the accuracy of the predictions depends on the size of the data base used to create them. Thus, such correlations developed by Henry (1981) and Seeger *et al.* (1986) have not been extended by other researchers, despite the available data base of experimental results having grown significantly in recent years.



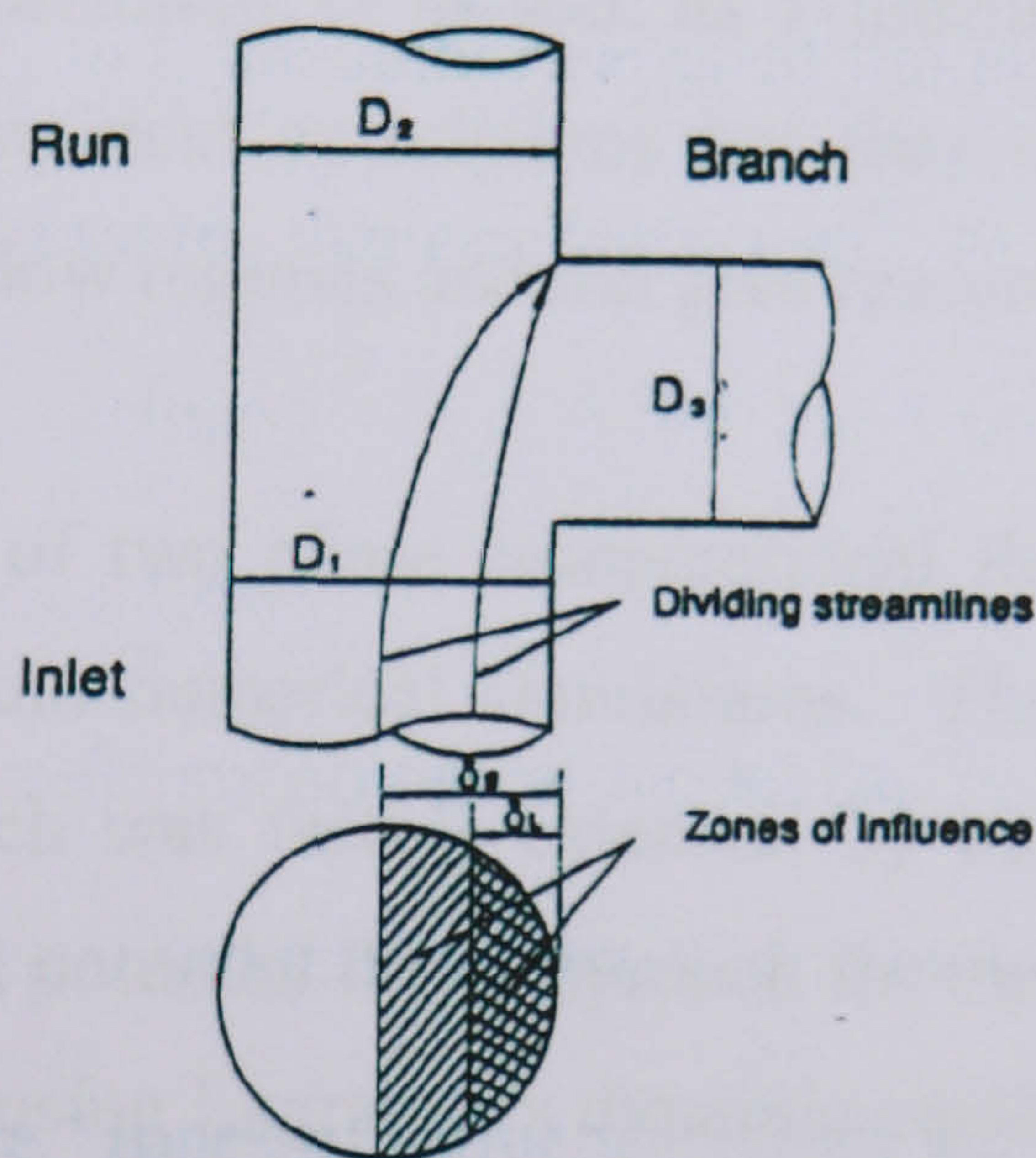
Phenomenological models have been growing in popularity over recent years. Such models provide a simple and practical analysis of the complicated two phase flow behaviour at a T-junction. The models are based on the assumption that the branch arm exerts a “zone of influence” on the two phase flow passing the inlet. As these models aim to apply the principles of fluid mechanics and the effects of the T-junction geometry they tend to be flow regime dependant and based on specific T-junction geometries. Some of the more developed phenomenological models have been adapted so they can be applied to various different T-junction configurations.

Studies of single phase flows, particularly that of McNown (1954), have shown that the fluid taken off through the side arm of the junction comes from an area approximated by the segment of the main pipe nearest the sidearm. Azzopardi and Whalley (1982) extended the single phase flow theory suggested by McNown (1954) to two-phase flows and developed a simple geometric model for vertical annular flow. Within this model a single zone of influence for both the gas and the liquid was used, see Figure 7-1 (A). This meant the dividing streamline (used to govern the fraction of the inlet flow which is diverted down the side arm and that which carries on) for the gas and liquid followed the same path. This approach was extended by Azzopardi (1984), to take into account the effect of branch arm diameter using geometric relationships, thus broadening the potential use of this method. Shoham *et al.* (1987) took this method further by considering the relative momentum fluxes of the two phases. This resulted in the gas and liquid having different dividing streamlines and thus different zones of influence, Figure 7-1 (B). The boundary of each zone was still considered to be a vertical chord. The initial model of Shoham *et al.* (1987) was to predict the phase split at a horizontal regular T-junction but has been extended to account for different branch arm diameters (Penmatcha *et al.*, 1996) and different branch arm inclinations (Penmatcha *et al.*, 1996; Marti and Shoham, 1997).

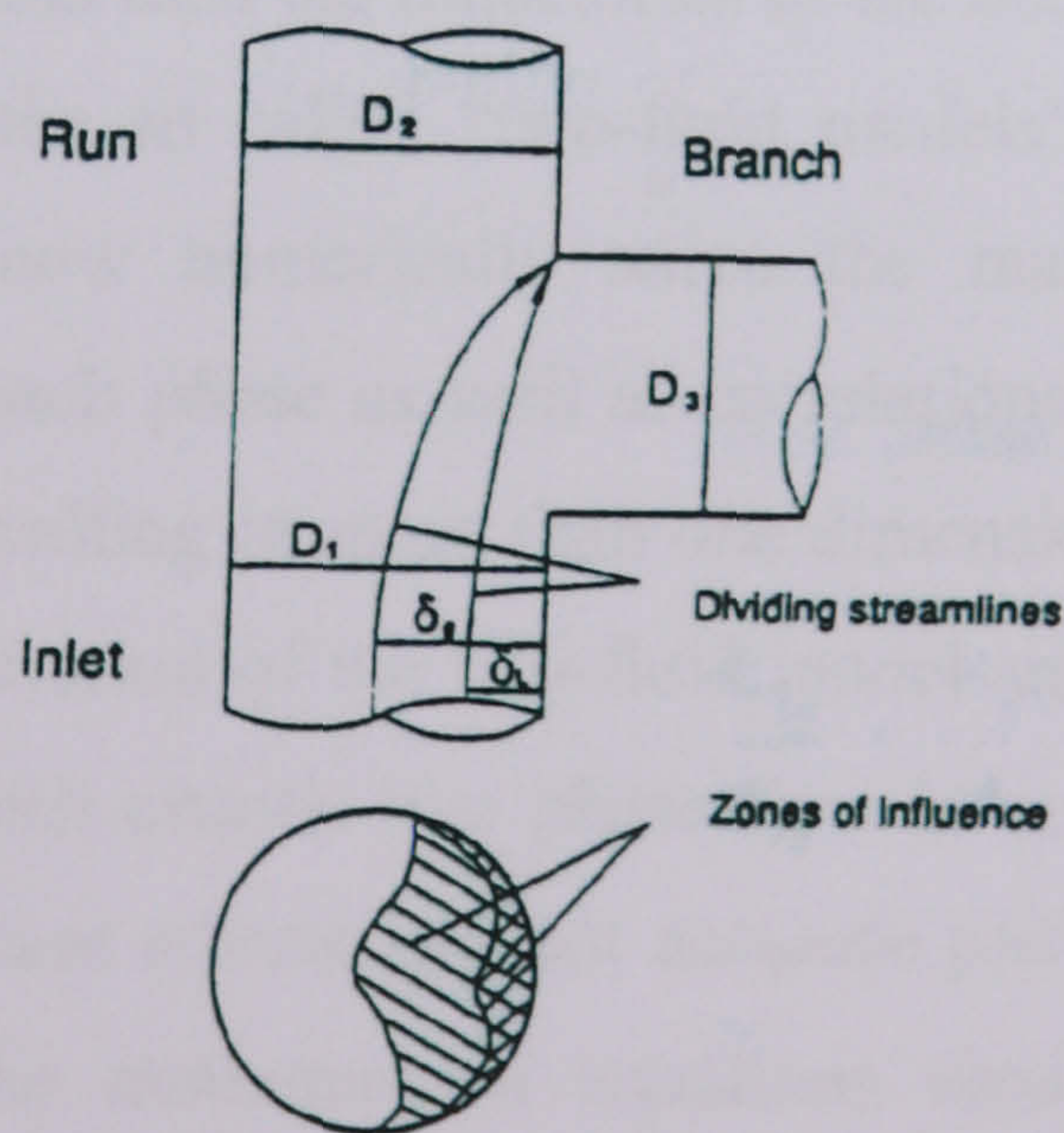




(A) Azzopardi and Whalley (1982)



(B) Shoham *et al.* (1987) and Hwang *et al.* (1988)



(C) Ballyk and Shoukri (1990)

Figure 7-1: The different zones of influence used within phenomenological models



However, when Ballyk and Shoukri (1990) developed a model for annular flow in a horizontal regular T-junction they determined the position of the gas and liquid dividing streamlines by plotting the path of the fluid particles using the theory of potential flow. This showed that the shape of the zone of influence boundaries were dependent on the horizontal elevation from the bottom of the pipe and did not follow a completely planar path, Figure 7-1 (C). Peng and Shoukri (1997) developed this idea further to include a gravitational term allowing for branch arm orientation to be changed from the horizontal.

Hwang *et al.* (1988) took the dividing streamline approach to predict the phase separation at regular horizontal Y- as well as T-junctions. The dividing streamlines were developed by empirical correlations but they claimed that their model was applicable for all inlet flow regimes and did give reasonable results.

The growth in the art of two phase computational fluid dynamics has allowed the development of two-fluid numerical simulations. The analysis of annular flow by McCreery (1984), which was further extended by McCreery and Banerjee (1990), used a two-dimensional potential flow approach for the gas stream and calculated the liquid drop trajectories using Lagrange's dynamic equations. Lemonnier and Hervieu (1987) redeveloped this approach for bubbly flow where the potential flow of the liquid was determined and then the trajectories of the bubbles sought. These were the first developments of the so called "two-fluid models". The use of sophisticated computer codes can now numerically solve the mass, momentum and energy conservation laws for each phase as well as correlations for the droplets/bubbles for the different phases travelling in more than one dimension. Lahey and Drew (1992) provide a complete derivation of the two-fluid model and as Lahey (1990) indicates, being able to predict such chaotic two phase flow behaviour in a three dimensional form does have significant advantages but accurate predictions still rely the closure relationships i.e. on the mathematical equations used to describe the processes occurring, notably the interfacial behaviour of the two phases which governs the transitions between different flow regimes. There is no doubt that the potential of this method of predicting the phase redistribution at a T-junction is significant, as the flow



can be visualised, providing valuable down stream information but to date few attempts have been made, and those are primarily by Lahey (1990), Issa and Oliveria (1994) and Adechy and Issa (1999).

### 7.1.2 The distribution of the two phases

The development of phenomenological models has allowed the distribution of the two phases at a junction to be described mathematically with a basis in reality. Depending on the authors' assumptions and how the mathematics is used to describe the physical reality the models can produce fairly accurate predictions. Normally, the published models are flow regime dependant although a few authors, Saba and Lahey (1984), Hwang *et al.* (1987) and Ma *et al.* (1990), have tried to produce models independent of inlet flow regime. The general techniques used for analysing how the two fluids flow together for modelling purposes can fall into two classes – homogenous flow and separated flow. If the flow is considered to be homogeneous then the mixture is treated as a pseudofluid that obeys the usual equations that can be written for single component flow meaning all of the standard methods of fluid mechanics can be applied. Suitable average properties are determined for the mixture's velocity, temperature, density and viscosity. These pseudo properties are weighted averages and are not necessarily the same as the properties of either phase. Differences in velocity, temperature and chemical potential between the phases will encourage momentum and heat and mass transfer. Often these processes proceed very rapidly, particularly when one phase is finely dispersed in the other, and it can be assumed that equilibrium is reached. In this case the average values of velocity, temperature and chemical potential are the same as the values for each component thus giving homogeneous equilibrium flow. The resulting equations are simple and easy to use making this technique attractive for quick design calculations. This was generally the approach taken by the early empirical correlations.

The second approach, the separated flow model, takes into account that the two phases can have differing properties and different velocities. It may be developed



with various degrees of complexity. In the most sophisticated version, separate equations of continuity, momentum, and energy are written for each phase and these six equations are solved simultaneously, together with rate equations, which describe how the phases interact with each other and with the walls of the pipe. In the simplest version, only one parameter, such as velocity is allowed to differ for the two phases while conservation equations are written for the combined flow. When the number of variables to be determined exceeds the available number of equations, correlations or simplifying assumptions are introduced.

### **7.1.3 Predicting the phase split with a downwards side arm**

Most previous analytical and experimental research has considered all arms of the T-junction to lie horizontally. Since such junctions are rarely found within industrial settings investigating the effects on phase split at a T-junction with an inclined branch arm are imperative. As discussed in Chapter 4 with the branch arm inclined vertically upwards (+90°) a gas rich stream is drawn off and inclining the branch arm vertically downwards (-90°) draws off a liquid rich stream. The previous sections indicate the different approaches used to predict the phase split at a T-junction but of the available published models few have been dedicated to the phase separation at a T-junction with a vertically downwards side arm. Peng *et al.* (1993) took the empirical relationships developed by Seeger *et al.* (1986) and the more phenomenological model presented by Ballyk and Shoukri (1990) and compared the predicted results with their experimental data for a regular 26mm diameter T-junction with annular flow, see Figure 7-2 and Figure 7-3 respectively.



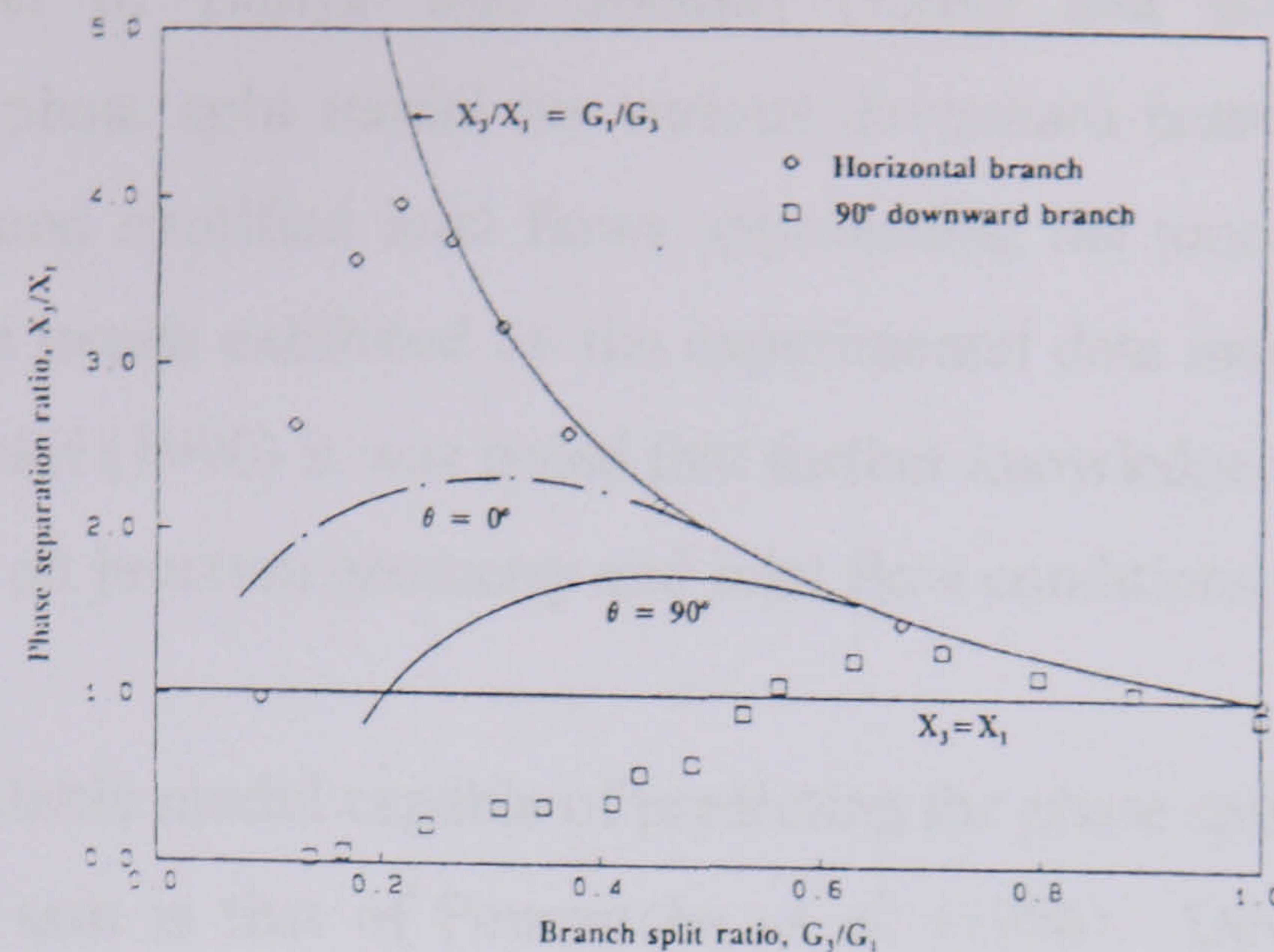


Figure 7-2: The model of Seeger *et al.* (1986) compared with the data of Peng *et al.* (1993)

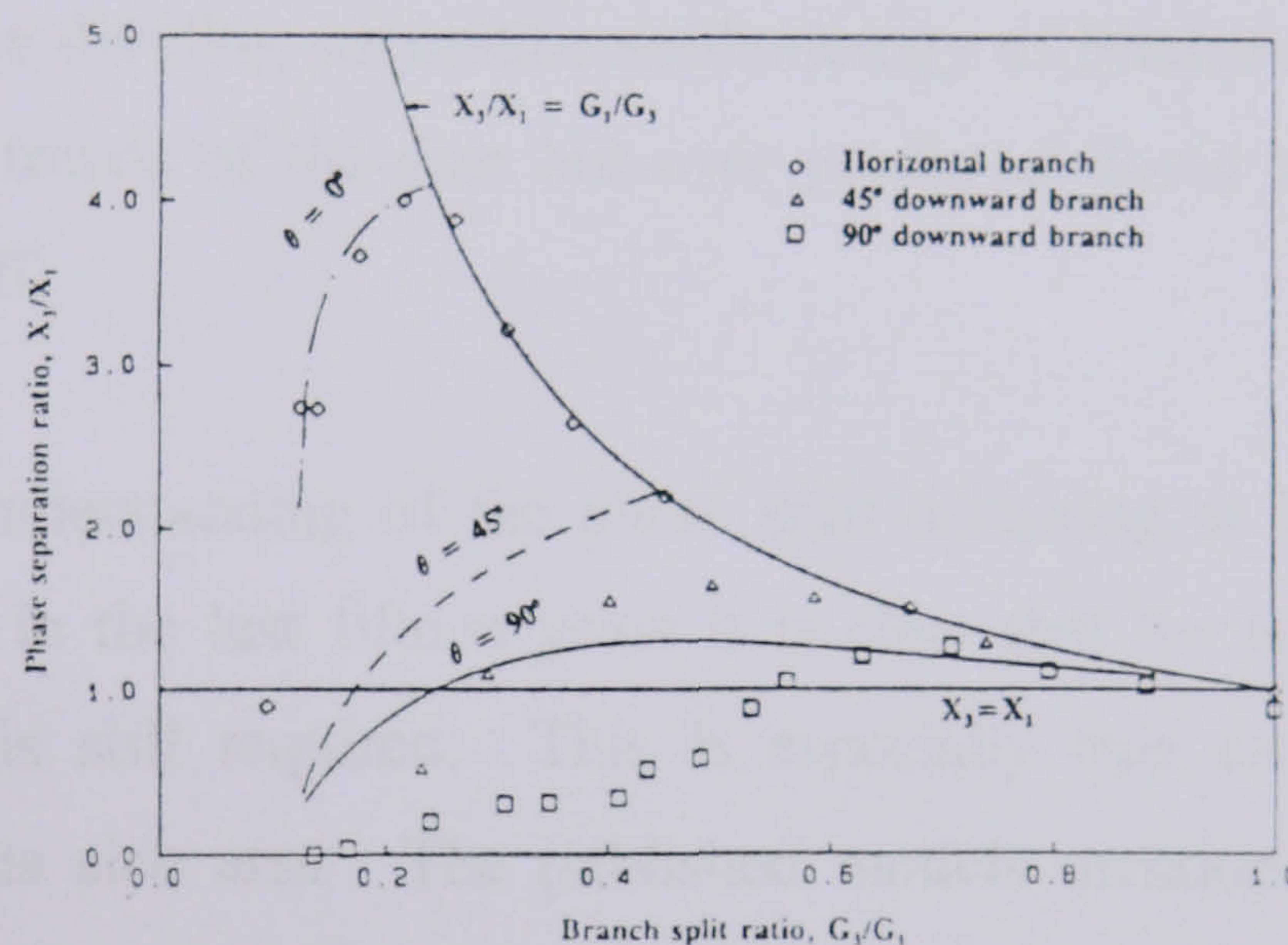


Figure 7-3: The model of Ballyk and Shoukri (1990) compared with the data of Peng *et al.* (1993)

The empirical correlations proposed by Seeger *et al.* (1986) vastly under predicted the data for the horizontal junction and over predicted the results of the junction with a downwards side arm. Not even the general trends exhibited by the data were followed, highlighting the limitations of empirically based models. The performance of the model by Ballyk and Shoukri (1990) deteriorated as the side arm was rotated downwards from the horizontal. Their model took into account the increasing effect of gravity as the side arm is rotated downwards but as the results indicate the phase split at such junctions is governed by more complicated mechanisms than increasing gravitational forces, especially with the side arm vertically downwards. Peng (1994)



adapted the model of Ballyk and Shoukri (1990) and published a general phenomenological phase split model for various downward branch arm orientations with both annular and stratified inlet flows approaching the junction. Although the model followed the trends exhibited by the experimental data more closely than that of Ballyk and Shoukri (1990) it was noted that further knowledge of gas pull-through and its dependence on junction geometry and inlet flow conditions was required.

The only other available model capable of predicting the phase split at a junction with a downwards side arm is that of Penmatcha *et al.* (1996). Developed initially to predict the phase split for stratified flow at a regular T-junction with a side arm orientated from the horizontal to vertically downwards the ideas were extended by Marti and Shoham (1997) for a reduced diameter side arm. In general their model, based initially on the dividing streamline methodology of Shoham *et al.* (1987), did exhibit the general trends of the data but over predicted liquid take off and under predicted gas take off.

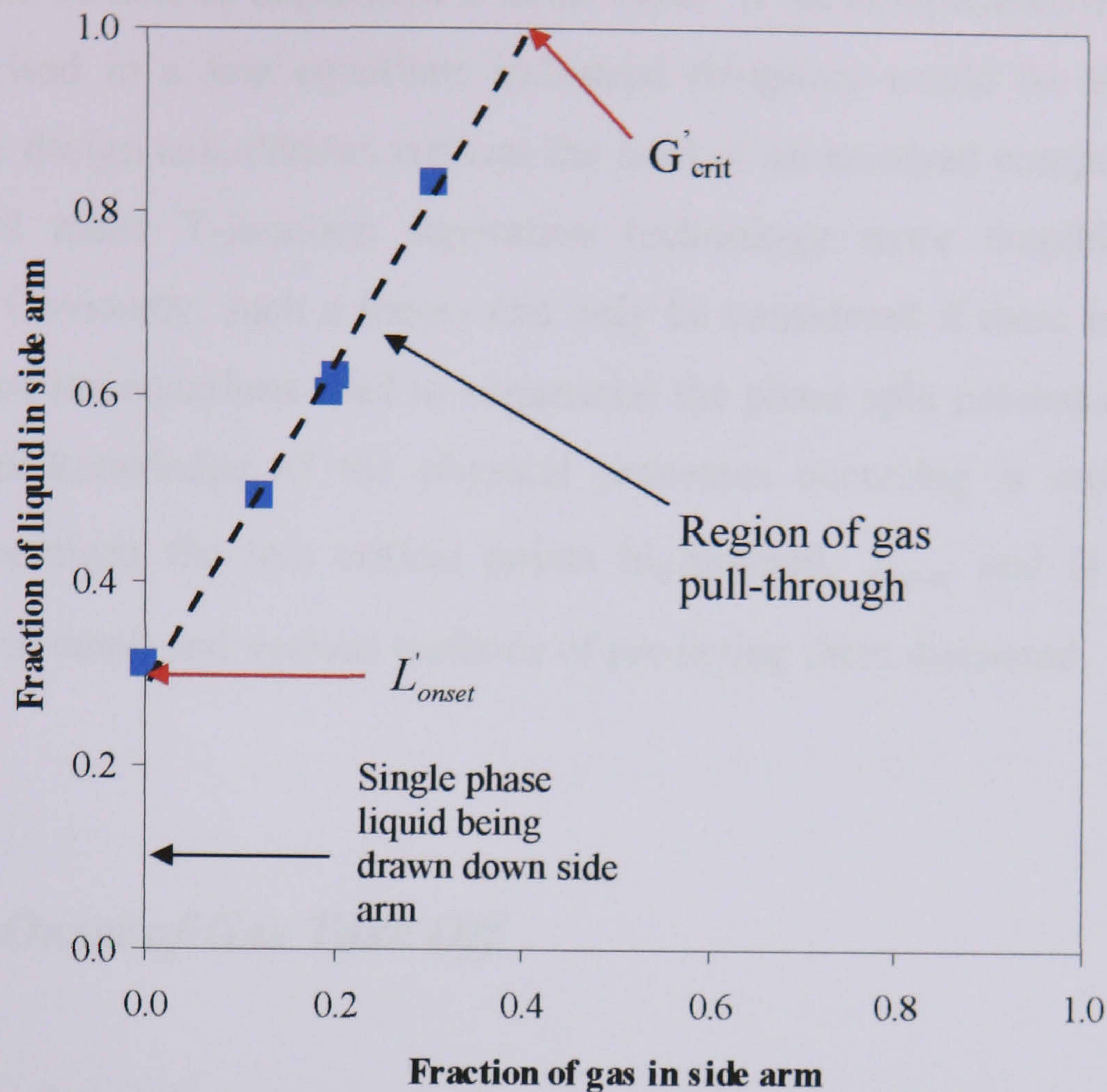
Thus, despite our understanding of the phase split occurring at T-junctions having grown significantly in the last fifteen years it is clear that for accurate predictions further knowledge is still required. This is especially true for junctions with a vertically downwards side arm. The published models mentioned above have all extended the principles behind the existence of zones of influence and applied them to junction orientations from the horizontal. As highlighted by the results, in all cases the physical reality is not being fully described and the predictions fall short of the experimental data. Therefore the theoretical work presented within this chapter considers the physical effects on the inlet flow passing a junction with a downwards side arm and suggests possible mechanisms to describe the observed phase split.

Figure 7-4 shows a typical set of phase split results for a large diameter, regular T-junction with a vertically downwards side arm. For all inlet conditions it was observed that initially a single phase liquid stream was drawn through the branch arm. At a critical value of the fraction of liquid drawn down the branch arm, gas is entrained. This point was considered to be the onset of gas take off and denoted,

$$L'_{onset}.$$


---





**Figure 7-4: Typical phase split results with the side arm vertically downwards**

$$U_{gs} = 8\text{m/s and } U_{ls} = 0.556\text{m/s}$$

Beyond this point, a two-phase stream emerges from the branch arm and this has been termed the region of gas pull-through. At a critical gas take off, all the liquid is diverted down the branch arm. This point was denoted  $G'_{crit}$ .

All the experimental data for a junction with a downwards side arm, detailed in Chapter 4, was seen to follow similar trends, following a linear trend from the onset of gas take off to the critical gas fraction where all the liquid has been diverted. It was considered that the linear nature of the phase split results could provide a simple solution to predicting the phase separation. If the onset of gas take off,  $L'_{onset}$  and the point where all the liquid has been diverted down the side arm for a critical gas fraction,  $G'_{crit}$ , can be found then the phase split for a specified liquid and gas fraction



can be determined easily. The advantages of providing a simple method of calculating the phase split at a downwards T-junction is that the ultimate users of this theory would be able to implement it in the field. If the complicated mechanisms can be summarised in a few equations industrial designers would be able to perform preliminary design calculations without the need of an involved computer simulation. This would make T-junction separation technology more tangible and readily available. Obviously, such a theory can only be considered if there is confidence in the results of the equations used to summarise the phase split process and to produce such results knowledge of the physical processes occurring is required. In the following sections the two critical points highlighted,  $L'_{onset}$  and  $G'_{crit}$ , have been considered in detail and various methods of predicting them discussed.

## 7.2 The Onset of Gas Take Off

As shown in Figure 7-4, the onset of gas take off is the point where gas is first drawn out of the side arm with the exiting liquid. Previous to this point a single phase liquid stream has been exiting through the side arm but at the onset of gas take off the single phase liquid stream turns into a two-phase gas-liquid flow. The data presented by Reimann *et al.* (1988) exhibits similar trends as does the data of Penmatcha *et al.* (1996), who studied various downwards branch arm angles, although no mention was made of this phenomenon within their predictive model.

The prediction of this point, the onset of gas take off  $L'_{onset}$ , was tackled from two points of view. Up to this point only a fraction of the inlet liquid flow has been diverted down the branch arm, the first approach therefore considered the gas exiting with the liquid to be pulled through the layer of liquid remaining in the pipeline. This was related to previous research into small breaks in pipelines, which have received significant attention due to the nuclear industry. The second idea considered what was happening to the flow diverted down the branch arm, rather than any phenomena occurring at the junction. During experimentation the entrained gas was seen as



bubbles trapped in liquid column in the branch arm and so their movement was considered.

### 7.2.1 Predictions using small break theory

Research into gas being pulled through a liquid layer, as would be experienced with stratified flow approaching the junction, was prevalent in the early 1980's when nuclear reactor safety was at the forefront of two-phase flow research. Loss of Coolant Accidents (LOCA) caused by a small break in a horizontal coolant pipe, for the purposes of experimental investigations, was often regarded as a T-junction with a very narrow branch arm diameter. Obviously, as the coolant pipe wall could fail at any point around its circumference research was performed with the narrow branch arm of the T-junction placed at various orientations from the horizontal. Reimann and Khan (1982, 1983) paid particular attention when this phenomenon occurred at the bottom of the horizontal pipe. They simulated the problem by using a T-junction where the main pipe diameter was 206mm and two different side arm diameters of 6mm and 12mm. Using air-water stratified flow conditions the onset of continuous gas pull through was related to the stratified liquid level height,  $h$ , and can be described by:

$$Fr \left( \frac{\rho_L}{\rho_L - \rho_G} \right)^{0.5} = 1.1 \left( \frac{h}{d} \right)^{2.5} \quad \text{Equation 7-1}$$

Since the Froude number,  $Fr = V_3^2 / gd$ , is dependant on the side arm (branch 3) velocity and diameter they determined that the onset of continuous gas pull through can become independent of side arm diameter,  $d$ , if the break mass flowrate is considered instead:

$$\dot{m}_{L3} / (g \rho_L (\rho_L - \rho_G))^{0.5} h^{2.5} = 0.736 \quad \text{Equation 7-2}$$



Experiments were performed in the range  $h/d \geq 1$ . Maciaszek and Micaelli (1988) used a similar T-junction arrangement with a large diameter main branch (0.102 – 0.284m) and a very small diameter branch arm (4 – 34mm) placed horizontally, vertically upwards and vertically downwards. They calculated the onset of gas take off by considering it as a balance between the horizontal and vertical inertial forces of the liquid phase:

$$h_{bge} = K \left( \frac{Q_{3L}^2}{g(\rho_L - \rho_G)\rho_L} \right)^n \quad \text{Equation 7-3}$$

K and n were found by experimental means for their system. K varied with the fraction of liquid drawn down the branch arm being close to unity for large fraction of liquid diverted and decreasing as the fraction of liquid in the branch arm was reduced. The value of n was found to be 0.2.

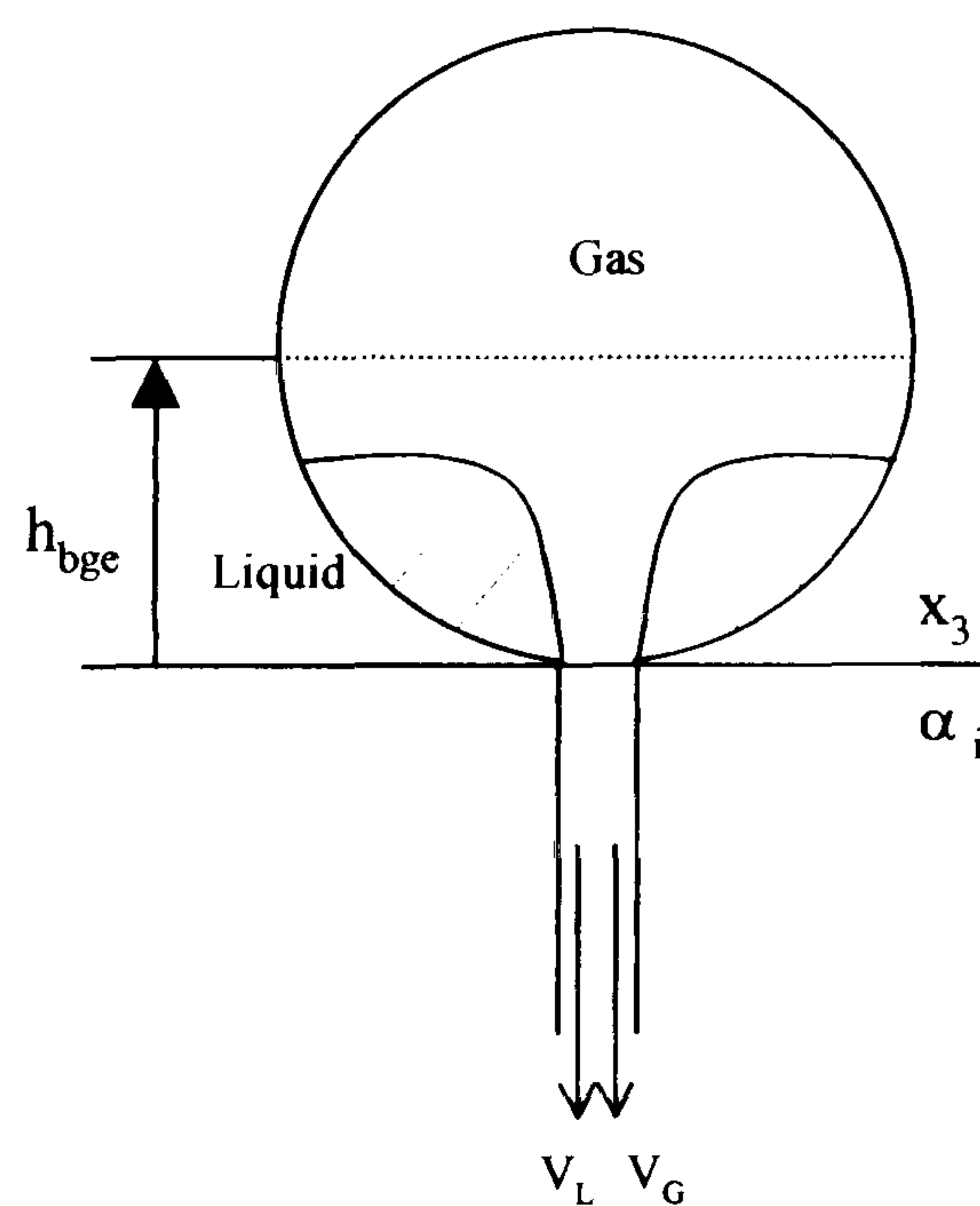


Figure 7-5: Onset of gas pull through, Maciaszek and Micaelli (1988)



As shown in Figure 7-5, this method of calculating the onset of gas pull through is in effect creating a dividing streamline where anything above the height,  $h_{bge}$  does not get drawn down the side arm. Hence, this method was applied to the large diameter T-junction currently under investigation and used to calculate the onset of gas take off,  $L'_{onset}$ . The effect on the predicted value of  $L'_{onset}$  can be seen in Table 7-1 for two arbitrary inlet conditions. Systematic empirical variation of both K and n was investigated. The values of K = 1.1 and n = 0.2 gave the best fit and were closest to the values quoted by Maciaszek and Micaelli (1988).

**Table 7-1: Comparison of the predicted and experimental values for the fraction of liquid drawn into the branch arm at the onset of gas take off,  $L'_{onset}$  for different inlet flow conditions for the large diameter regular T-junction using the small break theory**

Inlet Conditions	$L'_{onset}$ Experimental	$L'_{onset}$ Predicted	K	n
$U_{gs} = 8\text{m/s}$ $U_{ls} = 0.434\text{m/s}$	0.40	0.34	1.2	0.20
		0.42	1.1	0.20
		0.54	1.0	0.20
		0.79	1.1	0.22
		0.58	1.1	0.21
		0.30	1.1	0.19
$U_{gs} = 6\text{m/s}$ $U_{ls} = 0.31\text{m/s}$	0.68	0.48	1.2	0.20
		0.60	1.1	0.20
		0.77	1.0	0.20
		1.0	1.1	0.22
		0.86	1.1	0.21
		0.41	1.1	0.19

This method clearly indicates that there is an “onset of gas take off” for each set of inlet conditions and that it can be predicted, perhaps, in a manner not too dissimilar to the above methods described for the LOCA incidents. One major difference is that for LOCAs the diameter of the break was thought to be a fraction of the main pipe diameter but for T-junctions the diameter of the branch arm tends to be much larger as



junctions being used as partial phase separators need to separate the two phases into different streams and not significantly reduce the volumetric flowrate of one of the branches. Further enhancement of the above method would be obtained if an in-depth evaluation of the constants were made. The values initially used for  $K$  and  $n$  were taken around those suggested within the literature but a deeper investigation may highlight more suitable values.

The value of  $L'_{onset}$  using the small break theory was calculated for different inlet conditions with  $K = 1.1$  and  $n = 0.2$ . The error in the predicted value of  $L'_{onset}$  is shown in Figure 7-6. The systematic over and under prediction of  $L'_{onset}$  using the small break theory indicates that with some modifications the theory may be extended to large diameter pipelines.

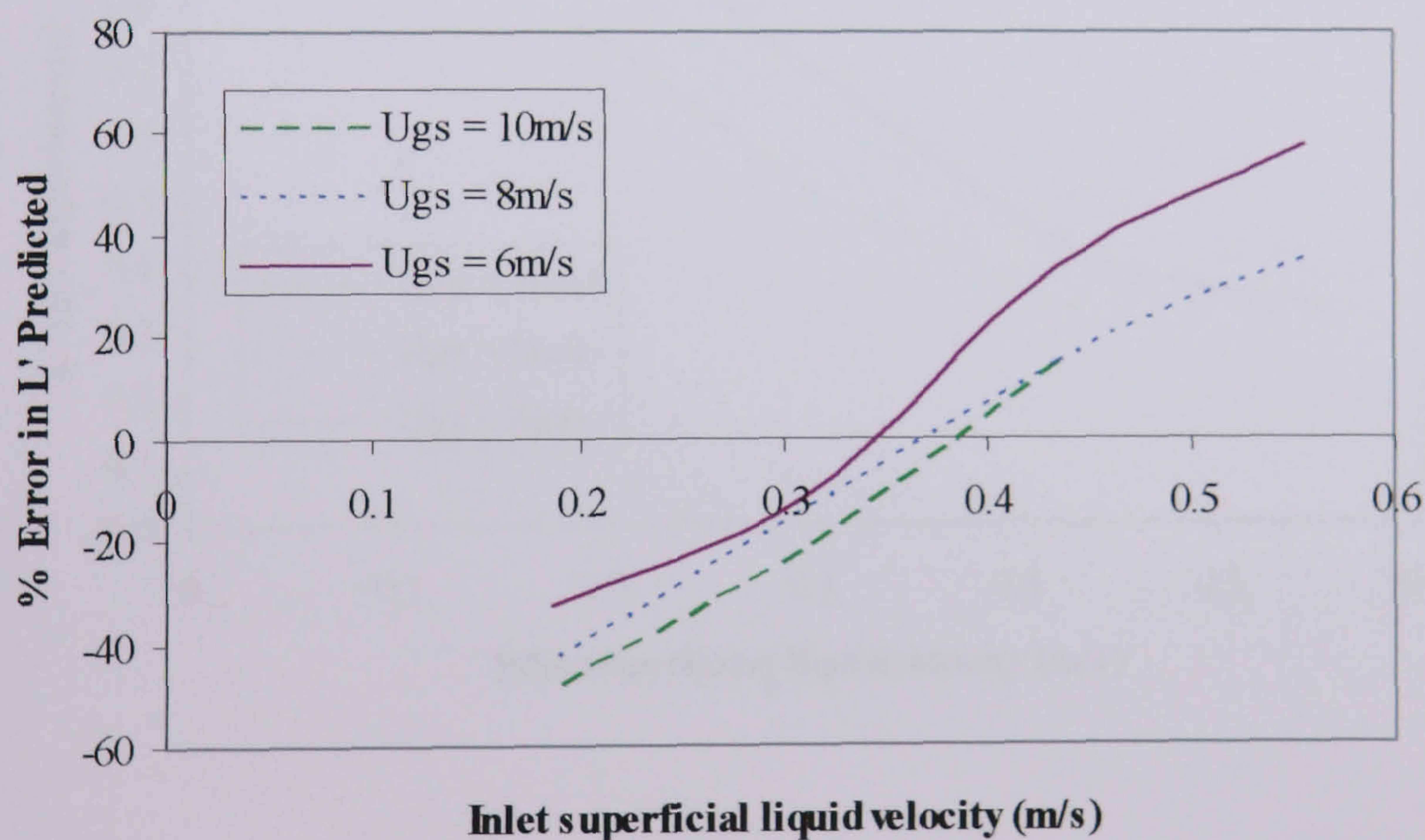
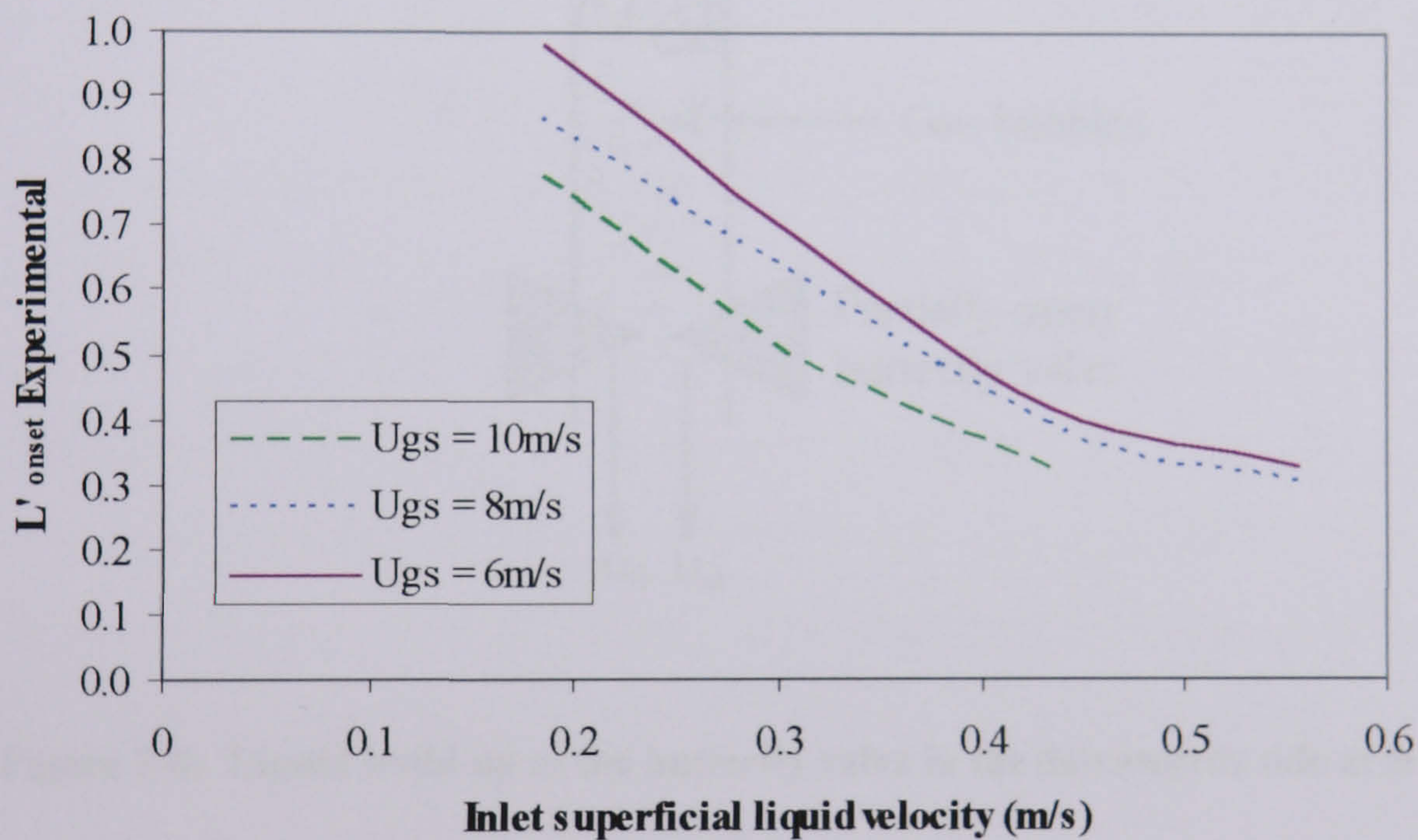


Figure 7-6: The effect on the predicted value of  $L'_{onset}$  for different inlet conditions



### 7.2.2 Predictions considering the gas-liquid flow in the branch arm

From inspection of the experimental values of  $L'_{onset}$  (tabulated in Appendix A for the raw data given in Appendix B) it was seen that for the same inlet gas superficial velocity,  $U_{gs}$ , the fraction of liquid that has to be diverted before the onset of gas take off,  $L'_{onset}$ , is reached increases as the inlet liquid superficial velocity,  $U_{ls}$ , is reduced. Plus, for the same inlet liquid superficial velocities,  $U_{ls}$ , and increasing inlet gas superficial velocity,  $U_{gs}$ , the value of  $L'_{onset}$  remains fairly steady, especially at the higher  $U_{ls}$  values, see Figure 7-7.



**Figure 7-7: Variation of experimental values of  $L'_{onset}$  with inlet gas and liquid superficial velocities**

This suggests that consideration has to be given to the processes occurring in the side arm in addition to the flow approaching the T-junction. For all experiments the phase redistribution at the T-junction was controlled by the butterfly valves on the downstream legs of the junction, one in the run arm and one in the branch arm (see Chapter 3 for full geometrical details). During the experiments it was observed that the initial



fractional movement of the butterfly valve in the branch arm from the fully closed position (towards fully open) caused the greatest difference in the amount of gas and liquid drawn off down the side arm. With the valve partially closed, the liquid drawn off down the branch arm at the T-junction would build up behind the valve, causing a plug of liquid that any entrained gas would have to pass through before being measured downstream of the valve.

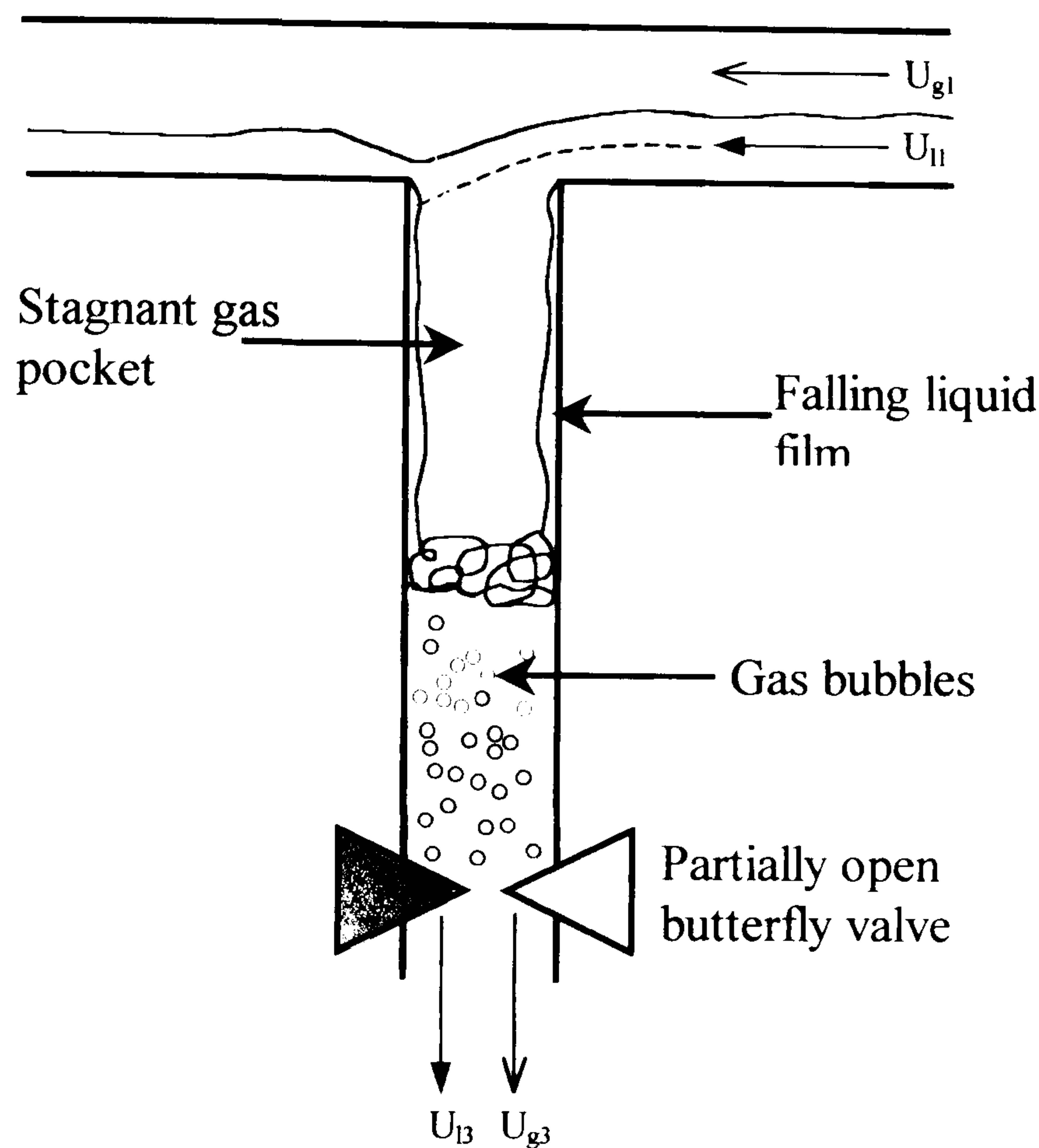


**Figure 7-8: Liquid build up at the butterfly valve in the downwards side arm**

The liquid drawn into the branch arm from the T-junction falls as a film down the pipe walls, either side of a stagnant gas pocket, as shown in Figure 7-8. With the butterfly valve partially closed the liquid can not drain away as fast as it is collecting, so a column of liquid builds up at the valve, backing up towards the T-junction. Within this column of liquid small gas bubbles are seen to be entrained. The stagnant gas pocket may act as a cushion, supporting the phase split phenomenon that is seen at the T-junction (described in Chapter 4 section 4.3, as a transparent banana being peeled). Once the valve is opened wide enough, the build up of liquid is released and



both the gas and liquid can be drawn simultaneously through the valve and be monitored further down stream.

With the aid of Figure 7-8 it can be seen that although the air can be drawn down the side arm at the T-junction with the falling liquid film it has to pass through the column of liquid before being measured downstream of the butterfly valve. Within the column of liquid many small gas bubbles can be seen, circulating with the flow. For any of the gas bubbles to escape with the liquid flowing through the valve their natural buoyancy within the liquid must be overcome. At the point where the terminal rise velocity of the bubble is less than or equal to the velocity of the exiting liquid, gas bubbles will be drawn out the side arm.

Many papers have been published describing the dependence of the terminal rise velocity of a single bubble on fluid properties, bubble concentration and the influence of containing walls, void fraction and vibrations. Haberman and Morton (1953) considered the effect of terminal rise velocity for air bubbles in water as a function of equivalent bubble diameter. They concluded that the terminal velocity remained fairly constant for any bubble over 0.6mm in diameter. Given that the vast majority of the bubbles seen in the present experiments were easily visible with the human eye then it can be assumed that the bubbles were larger than this critical diameter. In addition, any smaller gas bubbles that may have been drawn through the valve would have to be present in a huge concentration to produce any measurable gas flow.

From their comprehensive study, Peebles and Garber (1953) suggested that there were four different ranges of conditions in which specific correlations for the terminal rise velocity of a bubble were applicable. The boundaries of each region are given in terms of the bubble Reynolds number,  $Re_b$ . Successive regions consider faster moving bubbles with the specified correlations of the terminal rise velocity taking into account the appropriate drag coefficient. Region 1 considers very slow bubble movement where  $Re_b \leq 2$  and Regions 2 and 3 are defined by correlations considering the shape of the bubble drag coefficient curve when plotted against  $Re_b$ . Region 4 is distinguished from the other regions by the gas bubbles exhibiting a constant rising velocity, independent of the bubbles size. Both Haberman and Morton

---



(1953) and Peebles and Garber (1953) state that above a critical bubble diameter. 0.6mm, the terminal rise velocity is constant. From the experimental observations previously noted the bubbles were visible with the human eye therefore for the situation within the T-junction it was found that the correlations associated with ‘Region 4’ were the most appropriate. Within this region Peebles and Garber (1953) have defined the bubble rise velocity,  $v_{\infty}$  as

$$v_{\infty} = 1.18 \left( \frac{g\sigma}{\rho_L} \right)^{0.25} \quad \text{Equation 7-4}$$

Though more complicated predictions have been presented very recently for bubble rise velocity (Tomiyama *et al.*, 2001; Celata *et al.*, 2001) their implementation requires in depth knowledge of the two-phase system – including a bubble distortion factor and aspect ratio. Within industrial settings, beyond the average system flowrates, such properties are not known so the above correlation provides a suitable method to predict bubble rise velocity.

If the onset of gas take off is assumed to occur when the liquid flowrate through the valve is equal to or greater than the terminal rise velocity of the gas bubbles then it could be stated that the exiting liquid flowrate is equal to the calculated rise velocity. From an examination of the available experimental data it was seen that the Froude number for the liquid in the downwards branch arm:

$$Fr = \frac{V_{L3}^2}{gD_3} \quad \text{Equation 7-5}$$

was related to  $L'_{onset}$ , the fraction of liquid that is diverted down the side arm at the onset of gas take off. It was discovered that for all the experimental inlet superficial velocities that the Froude number remained constant at a value of 0.026.

The bubble rise velocity from Equation 7-4 was assumed to equal the exiting liquid velocity at the onset of gas take. Thus, by substitution of this calculated bubble rise

---



velocity into Equation 7-5 the Froude number was found to be 0.029. This value of Froude number provides a method of calculating the fraction of liquid diverted at the onset of gas take off for any inlet conditions. Figure 7-9 shows the variation in the experimental values of  $L'_{onset}$  with those calculated by the above methods. The diamonds represent the calculated values using the empirical Froude number of 0.026 and the circles represent the Froude number of 0.029 based on a bubble rise velocity. Obviously  $L'_{onset}$  can not be larger than one so even the over predicted values would collapse back to a value of one. Therefore, Figure 7-9 indicates that  $L'_{onset}$  can be reasonably predicted and is related to the bubble rise velocity of the entrained bubbles in the column of liquid held up in the down arm. It should be stated that the higher the liquid inlet velocity the more accurately  $L'_{onset}$  is predicted.

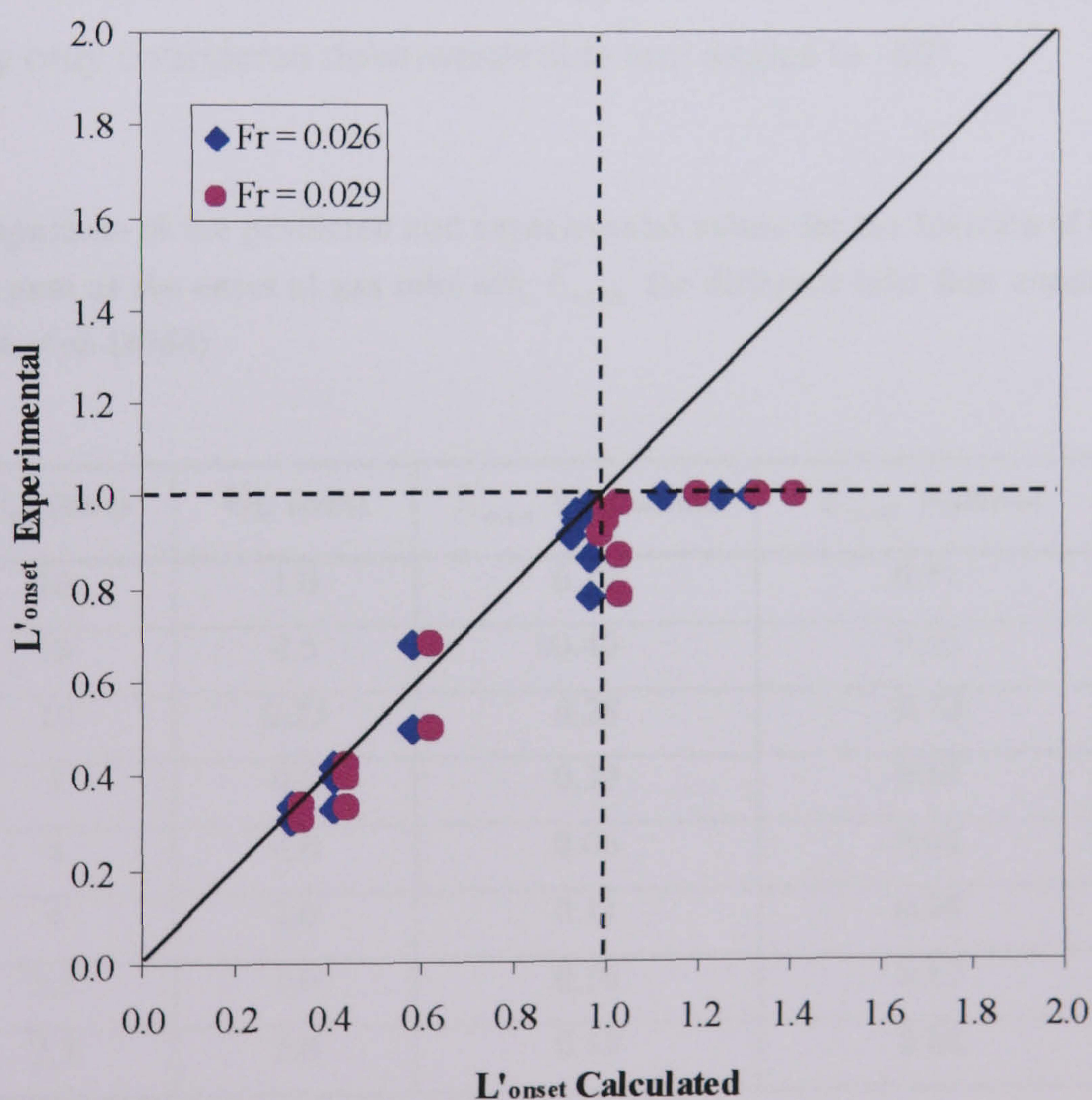


Figure 7-9: Calculated versus measured values of  $L'_{onset}$



Bubble rise velocity was also considered by Evans and Jameson (1995) who were investigating the hydrodynamics of a plunging liquid jet bubble column. They considered the gas drift flux of their system could be related to the terminal bubble rise velocity by the correlation highlighted by Wallis (1969). A similar approach was considered with the current data although a convergence could not be found in this case.

This simple method of predicting  $L'_{onset}$  was tested against data found in literature. The high pressure (5bar) air-water data of Reimann *et al.* (1988) approaching a regular 0.05m T-junction with a vertical downwards (-90°) side arm could be reasonably predicted, see Table 7-2. Again at very low inlet liquid flowrates ( $U_{ls} = 0.25\text{m/s}$ ) the predicted value of  $L'_{onset}$  quoted in Table 7-2 differs significantly, a similar trend observed in predicting  $L'_{onset}$  for the current data at a large diameter junction. The same method could not be applied to the data of Penmatcha *et al.* (1996), as they only considered downwards side arm angles to -60°.

**Table 7-2: Comparison of the predicted and experimental values for the fraction of liquid drawn into the branch arm at the onset of gas take off,  $L'_{onset}$  for different inlet flow conditions for the data of Reimann *et al.* (1988)**

$U_{gs}$ (m/s)	$U_{ls}$ (m/s)	$L'_{onset}$ Experimental	$L'_{onset}$ Predicted
10	1.0	0.19	0.17
10	0.5	0.40	0.35
10	0.25	0.28	0.70
5	0.5	0.39	0.35
4	4.0	0.06	0.04
4	2.0	0.11	0.08
2.5	1.0	0.16	0.17
2.5	2.0	0.10	0.08



In Chapter 2 the first industrial use of a T-junction as a partial phase separator was highlighted. Azzopardi *et al.* (2001) successfully employed a T-junction to perform a partial phase separation of a two-phase stream to allow the fractions to enter different points of a distillation column, thus restoring its efficiency. Although the junction is not strictly a horizontal junction with a vertical downwards side arm, see Figure 7-10, the above method for predicting  $L'_{onset}$  was considered for the industrial operating conditions. For this case the terminal bubble rise velocity,  $V_{\infty}$ , was calculated to be 0.135m/s and the downwards velocity of the liquid passing through the U-bend was found to be 0.09m/s. For the above theory to hold, the velocity of the liquid flowing through the U-bend must equal the bubble rise velocity. As can be seen the liquid velocity in the U-bend is lower than the bubble rise velocity indicating there is no gas present in the liquid only stream, which is deemed to be the case. So it can be stated that the above methodology can be applied to industrially relevant situations as well as data collected under laboratory conditions.

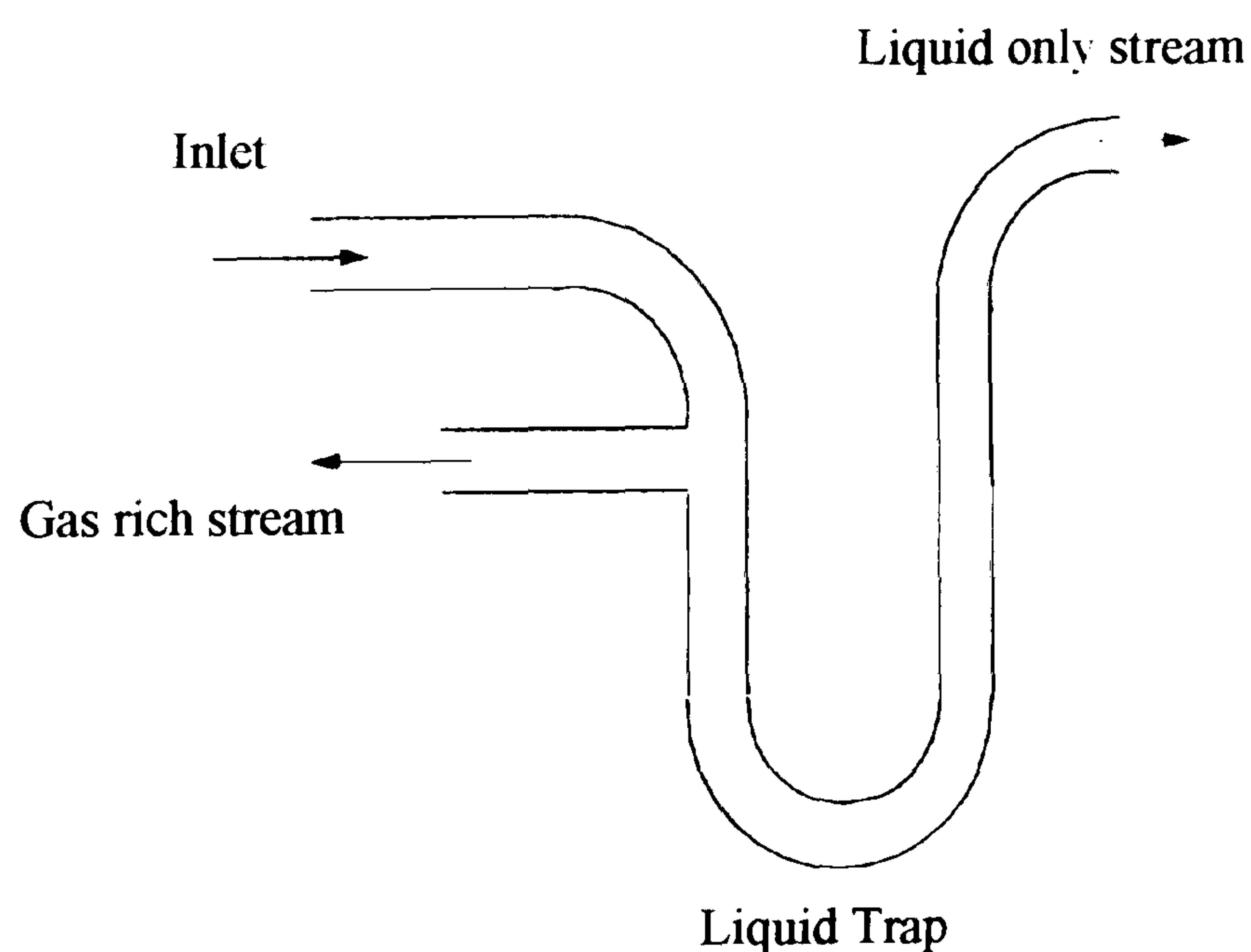


**Figure 7-10: The industrial partial phase T-junction separator at BP/Amoco, Hull**



### 7.3 The Critical Gas Fraction and Gas Pull Through

In the previous section it was shown that the fraction of liquid diverted at the onset of gas take off,  $L'_{onset}$ , can be reasonably predicted by calculating the bubble rise velocity for the gas-liquid flow trapped in the branch arm. From the onset of gas take off,  $L'_{onset}$ , the data in the region of gas pull through follows a linear trend resulting in total liquid removal down the side arm at a critical gas fraction,  $G'_{crit}$ . Beyond this point only an increase in the fraction of gas drawn down the branch arm is observed. If the value of  $G'_{crit}$  can be predicted in a straightforward manner, as for  $L'_{onset}$ , then the phase split at a T-junction with a downwards side arm can be easily predicted. Calculating the value of  $G'_{crit}$  was approached from three points of view. The first was through empirical manipulation of the data to gain an understanding of the mechanisms taking place. The second and third approaches are related. As a basic assumption they considered the flow across the junction to be a “particle”. The forces acting on the particle were then considered and the predictive results obtained were compared with the experimental data.

#### 7.3.1 Empirical relationships

Since the relationship between the fraction of liquid diverted,  $L'$  and the fraction of gas diverted,  $G'$  down the side arm, in the gas pull through region is linear, it can be said that

$$L' = M G' + L'_{onset} \quad \text{Equation 7-6}$$

where  $M$  is the gradient of the phase split data.



It was suggested that the gradient of the phase split data,  $M$ , was related to the ratio of the superficial flux of the gas and liquid phases in the side arm as in Equation 7-7.

$$\text{Phase Split Gradient, } M \approx \sqrt{\frac{\rho_L V_{L3}^2}{\rho_G V_{G3}^2}} \quad \text{Equation 7-7}$$

Hence the phase split data can be described by the following equation:

$$L' = \sqrt{\frac{\rho_L V_{L3}^2}{\rho_G V_{G3}^2}} G' + L'_{onset} \quad \text{Equation 7-8}$$

This relationship was used to predict the trend of the phase split data collected in the present experimental investigation. Figure 7-11 shows the results for various inlet liquid flowrates at a constant gas velocity,  $U_{gs} = 10\text{m/s}$ . The phase split results are reasonably determined however, for the very low inlet liquid flowrates the predicted value of  $L'_{onset}$  is over estimated resulting in a poor overall prediction.

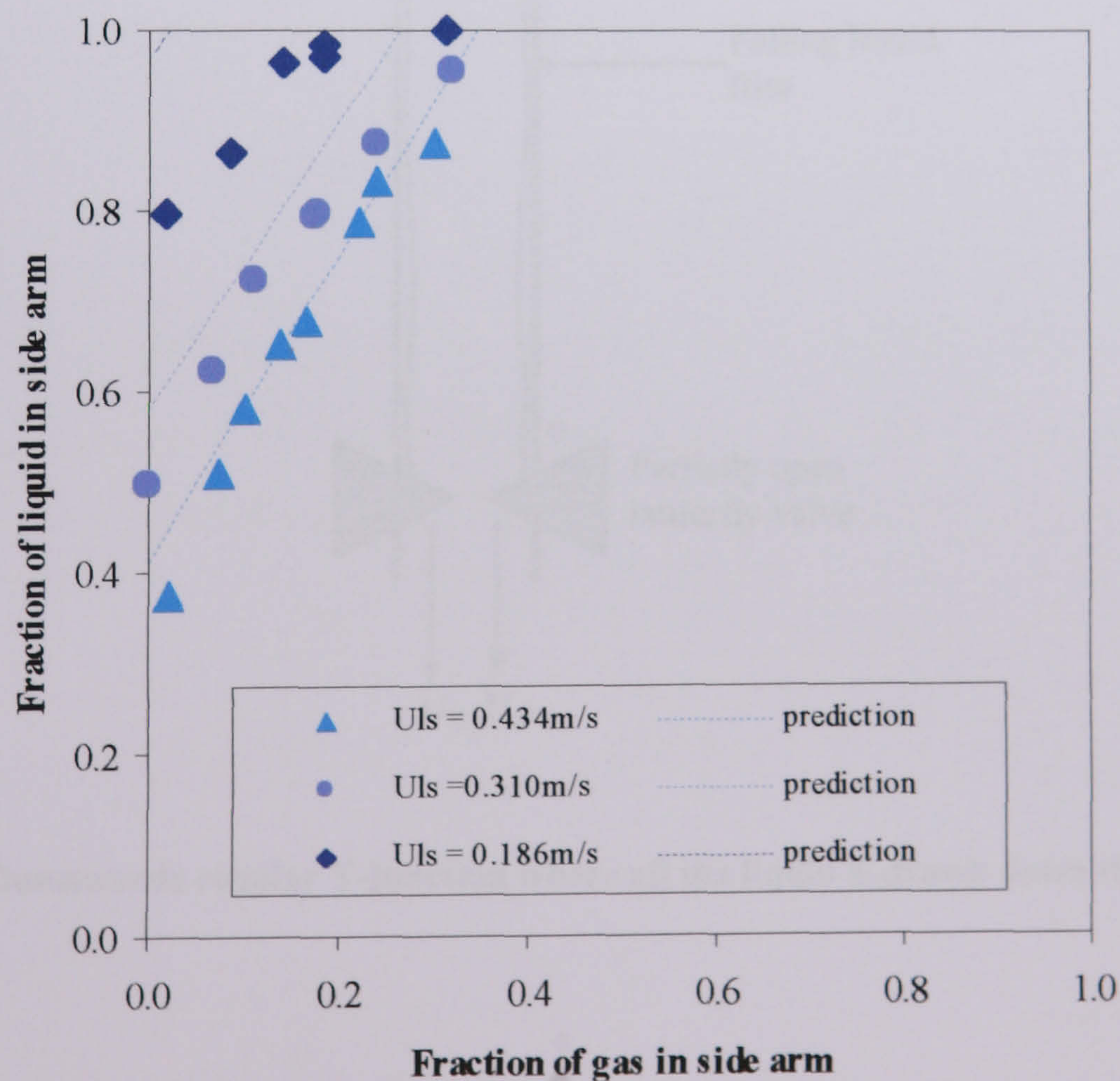


**Figure 7-11: Empirical phase split predictions for a large diameter regular T-junction,**  
 $U_{gs} = 10\text{m/s}$



### 7.3.2 Considering the pressure drop across the T-junction

As stated earlier in this chapter examination of the data leading to empirical correlations can provide an insight into what physical processes are occurring within a system but the resulting relationships often do not hold beyond the data base used to create them. A more powerful approach would be to employ a model based on the physics of the system, as with phenomenological analysis. Thus, to relate the gas pull through seen in the experimental data to physical phenomena an initial start was made by considering what was happening at the point of critical gas take off,  $G'_{crit}$ , the point where all the liquid had been drawn down the branch arm, as indicated in Figure 7-12.

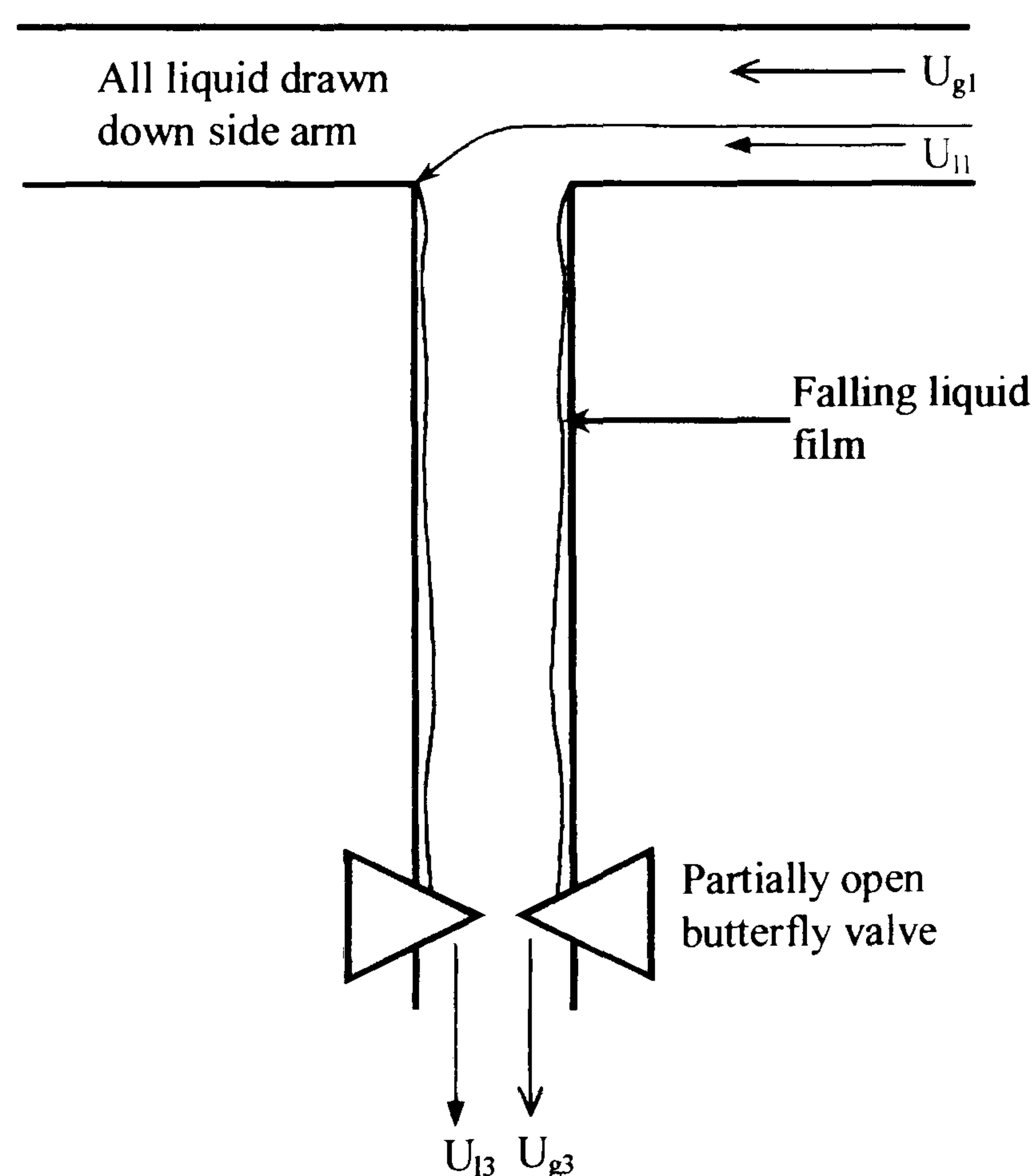


Figure 7-12: Downwards regular T-junction where all the liquid is drawn down the side arm



At this point all the liquid is drawn down the side arm for a certain gas fraction diverted. If the last particle of liquid to be drawn down the side arm is considered to be travelling at the gas-liquid interface then it is at the maximum height of the liquid,  $h$ , and travelling along the axes of the pipe at the interface velocity,  $V_{LH}$ . A particle of gas at the interface will be at a very similar height and travelling at a very similar velocity.

The following equations can be used to describe the horizontal,  $x$ , and vertical,  $y$ , motion of the liquid particle as it falls into the branch arm. The exact determination of these equations can be found in Appendix C.

In the horizontal direction, the distance travelled by the particle,  $x$ , is related to the interface velocity,  $V_{LH}$  by

$$x = V_{LH}t - \frac{C_1}{\rho_L} \frac{t^2}{2} \quad \text{Equation 7-9}$$

The motion in the vertical,  $y$ , can be described by

$$y = \frac{C_2}{\rho_L} \frac{t^2}{2} \quad \text{Equation 7-10}$$

The value of the constants  $C_1$  and  $C_2$  are found by considering the horizontal and vertical pressure drops across the junction. For simplicity the pressure drop correlation of Gardel (1957) was considered for the gas phase only as it passed the T-junction thus

$$C_1 = \frac{dP}{dx} = \frac{P_2 - P_1}{D_3} \quad \text{Equation 7-11}$$

and

$$C_2 = \rho_L g + \frac{dP}{dy} = \rho_L g + \frac{\bar{P} - P_3}{D_1/2} \quad \text{Equation 7-12}$$



Substituting for time,  $t$  from Equation 7-10 into Equation 7-9 gives the overall relationship for the particles horizontal and vertical motion

$$x = V_{LH} \sqrt{\frac{2\rho_L}{C_2}} y^{0.5} - \frac{C_1}{C_2} y \quad \text{Equation 7-13}$$

The point where total liquid take off has been achieved for a specific fraction of gas diverted down the side arm is reached when  $x$  in Equation 7-13 to equal  $D_3$  (0.127m) at  $y = h$  for the particle travelling at the interfacial velocity  $V_{LH}$ . Below this value the point of total liquid extraction has been passed and beyond this value total liquid extraction has not been achieved.

From Equation 7-13 the value used for the stratified liquid height plays a critical role. The customary technique of calculating the stratified liquid height for given inlet conditions is to use methodology of Taitel and Dukler (1976). However, the experimental analysis of Rea (1998) showed that for the high liquid flowrates and the large tube diameter used in this case the methodology of Taitel and Dukler (1976) under predicts film thickness.

As can be seen in Figure 7-13 for small film thicknesses the measured and calculated film thicknesses are identical. As film thickness increases the calculated film thickness is over predicted. Sufficient measurements at various inlet conditions were provided by Rea (1998) for an accurate value to be provided for the present experimental conditions. The values have been tabulated in Appendix A for reference. Obviously for large industrial sized pipelines an accurate method of predicting liquid height would be needed.



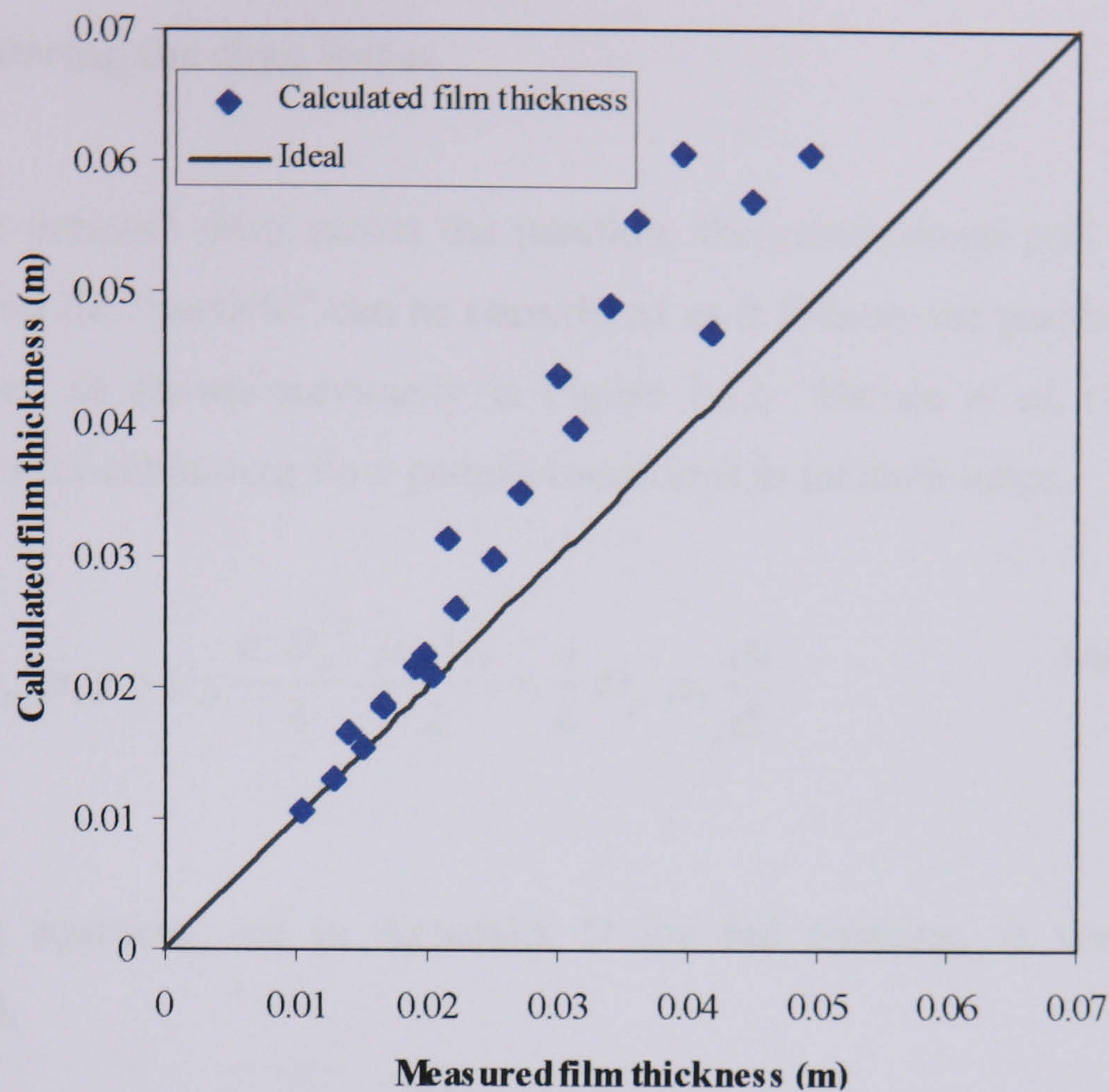


**Figure 7-13: The comparison of measured film thickness to those calculated using the methodology of Taitel and Dukler (1976) highlighted by Rea (1998)**

Thus, using knowledge of the liquid height for specific inlet conditions the result of Equation 7-13 was calculated for various gas fractions diverted down the side arm. The sensitivity in  $x$  was found with respect to the different fractions of gas diverted down the side arm was found to be limited. This indicates that the calculated pressure drops across the junction were negligible and hence  $C_2 \gg C_1$ . This further implies that the horizontal distance travelled by the particle is heavily dependant on the interfacial velocity. Although only the pressure drop for a single phase is considered and it can be argued that the two-phase pressure drop is considerably higher, the values calculated for the horizontal distance,  $x$ , were thought to be more dependant on a different resistive force.



### 7.3.3 Considering the drag forces

Instead of the pressure drop across the junction, the gravitational pull and the drag forces acting on the “particle” can be considered as it follows the parabolic path into the branch arm, as shown previously in Figure 7-12. Barnea *et al.* (1985) used a similar process for estimating flow pattern transitions in inclined tubes.

$$\frac{\pi}{6} D_p^3 \rho_L g + C_D \frac{\pi D_p^2}{4} \frac{\rho_G u_G^2}{2} = \frac{\pi}{6} D_p^3 \rho_L \frac{dv}{dt} \quad \text{Equation 7-14}$$

The resulting equation, see in Appendix D for full working, is very similar to Equation 7-13,

$$x = V_{LH} \sqrt{\frac{2h}{g'}} \quad \text{Equation 7-15}$$

where

$$g' = g + \frac{3 C_D}{4} \frac{\rho_G}{D_p \rho_L} V_{G3}^2 \quad \text{Equation 7-16}$$

Equation 7-15, indicates that the horizontal distance travelled,  $x$ , depends on the particle diameter,  $D_p$  and the horizontal liquid phase velocity at the interface,  $V_{LH}$ . The value of  $C_D$  was calculated as a function of the particles Reynolds number.



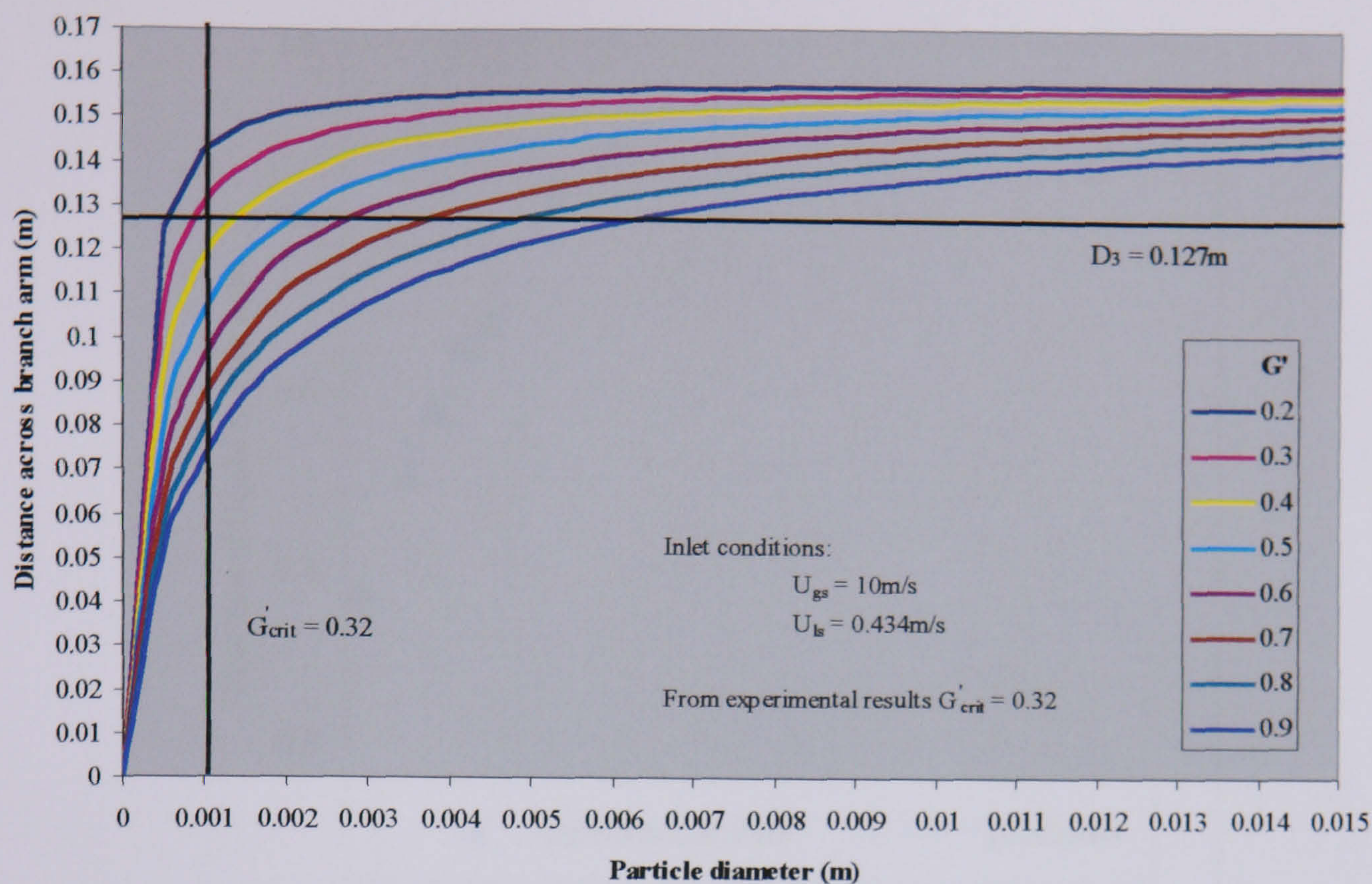


**Figure 7-14: The dependence of horizontal distance travelled on particle diameter**

$$U_{gs} = 10\text{m/s and } U_{ls} = 0.434\text{m/s}$$

The dependency on particle size can be seen in Figure 7-14. For different fractions of the inlet gas flow drawn down the branch arm,  $G'$ , the horizontal distance travelled by the particle,  $x$ , was calculated as a function of particle diameter,  $D_p$ . From the experimental results it is known for total liquid removal ( $L' = 1$ ) down the branch arm the corresponding critical gas fraction,  $G'_{crit}$ , is 0.32, for the inlet conditions  $U_{gs} = 10\text{m/s}$  and  $U_{ls} = 0.434\text{m/s}$  shown in Figure 7-14. This means the size of particle that has travelled the horizontal distance equivalent to the branch arm diameter,  $D_3 = 0.127\text{m}$ , is 0.0012m. A similar analysis was performed for all the inlet conditions and an average particle diameter was calculated to be 0.0015m.



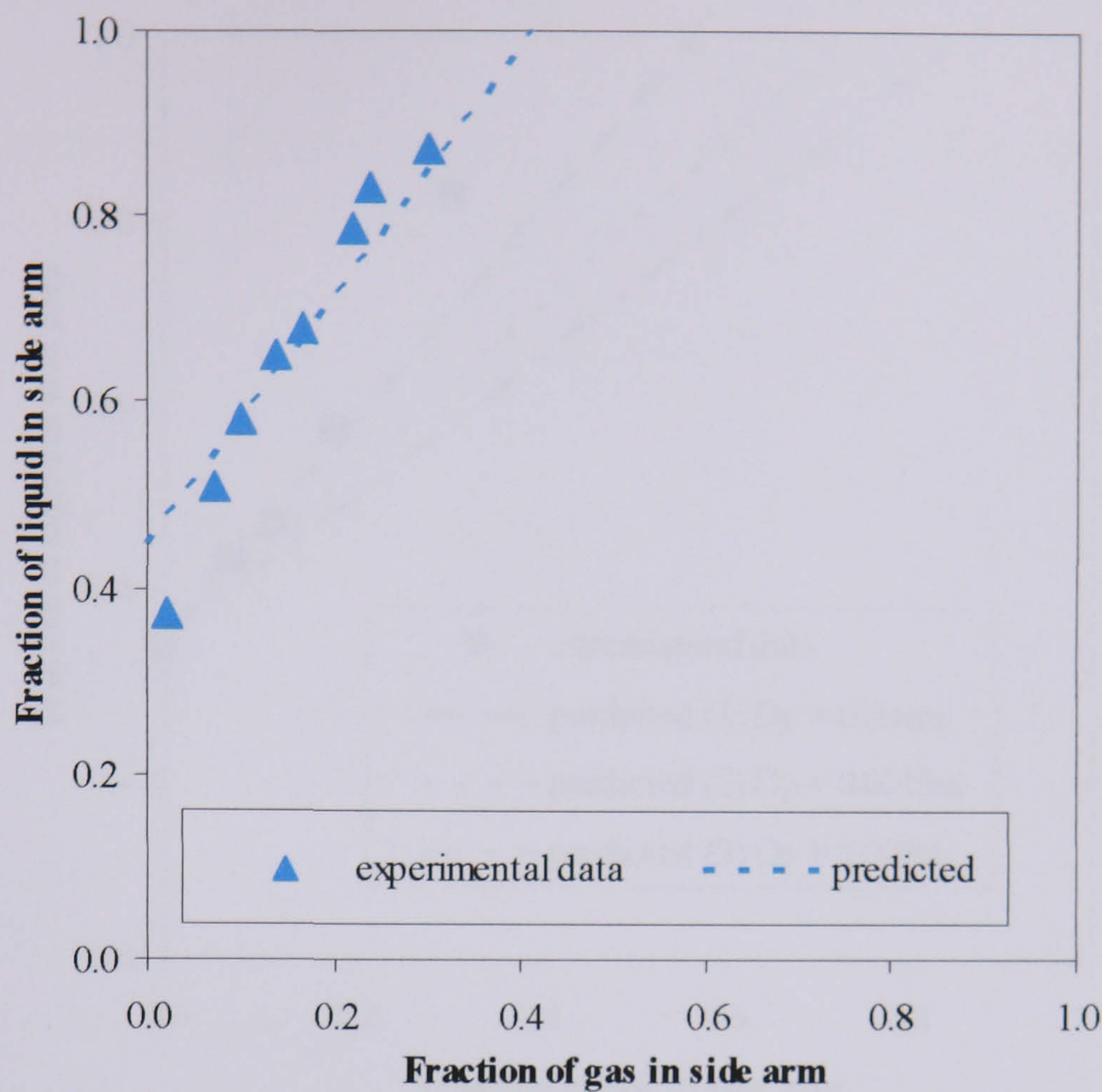


**Figure 7-15: Predicted phase split knowing  $L'_{onset}$  and  $G'_{crit}$  for  $U_{gs} = 10\text{m/s}$ ,  $U_{ls} = 0.434\text{m/s}$**

Using  $0.0015\text{m}$  as a standard particle diameter the critical gas take off for all liquid removed down the side arm,  $G'_{crit}$ , can be calculated. Figure 7-15 shows the predicted phase split for inlet conditions  $U_{gs} = 10\text{m/s}$  and  $U_{ls} = 0.434\text{m/s}$  by calculating  $L'_{onset}$  (from calculating the bubble rise velocity in the branch arm as described in Section 7.2.2) and  $G'_{crit}$  (from Equation 7-15). By using knowledge of the physics of the system the predicted phase split can be justified unlike the empirical manipulations presented in Figure 7-11.



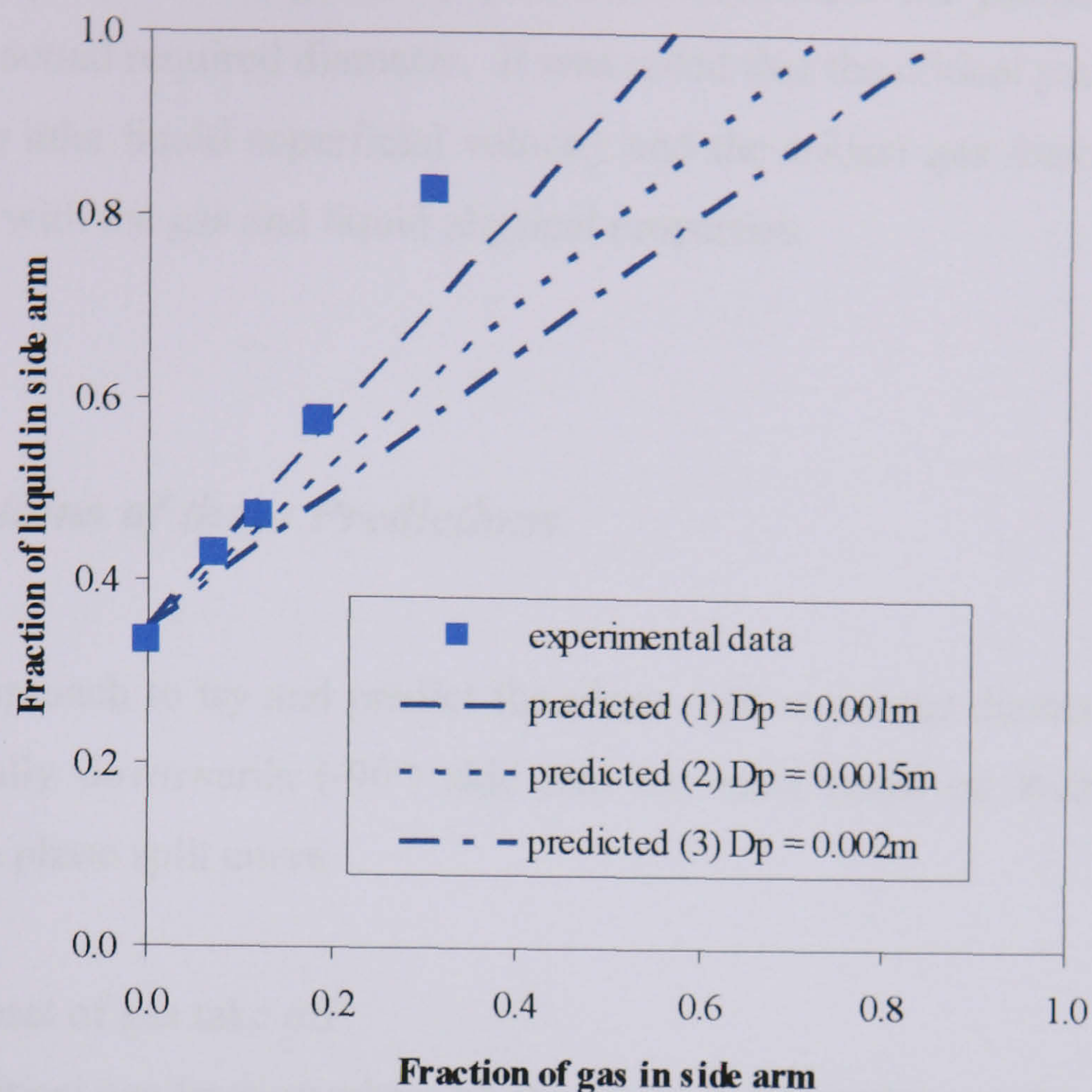


**Figure 7-16: Phase split predictions for different particle diameters,**  
 $U_{gs} = 6m/s$  and  $U_{gs} = 0.556m/s$

Unfortunately, this method of predicting the phase split is heavily dependant on the particle diameter used within Equation 7-15. Using the average particle diameter of 0.0015m may mean for some cases the value of  $G'_{crit}$  is heavily over predicted. For example for inlet conditions,  $U_{gs} = 6m/s$  and  $U_{ls} = 0.556m/s$  the particle diameter that best describes the parabolic motion and falls at the point  $x = D_3 = 0.127m$  is 0.00075m. Figure 7-16 shows the dependence on particle diameter for inlet conditions  $U_{gs} = 6m/s$  and  $U_{ls} = 0.556m/s$

predicted (1) uses particle diameter,  $D_p$  of 0.001m

predicted (2) uses particle diameter,  $D_p$  of 0.0015m

predicted (3) uses particle diameter,  $D_p$  of 0.002m



Thus the average particle diameter of 0.0015m will overpredict  $G'_{crit}$  as shown and the most accurate prediction is given by prediction (1) where the particle diameter is closest to the actual required diameter. It was noted that the critical particle diameter was related to inlet liquid superficial velocity and the critical gas fraction drawn off and may vary with the gas and liquid physical properties.

#### 7.4 Limitations of these Predictions

This initial approach to try and predict the phase split at a large diameter T-junction with a vertically downwards (-90°) side arm has been based on locating two key features of the phase split curve

1. The onset of gas take off
2. The critical gas fraction where all the liquid is diverted down the side arm

The onset of gas take off,  $L'_{onset}$  is found by determining the liquid fraction drawn through the side arm when the first gas is drawn through. It was seen to be reasonably predicted with reference to the terminal rise velocity of a single bubble through a column of liquid for both industrial situations and data collected under laboratory conditions. However, for both the current data and for that of Reimann *et al.* (1988) this method could not predict  $L'_{onset}$  for very low inlet liquid flowrates although it could be argued that industrial pipelines do not operate at such low velocities. The small break theory considered initially is very flow regime dependant and may only be considered for stratified flows.

From the onset of gas take off the gas is pulled through the liquid layer until a critical gas take off is reached,  $G'_{crit}$ , where all the liquid is diverted down the side arm, leaving a pure gas stream in the run arm. This point was predicted by considering a particle travelling at the height of the liquid interface and at the liquid interfacial velocity and falls with a parabolic motion downwards. The horizontal distance the particle travels is calculated considering its horizontal and vertical motion and at the

---



point where the horizontal distance travelled is equal to the side arm diameter, the critical gas take off is calculated.

The motion of the particle was found to be very dependent on the particle diameter and on the interfacial velocity. The interfacial velocity used within the prediction was based on the turbulent liquid-turbulent gas assumptions of Agrawal *et al.* (1973) where they assumed the velocity profile for the turbulent liquid followed the well established empirical one-seventh power law. This empirical correlation was easy to implement and gave reasonable results, especially for the higher inlet liquid flowrates considered here. However, for the low liquid inlet flowrates the calculated interfacial velocity does not give the particle enough horizontal momentum to travel across the opening of the branch arm, even at very low gas fractions drawn down the branch arm, as can be seen by Figure 7-17.

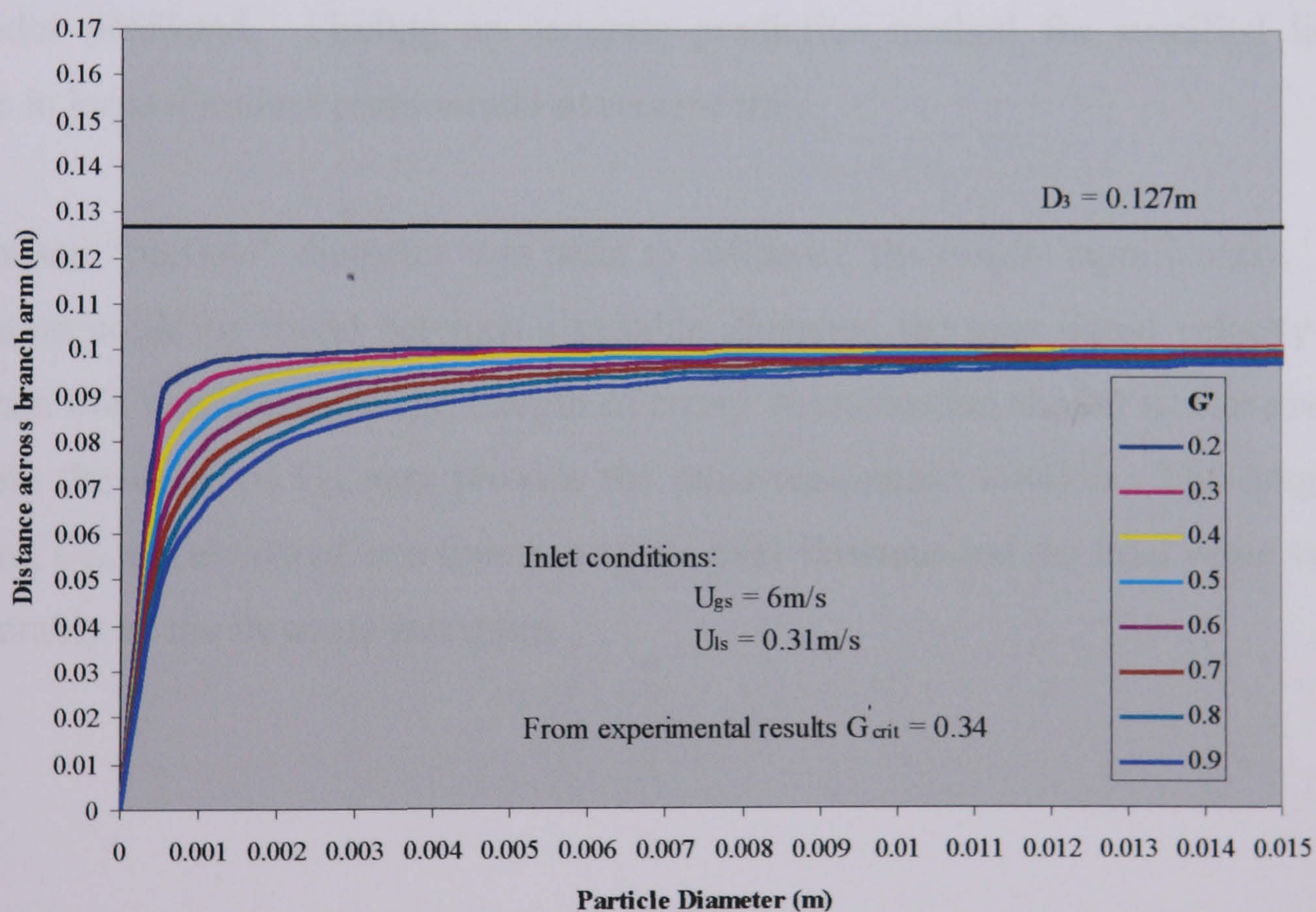


**Figure 7-17: Low liquid flow  $U_{gs} = 6\text{m/s}$**

This means, at these low interfacial velocities, not even the smallest particle diameter would provide a convergence between the fraction of gas drawn down the side arm,  $G'$  and the horizontal distance travelled across the branch arm.



An improvement in predicting a more accurate velocity profile may be found by considering the theoretical studies of horizontal stratified gas-liquid flow by Cheremisinoff and Davis (1979) or Shoham and Taitel (1984). Although both correlations claim to give reasonable results they are both very involved and lead the proposed theory away from being a quick and easy predictive method for calculating the phase split at a T-junction with a vertically downwards side arm.

As previously mentioned the above theory is also dependant on accurate liquid height predictions. The methodology of Taitel and Dukler (1976) was seen to under predict liquid height when applied to large diameter pipes at high liquid flowrates. Within this investigation liquid heights could be extrapolated from the measured heights published by Rea (1998) and so reasonable results could be obtained. If the methodology of Taitel and Dukler (1976) is applied within this theory then the results are under predicted. Finding an accurate predictive method for stratified liquid heights in large diameter pipes would overcome this.

The chosen “particle” diameter was seen to influence the results significantly. If a correlation could be found between a suitable diameter, the inlet liquid velocity and  $G'_{crit}$  then this would narrow the margin of error. A correlation similar to that used to calculate the value of  $C_D$  may provide the most reasonable solution. The drag coefficient,  $C_D$ , is calculated as a function of the inlet flowrate and the final value varies considerably as the flowrate increases.



## CHAPTER 8

### Conclusions and Further Work

#### *8.1 Final Considerations and Conclusions*

Within the present work, knowledge of the split of two-phase gas-liquid flows at a large diameter T-junction has been extended in several areas. Special consideration was given to the geometry of the T-junction with the aim of enhancing the phase separation qualities of the junction in a predictable manner. This would allow the simple T-junction to be used with confidence as a partial phase separator.

If the phase separation of the gas-liquid flows at a T-junction can be relied on then such partial phase separators require nominal maintenance, above that of general up keep and can therefore be placed in inaccessible sites, such as on sea beds or in remote geographical locations. In addition, the naturally low inventory of T-junctions makes them attractive phase separation alternatives where space is at a premium, for example on off-shore oil platforms, or in the handling of flammable fluids where the storage of large volumes can have serious safety implications.

Thus, with the above considerations in mind, attention was given to the effect of altering the side arm orientation of the regular 0.127m junction and the reduced 0.127-0.076m T-junction from the horizontal. The effects on gas and liquid take off were investigated with both stratified and annular flow and experimental trends were validated against previously published data for smaller diameter T-junctions.

From the knowledge gained from studying the phase split at a single junction the effect of using an insert was considered. Detailed experimentation highlighted specific cases where the inclusion of a simple insert protruding from the side arm into the main run pipe causes the junction to act as a partial phase separator and others



where the junction acted as an equal flow divider between the two outlets. An advance on single T-junction phase separation technology was also made by placing two T-junctions in series where significant improvement in the quality of the gas and liquid rich streams can be seen.

Particular attention has been given to the case of a horizontal T-junction with a vertically downwards side arm and to the predictive methods of defining the phase split at such a junction. The simple methods proposed have summarised the complicated mechanisms occurring and the results give good predictions.

Thus, the following conclusions can be drawn from the current investigation of the phase split at large diameter T-junctions.

- 1) The current air-water phase split experiments can be successfully compared with previously published data with similar void fractions taken in smaller diameter experimental facilities.
- 2) The phase separation qualities of a T-junction are very dependant on the flow regime approaching it, even for the large diameter junctions considered in this work.
- 3) Comparisons drawn between the regular and reduced T-junctions indicate that for all branch arm orientations there is no detrimental effect of using a reduced T-junction and in most cases it can enhance the phase separation qualities of the junction.
- 4) By introducing a simple insert at a horizontal junction the phase split can be enhanced or the junction can be made to act as a flow divider. Careful consideration is required before the instalment of such a device as the results were found to be very flow regime dependant.



- 5) Significant improvement can be made in side arm quality through branch arm orientation. With a vertically upwards side arm gas take off was found to be similar for different operating systems with similar inlet conditions. The limit of all gas take off was rarely found to be below 80% of high inlet liquid velocities.
- 6) With a downwards orientated side arm the onset of gas take off was seen to increase with reducing liquid inlet flowrate. This effect was diminished with the inclusion of a U-bend which further reduced gas take off.
- 7) Two T-junctions placed in series reduces the possibility of a hydraulic jump forming within the system thus a pure gas stream can be created for all inlet flow conditions. By combining the output of two branch arms total liquid extraction can be achieved with minimal gas take off or a high gas take off with minimal liquid removed.
- 8) The performance of two T-junctions placed in series was found to be more complex than the simple analysis of two single junctions. In addition, the two junction system was found to be more versatile and able to handle more liquid dominated inlet conditions with little detrimental affect to the phase split results.
- 9) Analytical interpretation of the phase split results of a single regular junction with a downwards side arm indicated that the split can be predicted by understanding the physical behaviour of the system at two key points. By determining the fraction of liquid where the onset of gas take off occurs and fraction of gas where complete liquid extraction is expected then the linear nature of the results can be predicted.
- 10) The onset of gas take off was found to be reasonably predicted by considering the bubble rise correlation of Peebles and Garber (1953). The analysis can be considered flow regime independent and was found to be applicable to other



system conditions and relevant to an industrially employed T-junction as a partial phase separator.

- 11) To determine the fraction of gas removed for complete liquid extraction the predicted method presented relied on providing an accurate gas-liquid interfacial velocity and a realistic film thickness value for the system. For large diameter pipes under consideration the methodology of Taitel and Dukler (1976) to calculate film thickness was found to under predict.
- 12) Evidence of a pressure reversal phenomena occurring at the large diameter T-junction with a downwards sidearm was collected.

## **8.2 *Future Work***

From this study of two-phase flow approaching large diameter T-junctions, knowledge of how junction geometry can effect the phase split has been augmented. However, the following recommendations for future work can be made.

- 1) In order to improve phase split predictions, current methods for calculating film thickness and interfacial phase velocity need extending to industrially relevant pipe diameters.
- 2) The phase split predictions presented have only been applied to the regular T-junction. Their application to reduced junctions needs consideration and verification.
- 3) The inclusion of a U-bend on the downwards side arm was found to reduce the fraction of gas taken over. Further investigation is required to gain a better understanding of how best to employ such a system. Detailed investigation should include altering the U-bend diameter, shape and distance from the



junction. Limited air supply in the present investigation prevented such in-depth analysis.

- 4) Pressure drop measurements across the junction should be carried out to complement the present data. These would be of interest for the phase split predictions and in determining the nature of the pressure reversal phenomena observed during experimentation.
- 5) Although the available database has been expanded by considering more industrially relevant pipe diameters, consideration should be paid to the use of more industrially relevant fluids. Investigating the effect of fluid properties (density, viscosity, surface tension), temperature and system pressure on the phase split would be invaluable.
- 6) The controllability of the two T-junction system should be further investigated. Over the lifetime of an oil field there will be considerable fluctuation in the production rates of the extracted oil and gas. This in turn will affect the flow pattern of the approaching fluids and it is known that the approaching flow pattern has a significant effect on the predicted phase split at a T-junction. In addition, movement of the valves on the outlet streams of the two T-junction system was shown to effect the quality of the flow. Thus, if the outlets of the two-T-junction system are to remain gas rich and liquid rich and the approaching flow pattern can be determined, then it would be possible to use the valves on the outlets as control valves and manage them in such a way to allow the quality of the separated streams to remain independent of the approaching flow pattern.



## Bibliography

- Adechy, D. and Issa, R. I., (1999), "Numerical modelling of horizontal annular flows", 2nd International Symposium on Two-Phase Flow Modelling and Experimentation, Pisa, Italy.
- Agrawal, S. S., Gregory, G. A., and Govier, G. W., (1973), "An analysis of horizontal stratified two phase flow in pipes", *Canadian Journal of Chemical Engineering*, Vol. 51, pp. 280-286.
- Anderson, J. L., (1987), "Steam/Water Entrainment and pull-through phenomena at a pipe branch", AIChE Annual Meeting, New York City.
- Arirachakaran, S., (1990), "Two-phase slug flow splitting phenomenon at a regular horizontal side-arm tee", *Ph. D. Thesis*, University of Tulsa, Tulsa, USA.
- Azzopardi, B. J., (1984), "The effect of the side arm diameter on the two-phase flow split at a T-junction", *International Journal of Multiphase Flow*, Vol. 10, No. 4, pp. 509-512.
- Azzopardi, B. J., (1988), "Measurements and observations of the spilt of annular flow at a vertical T-junction", *International Journal of Multiphase Flow*, Vol. 14, No. 6, pp. 701-710.
- Azzopardi, B. J., (1999), "Phase separation at T-junctions", *Multiphase Science and Technology*, Vol. 11, pp. 223-329.
- Azzopardi, B. J., Colman, D. A., and Fay, D., (2001), "Plant application of a T-junction as a partial phase separator", *Awaiting publication in International Journal of Multiphase Flow*, Vol.
- Azzopardi, B. J. and Hervieu, E., (1994), "Phase separation at T-junctions". *Multiphase Science and Technology*, Vol. 8, pp. 645-714.
-



- 
- Azzopardi, B. J. and Smith, P. J., (1992), "Two-phase flow split at T-junctions: Effect of side arm orientation and downstream geometry". *International Journal of Multiphase Flow*, Vol. 18, No. 6, pp. 861-875.
- Azzopardi, B. J., Wagstaff, D., Patrick, L., Memory, S. B. and Dowling, J.. (1988). "The split of two-phase flow at a horizontal T - Annular and stratified flow". UKAEA, Report AERE R 13059.
- Azzopardi, B. J. and Whalley, P. B., (1982), "The effect of flow patterns on two-phase flow in a T-junction", *International Journal of Multiphase Flow*, Vol. 8, No. 5, pp. 491-507.
- Baker, O., (1954), "Simultaneous flow of oil and gas", *Oil and Gas Journal*, Vol. 53, pp. 385-389.
- Ballyk, J. D. and Shoukri, M., (1990), "On the development of a model for predicting phase separation phenomena in dividing two-phase flow", *Nuclear Engineering and Design*, Vol. 123, pp. 67-75.
- Ballyk, J. D., Shoukri, M., and Peng, F., (1991), "The effect of branch size and orientation on two-phase annular flow in T-junctions with horizontal inlet", International Conference on Multiphase Flows, Tsukuba, Japan.
- Barnea, D., (1991), "Stability analysis of annular flow structure, using a discrete form of the "Two-Fluid Model"", *International Journal of Multiphase Flow*, Vol. 17, No. 6, pp. 705-716.
- Barnea, D., Shoham, O., Taitel, Y., and Dukler, A. E., (1985), "Gas-Liquid flow in inclined tubes: Flow pattern transitions for upward flow", *Chemical Engineer Science*, Vol. 40, No. 1, pp. 131-136.
- Barnea, D. and Taitel, Y., (1985), "Flow pattern transition in two-phase gas-liquid flows", *Encyclopaedia of Fluid Mechanics*, Vol. 2, Chap. 16, Gulf Publishing Company, Houston, Texas.
-



- Bevilacqua, M., Giacchetta, G., and Nielsen, K. L., (2000), "Two-phase liquid gas separation with a new conception comb separator", 7th International Conference of Multiphase Flow in Industrial Plants, Bologna, Italy.
- Buell, J. R., Soliman, H. M., and Sims, G. E., (1994), "Two-phase pressure drop and phase distribution at a horizontal T-junction", *International Journal of Multiphase Flow*, Vol. 20, No. 5, pp. 819-836.
- Butterworth, D., (1980), "Unresolved problems in heat exchanger design", Interflow '80 - The Fluid Handling Conference, Harrogate, England.
- Celata, G. P., Cumo, M., Francesco, D., and Tomiyama, A., (2001), "Terminal bubble rising velocity in one-component systems", 39th European Two-Phase Flow Group Meeting, Aveiro, Portugal.
- Charron, Y. and Whalley, P. B., (1995), "Gas-liquid annular flow at a vertical T-junction - Part I: Flow separation", *International Journal of Multiphase Flow*, Vol. 21, No. 4, pp. 569-589.
- Collier, J. G., (1976), "Single-phase and two-phase flow behaviour in primary circuit components", NATO Advanced Study Institute on Two-Phase Flow & Heat Transfer, Report
- Coney, M. W. E., (1980), "Two-Phase flow distribution in a manifold system", European Two-Phase Flow Group Meeting, Glasgow, Scotland.
- Conte, G., (2000), "An experimental study for the characteristics of gas/liquid flow splitting at T-junctions", *Ph. D. Thesis*, University of Nottingham, Nottingham, England.
- Davies, E and Watson, P., (1979), "Miniaturised separators for offshore platforms", 1st New Technology for Exploration and Exploitation of Oil and Gas Reserves Symposium, Luxembourg.
- Domasnki, R., Reimann, J., and Muller, U., (1987), "Phase redistribution and pressure drop in T-junctions with different diameter ratios", European Two-Phase Flow Group Meeting, Trondheim, Norway.
-



- 
- Eaton, B. A., Andrews, D. E., Knowles, C. R., Silberberg, I. H., and Brown, K. E., (1967), "The Prediction of flow patterns liquid holdup and pressure losses occurring during continuous two-phase flow in horizontal pipelines", *Journal of Petroleum Technology*, Vol. June, pp. 815-828.
- Evans, G. M. and Jameson, G. J., (1995), "Hydrodynamics of a plunging liquid jet bubble column", *Trans I ChemE*, Vol. 73, No. A, pp. 679-684.
- Fouda, A. E. and Rhodes, E., (1974), "Two-phase annular flow stream division in a simple Tee", *Transactions of the Institute of Chemical Engineers*, Vol. 52, pp. 354-360.
- Fryar, J. R., (1980), "Options are available for pipeline and compressor-station drip design", *Oil and Gas Journal*, Vol. March, pp. 154-161.
- Gardel, A., (1957), "Les pertes de charge dans les écoulements au travers de branchements en tee", *Bulletin Technique de la Suisse Romande*, Vol. 25, pp. 363-391.
- Haberman, W. L. and Morton, R. K., (1953), "David W Taylor Model Basin", Report 802.
- Hart, J., Hamersma, P. J., and Fortuin, J. M. H., (1991), "A model for predicting liquid route preference during gas-liquid flow through horizontal branched pipelines", *Chemical Engineering Science*, Vol. 46, No. 7, pp. 1609-1622.
- Henry, J. A. R., (1981), "Dividing annular flow in a horizontal Tee", *International Journal of Multiphase Flow*, Vol. 7, No. 3, pp. 343-355.
- Hewitt, G. F., Gill, L. E., Roberts, D. N., and Azzopardi, B. J., (1990), "The split of low inlet quality gas-liquid flow at a vertical T - Experimental data", UKAEA, Report AERE M3801.
- Holt, A., (1996), "Two-phase pressure drop and void fraction in narrow channels". *Ph. D. Thesis*, University of Nottingham, Nottingham, England.
-



- 
- Hong, K. C., (1978), "Two-phase flow splitting at a pipe tee", *Journal of Petroleum Technology*, Vol. 2, pp. 290-296.
- Hwang, S. T., Soliman, H. M., and Lahey, R. T., (1988), "Phase separation in dividing two-phase flows", *International Journal of Multiphase Flow*, Vol. 14, No. 4, pp. 439-458.
- Issa, R. I and Olivera, P. J., (1994), "Numerical prediction of phase separation in two-phase flow through T-junctions", *Computer Fluids*, Vol. 23, pp. 347-372.
- Katsaounis, A., Papanikas, D. G., Fertis, D. K., and Margaris, D. P., (1997), "Dynamic T-junction separator for multiphase transport pipelines", 4th World Conference on Experimental Heat Transfer, Fluid Mechanics and Thermodynamics, Brussels.
- Katsaounis, A. and Schultheiss, G. F., (1987), "Diverging two-phase flow patterns in a T-junction and their influence on the form-resistance pressure drop", 23rd National Heat Transfer Conference, Denver, Colorado.
- Kawaji, M., Muhammad, A., Ciastek, A., and Lorencez, C., (1995), "Study of liquid flow structure in horizontal co-current gas-liquid slug flow", National Heat Conference, Portland, Ontario.
- Kolnes, J. and Asheim, H., (1990), "New offshore slug catcher design", International Conference on Basic Principles and Industrial Applications of Multiphase Flow, London, England.
- Kvernvold, O., Vindoy, V., Sontvedt, T., Saasen, A., and Selmer-Olsen, S., (1984), "Velocity distribution in horizontal slug flow", *International Journal of Multiphase Flow*, Vol. 10, No. 4, pp. 441-457.
- Lahey, R. T., (1990), "The analysis of phase separation and phase distribution phenomena using two-fluid models", *Nuclear Engineering and Design*, Vol. 122, pp. 17-40.
- Lahey, R. T., (1986), "Current understanding of phase separation mechanisms in branching conduits", *Nuclear Engineering and Design*, Vol. 95, pp. 145-161.
-



- 
- Lahey, R. T. and Drew, D. A., (1992), "On the development of multidimensional two-fluid models for vapour-liquid two-phase flows". *Chemical Engineering Communication*, Vol. 118, pp. 125-139.
- Ma Y. P., Pei, B. S., Lin, W. K., and Hsu, Y. Y., (1990), "Analysis of a fluid-mechanic model of a horizontal T-junction", *Heat Transfer and Fluid Flow*, Vol. 92, pp. 134-140.
- Maciaszek, T. and Momponteil, A., (1986), "Experimental study on phase separation in a T-junction for steam-water stratified inlet flow". European Two-Phase Flow Group Meeting, Munich, Germany.
- Maciaszek, T. and Micaelli, J. C., (1988), "A phase separation model for T-junctions application to a PWR safety code", National Heat Transfer Conference, Houston, Texas.
- Mandhane, J. M., Gregory, G. A., and Aziz, K., (1974), "A flow pattern map for gas-liquid flow in horizontal pipes", *International Journal of Multiphase Flow*, Vol. 1, pp. 537-553.
- Marti, S. and Shoham, O., (1997), "A unified model for stratified-wavy two-phase flow splitting at a reduced T-junction with an inclined branch arm", *International Journal of Multiphase Flow*, Vol. 23, No. 4, pp. 725-748.
- McCreery, G. E., (1984), "A correlation for phase separation in a tee", *Multiphase Flow and Heat Transfer III, Part B: Applications*, Editors Veriroglu, T. N. and Bergles, A. E., Elsevier Science Publications, Amsterdam, pp165-178.
- McCreery, G. E. and Banerjee, S., (1990), "Phase separation of dispersed mist and dispersed annular (rivulet or thin film) flow in a tee - Part I", *International Journal of Multiphase Flow*, Vol. 16, No. 3, pp. 429-445.
- McNown, J. S., (1954), "Mechanics of manifold flow", *Transactions of the American Society of Civil Engineers*, Vol. 119, pp. 1103-1142.
-



- 
- Mudde, R. F., Groen, J. S., and van den Akker, H. E. A., (1993), "Two-phase flow redistribution phenomena in a large diameter T-junction", *International Journal of Multiphase Flow*, Vol. 19, No. 4, pp. 563-573.
- Muller, U. and Reimann, J., (1991), "Redistribution of two-phase flow in branching conduits: A survey", International Conference Multiphase Flows, Tsukuba, Japan.
- Oranje, L., (1983), "Handling two-phase gas", *Oil and Gas Journal*, Vol. April, pp. 103-142.
- Ottens, M., Hoefsloot, H. C. J., and Hamersma, P. J., (1999), "Effect of small branch inclination on gas-liquid flow separation in T-junctions", *AIChE Journal*, Vol. 45, No. 3, pp. 465-474.
- Peebles, F. N. and Garber, H. J., (1953), "Studies on the motion of gas bubbles in liquids", *Chemical Engineering Progress*, Vol. 49, No. 2, pp. 88-97.
- Peng, F. and Shoukri, M., (1997), "Modelling of phase redistribution of horizontal annular flow divided in T-junctions", *Canadian Journal of Chemical Engineering*, Vol. 75, pp. 264-270.
- Peng, F., Shoukri, M., and Ballyk, J. D., (1998), "An experimental investigation of stratified steam-water flow in T-junctions", 3rd International Conference on Multiphase Flow, Lyon, France.
- Peng, F., Shoukri, M., and Chan, A., (1993), "Annular flow in T-junctions with horizontal inlet and downwardly inclined branches", *ASME - FED Gas-Liquid Flows*, Vol. 165, pp. 13-24.
- Peng, F., Shoukri, M., and Chan, A., (1996), "Effect of branch orientation on annular two-phase flow in T-junctions", *Transactions of the ASME*, Vol. 118, pp. 166-171.
- Penmatcha, V. R., Ashton, P. J., and Shoham, O., (1996), "Two-phase stratified flow splitting at a T-junction with an inclined branch arm", *International Journal of Multiphase Flow*, Vol. 22, No. 6, pp. 1105-1122.
-



- 
- Premoli, A., Francesco, D., and Prina, A., (1970). "An empirical correlation for evaluating two-phase mixture density under adiabatic conditions". European Two-Phase Flow Group Meeting.
- Rea, S., (1998), "Stratified flow at T-junctions", *Ph. D. Thesis*, University of Nottingham, Nottingham, England.
- Reimann, J., Brinkmann, H. J., and Domanski, R., (1988), "Gas-Liquid flow in dividing T-junctions with a horizontal inlet and different branch orientations and diameters", Kernforschungszentrum Karlsruhe, Institut für Reaktorbauelemente, Report KfK 4399.
- Reimann, J. and Khan, M., (1983), "Flow through a small break at the bottom of a large pipe with stratified flow", 2nd International Topical Meeting on Nuclear Reactor Thermohydraulics, Santa Barbara, California.
- Reimann, J. and Khan, M., (1982), "Flow through a small pipe at the bottom of a large pipe with stratified flow", Annual Meeting of the European Two-Phase Flow Group, Paris, France.
- Roberts, P. A., (1995), "Two-phase flow at T-junctions", *Ph. D. Thesis*, University of Nottingham, Nottingham, England.
- Saba, N. and Lahey, R. T., (1984), "The analysis of phase separation phenomena in branching conduits", *International Journal of Multiphase Flow*, Vol. 10, No. 1, pp. 1-20.
- Scott, S. L., Shoham, O., and Brill, J. P., (1987), "Modelling slug growth in large diameter pipes", 3rd International Conference on Multiphase Flow, The Hague, Netherlands.
- Seeger, W., Reimann, J., and Muller, U., (1986), "Two-phase flow in a T-junction with a horizontal inlet. Part I: Phase separation", *International Journal of Multiphase Flow*, Vol. 12, No. 4, pp. 575-585.
- Sharma, S., Lewis, S., and Kojasoy, G., (1998), "Local studies in horizontal gas-liquid slug flow", *Nuclear Engineering and Design*, Vol. 184, pp. 305-318.
-



- Shoham, O., Arirachakaran, S., and Brill, J. P., (1989). "Two-phase flow splitting in a horizontal reduced pipe tee", *Chemical Engineering Science*, Vol. 44, No. 10, pp. 2388-2391.
- Shoham, O., Brill, J. P., and Taitel, Y., (1987), "Two-phase flow splitting in a T-junction - experimental and modelling", *Chemical Engineering Science*, Vol. 42, No. 11, pp. 2667-2676.
- Smith, P. A. and Azzopardi, B. J., (1990), "The split of two-phase flow at a T-junction with a horizontal main tube and a vertically upward side arm". UKAEA, Report AERE R 13721.
- Smoglie, C., Reimann, J., and Muller, U., (1985). "Two-phase flow through small breaks in a horizontal pipe with stratified flow", 3rd International Topical Meeting on Reactor Thermal Hydraulics, Newport, Rhode Island, USA.
- Taitel, Y. and Dukler A.E., (1976), "A model for predicting flow regime transitions in horizontal and near horizontal gas-liquid flow", *AIChE Journal*, Vol. 22, No. 1, pp. 47-55.
- Tomiyama, A., Celata, G. P., Hosokawa, S., and Yoshida, S., (2001), "Terminal velocity of single bubbles in surface tension force dominant regime", 39th European Two-phase Flow Group Meeting, Aveiro, Portugal.
- Walters, L. C., Soliman, H. M., and Sims, G. E., (1998), "Two-phase pressure drop and phase distribution at reduced T-junctions", *International Journal of Multiphase Flow*, Vol. 24, pp. 775-792.
- Whalley, P. B. and Azzopardi, B. J., (1980), "Two-phase flow in a T-junction". UKAEA, Report AERE R 9699.



## Nomenclature

$A$	cross-sectional area of pipe	$m^2$
$C_D$	drag coefficient	
$d$	break diameter	$m$
$D$	pipe diameter	$m$
$D_p$	particle diameter	$m$
$Fr$	Froude Number $(V^2/gD)$	
$G$	mass flux	$kg/m^2 \text{ s}$
$G'$	fraction of inlet gas drawn down the branch arm	
$G'_{crit}$	fraction of inlet gas drawn down branch arm at total liquid removal	
$g$	acceleration due to gravity	$m/s^2$
$h$	stratified liquid level height	$m$
$h_{bge}$	height at the beginning of gas entrainment	$m$
$K$	constant in Equation 7-3	
$L'$	fraction of inlet liquid drawn down the branch arm	
$L'_{onset}$	fraction of inlet liquid drawn down branch arm at the onset of gas take off	
$\dot{m}$	mass flowrate	$kg/s$
$n$	constant in Equation 7-3	
$P$	pressure	$Pa$
$\bar{P}$	average pressure $((P_1 - P_2)/2)$	$Pa$
$Q$	volumetric flowrate	$m^3/s$
$R_b$	equivalent bubble radius	$m$
$Re_b$	gas bubble Reynolds number $(2\rho_L V_\infty R_b/\mu_L)$	
$t$	time	$s$
$U_G$	superficial gas velocity	$m/s$
$U_L$	superficial liquid velocity	$m/s$
$V_G$	gas velocity	$m/s$
$V_L$	liquid velocity	$m/s$



$V_{LH}$	liquid velocity at gas-liquid interface	m s
$V_{\infty}$	terminal bubble rise velocity	m/s
$x$	distance in the horizontal plane	m
$y$	distance in the vertical plane	m
$\mu$	viscosity	kg/m s
$\rho$	density	kg/m <sup>3</sup>
$\sigma$	surface tension	N/m

Subscripts

G	gas
L	liquid
1	inlet
2	run arm
3	branch arm



# APPENDIX A

## Error Analysis and Data Obtained from Experimental Results

### *A.1 Error Analysis*

Measurements for all the phase split data were only noted when the error in the air mass balance was within 10% and the error in the water mass balance was within 5%. Given below is a brief analysis for a randomly selected phase split result for the regular 0.127m diameter T-junction with a downwards side arm with both the run and branch arm butterfly valves left open. This point generally represents the mid-point of a set of results and thus was chosen. For this case, the inlet gas superficial velocity,  $U_{gs}$ , is 8m/s and the inlet liquid superficial velocity,  $U_{ls}$ , is 0.186m/s. Errors in all cases were kept to a minimum by taking an average of several readings before noting the final value. The final overall error in both the fraction of liquid diverted down the branch arm ( $L'$ ) and the fraction of gas diverted ( $G'$ ) were found to be 5% and 6% and this was found to be consistent for other randomly selected phase split results.

#### *Error analysis on the air mass balance*

##### *Inlet air flowrate:*

Error in reading a manometer is  $\pm 0.5\text{mm}$  and the average combined error in reading a manometer can be given as,  $E = \sqrt{e_1^2 + e_2^2} = \sqrt{0.5^2 + 0.5^2} = 0.7\text{mm}$ .

For the inlet flow, average manometer reading was  $221 \pm 0.7\text{mmH}_2\text{O}$ , giving an inlet flow of  $8.01 \pm 0.01\text{m/s}$ .



*Outlet air flowrate:*

For run arm, average manometer reading was  $228 \pm 0.7 \text{ mmH}_2\text{O}$  giving a flowrate of  $6.37 \pm 0.01 \text{ m/s}$ .

For branch arm, average manometer reading was  $152 \pm 0.7 \text{ mmH}_2\text{O}$  giving a flowrate of  $1.91 \pm 0.01 \text{ m/s}$ .

*Overall Mass Balance and Error in  $G'$ :*

Thus, overall measured outlet air mass balance is  $8.28 \pm 0.14 \text{ m/s}$ , falling within the 10% margin stated as being acceptable for the results to be noted.

Overall error in  $G'$ , fraction of gas diverted down the branch arm is  $0.231 \pm 0.014$  (6% error).

*Error analysis on the water mass balance*

Error in reading stop clock:  $\pm 0.5 \text{ s}$

Error in measuring mass flow from cyclone to weigh tank:  $\pm 0.1 \text{ kg}$

Error in measuring rise in height of liquid in separator tank:  $\pm 0.5 \text{ mm}$

Error in reading inlet turbine meter:  $\pm 1$  gallons per minute

*Inlet water flowrate:*

Turbine meter reading indicated  $30 \pm 1 \text{ IGPM}$  which gives a mass flowrate of  $2.35 \pm 0.08 \text{ kg/s}$

*Outlet water flowrate:*

Average mass water collected from run arm in weigh tank  $2.4 \pm 0.1 \text{ kg}$  within  $128 \pm 0.5 \text{ s}$  giving a combined error in the mass flowrate of  $0.018 \pm 0.001 \text{ kg/s}$ .

Average rise in water in separating tank from branch arm was  $380 \pm 0.5 \text{ mm}$  within  $128 \pm 0.5 \text{ s}$ , giving a combined error in the mass flowrate of  $2.33 \pm 0.02 \text{ kg/s}$ .



*Overall mass balance and Error in L':*

Thus, overall outlet water mass balance is  $2.35 \pm 0.09$  kg/s which when compared to the inlet flowrate of  $2.34 \pm 0.08$  kg/s, is within the 5% margin that was acceptable for the results to be noted.

Overall error in L', the fraction of water diverted down the branch arm, is  $0.99 \pm 0.05$  (5% error).

*Reference Books:*

Pentz, M. and Shott, M., (1989), "*Handling Experimental Data*", Editor Aprahamian, F., Open University Press, Milton Keynes.

Taylor, J. R., (1997), "*An Introduction to Error Analysis. The Study of Uncertainties in Physical Measurements*", Second Edition, University Science Books, Sausalito, CA.



## A.2 Data Obtained from Experimental Results

To predict the phase split at a regular 0.127m T-junction with a vertically downwards (-90°) side arm the following data was required.

The following values of  $L'_{onset}$  and  $G'_{crit}$  were determined from the experimental data tabulated in Appendix B, Table B4 and have been used within Chapter 7.

**Table A-1: Values of  $L'_{onset}$  and  $G'_{crit}$  for the regular T-junction with a vertically downwards (-90°) side arm**

$U_{gs}$ (m/s)	$U_{ls}$ (m/s)	$L'_{onset}$	$G'_{crit}$
12	0.434	0.38	0.35
	0.310	0.51	0.32
	0.186	0.70	0.28
10	0.434	0.33	0.32
	0.310	0.50	0.32
	0.186	0.78	0.22
8	0.556	0.31	0.42
	0.434	0.40	0.43
	0.186	0.87	0.23
6	0.556	0.33	0.42
	0.434	0.42	0.35
	0.310	0.66	0.31
	0.186	0.98	0.23

The method presented in Chapter 7 to predict the fraction of gas when all the liquid is diverted down the side arm,  $G'_{crit}$  required accurate film thickness values. These were extrapolated from the values measured by Rea (1998) for the current experimental conditions. In the figures below the solid points represent film thicknesses measured by Rea (1998) and the hollow points are film heights extrapolated from the surrounding data.



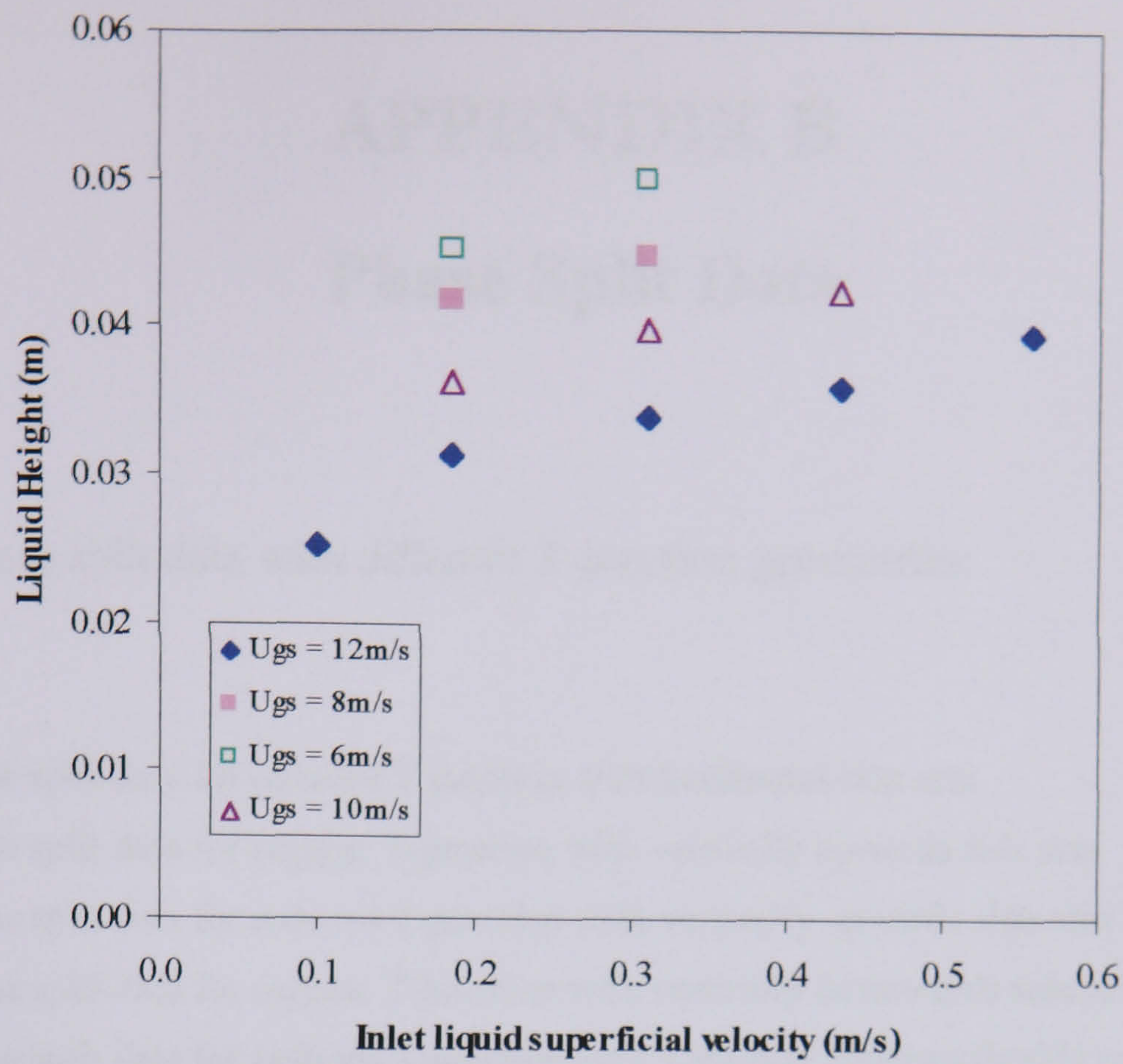


Figure A-1: Variation of liquid height,  $h$  with inlet liquid superficial velocity (m/s)

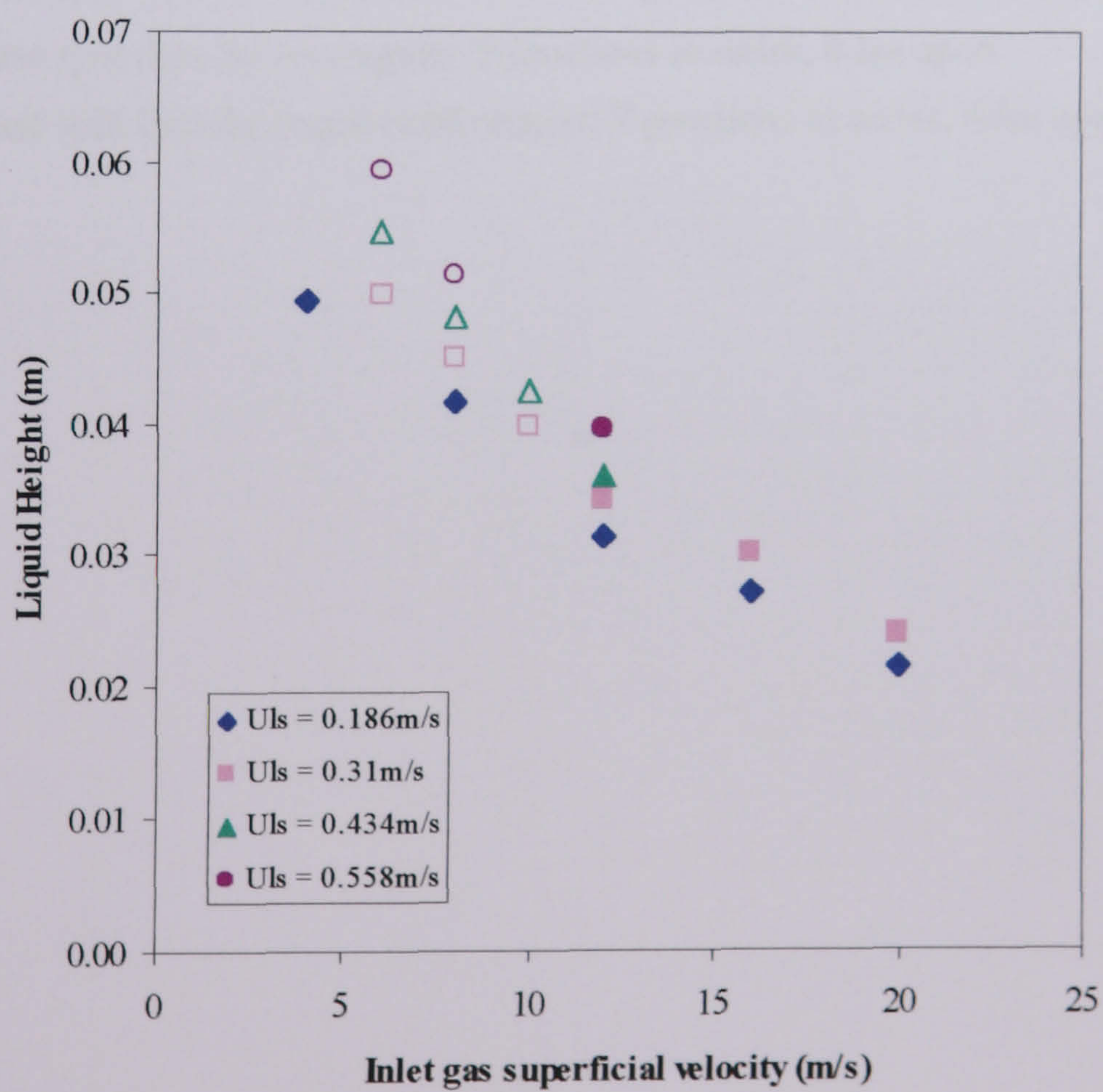


Figure A-2: Variation of liquid height,  $h$  with inlet gas superficial velocity (m/s)



**APPENDIX B**

**Phase Split Data**

Air/Water phase split data with different T-junction geometries:

Table B1: Phase split data for reduced T-junction with horizontal side arm	B2
Table B2: Phase split data for regular T-junction with vertically upwards side arm	B4
Table B3: Phase split data for reduced T-junction with vertically upwards side arm	B6
Table B4: Phase split data for regular T-junction with vertically downwards side arm	B7
Table B5: Phase split data for reduced T-junction with vertically downwards side arm	B10
Table B6: Phase split data for horizontal T-junctions with inserts	B14
Table B7: Phase split data for regular T-junction with downwards side arm and U-bend	B18
Table B8: Phase split data for reduced T-junction with downwards side arm and U-bend	B19
Table B9: Phase split data for two regular T-junctions in series, 1.2m apart	B20
Table B10: Phase split data for regular and reduced T-junctions in series, 1.2m apart	B23
Table B11: Phase split data for two regular T-junctions in series, 0.5m apart	B26
Table B12: Phase split data for regular and reduced T-junctions in series, 0.5m apart	B29



**Table B1: Phase split data for reduced T-junction with horizontal side arm**

U <sub>gs</sub> (m/s)	U <sub>ls</sub> (m/s)	D <sub>3</sub> / D <sub>1</sub>	Geometry	G'	L'
24	0.0283	0.6	0°	0.114	0.023
				0.171	0.037
				0.224	0.058
				0.319	0.128
24	0.0401	0.6	0°	0.112	0.013
				0.168	0.033
				0.205	0.051
				0.257	0.063
				0.322	0.108
				0.402	0.185
24	0.0535	0.6	0°	0.111	0.012
				0.162	0.032
				0.211	0.053
				0.289	0.077
				0.338	0.115
				0.407	0.160
12	0.0283	0.6	0°	0.204	0.000
				0.362	0.004
				0.476	0.062
				0.517	0.076
				0.615	0.138
				0.794	0.256
				0.889	0.729
12	0.0401	0.6	0°	0.250	0.000
				0.360	0.010
				0.468	0.070
				0.513	0.083
				0.619	0.147
				0.816	0.388
				0.877	0.589
				1.000	1.000
12	0.0535	0.6	0°	0.209	0.000
				0.359	0.014
				0.461	0.071
				0.514	0.101
				0.628	0.160
				0.812	0.424
				0.885	0.742
12	0.31	0.6	0°	0.232	0.018
				0.350	0.028
				0.458	0.045
				0.639	0.056
				0.810	0.076



**Table B1: continued**

Ugs (m/s)	Uls (m/s)	D <sub>3</sub> / D <sub>1</sub>	Geometry	G'	L'
4	0.31	0.6	0°	0.108	0.020
				0.465	0.025
				0.513	0.038
				0.606	0.050
				0.823	0.275
				1.000	0.542
4	0.434	0.6	0°	0.000	0.000
				0.161	0.022
				0.476	0.037
				0.537	0.046
				0.573	0.051
				0.741	0.053
				0.825	0.320
				1.000	0.818
4	0.558	0.6	0°	0.000	0.000
				0.151	0.017
				0.507	0.028
				0.556	0.038
				0.562	0.032
				0.815	0.070
				0.869	0.391
				1.000	0.930



**Table B2: Phase split data for regular T-junction with vertically upwards side arm**

Ugs (m/s)	Uls (m/s)	D <sub>3</sub> / D <sub>1</sub>	Geometry	G'	L'
24	0.0283	1	+90°	0.450	0.000
				0.640	0.000
				0.830	0.000
				0.940	0.020
				0.960	0.370
				0.960	0.810
24	0.0401	1	+90°	0.450	0.000
				0.630	0.000
				0.850	0.000
				0.880	0.010
				0.980	0.470
				0.980	0.980
24	0.0535	1	+90°	0.460	0.000
				0.640	0.000
				0.830	0.000
				0.960	0.160
				0.960	0.620
				0.960	1.000
12	0.0283	1	+90°	0.520	0.000
				0.630	0.000
				0.840	0.000
				0.890	0.000
				0.930	0.020
				0.930	0.960
12	0.0401	1	+90°	0.480	0.000
				0.530	0.000
				0.630	0.000
				0.780	0.000
				0.910	0.190
				0.920	0.970
12	0.0535	1	+90°	0.480	0.000
				0.530	0.000
				0.630	0.000
				0.780	0.000
				0.910	0.190
				0.920	0.970



**Table B2: continued**

Ugs (m/s)	Uls (m/s)	D <sub>3</sub> / D <sub>1</sub>	Geometry	G'	L'
8	0.31	1	+90°	0.522	0.000
				0.705	0.000
				0.807	0.000
				1.000	0.128
4	0.186	1	+90°	0.502	0.000
				0.517	0.000
				0.571	0.000
				0.729	0.000
				1.000	0.316
4	0.31	1	+90°	0.538	0.000
				0.626	0.000
				0.905	0.000
				1.000	0.311
4	0.434	1	+90°	0.539	0.000
				0.662	0.000
				0.754	0.000
				1.000	0.127
4	0.558	1	+90°	0.551	0.000
				0.714	0.000
				0.871	0.000
				1.000	0.089



**Table B3: Phase split data for reduced T-junction with vertically upwards side arm**

U <sub>gs</sub> (m/s)	U <sub>ls</sub> (m/s)	D <sub>3</sub> / D <sub>1</sub>	Geometry	G'	L'
24	0.0283	0.6	+90°	0.070	0.000
				0.152	0.000
				0.285	0.000
				0.499	0.002
24	0.0401	0.6	+90°	0.065	0.000
				0.155	0.000
				0.288	0.002
				0.535	0.005
24	0.0535	0.6	+90°	0.069	0.000
				0.158	0.000
				0.295	0.001
				0.494	0.002
12	0.0283	0.6	+90°	0.360	0.000
				0.475	0.000
				0.511	0.000
				0.617	0.000
				0.828	0.000
				0.914	0.223
12	0.0401	0.6	+90°	0.329	0.000
				0.466	0.000
				0.502	0.000
				0.617	0.000
				0.804	0.000
				0.861	0.339
12	0.0535	0.6	+90°	0.328	0.000
				0.470	0.000
				0.511	0.000
				0.629	0.000
				0.851	0.000
				0.918	0.186
4	0.434	0.6	+90°	0.000	0.000
				0.537	0.000
				0.584	0.000
				0.724	0.000
				0.875	0.000
				1.000	0.169
4	0.558	0.6	+90°	0.000	0.000
				0.000	0.000
				0.567	0.000
				0.628	0.000
				0.870	0.000
				1.000	0.182



**Table B4: Phase split data for regular T-junction with vertically downwards side arm**

U <sub>gs</sub> (m/s)	U <sub>ls</sub> (m/s)	D <sub>3</sub> / D <sub>1</sub>	Geometry	G'	L'
12	0.186	1	-90°	0.210	0.897
				0.320	0.993
				0.679	0.993
				0.194	0.923
				0.101	0.808
				0.054	0.783
				0.138	0.877
				0.111	0.860
				0.085	0.811
12	0.31	1	-90°	0.000	0.464
				0.084	0.638
				0.137	0.721
				0.175	0.812
				0.177	0.796
				0.311	0.956
12	0.434	1	-90°	0.029	0.408
				0.085	0.548
				0.133	0.628
				0.167	0.692
				0.280	0.882
10	0.186	1	-90°	0.017	0.797
				0.086	0.865
				0.141	0.966
				0.185	0.983
				0.185	0.971
				0.313	0.999
10	0.31	1	-90°	0.000	0.497
				0.068	0.621
				0.110	0.722
				0.175	0.792
				0.177	0.798
				0.241	0.875
				0.321	0.955
10	0.434	1	-90°	0.023	0.374
				0.074	0.510
				0.102	0.582
				0.137	0.653
				0.166	0.679
				0.221	0.786
				0.239	0.833
				0.303	0.875



**Table B4: continued**

Ugs (m/s)	Uls (m/s)	D <sub>3</sub> / D <sub>1</sub>	Geometry	G'	L'
8	0.0283	1	-90°	0.000	1.000
				0.103	1.000
				0.255	1.000
8	0.0401	1	-90°	0.253	1.000
				0.144	1.000
				0.000	1.000
8	0.0535	1	-90°	0.000	1.000
				0.142	1.000
				0.252	1.000
8	0.136	1	-90°	0.239	0.999
				0.111	0.996
				0.000	0.988
8	0.186	1	-90°	0.000	0.867
				0.099	0.913
				0.200	0.986
				0.228	0.993
				0.231	0.992
				0.326	1.000
8	0.31	1	-90°	0.022	0.653
				0.129	0.769
				0.222	0.854
				0.225	0.852
				0.332	0.970
				0.471	1.000
8	0.434	1	-90°	0.000	0.397
				0.083	0.495
				0.125	0.551
				0.201	0.670
				0.203	0.662
				0.331	0.856
8	0.558	1	-90°	0.000	0.309
				0.122	0.493
				0.195	0.604
				0.200	0.622
				0.305	0.832
6	0.136	1	-90°	0.000	0.995
				0.140	1.000
				0.229	1.000



**Table B4: continued**

<b>U<sub>gs</sub> (m/s)</b>	<b>U<sub>ls</sub> (m/s)</b>	<b>D<sub>3</sub> / D<sub>1</sub></b>	<b>Geometry</b>	<b>G'</b>	<b>L'</b>
6	0.186	1	-90°	0.000	0.976
				0.152	0.998
				0.241	0.998
				0.245	1.000
6	0.31	1	-90°	0.044	0.720
				0.091	0.761
				0.206	0.840
				0.211	0.828
				0.311	0.976
				0.455	0.997
6	0.434	1	-90°	0.000	0.468
				0.028	0.481
				0.065	0.516
				0.102	0.562
				0.113	0.585
				0.179	0.741
				0.181	0.728
				0.303	0.889
				0.500	0.976
6	0.558	1	-90°	0.000	0.334
				0.072	0.431
				0.118	0.471
				0.182	0.572
				0.187	0.578
				0.309	0.829
4	0.186	1	-90°	0.042	1.000
				0.340	1.000
				0.455	1.000
4	0.31	1	-90°	0.427	1.000
				0.456	1.000
				0.531	1.000
4	0.434	1	-90°	0.068	0.561
				0.169	0.652
				0.221	0.749
				0.280	0.779
				0.381	0.842
				0.381	0.827
				0.422	0.914
				0.469	0.973
4	0.558	1	-90°	0.065	0.445
				0.113	0.515
				0.161	0.582
				0.222	0.612
				0.336	0.730
				0.409	0.877
				0.492	0.925



**Table B5: Phase split data for reduced T-junction with vertically downwards side arm**

Ugs (m/s)	Uls (m/s)	D <sub>3</sub> / D <sub>1</sub>	Geometry	G'	L'
12	0.0283	0.6	-90°	0.013	0.909
				0.096	0.932
				0.197	0.953
				0.216	0.958
				0.224	0.954
				0.229	0.976
				0.322	0.988
12	0.0401	0.6	-90°	0.192	0.984
				0.201	0.985
				0.227	0.990
				0.273	0.993
				0.323	0.997
				0.192	0.984
				0.000	0.812
				0.096	0.970
12	0.0535	0.6	-90°	0.000	0.740
				0.095	0.940
				0.185	0.972
				0.187	0.972
				0.199	0.978
				0.220	0.979
				0.273	0.987
				0.352	0.995
12	0.1	0.6	-90°	0.020	0.609
				0.125	0.887
				0.222	0.937
				0.223	0.933
				0.318	0.972
				0.399	0.980
12	0.186	0.6	-90°	0.000	0.238
				0.000	0.252
				0.072	0.842
				0.074	0.860
				0.131	0.889
				0.132	0.889
				0.137	0.881
				0.146	0.894
				0.157	0.904
				0.175	0.916
				0.220	0.928
				0.276	0.955



**Table B5: continued**

Ugs (m/s)	Uls (m/s)	D <sub>3</sub> / D <sub>1</sub>	Geometry	G'	L'
12	0.31	0.6	-90°	0.000	0.567
				0.045	0.663
				0.091	0.773
				0.092	0.785
				0.122	0.814
				0.139	0.822
				0.187	0.838
12	0.434	0.6	-90°	0.000	0.492
				0.039	0.580
				0.063	0.664
				0.077	0.678
				0.077	0.670
				0.101	0.736
				0.117	0.753
10	0.0401	0.6	-90°	0.136	1.000
10	0.0535	0.6	-90°	0.248	0.984
				0.016	0.914
				0.116	0.951
				0.242	0.973
				0.339	0.989
				0.419	1.000
10	0.186	0.6	-90°	0.016	0.369
				0.122	0.873
				0.184	0.890
				0.186	0.900
				0.300	0.951
10	0.31	0.6	-90°	0.017	0.225
				0.055	0.710
				0.116	0.770
				0.117	0.774
				0.240	0.871
10	0.434	0.6	-90°	0.000	0.092
				0.039	0.590
				0.100	0.705
				0.101	0.708
				0.261	0.787
10	0.558	0.6	-90°	0.050	0.463
				0.096	0.615
				0.271	0.698



**Table B5: continued**

Ugs (m/s)	Uls (m/s)	D <sub>3</sub> / D <sub>1</sub>	Geometry	G'	L'
8	0.0535	0.6	-90°	0.020	0.877
				0.130	0.958
				0.243	0.966
				0.341	0.986
8	0.186	0.6	-90°	0.020	0.879
				0.050	0.910
				0.086	0.914
				0.158	0.915
				0.160	0.926
				0.277	0.962
				0.455	0.990
8	0.31	0.6	-90°	0.010	0.213
				0.040	0.717
				0.083	0.771
				0.111	0.814
				0.241	0.889
8	0.434	0.6	-90°	0.007	0.120
				0.035	0.549
				0.078	0.686
				0.093	0.708
				0.224	0.826
8	0.558	0.6	-90°	0.021	0.346
				0.049	0.595
				0.072	0.643
				0.083	0.655
				0.275	0.748
6	0.0535	0.6	-90°	0.000	0.919
				0.064	0.975
				0.188	0.980
				0.340	1.000
6	0.1	0.6	-90°	0.000	0.535
				0.102	0.948
				0.309	0.987
				0.483	0.997
6	0.186	0.6	-90°	0.094	0.913
				0.046	0.892
				0.015	0.245
				0.160	0.923
				0.276	0.940
				0.443	0.966



**Table B5: continued**

Ugs (m/s)	Uls (m/s)	D <sub>3</sub> / D <sub>1</sub>	Geometry	G'	L'
6	0.31	0.6	-90°	0.017	0.193
				0.076	0.812
				0.109	0.848
				0.211	0.903
				0.390	0.939
6	0.434	0.6	-90°	0.022	0.291
				0.087	0.732
				0.113	0.750
				0.199	0.816
				0.369	0.879
6	0.558	0.6	-90°	0.123	0.701
				0.245	0.755
				0.354	0.796
				0.096	0.689
				0.018	0.194
4	0.186	0.6	-90°	0.220	0.914
				0.226	0.908
				0.238	0.940
				0.275	0.935
				0.270	0.936
				0.221	0.920
				0.043	0.903
				0.152	0.911
4	0.31	0.6	-90°	0.039	0.644
				0.069	0.856
				0.088	0.866
				0.125	0.879
				0.164	0.892
				0.208	0.901
				0.211	0.909
				0.214	0.916
				0.226	0.919
				0.236	0.927
4	0.434	0.6	-90°	0.027	0.159
				0.101	0.745
				0.248	0.804
				0.254	0.788
				0.297	0.832
				0.434	0.890
4	0.558	0.6	-90°	0.080	0.645
				0.104	0.670
				0.139	0.701
				0.172	0.736
				0.215	0.748
				0.289	0.782



**Table B6: Phase split data for horizontal T-junctions with inserts**

U <sub>gs</sub> (m/s)	U <sub>ls</sub> (m/s)	D <sub>3</sub> / D <sub>1</sub>	Geometry	G'	L'
24	0.0283	1	45° ½D forwards	0.000	0.000
				0.147	0.043
				0.242	0.100
				0.261	0.143
				0.266	0.147
				0.266	0.143
				0.266	0.138
				0.298	0.170
				0.359	0.228
				0.389	0.275
				0.470	0.353
				0.566	0.483
				0.661	0.576
				0.777	0.473
				0.886	0.569
				0.959	1.000
				0.959	0.854
24	0.0283	1	45° ½D backwards	0.000	0.000
				0.006	0.000
				0.060	0.014
				0.066	0.025
				0.141	0.074
				0.150	0.074
				0.162	0.060
				0.290	0.162
				0.528	0.345
				0.801	0.458
				0.957	0.580
				0.958	0.834
				0.958	1.000
24	0.0283	1	45° ¾D forwards	0.000	0.000
				0.232	0.072
				0.362	0.130
				0.426	0.208
				0.517	0.299
				0.564	0.347
				0.566	0.343
				0.583	0.369
				0.615	0.393
				0.665	0.440
				0.737	0.526
				0.833	0.584
				0.939	0.673
				1.000	1.000



**Table B6: continued**

<b>U<sub>gs</sub> (m/s)</b>	<b>U<sub>ls</sub> (m/s)</b>	<b>D<sub>3</sub> / D<sub>1</sub></b>	<b>Geometry</b>	<b>G'</b>	<b>L'</b>
24	0.0283	1	45° ¾D backwards	0.012	0.008
				0.026	0.016
				0.039	0.025
				0.253	0.037
				0.581	0.059
				0.815	0.082
				0.925	0.123
				1.000	1.000
24	0.0535	1	45° ½D forwards	0.000	0.000
				0.124	0.064
				0.234	0.102
				0.298	0.130
				0.439	0.190
				0.503	0.229
				0.621	0.308
				0.829	0.437
24	0.0535	1	45° ½D backwards	1.000	1.000
				0.067	0.027
				0.160	0.082
				0.302	0.203
				0.463	0.418
				0.556	0.423
				0.753	0.512
				0.855	0.724
24	0.0535	1	45° ¾D forwards	1.000	1.000
				0.000	0.000
				0.186	0.131
				0.433	0.255
				0.578	0.354
				0.587	0.392
				0.636	0.412
				0.669	0.447
24	0.0535	1	45° ¾D backwards	0.833	0.547
				0.865	0.598
				0.929	0.659
				1.000	1.000
				0.017	0.015
				0.031	0.025
				0.226	0.051
				0.481	0.076
24	0.0535	1	45° ¾D backwards	0.644	0.110
				0.765	0.151
				0.876	0.246
				1.000	1.000



**Table B6: continued**

<b>U<sub>gs</sub> (m/s)</b>	<b>U<sub>ls</sub> (m/s)</b>	<b>D<sub>3</sub> / D<sub>1</sub></b>	<b>Geometry</b>	<b>G'</b>	<b>L'</b>
12	0.31	1	45° ½D forwards	0.313	0.199
				0.519	0.226
				0.546	0.250
				0.646	0.269
				0.851	0.318
12	0.31	1	45° ½D backwards	0.324	0.019
				0.445	0.059
				0.448	0.041
				0.504	0.070
				0.621	0.108
				0.872	0.121
				1.000	1.000
12	0.31	1	45° ¾D forwards	0.428	0.328
				0.483	0.372
				0.578	0.410
				0.585	0.417
				0.650	0.433
				0.753	0.499
12	0.31	1	45° ¾D backwards	0.329	0.021
				0.473	0.035
				0.591	0.051
				0.765	0.168
12	0.31	1	30° ½D forwards	0.306	0.236
				0.508	0.276
				0.641	0.294
				0.782	0.349
				0.962	0.642
12	0.31	1	30° ½D backwards	0.465	0.062
				0.604	0.124
				0.833	0.222
				0.347	0.016
12	0.31	1	30° ¾D forwards	0.338	0.332
				0.480	0.408
				0.563	0.439
				0.609	0.474
				0.750	0.515
				0.897	0.603
12	0.31	1	30° ¾D backwards	0.332	0.056
				0.408	0.051
				0.439	0.063
				0.562	0.081
				0.852	0.262



**Table B6: continued**

<b>U<sub>gs</sub> (m/s)</b>	<b>U<sub>ls</sub> (m/s)</b>	<b>D<sub>3</sub> / D<sub>1</sub></b>	<b>Geometry</b>	<b>G'</b>	<b>L'</b>
12	0.31	0.6	45° ½D forwards	0.339	0.063
				0.477	0.074
				0.621	0.105
				0.757	0.148
				0.853	0.462
12	0.31	0.6	45° ½D backwards	0.156	0.008
				0.300	0.021
				0.442	0.027
				0.621	0.055
				0.830	0.118
				0.877	0.660
12	0.31	0.6	45° ¾D forwards	0.472	0.045
				0.617	0.068
				0.720	0.162
				0.877	0.446
12	0.31	0.6	45° ¾D backwards	0.172	0.003
				0.370	0.014
				0.605	0.023
				0.758	0.101
				0.877	0.478



**Table B7: Phase split data for regular T-junction with downwards side arm and U-bend**

U <sub>gs</sub> (m/s)	U <sub>ls</sub> (m/s)	D <sub>3</sub> / D <sub>1</sub>	Geometry	G'	L'
12	0.1	1	-90° U-bend	0.000	0.841
				0.000	0.841
				0.000	0.828
				0.000	0.000
				0.006	0.871
				0.006	0.865
				0.009	0.855
				0.009	0.855
				0.009	0.844
				0.010	0.926
				0.012	0.932
				0.078	0.985
				0.096	0.990
12	0.1	1	-90° U-bend	0.000	0.720
				0.000	0.729
				0.000	0.567
				0.000	0.628
				0.010	0.720
				0.012	0.703
				0.013	0.719
				0.013	0.728
				0.027	0.858
4	0.31	1	-90° U-bend	0.000	0.451
				0.033	0.929
				0.035	0.930
				0.049	0.915
				0.051	0.911
				0.055	0.920
				0.055	0.918
4	0.558	1	-90° U-bend	0.039	0.178
				0.041	0.463
				0.058	0.504
				0.067	0.521
				0.068	0.514
				0.073	0.455
				0.077	0.443
				0.086	0.535



**Table B8: Phase split data for reduced T-junction with downwards side arm and U-bend**

<b>U<sub>gs</sub> (m/s)</b>	<b>U<sub>ls</sub> (m/s)</b>	<b>D<sub>3</sub> / D<sub>1</sub></b>	<b>Geometry</b>	<b>G'</b>	<b>L'</b>
12	0.0283	0.6	-90° U-bend	0.000	0.878
				0.000	0.823
				0.004	0.865
				0.005	0.855
				0.090	0.898
12	0.0401	0.6	-90° U-bend	0.004	0.734
				0.004	0.714
				0.006	0.783
				0.006	0.801
				0.093	0.973
12	0.0535	0.6	-90° U-bend	0.000	0.653
				0.004	0.724
				0.005	0.694
				0.006	0.714
				0.007	0.717
				0.091	0.958
				0.112	0.962
12	0.186	0.6	-90° U-bend	0.000	0.416
				0.000	0.454
				0.004	0.407
				0.006	0.472
				0.011	0.488
				0.051	0.879
12	0.31	0.6	-90° U-bend	0.000	0.208
				0.005	0.323
				0.007	0.311
				0.010	0.362
				0.018	0.538
				0.052	0.506
4	0.31	0.6	-90° U-bend	0.031	0.669
				0.038	0.701
				0.039	0.645
				0.042	0.658
				0.058	0.588
				0.095	0.827
				0.043	0.619
				0.013	0.226
				0.000	0.792
4	0.558	0.6	-90° U-bend	0.043	0.914
				0.058	0.620
				0.063	0.791
				0.073	0.734
				0.074	0.544
				0.114	0.778
				0.119	0.931
				0.125	0.811
				0.130	0.831



Table B9: Phase split data for two regular T-junctions in series, 1.2m apart

Ugs (m/s)	Uls (m/s)	D <sub>3</sub> / D <sub>1</sub> for +90° T-junction	D <sub>3</sub> / D <sub>1</sub> for 90° T-junction	T-junction separation distance (m)	G' in +90° arm	L' in +90° arm	G' in -90° arm	L' in -90° arm	G' in run arm	L' in run arm
12	0.186	1	1	1.2	0.356	0.000	0.124	0.907	0.520	0.093
					0.440	0.000	0.157	0.979	0.403	0.021
					0.518	0.000	0.189	0.991	0.292	0.009
					0.739	0.000	0.261	1.000	0.000	0.000
					0.387	0.000	0.089	0.873	0.524	0.127
					0.409	0.000	0.034	0.842	0.557	0.158
					0.433	0.000	0.000	0.000	0.567	1.000
					0.243	0.000	0.145	0.958	0.612	0.042
					0.000	0.000	0.191	0.941	0.809	0.059
					1.000	0.000	0.000	0.999	0.000	0.001
12	0.31	1	1	1.2	0.385	0.000	0.121	0.749	0.494	0.251
					0.481	0.000	0.107	0.839	0.412	0.161
					0.537	0.000	0.166	0.906	0.297	0.094
					0.759	0.000	0.241	1.000	0.000	0.000
					0.403	0.000	0.080	0.679	0.516	0.321
					0.413	0.000	0.050	0.626	0.537	0.374
					0.469	0.000	0.000	0.000	0.531	1.000
					0.236	0.000	0.141	0.801	0.623	0.199
					0.000	0.000	0.179	0.832	0.821	0.168
					0.987	0.012	0.013	0.988	0.000	0.000
12	0.434	1	1	1.2	0.395	0.000	0.111	0.610	0.494	0.390
					0.508	0.000	0.148	0.726	0.344	0.274
					0.602	0.000	0.175	0.769	0.223	0.231
					0.783	0.000	0.217	1.000	0.000	0.000
					0.423	0.000	0.074	0.509	0.503	0.491
					0.449	0.000	0.052	0.458	0.499	0.542
					0.555	0.000	0.000	0.000	0.445	1.000
					0.265	0.000	0.135	0.662	0.600	0.338
					0.000	0.000	0.183	0.719	0.817	0.281
					0.965	0.000	0.035	1.000	0.000	0.000



Table B9: continued

Ugs (m/s)	Uls (m/s)	D <sub>3</sub> / D <sub>1</sub> for first T-junction	D <sub>3</sub> / D <sub>1</sub> for second T-junction	T-junction separation distance (m)	G' in +90° arm	L' in +90° arm	G' in -90° arm	L' in -90° arm	G' in run arm	L' in run arm
8	0.186	1	1	1.2	0.459	0.000	0.055	0.982	0.486	0.018
					0.566	0.000	0.064	0.993	0.370	0.007
					0.659	0.000	0.075	1.000	0.267	0.000
					0.893	0.000	0.107	1.000	0.000	0.000
					0.462	0.000	0.048	0.986	0.490	0.014
					0.481	0.000	0.023	0.985	0.496	0.015
					0.543	0.000	0.000	0.000	0.457	1.000
					0.207	0.000	0.081	0.985	0.713	0.015
					0.000	0.000	0.103	0.980	0.897	0.020
8	0.31	1	1	1.2	0.454	0.000	0.059	0.757	0.487	0.243
					0.637	0.000	0.083	0.774	0.280	0.226
					0.678	0.000	0.089	0.914	0.233	0.086
					0.888	0.000	0.112	1.000	0.000	0.000
					0.463	0.000	0.045	0.759	0.493	0.241
					0.470	0.000	0.027	0.714	0.502	0.286
					0.532	0.000	0.000	0.000	0.468	1.000
					0.245	0.000	0.078	0.766	0.676	0.234
					0.000	0.000	0.103	0.789	0.897	0.211
					0.967	0.155	0.033	0.845	0.000	0.000
4	0.186	1	1	1.2	0.425	0.000	0.140	1.000	0.434	0.000
					0.452	0.000	0.148	1.000	0.399	0.000
					0.457	0.000	0.073	1.000	0.470	0.000
					0.379	0.000	0.151	1.000	0.470	0.000



Table B9: continued

U <sub>gs</sub> (m/s)	U <sub>ls</sub> (m/s)	D <sub>3</sub> / D <sub>1</sub> for +90° T- junction	D <sub>3</sub> / D <sub>1</sub> for 90° T- junction	T-junction separation distance (m)	G' in +90° arm	L' in +90° arm	G' in -90° arm	L' in -90° arm	G' in run arm	L' in run arm
4	0.31	1	1	1.2	0.428	0.000	0.138	1.000	0.434	0.000
					0.444	0.000	0.143	1.000	0.413	0.000
					0.756	0.000	0.244	1.000	0.000	0.000
					0.461	0.000	0.084	1.000	0.455	0.000
					0.466	0.000	0.063	1.000	0.471	0.000
					0.502	0.000	0.000	0.000	0.498	1.000
					0.378	0.000	0.150	1.000	0.472	0.000
					0.000	0.000	0.243	1.000	0.757	0.000
					0.949	0.000	0.051	0.869	0.000	0.131
4	0.434	1	1	1.2	0.429	0.000	0.138	0.783	0.433	0.217
					0.461	0.000	0.145	0.757	0.394	0.243
					0.497	0.000	0.150	0.818	0.353	0.182
					0.775	0.000	0.225	1.000	0.000	0.000
					0.453	0.000	0.094	0.714	0.453	0.286
					0.464	0.000	0.063	0.636	0.473	0.364
					0.476	0.000	0.000	0.000	0.524	1.000
					0.322	0.000	0.160	0.736	0.518	0.264
					0.000	0.000	0.233	0.762	0.767	0.238
					0.891	0.029	0.109	0.971	0.000	0.000
4	0.558	1	1	1.2	0.438	0.000	0.145	0.606	0.418	0.394
					0.569	0.000	0.166	0.662	0.265	0.338
					0.576	0.000	0.171	0.784	0.253	0.216
					0.768	0.000	0.232	1.000	0.000	0.000
					0.459	0.000	0.080	0.511	0.462	0.489
					0.471	0.000	0.065	0.460	0.464	0.540
					0.575	0.000	0.000	0.000	0.425	1.000
					0.338	0.000	0.146	0.579	0.516	0.421
					0.000	0.000	0.228	0.650	0.772	0.350
					0.879	0.000	0.121	0.956	0.000	0.044



Table B10: Phase split data for regular and reduced T-junctions in series, 1.2m apart

Ugs (m/s)	Uls (m/s)	D <sub>3</sub> / D <sub>1</sub> for +90° T-junction	D <sub>3</sub> / D <sub>1</sub> for 90° T-junction	T-junction separation distance (m)	G' in +90° arm	L' in +90° arm	G' in -90° arm	L' in -90° arm	G' in run arm	L' in run arm
12	0.186	1	0.6	1.2	0.388	0.000	0.069	0.905	0.543	0.095
					0.536	0.000	0.112	0.961	0.352	0.039
					0.628	0.000	0.137	0.957	0.235	0.043
					0.805	0.000	0.195	1.000	0.000	0.000
					0.401	0.000	0.050	0.893	0.549	0.107
					0.417	0.000	0.022	0.656	0.561	0.344
					0.437	0.000	0.000	0.000	0.563	1.000
					0.225	0.000	0.107	0.884	0.667	0.116
					0.000	0.000	0.135	0.868	0.865	0.132
					0.980	0.178	0.020	0.822	0.000	0.000
12	0.31	1	0.6	1.2	0.413	0.000	0.049	0.782	0.538	0.218
					0.577	0.000	0.081	0.849	0.342	0.151
					0.672	0.000	0.094	0.868	0.233	0.132
					0.876	0.000	0.124	1.000	0.000	0.000
					0.419	0.000	0.034	0.730	0.547	0.270
					0.424	0.000	0.026	0.674	0.550	0.326
					0.433	0.000	0.000	0.000	0.567	1.000
					0.249	0.000	0.065	0.759	0.687	0.241
					0.000	0.000	0.097	0.766	0.903	0.234
					0.972	0.060	0.028	0.940	0.000	0.000
12	0.434	1	0.6	1.2	0.415	0.000	0.045	0.673	0.540	0.327
					0.679	0.000	0.081	0.769	0.239	0.231
					0.755	0.000	0.094	0.791	0.151	0.209
					0.893	0.000	0.107	1.000	0.000	0.000
					0.428	0.000	0.035	0.592	0.537	0.408
					0.477	0.000	0.023	0.308	0.500	0.692
					0.550	0.000	0.000	0.000	0.450	1.000
					0.208	0.000	0.061	0.675	0.731	0.325
					0.000	0.000	0.087	0.674	0.913	0.326
					0.954	0.002	0.046	0.998	0.000	0.000



Table B10: continued

U <sub>gs</sub> (m/s)	U <sub>ls</sub> (m/s)	D <sub>3</sub> / D <sub>1</sub> for +90° T- junction	D <sub>3</sub> / D <sub>1</sub> for 90° T- junction	T-junction separation distance (m)	G' in +90° arm	L' in +90° arm	G' in -90° arm	L' in -90° arm	G' in run arm	L' in run arm
8	0.186	1	0.6	1.2	0.481	0.000	0.021	0.933	0.498	0.067
					0.597	0.000	0.031	0.949	0.372	0.051
					0.751	0.000	0.048	0.966	0.201	0.034
					0.928	0.000	0.072	1.000	0.000	0.000
					0.487	0.000	0.012	0.912	0.501	0.088
					0.497	0.000	0.009	0.649	0.494	0.351
					0.535	0.000	0.000	0.000	0.465	1.000
					0.241	0.000	0.046	0.926	0.713	0.074
					0.000	0.000	0.056	0.891	0.944	0.109
8	0.31	1	0.6	1.2	0.485	0.000	0.028	0.650	0.487	0.350
					0.626	0.000	0.052	0.855	0.322	0.145
					0.785	0.000	0.068	0.934	0.147	0.066
					0.918	0.000	0.082	1.000	0.000	0.000
					0.469	0.000	0.038	0.818	0.493	0.182
					0.510	0.000	0.012	0.168	0.477	0.832
					0.530	0.000	0.000	0.000	0.470	1.000
					0.269	0.000	0.055	0.828	0.676	0.172
					0.000	0.000	0.079	0.820	0.921	0.180
					0.968	0.103	0.032	0.897	0.000	0.000



Table B10: continued

U <sub>gs</sub> (m/s)	U <sub>ls</sub> (m/s)	D <sub>3</sub> / D <sub>1</sub> for first T-junction	D <sub>3</sub> / D <sub>1</sub> for second T-junction	T-junction separation distance (m)	G' in +90° arm	L' in +90° arm	G' in -90° arm	L' in -90° arm	G' in run arm	L' in run arm
4	0.31	1	0.6	1.2	0.440	0.000	0.108	0.889	0.452	0.111
					0.477	0.000	0.124	0.890	0.399	0.110
					0.592	0.000	0.156	0.953	0.251	0.047
					0.789	0.000	0.211	1.000	0.000	0.000
					0.458	0.000	0.077	0.917	0.465	0.083
					0.474	0.000	0.045	0.615	0.481	0.385
					0.506	0.000	0.000	0.000	0.494	1.000
					0.333	0.000	0.137	0.869	0.531	0.131
					0.000	0.000	0.216	0.917	0.784	0.083
					0.942	0.081	0.058	0.919	0.000	0.000
4	0.434	1	0.6	1.2	0.426	0.000	0.127	0.553	0.447	0.447
					0.471	0.000	0.145	0.848	0.383	0.152
					0.542	0.000	0.165	0.908	0.293	0.092
					0.792	0.000	0.208	1.000	0.000	0.000
					0.427	0.000	0.101	0.774	0.471	0.226
					0.439	0.000	0.073	0.665	0.488	0.335
					0.512	0.000	0.000	0.000	0.488	1.000
					0.355	0.000	0.129	0.808	0.516	0.192
					0.000	0.000	0.196	0.820	0.804	0.180
					0.923	0.249	0.077	0.751	0.000	0.000
4	0.558	1	0.6	1.2	0.485	0.000	0.028	0.650	0.487	0.350
					0.492	0.000	0.191	0.812	0.316	0.188
					0.575	0.000	0.199	0.886	0.226	0.114
					0.764	0.000	0.236	1.000	0.000	0.000
					0.409	0.000	0.142	0.758	0.449	0.242
					0.472	0.000	0.053	0.344	0.475	0.656
					0.528	0.000	0.000	0.000	0.472	1.000
					0.349	0.000	0.150	0.724	0.501	0.276
					0.000	0.000	0.207	0.780	0.793	0.220
					0.884	0.053	0.116	0.947	0.000	0.000



Table B11: Phase split data for two regular T-junctions in series, 0.5m apart

Ugs (m/s)	Uls (m/s)	D <sub>3</sub> / D <sub>1</sub> for +90° T-junction	D <sub>3</sub> / D <sub>1</sub> for 90° T-junction	T-junction separation distance (m)	G' in +90° arm	L' in +90° arm	G' in -90° arm	L' in -90° arm	G' in run arm	L' in run arm
12	0.186	1	1	0.5	0.376	0.000	0.122	0.870	0.502	0.130
					0.447	0.000	0.149	0.983	0.404	0.017
					0.540	0.000	0.180	0.995	0.280	0.005
					0.738	0.000	0.262	1.000	0.000	0.000
					0.394	0.000	0.073	0.841	0.534	0.159
					0.418	0.000	0.000	0.830	0.582	0.170
					0.453	0.000	0.000	0.000	0.547	1.000
					0.238	0.000	0.149	0.938	0.613	0.062
					0.000	0.000	0.192	0.948	0.808	0.052
12	0.31	1	1	0.5	0.393	0.000	0.106	0.723	0.501	0.277
					0.484	0.000	0.142	0.831	0.374	0.169
					0.578	0.000	0.173	0.887	0.249	0.113
					0.766	0.000	0.234	1.000	0.000	0.000
					0.408	0.000	0.074	0.660	0.517	0.340
					0.422	0.000	0.038	0.557	0.540	0.443
					0.475	0.000	0.000	0.000	0.525	1.000
					0.212	0.000	0.141	0.789	0.648	0.211
					0.000	0.000	0.180	0.808	0.820	0.192
					1.000	0.263	0.000	0.705	0.000	0.031
12	0.434	1	1	0.5	0.405	0.000	0.113	0.534	0.482	0.466
					0.539	0.000	0.153	0.656	0.309	0.344
					0.597	0.000	0.179	0.734	0.224	0.266
					0.783	0.000	0.217	1.000	0.000	0.000
					0.432	0.000	0.083	0.464	0.486	0.536
					0.491	0.000	0.018	0.339	0.490	0.661
					0.551	0.000	0.000	0.000	0.449	1.000
					0.176	0.000	0.151	0.623	0.674	0.377
					0.000	0.000	0.187	0.672	0.813	0.328



Table B11: continued

Ugs (m/s)	Uls (m/s)	D <sub>3</sub> / D <sub>1</sub> for first T-junction	D <sub>3</sub> / D <sub>1</sub> for second T-junction	T-junction separation distance (m)	G' in +90° arm	L' in +90° arm	G' in -90° arm	L' in -90° arm	G' in run arm	L' in run arm
8	0.31	1	1	0.5	0.469	0.000	0.058	0.786	0.472	0.214
					0.636	0.000	0.077	0.781	0.287	0.219
					0.762	0.000	0.090	0.939	0.148	0.061
					0.895	0.000	0.105	1.000	0.000	0.000
					0.475	0.000	0.045	0.747	0.481	0.253
					0.487	0.000	0.024	0.701	0.489	0.299
					0.540	0.000	0.000	0.000	0.460	1.000
					0.296	0.000	0.074	0.748	0.630	0.252
4	0.186	1	1	0.50	0.000	0.000	0.101	0.781	0.899	0.219
					0.973	0.294	0.027	0.706	0.000	0.000
					0.429	0.000	0.135	1.000	0.436	0.000
					0.450	0.000	0.142	1.000	0.408	0.000
					0.466	0.000	0.063	1.000	0.472	0.000
					0.398	0.000	0.142	1.000	0.460	0.000



Table B11: continued

Ugs (m/s)	Uls (m/s)	D <sub>3</sub> / D <sub>1</sub> for +90° T- junction	D <sub>3</sub> / D <sub>1</sub> for 90° T- junction	T-junction separation distance (m)	G' in +90° arm	L' in +90° arm	G' in -90° arm	L' in -90° arm	G' in run arm	L' in run arm
4	0.31	1	1	0.5	0.426	0.000	0.134	1.000	0.440	0.000
					0.449	0.000	0.140	1.000	0.411	0.000
					0.679	0.000	0.214	1.000	0.106	0.000
					0.449	0.000	0.097	1.000	0.454	0.000
					0.484	0.000	0.037	0.535	0.479	0.465
					0.506	0.000	0.000	0.000	0.494	1.000
					0.282	0.000	0.170	1.000	0.548	0.000
					0.000	0.000	0.237	1.000	0.763	0.000
4	0.434	1	1	0.5	0.434	0.000	0.137	0.683	0.428	0.317
					0.493	0.000	0.153	0.677	0.353	0.323
					0.555	0.000	0.172	0.722	0.273	0.278
					0.767	0.000	0.233	1.000	0.000	0.000
					0.454	0.000	0.096	0.627	0.450	0.373
					0.483	0.000	0.035	0.313	0.482	0.687
					0.534	0.000	0.000	0.000	0.466	1.000
					0.363	0.000	0.151	0.691	0.487	0.309
					0.000	0.000	0.232	0.685	0.768	0.315
4	0.558	1	1	0.5	0.432	0.000	0.129	0.578	0.440	0.422
					0.697	0.000	0.207	0.673	0.095	0.327
					0.515	0.000	0.159	0.631	0.327	0.369
					0.764	0.000	0.236	1.000	0.000	0.000
					0.461	0.000	0.089	0.540	0.450	0.460
					0.455	0.000	0.066	0.485	0.479	0.515
					0.534	0.000	0.023	0.115	0.443	0.885
					0.302	0.000	0.157	0.601	0.540	0.399
					0.155	0.000	0.205	0.637	0.640	0.363



Table B12: Phase split data for regular and reduced T-junctions in series, 0.5m apart

U <sub>gs</sub> (m/s)	U <sub>ls</sub> (m/s)	D <sub>3</sub> / D <sub>1</sub> for +90° T- junction	D <sub>3</sub> / D <sub>1</sub> for 90° T- junction	T-junction separation distance (m)	G' in +90° arm	L' in +90° arm	G' in -90° arm	L' in -90° arm	G' in run arm	L' in run arm
12	0.186	1	0.6	0.5	0.231	0.000	0.088	0.880	0.681	0.1201362
					0.540	0.000	0.107	0.930	0.352	0.0698557
					0.662	0.000	0.147	0.945	0.191	0.055
					0.807	0.000	0.193	1.000	0.000	0.000
					0.396	0.000	0.053	0.890	0.551	0.110
					0.418	0.000	0.018	0.481	0.564	0.519
					0.436	0.000	0.000	0.000	0.564	1.000
					0.200	0.000	0.092	0.893	0.707	0.107
					0.000	0.000	0.126	0.879	0.874	0.121
					1.000	0.001	0.000	0.999	0.000	0.000
12	0.31	1	0.6	0.5	0.408	0.000	0.044	0.747	0.548	0.253
					0.591	0.000	0.079	0.828	0.330	0.172
					0.704	0.000	0.101	0.843	0.195	0.157
					0.871	0.000	0.129	1.000	0.000	0.000
					0.435	0.000	0.032	0.718	0.533	0.282
					0.449	0.000	0.000	0.311	0.551	0.689
					0.473	0.000	0.000	0.000	0.527	1.000
					0.239	0.000	0.067	0.758	0.694	0.242
					0.000	0.000	0.094	0.768	0.906	0.232
					0.981	0.096	0.019	0.904	0.000	0.000
12	0.434	1	0.6	0.5	0.417	0.000	0.044	0.647	0.539	0.353
					0.685	0.000	0.078	0.745	0.236	0.255
					0.786	0.000	0.097	0.762	0.117	0.238
					0.885	0.000	0.115	1.000	0.000	0.000
					0.424	0.000	0.037	0.601	0.539	0.399
					0.490	0.000	0.000	0.300	0.510	0.700
					0.537	0.000	0.000	0.000	0.463	1.000
					0.214	0.000	0.057	0.655	0.729	0.345
					0.000	0.000	0.082	0.683	0.918	0.317
					0.959	0.019	0.041	0.981	0.000	0.000



Table B12: continued

U <sub>gs</sub> (m/s)	U <sub>ls</sub> (m/s)	D <sub>3</sub> / D <sub>1</sub> for first T-junction	D <sub>3</sub> / D <sub>1</sub> for second T-junction	T-junction separation distance (m)	G' in +90° arm	L' in +90° arm	G' in -90° arm	L' in -90° arm	G' in run arm	L' in run arm
8	0.31	1	0.6	0.5	0.490	0.000	0.037	0.632	0.473	0.368
					0.645	0.000	0.050	0.843	0.304	0.157
					0.786	0.000	0.069	0.911	0.145	0.089
					0.920	0.000	0.080	1.000	0.000	0.000
					0.471	0.000	0.041	0.809	0.488	0.191
					0.511	0.000	0.016	0.414	0.472	0.586
					0.540	0.000	0.000	0.000	0.460	1.000
					0.255	0.000	0.058	0.803	0.686	0.197
					0.000	0.000	0.079	0.797	0.921	0.203
4	0.31	1	0.6	0.5	0.443	0.000	0.112	0.882	0.445	0.118
					0.480	0.000	0.125	0.875	0.395	0.125
					0.580	0.000	0.152	0.938	0.268	0.062
					0.790	0.000	0.210	1.000	0.000	0.000
					0.458	0.000	0.080	0.908	0.462	0.092
					0.498	0.000	0.023	0.192	0.479	0.808
					0.504	0.000	0.000	0.000	0.496	1.000
					0.309	0.000	0.145	0.873	0.546	0.127
					0.000	0.000	0.213	0.884	0.787	0.116
					0.937	0.000	0.063	1.000	0.000	0.000
4	0.434	1	0.6	0.5	0.458	0.000	0.077	0.576	0.465	0.424
					0.503	0.000	0.129	0.839	0.368	0.161
					0.580	0.000	0.146	0.898	0.274	0.102
					0.811	0.000	0.189	1.000	0.000	0.000
					0.447	0.000	0.097	0.790	0.455	0.210
					0.459	0.000	0.080	0.747	0.461	0.253
					0.526	0.000	0.000	0.000	0.474	1.000
					0.362	0.000	0.129	0.633	0.509	0.367
					0.000	0.000	0.196	0.824	0.804	0.176
					0.891	0.000	0.109	1.000	0.000	0.000



Table B12: continued

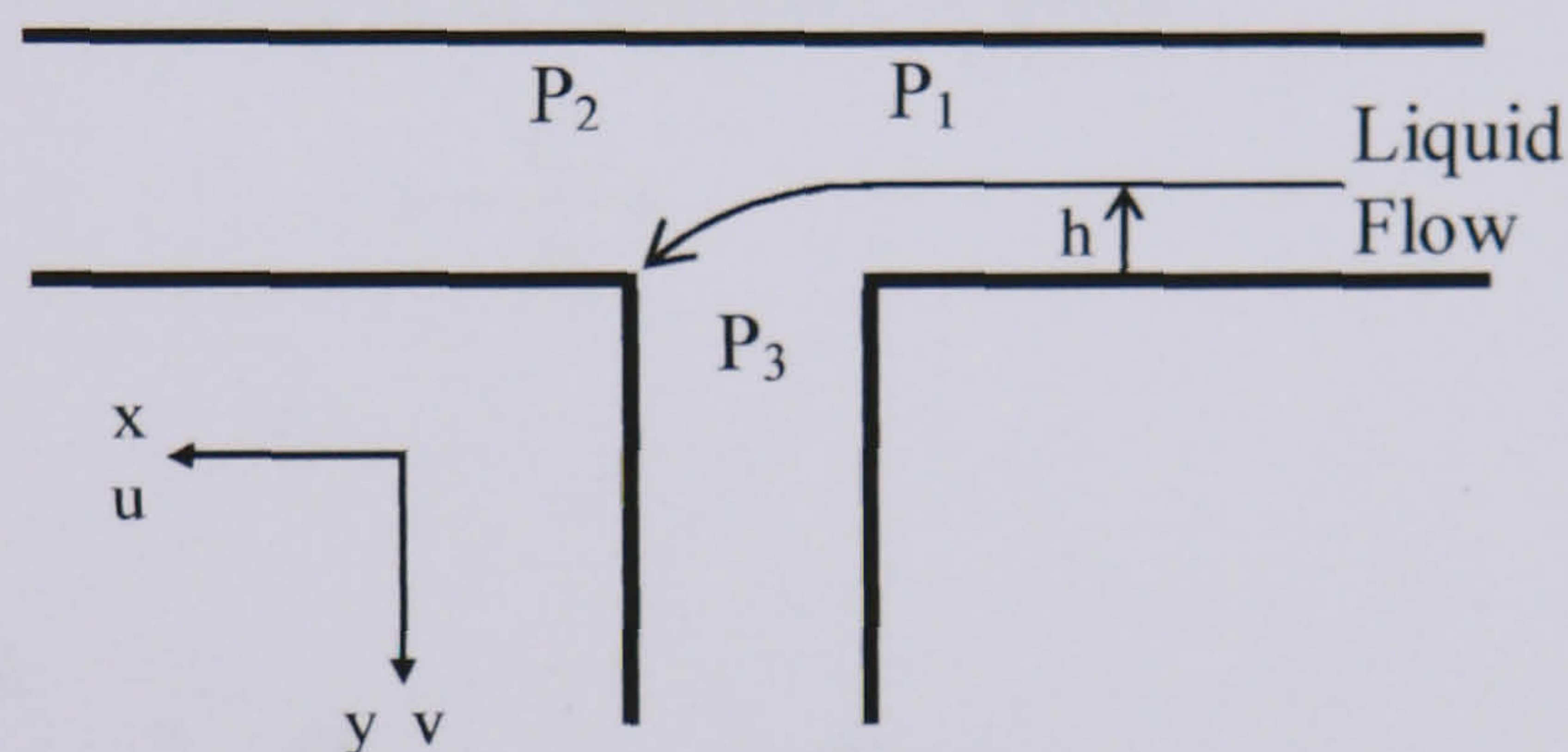
Ugs (m/s)	Uls (m/s)	D <sub>3</sub> / D <sub>1</sub> for first T- junction	D <sub>3</sub> / D <sub>1</sub> for second T- junction	T-junction separation distance (m)	G' in +90° arm	L' in +90° arm	G' in -90° arm	L' in -90° arm	G' in run arm	L' in run arm
4	0.558	1	0.6	0.5	0.455	0.000	0.062	0.433	0.483	0.567
					0.544	0.000	0.171	0.799	0.285	0.201
					0.602	0.000	0.178	0.889	0.220	0.111
					0.781	0.000	0.219	1.000	0.000	0.000
					0.430	0.000	0.142	0.742	0.428	0.258
					0.461	0.000	0.085	0.624	0.454	0.376
					0.547	0.000	0.000	0.000	0.453	1.000
					0.373	0.000	0.158	0.729	0.470	0.271
					0.000	0.000	0.148	0.732	0.852	0.268
					0.865	0.000	0.135	1.000	0.000	0.000



## APPENDIX C

### Considering Single Phase Pressure Drop

If a liquid particle is considered to be travelling across the junction at the height of the gas-liquid interface,  $h$ , and reacts to the junction pressure changes then



In the horizontal ( $x$ ) direction

$$\rho_L \frac{du}{dt} = -\frac{dP}{dx} = -C_1 \quad \text{Equation C-1}$$

Hence

$$C_1 = \frac{dP}{dx} = \frac{P_2 - P_1}{D_3} \quad \text{Equation C-2}$$



Since  $u = U_{LH}$  at  $t = 0$ , integrating Equation C-1 gives

$$u = -\frac{C_1}{\rho_L}t + U_{LH} \quad \text{Equation C-3}$$

where  $U_{LH}$  is the gas-liquid interfacial velocity.

In the vertical ( $y$ ) direction

$$\rho_L \frac{dv}{dt} = \rho_L g + \frac{dP}{dy} = C_2 \quad \text{Equation C-4}$$

Since  $v = 0$  at  $t = 0$ , integrating Equation C-4 gives

$$v = \frac{C_2}{\rho_L}t \quad \text{Equation C-5}$$

Now considering

$$u = \frac{dx}{dt} \quad \text{and} \quad v = \frac{dy}{dt} \quad \text{Equation C-6}$$

Since  $x = 0$  at  $t = 0$ , integrating Equation C-3 gives

$$x = U_{LH}t - \frac{C_1}{\rho_L} \frac{t^2}{2} \quad \text{Equation C-7}$$

and since  $y = 0$  at  $t = 0$ , integrating Equation C-5 gives

$$y = \frac{C_2}{\rho_L} \frac{t^2}{2} \quad \text{Equation C-8}$$



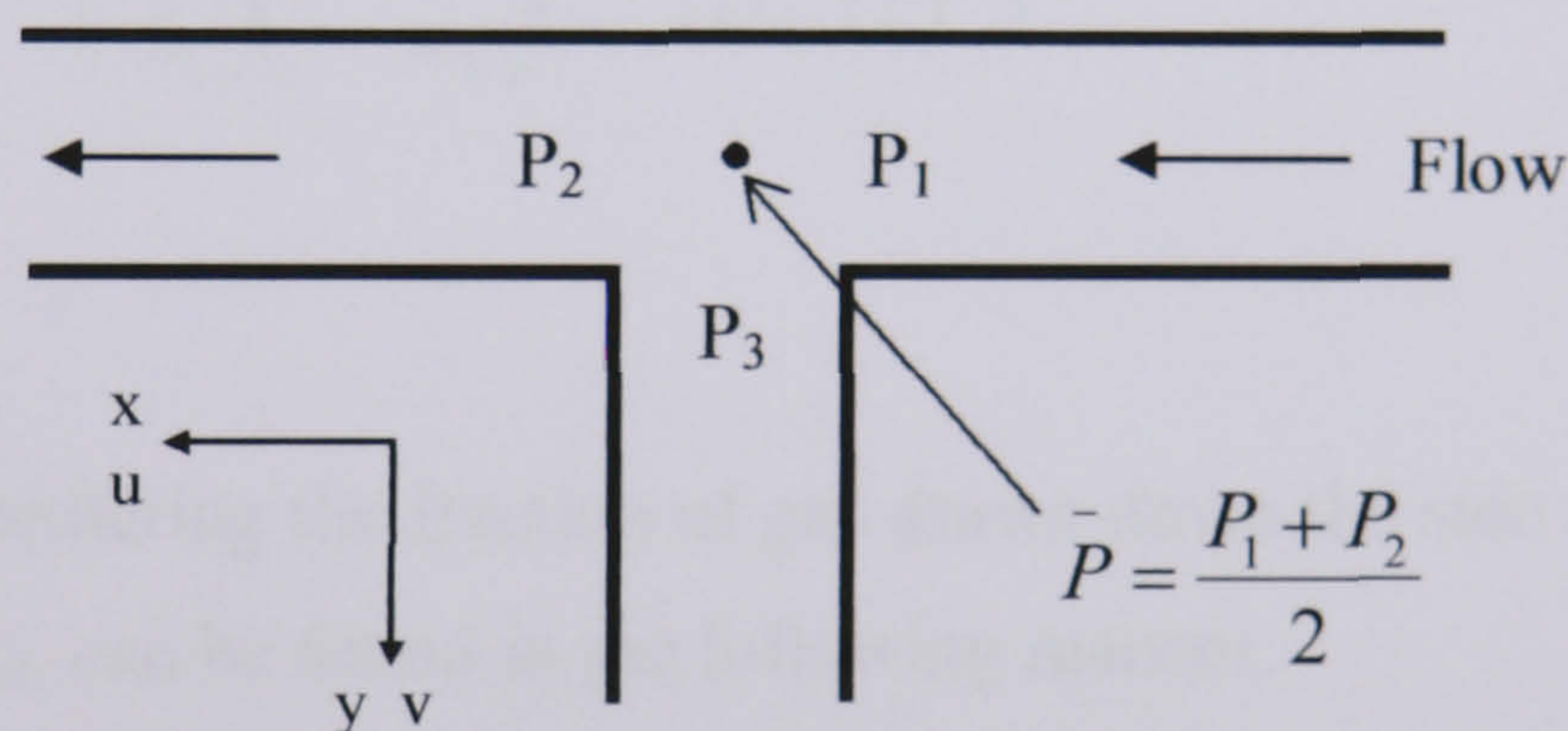
Rearranging Equation C-8 for time,  $t$

$$t = \sqrt{\frac{2\rho_L y}{C_2}} \quad \text{Equation C-9}$$

Substituting for time,  $t$  in Equation C-7

$$x = V_{LH} \sqrt{\frac{2\rho_L}{C_2}} y^{0.5} - \frac{C_1}{C_2} y \quad \text{Equation C-10}$$

where vertical distance  $y$  is equal to the height of the gas-liquid interface,  $h$  and  $V_{LH}$  is the gas-liquid interfacial velocity. The values of  $C_1$  and  $C_2$  are dependant on the pressure changes across the T-junction and can be determined from the single phase pressure drop described below.



From the single phase pressure drop model of Gardel (1957), for a gas flow passing a T-junction the pressure drop can be calculated as follows.

The pressure drop across the inlet and run arms can be calculated by

$$P_2 - P_1 = K_{12} \frac{G_1^2 - G_2^2}{\rho_G} \quad \text{Equation C-11}$$

where

$$G = \frac{\dot{m}}{A} \quad \text{Equation C-12}$$

with  $A$  being the cross-sectional area of the pipe



and

$$K_{12} = 0.57 - 0.102 \left( \frac{\dot{m}_3}{\dot{m}_1} \right) - 0.107 \left( \frac{\dot{m}_3}{\dot{m}_1} \right)^2 \quad \text{Equation C-13}$$

The pressure drop across the inlet and down arm can be calculated by

$$P_1 - P_3 = \frac{G_3^2 - G_1^2}{2\rho_G} + K_{13} \frac{G_1^2}{2\rho_G} \quad \text{Equation C-14}$$

where

$$K_{13} = 0.95 \left( 1 - \frac{\dot{m}_3}{\dot{m}_1} \right)^2 + \left( \frac{\dot{m}_3}{\dot{m}_1} \right)^2 \left[ 1 + \frac{0.4/(D_3/D_1)^2 - 0.1}{(D_3/D_1)^2} \right] \\ + 0.4 \left( \frac{\dot{m}_3}{\dot{m}_1} \right) \left( 1 - \frac{\dot{m}_3}{\dot{m}_1} \right) \left( 1 + \frac{1}{(D_3/D_1)^2} \right) \quad \text{Equation C-15}$$

Methodology for predicting the fraction of gas drawn down the side arm for complete liquid removal,  $G'_{\text{crit}}$ , can be found in the following manner.

1. If the liquid phase is neglected, for a known fraction of gas diverted down the

$$\text{side arm, } G' \equiv \frac{\dot{m}_{G3}}{\dot{m}_{G1}}$$

2. Thus the junction pressure drops can be calculated assuming the pressure drop

in the vertical direction can be approximated by  $\frac{dP}{dy} = \frac{\bar{P} - P_3}{D_1/2}$  where  $\bar{P}$  is the

average pressure at the centre of the junction

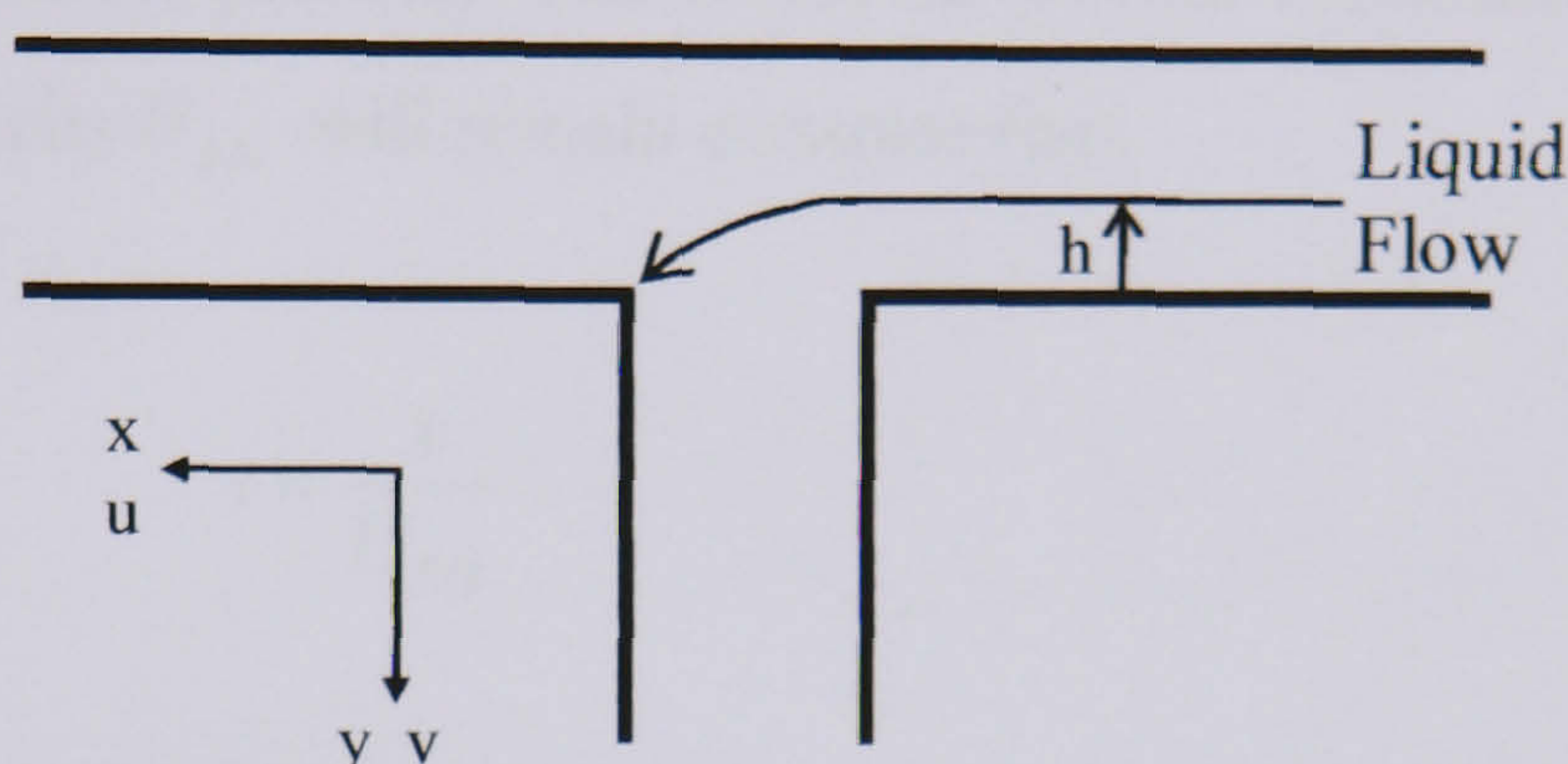
3. The horizontal distance,  $x$  can therefore be determined from Equation C-10

Closure of the problem is assumed when the calculated horizontal distance  $x$  is equal to the branch arm diameter  $D_3$ . Thus  $G'_{\text{crit}}$  has been determined.



## APPENDIX D

### Considering Drag Forces



If a liquid particle is considered to be travelling across the junction at the height of the gas-liquid interface,  $h$  then the gravitational and drag forces can be considered as it falls into the branch arm giving

$$\frac{\pi}{6} D_p^3 \rho_L g + C_D \frac{\pi D_p^2}{4} \frac{\rho_G u_G^2}{2} = \frac{\pi}{6} D_p^3 \rho_L \frac{dv}{dt} \quad \text{Equation D-1}$$

Which can be reduced to

$$\frac{dv}{dt} = \left[ g + \frac{3C_D}{4D_p} \frac{\rho_G u_G^2}{\rho_L} \right] \quad \text{Equation D-2}$$

Since  $v = 0$  at  $t = 0$ , integrating Equation D-2 gives

$$v = gt + \frac{3C_D}{4D_p} \frac{\rho_G u_G^2}{\rho_L} t \quad \text{Equation D-3}$$

Now if

$$v = \frac{dy}{dt} \quad \text{Equation D-4}$$



Since  $y = 0$  at  $t = 0$ , integrating Equation D-3 gives

$$y = \left[ g + \frac{3C_D}{4D_p} \frac{\rho_G}{\rho_L} \frac{u_{G3}^2}{\rho_L} \right] \frac{t^2}{2} \quad \text{Equation D-5}$$

If the pressure drop across the junction is considered negligible and by assuming there is no gravitational component or resistance to movement the  $x$  in direction, then no forces will be acting on the particle. Therefore, the particle is not accelerating and the liquid interfacial velocity  $U_{LH}$  will remain constant thus

$$t = \frac{x}{U_{LH}} \quad \text{Equation D-6}$$

Substituting for time,  $t$  in Equation D-5

$$y = g' \frac{x^2}{2U_{LH}^2} \quad \text{Equation D-7}$$

where

$$g' = g + \frac{3C_D}{4D_p} \frac{\rho_G}{\rho_L} \frac{u_{G3}^2}{\rho_L} \quad \text{Equation D-8}$$

If the particle starts at the vertical height  $h$ , then for  $y = h$ , the horizontal distance,  $x$  travelled by the particle can be found from Equation D-7

$$x = U_{LH} \sqrt{\frac{2h}{g'}} \quad \text{Equation D-9}$$



Equation D-9 is very similar to Equation C-15 except heavily dependant on particle diameter  $D_p$ . The fraction of gas drawn down the side arm for complete liquid removal,  $G'_{crit}$  can be determined in the following manner -

1. For a known fraction of gas removed down the side arm  $G' \equiv \frac{\dot{m}_{G3}}{\dot{m}_{G1}}$
2. Hence  $\dot{m}_{G3} = \rho_G \frac{\pi}{4} D_3^2 u_{G3}$
3. A particle diameter,  $D_p$  was assumed and the relevant value of  $C_D$  calculated by considering the particle Reynolds number
4. The values obtained for  $u_{G3}$ ,  $C_D$  and  $D_p$  were substituted into Equation D-9 to determine the horizontal distance travelled,  $x$  by the particle

Closure of the problem is assumed when the calculated horizontal distance  $x$  is equal to the branch arm diameter  $D_3$ . Thus  $G'_{crit}$  has been determined.